MECHANISTIC BASIS FOR THE ROLE OF RESISTANCE AND TOLERANCE DETERMINANTS IN ANTIBIOTIC TREATMENT FAILURE

by

MISHA IQBAL KAZI

DISSERTATION

Submitted in partial fulfillment of the requirements
to the faculty of the University of Texas at Arlington
for the degree of

DOCTOR OF PHILOSOPHY

The University of Texas at Arlington
Arlington, Texas
May, 2022

Approved by Supervisory Committee:

Joseph Boll, PhD, Supervising Professor and Committee Chair
Bryan Davies, PhD, Committee Member
Cara Boutte, PhD, Committee Member
Todd Castoe, PhD, Committee Member
Laura Mydlarz, PhD, Committee Member

DEDICATION

To my parents, whose sacrifices, love, and unwavering support have made it possible for me to realize my full potential and pursue my ambitions.

ACKNOWLEDGMENTS

I would like to thank my graduate advisor Dr. Joseph Boll for giving me the opportunity to explore many different topics under his supervision, I have truly learned so much. Your support, mentorship and friendship over the years have helped me gain confidence as a scientist, a writer and a public speaker. I am grateful for the countless hours you spent working with me to help improve my presentation skills. I have come a long way from my very first talk at UT Austin. Thanks to members of my graduate committee, Drs. Bryan Davies, Cara Boutte, Todd Castoe, and Laura Mydlarz, whose diverse perspectives have encouraged me to think critically about my research. Special thanks to Dr. Bryan Davies who gave me the opportunity to start my scientific career as a research technician in his lab and continues to be an important catalyst for my growth as a scientist. Thank you for putting up with me for so long. I would like to give a shout out to my undergraduate researchers, Victor Obuekwe, Tashjae Scales, Hana Ali and Richard Schargel, who helped support my graduate research. Thanks to members of the Boll lab for “tolerating” me every day, specially Nowrosh Islam and Feroz Ahmed, who have made working in the lab enjoyable and saved me numerous trips to lab on Sundays to start my cultures. I am going to miss the camaraderie we have established. A special shout out to the Boutte lab for always being so generous with their equipment, supplies and time. You guys have saved me more times than I can remember during supply shortages or when I just needed a sounding board. Thanks to Dr. Nigel Atkinson and Brooks Robinson for letting me be a part of their group as an undergraduate researcher at UT Austin. I am grateful for the opportunity you gave me to discover my passion for scientific research and pursue it.

TABLE OF CONTENTS

ABSTRACT

MECHANISTIC BASIS FOR THE ROLE OF RESISTANCE AND TOLERANCE DETERMINANTS IN ANTIBIOTIC TREATMENT FAILURE

Misha Iqbal Kazi, Ph.D.

The University of Texas at Arlington, 2022

Supervising Professor: Joseph Boll

Failure of antibiotics in treatment of nosocomial Gram-negative bacterial infections has created a substantial burden for global public health. The β-lactam class of antibiotics includes last resort carbapenems, which are used to combat multidrug resistant Gram-negative bacterial infections. Production of β-lactamase enzymes that degrade these antibiotics is the primary mechanism β-lactam resistance in Gram-negative bacteria. While FDA-approved serine-β-lactamase inhibitors are co-formulated with β-lactam antibiotics to prevent their inactivation during treatment, no metallo-β-lactamase inhibitors have been approved for clinical use. The first study employs an innovative antimicrobial discovery platform to identify peptide inhibitors against the New Delhi metallo-β-lactamase-1 (NDM-1), which is a concerning resistance enzyme that inactivates carbapenems. The activity of lead inhibitors to enhance carbapenem susceptibility was validated against NDM-1 encoded Enterobacteriaceae using minimum inhibitory concentration (MIC) and minimum bactericidal concentration (MBC) assays. Biochemical analysis using the chromogenic β-lactam analog nitrocefin and purified NDM-1 enzyme

revealed direct binding of four peptide sequences to NDM-1. Kinetic studies showed that three of the four lead inhibitors competitively bound NDM-1, while one peptide demonstrated non-competitive inhibition. The translational potential of lead peptides was determined using MTT and hemolysis assays where all four inhibitors showed minimal hemolytic and cytotoxic activity against mammalian cell lines. These studies provide a starting point for optimization and development of potent metallo-β-lactamase inhibitors with strong translational potential.

While resistance is a major contributor to antibiotic treatment failure, growing evidence suggests that antibiotic tolerance also plays a significant role in bacterial evasion of antimicrobial therapeutics. Many clinically significant Gram-negative pathogens demonstrate spheroplast-mediated tolerance to carbapenems. The second study uses *Enterobacter cloacae* to identify determinants of carbapenem tolerance in Enterobacteriaceae. These studies highlight the importance of PhoPQ-dependent L-Ara4N (positively charged moiety) addition to lipid A for *E. cloacae* carbapenem tolerance. Our analysis also suggests that PhoPQ-mediated lipid A modification is a highly conserved carbapenem tolerance mechanism across Enterobacteriaceae. This novel role for the highly conserved PhoPQ TCS presumably protects spheroplasts during treatment by increasing outer membrane stability and integrity. The third study expands my work on tolerance into the nosocomial Gram-negative pathogen *Acinetobacter baumannii.* Global differential gene expression profile of tolerant *A. baumannii* was determined by RNA-sequencing analysis, which revealed increased expression of genes encoding efflux pumps, putative lipoproteins and lipoprotein transport machinery and downregulation of genes encoding outer membrane porins in meropenem treated versus untreated

samples. Tn-seq was performed to pinpoint fitness determinants contributing to spheroplast-mediated carbapenem tolerance in *A. baumannii*. Subsequent validation and biochemical analysis demonstrated importance of outer membrane and peptidoglycan maintenance in *A. baumannii* carbapenem tolerance. These findings further emphasize the importance of maintaining outer membrane rigidity and stability for carbapenem tolerance and specifically spheroplast formation in Gram-negative bacteria.

The fourth study provides a detailed outline for a highly efficient Tn-seq method. This method relies on bacterial conjugation to generate saturated transposon insertion libraries and uses mechanical shearing for genomic DNA fragmentation which streamlines the entire method to provide robust and reproducible results. Together, these studies exploit innovative techniques to address important questions regarding clinical antibiotic treatment failure and provide novel targets for therapeutic development to potentially slow the spread of resistance and extend clinical efficacy of β-lactam antibiotics.

PRIOR PUBLICATIONS

*Denotes co-first authors

9. *Murtha AN, ***Kazi MI**, Schargel RD, et al. High-Level Carbapenem Tolerance Requires Antibiotic-Induced Outer Membrane Modifications. *PLoS Pathog.* 2022; *In Press*

8. Hunt-Serracín AC, **Kazi MI**, Boll JM, Boutte CC. In *Mycobacterium abscessus* , the stringent factor Rel regulates metabolism, but is not the only (p)ppGpp synthase. *J Bacteriol*. Published online December 13, 2021:JB.00434-21. doi:10.1128/JB.00434-21

7. *Islam N, ***Kazi MI**, Kang KN, et al. Peptidoglycan Recycling Contributes to Outer Membrane Integrity and Carbapenem Tolerance in *Acinetobacter Baumannii*. *bioRxiv;* 2021. doi:10.1101/2021.11.23.469614

6. Kang KN, **Kazi MI**, Biboy J, et al. Septal Class A Penicillin-Binding Protein Activity and LD -Transpeptidases Mediate Selection of Colistin-Resistant Lipooligosaccharide-Deficient *Acinetobacter baumannii*. *mBio*. 2021;12(1). doi:10.1128/mBio.02185-20

5. **Kazi MI**, Schargel RD, Boll JM. Generating Transposon Insertion Libraries in Gram-Negative Bacteria for High-Throughput Sequencing. *J Vis Exp*. 2020;(161). doi:10.3791/61612

4. **Kazi MI**, Perry BW, Card DC, et al. Discovery and characterization of New Delhi metallo-β-lactamase-1 inhibitor peptides that potentiate meropenem-dependent killing of carbapenemase-producing Enterobacteriaceae. *J Antimicrob Chemother*. 2020;75(10):2843-2851. doi:10.1093/jac/dkaa242

3. Kang KN, Klein DR, **Kazi MI**, et al. Colistin heteroresistance in *Enterobacter cloacae* is regulated by PhoPQ-dependent 4-amino-4-deoxy- L -arabinose addition to lipid A. *Mol Microbiol*. 2019;111(6):1604-1616. doi:10.1111/mmi.14240

2. Knauf GA, Cunningham AL, **Kazi MI**, et al. Exploring the Antimicrobial Action of Quaternary Amines against *Acinetobacter baumannii*. *mBio*. 2018;9(1). doi:10.1128/mBio.02394-17

1. **Kazi MI**, Conrado AR, Mey AR, Payne SM, Davies BW. ToxR Antagonizes H-NS Regulation of Horizontally Acquired Genes to Drive Host Colonization. *PLoS Pathog*. 2016;12(4):e1005570. doi:10.1371/journal.ppat.1005570

LIST OF TABLES

LIST OF FIGURES

CHAPTER 1

INTRODUCTION

The increased prevalence of antibiotic treatment failure has posed a major crisis for global public health. Bacterial infections that were once easily cleared with antibiotics, no longer respond to classic treatment protocols[1]. Nosocomial-associated Gram-negative pathogens, including members of the Enterobacteriaceae family and *Acinetobacter baumannii,* continue to rank among urgent threats and critical targets for new antibiotic development both by the Center for Disease Control and Prevention (CDC) and the World Health Organization (WHO), respectively[2,3]. Due to increasing incidence of multidrug resistant Gram-negative pathogens associated with life-threatening nosocomial infections there is an urgent need to characterize new drug targets and establish novel antimicrobial treatment protocols to counter antibiotic treatment failure and slow the spread of resistance.

β-lactams are a clinically important class of antibiotics that exert antimicrobial activity through perturbing cell wall biosynthesis[4,5]. Carbapenem β-lactams, such as imipenem and meropenem, are increasingly useful therapeutics because they are highly resistant to many of the common β-lactam resistance mechanisms and are last-resort therapeutics used to treat multidrug resistant Gram-negative infections[6,7]. Despite limiting carbapenem treatment to combat only multidrug resistant infections, many Gram-negative pathogens have adapted diverse mechanisms to evade carbapenem-dependent killing.

Antibiotic resistance is a major factor contributing to antibiotic treatment failure. The primary mechanism of β-lactam resistance in Gram-negative bacteria centers on β-

lactamase enzymes. β-lactamases cleave the amide bond in the four-membered β-lactam ring to destroy the antibiotic[7,8]. Diverse classes of β-lactamases exist, including metallo-β-lactamases, which are unique metal dependent β-lactamases, especially problematic in healthcare settings because they demonstrate an uncharacteristic broad substrate specificity that enables inactivation of all bicyclic β-lactams, including carbapenems. The New Delhi metallo-β-lactamase (NDM-1) has emerged since 2008 and is unusually problematic in hospitals and healthcare communities because it is plasmid encoded, which has facilitated rapid expansion among clinically important Gram-negative pathogens[9,10]. While serine-dependent β-lactamase inhibitors, such as clavulanic acid, sulbactam, and avibactam, are formulated with commonly prescribed β-lactam antibiotics to overcome serine-dependent drug resistance, no metallo-β-lactamase inhibitors have been approved for clinical use yet[11].

Antibiotic tolerance is another major factor contributing to the failure of antimicrobial therapy as well as recurrent bacterial infections[12,13]. Tolerance is described as the ability of susceptible bacteria to temporarily survive exposure to otherwise lethal concentrations of bactericidal antibiotics without altering the minimal inhibitory concentration[12,14,15]. While this mechanism directly contributes to antibiotic treatment failure in the short-term, it also contributes to acquisition of antibiotic resistance by extending pathogen survival, which increases the likelihood for resistance-conferring mutations or horizontal gene transfer to occur[16,17]. Previous studies have reported that several clinically important Gram-negative pathogens, including members of the Enterobacteriaceae family like *Klebsiella spp.* and *Enterobacter spp.* as well as *Acinetobacter baumannii*, exhibit high-levels carbapenem tolerance, mediated by

formation of viable, but non-dividing spheroplasts (bacteria with damaged peptidoglycan)[15,18–21]. Moreover, carbapenem-tolerant spheroplasts revert to characteristic wild type morphology and growth once the antibiotic is removed, suggesting it might pose a serious threat of relapse infections[21]. While mechanisms of β-lactam resistance have been extensively studied in various clinically relevant Gram-negative pathogens, factors regulating carbapenem tolerance in nosocomial-associated Gram-negative pathogens remain largely unknown.

Since carbapenem tolerance has previously been reported to be mediated by formation of spheroplast with a compromised cell-wall[18–21], it suggest that carbapenem-induced spheroplast integrity and survival is largely dependent on the outer membrane. The Gram-negative bacterial cell envelope is an important tripartite structure consisting of an outer membrane, and an inner membrane separated by the periplasm which contains a thin peptidoglycan layer[22,23]. The essential peptidoglycan cell wall provides cell shape and protects the bacterial cell from lysing due to internal turgor pressure[21,22]. The outer membrane of the Gram-negative cell envelope serves as a permeability barrier against harmful antibiotics and other hostile environments, and was recently shown to also serve as a load-bearing structure to counter the internal turgor[21,22].

Acinetobacter baumannii is another important gram-negative pathogen that poses a serious threat to the efficacy of our current β-lactam antibiotic repertoire*. A. baumannii* is an opportunistic, nosocomial pathogen that has dramatically increased in clinical importance over the past few decades[24,25]. Presently, *A. baumannii* is the most important and most challenging to treat organism associated with hospital-acquired infections due to its incredible ability to acquire antimicrobial resistance and high risk of epidemic[26–29].

However, investigation into the prevalence of carbapenem tolerance and the mechanisms regulating this in *A. baumannii* is lacking.

Here, I utilized innovative techniques to study resistance and tolerance mechanisms in a diverse array of Gram-negative pathogens. First, I discovered four potent inhibitor peptides against the NDM-1 resistance enzyme using a high-throughput antimicrobial discovery platform. Next, I investigated carbapenem tolerance in Enterobacteriaceae and discovered that the outer membrane becomes essential for supporting carbapenem-induced spheroplast formation in the presence of a defective cell wall. I also showed that spheroplast-mediated meropenem tolerance is widely observed in carbapenem susceptible lab-adapted *A. baumannii* strains as well as in recent clinical isolates. Tolerant *A. baumannii* isolates also resume growth and restore the coccobacilli morphology upon removal of meropenem.

I also optimized a transposon insertion sequencing (Tn-seq) protocol by streamlining the generation and sequencing of *A. baumannii* saturating mutant libraries under various conditions to obtain reproducible results and robust downstream analyses. Development and implementation of these new methods was critical in linking peptidoglycan recycling to outer membrane integrity and carbapenem tolerance in *A. baumannii*.

Together, these studies give insight into factors leading to failure of clinical antimicrobial therapeutics and mechanisms that regulate bacterial responses to antibiotics. Lastly, antibiotic tolerance is potentially a widespread cause of antimicrobial treatment failure and we have characterized new therapeutic targets to increase the

efficacy of our current β-lactam antibiotic arsenal and potentially slow the spread of antibiotic resistance mechanisms in clinically significant Gram-negative pathogens.

CHAPTER 2

LITERATURE REVIEW

History of β-lactam antibiotics

The discovery of antibiotics dates as far back as the late 19th century when two German physicians, Rudolph Emmerich and Oscar Löw, found that *Pseudomonas aeruginosa* and its extracts showed therapeutic potential against various bacterial diseases[30–32]. Following these observations, Emmerich and Löw developed pyocyanase in 1899, which was the first antimicrobial drug used as a clinical therapeutic[30,31]. While initially thought to be an enzyme, it was later determined that the antibacterial compound produced by *P. aeruginosa* was in fact a quorum sensing molecule[30,31,33]. However, due to its inconsistent efficacy and high host toxicity, clinical use of pyocyanase as a therapeutic was short-lived[30,31].

The best-known account of early antibiotics is likely Alexander Fleming's serendipitous discovery of penicillin, which revolutionized the use of antimicrobial agents as clinical therapeutics. In 1928, Fleming found that *Staphylococcus aureus* growth was inhibited by a contaminating mold; later identified as the fungus, *Penicillium notatum*[30,31,34,35]. However, it was more than a decade before penicillin became available for clinical use[30,31,34,36,37]. In 1940, Howard Florey, Norman Heatley and Ernest Chain published a study detailing the purification and therapeutic potential of penicillin in experimental mice infected with various bacterial pathogens, including *Streptococcus pyogenes*, *Staphylococcus aureus,* and *Clostridium septique*[30,31,36–38]. It was another 3 years before Mary Hunt isolated *Penicillium chrysogenum* from a moldy cantaloupe to

enable mass production of penicillin, which was instrumental in treating infections during World War II[34]. In 1945, Dorothy Hodgkin identified the β-lactam ring as the structure responsible for the antimicrobial activity of penicillin[31,33,39]. This was significant because it opened the door for development of synthetic and semi-synthetic derivatives of penicillin and propelled antibiotic discovery research[31,33].

While the concept of antibiosis, where one microorganism produces a toxic substance to out compete another, had been previously observed, Fleming's discovery of penicillin coupled with its success as an antimicrobial agent demonstrated the true potential of such compounds in treatment of infectious diseases[33,40,41]. In 1945, Giuseppe Brotzu isolated the second class of β-lactams after penicillin from the fungus *Cephalosporium acremonium* found in sewage water in Italy[34]. Brotzu observed that *Cephalosporium acremonium* exhibited growth inhibitory activity against various Gram-negative bacteria, including *Salmonella typhi, Vibrio cholerae* and *Staphylococcus aureus*[34,42]*.* Later, several species of soil bacteria were also identified to produce diverse cephalosporin substances[34]. Currently the β-lactam class of antibiotics consists of penicillins (penams), cephalosporins (cephams), monobactams and carbapenems[14,43]. Unfortunately, penicillins have lost their clinically efficacy as monotherapy due to widespread β-lactamase production in nosocomial pathogens[44,45]. Ampicillin and amoxicillin are two widely known penicillins that have maintained their effectiveness largely due to their co-formulations with clinically approved β-lactamase inhibitors[44]. Monobactams are unique β-lactams because they only contain the characteristic four-member β-lactam ring and are therefore monocyclic while penicillins, cephalosporins, and

carbapenems are bicyclic. Aztreonam is a commonly prescribed monobactam and it is the only monocyclic β-lactam approved for clinical use[44].

Thienamycin was the first carbapenem β-lactam discovered in 1970s but due to its instability it was never introduced into clinical practice[44,46]. However, imipenem was eventually derived from thienamycin by modifying its chemical structure with addition of *N*-formimidoyl group to produce a more stable compound[44]. Imipenem and meropenem are now two widely used carbapenems due to their broad-spectrum activity against Gram-negative and Gram-positive pathogens[47–49]. Meropenem exhibits more potent activity against Gram-negative bacteria and is a more stable compound than imipenem, making it valuable clinical therapeutic[50–52].

The trend of discovering new classes of antimicrobial agents continued throughout the mid-to-late 20th century. Since the end of the so-called golden age of antibiotics, when discovery of novel antibiotic classes was rampant, no major classes of antimicrobials have been developed. For more than 50 years now, the development of new drugs has relied on finding derivatives of existing antimicrobial agents. However, the rapid emergence of novel bacterial resistance mechanisms and the decline of our current antibiotic arsenal warrants discovery and development of innovative targets to combat the global antibiotic resistance crisis we face today.

Failure of antimicrobial therapeutics

The occurrence of clinical antibiotic treatment failure has exceeded the rate of new antibiotic development, which is causing a serious global public health crisis because we may not be able to treat infections that were once easily cleared[53]. Microbes quickly evolve to survive when faced with environmental threats or stressful conditions. Genomic

mutations conveying resistance or acquisition of resistance mechanisms through horizontal gene transfer enables survival[54]. Bacterial insensitivity to antimicrobial agents has been observed since development of the first antibiotics in the early 20th century. Resistance to β-lactam antibiotics was observed in 1940 with identification of β-lactamase enzymes, penicillinases, that inactivate penicillin before the drug was even commercially available for clinical use and reports of penicillin resistant isolates of *S. aureus* followed soon thereafter[54–57]. In order to overcome penicillinase-mediated inactivation of the drug, chemically modified penicillin derivatives were synthesized leading to the development of methicillin[54,55,58]. However, methicillin-resistant *S. aureus* strains (MRSA) emerged soon after methicillin was introduced as a clinical therapeutic[54,58]. In fact, Fleming, the discoverer of penicillin the drug that changed history, himself warned about the dangers of penicillin misuse giving rise to penicillin-resistant pathogens[59].

Antibiotic resistance

Bacterial resistance to antibiotics is a major factor contributing to the failure of antimicrobial therapy in the clinic. The loss of the current antibiotic repertoire is exacerbated by a complete void in new antibiotic development over the past thirty years[60–62]. Resistance is defined as the inherited ability of bacterial populations to grow in the presence of an antibiotic and is quantified by an increase in the minimum inhibitory concentration (MIC)[13,63–65]. There are several well-characterized resistance mechanisms, including reduced cell permeability, efflux, modification of the antibiotic target and production of antibiotic degrading enzymes (**Figure 1**). In Gram-negative bacteria, acquisition of resistance can occur through *de novo* mutations or through horizontal gene transfer to promote inactivation or degradation of the toxic compound[14]. While resistance

is a well-defined cause of antibiotic treatment failure, other less studied factors, such as tolerance, can also contribute to failure of clinical antimicrobial therapy and promote acquisition/evolution of canonical resistance.

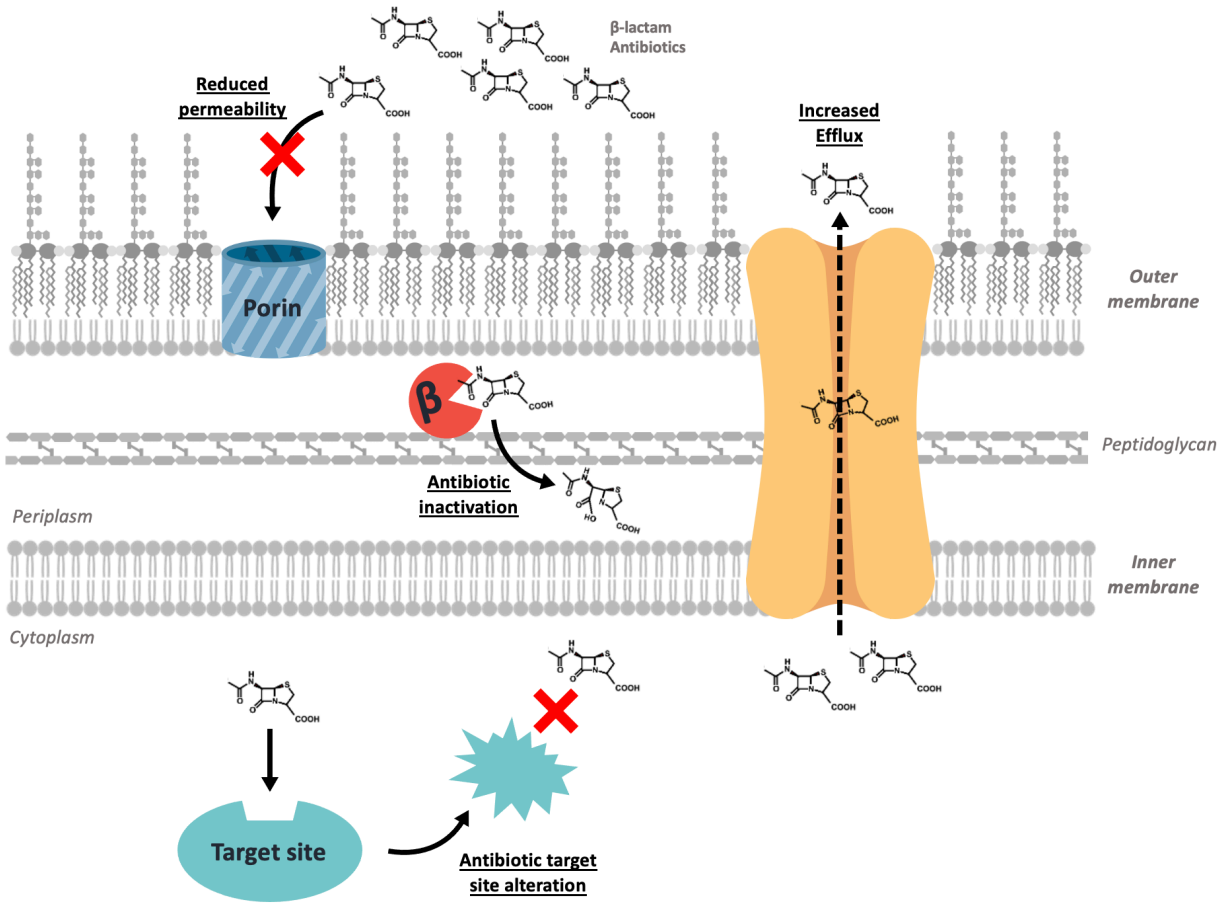

Figure 1: Mechanisms of antibiotic resistance in Gram-negative bacteria. Schematic showing various antibiotic resistance mechanisms encoded by Gram-negative bacteria. Gram-negative bacterial species can escape antimicrobial therapy by decreasing influx through reduced permeability, increasing efflux of toxic compound out of the cell, enzymatically inactivating the drug or altering the antibiotic target site.

Antibiotic tolerance

Like resistance, bacterial tolerance to antimicrobial agents was also identified during early decades of antibiotic discovery, not too long following the development of penicillin as a clinical therapeutic[12–14,66–68]. Tolerance is described as the ability of a susceptible bacterial population (no change in MIC) to temporarily survive exposure to

bactericidal antibiotics, such as carbapenem β-lactams, at otherwise lethal concentrations[12,14,15]. Antibiotic tolerance is usually observed with bactericidal agents during stationary phase of the bacterial life cycle when there are limited nutrients and reduced proliferation without significant alteration in MIC of the drug[69–71]. In 1980s, Alexander Tomasz and colleagues reported that many clinical isolates of *Streptococcus pneumoniae* did not lyse as excepted when exposed to high levels (20X MIC) of penicillin and that repeated exposure to higher than MIC penicillin levels gives rise to tolerant populations[72]. This was one of the early indications that tolerant populations likely promote acquisition of true resistance by increasing the probability for resistance mutations to occur[14,72]. Additionally, this was further supported by observations that vancomycin-tolerant *S. pneumoniae* exhibit increased capacity for acquisition of resistance genes relative to susceptible, non-tolerant isolates[73]. More recently studies have demonstrated that antibiotic tolerance is a prerequisite for the evolution of true resistance and that the development of antimicrobial resistance has a positive correlation with the level of tolerance exhibited by a bacterial population[74,75]. Based on growing evidence, antibiotic tolerance is now widely associated with the failure of antimicrobial therapy and regarded as a serious threat to the efficacy of clinically used antibiotics[12,13,16]. Despite also contributing to recurrent/relapse infections and posing a major risk to public health, little is known about mechanisms regulating antibiotic tolerance in Gram-negative bacteria[12,13,16,17].

ESKAPE pathogens

The dissemination of antimicrobial resistance has given rise to the ESKAPE pathogens. ESKAPE is an acronym defining a group of the six most clinically problematic Gram-positive and Gram-negative bacterial species, including ***E****nterococcus faecium*, ***S****taphylococcus aureus*, ***K****lebsiella pneumoniae,* ***A****cinetobacter baumannii,* ***P****seudomonas aeruginosa*, and members of the **E**nterobacteriaceae family[76,77]. ESKAPE pathogens are a serious threat to global public health because these bacterial species account for the majority of nosocomial bacterial infections worldwide, especially endangering our most vulnerable patient populations including children, neonatal patients, immunocompromised individuals, as well as critically ill elderly patients[76–79]. As suggested by their acronym, these bacterial species notoriously "escape" commonly used clinical antimicrobial therapeutics and are characterized by exhibiting multiple mechanisms of multidrug resistance[78,80]. Additionally, ESKAPE pathogens are reported to cause life-threatening hospital-acquired infections and are associated with high morbidity and mortality rates causing a substantial financial health care burden[78,79]. Of these carbapenem-resistant Enterobacteriaceae (CRE) and carbapenem-resistant *Acinetobacter baumannii* (CRAB) are ranked as the most dangerous public health threats by the CDC and the WHO[2,3].

Members of the Enterobacteriaceae family, including *E. cloacae* and *K. pneumoniae*, are commonly associated with serious nosocomial infections, including urinary tract infections, bloodstream infections, as well as various types of pneumonia infections[81]. The increasing prevalence of carbapenem-resistant Enterobacteriaceae has greatly limited treatment options available against infections caused by

Enterobacteriaceae species. The main mechanisms of carbapenem resistance in Enterobacteriaceae bacterial populations is the acquisition and production of carbapenem inactivating enzymes such as *K. pneumoniae* carbapenemase (KPC) and the NDM, VIM, IMP class B metallo-β-lactamases[81]. This has resulted in emergence of multidrug resistant, extensive drug resistant, and even pan drug resistant Enterobacteriaceae isolates[60,82].

Acinetobacter baumannii is an opportunistic, nosocomial, Gram-negative pathogen that has dramatically increased in clinical importance over the past few decades[24,25]. *A. baumannii* has emerged as the most important organism associated with hospital-acquired infections throughout the world due to its capacity for acquiring antimicrobial resistance and high risk of epidemic[26–29]. Infections caused by *A. baumannii* are commonly associated with intensive care units (ICUs) and can manifest as urinary tract infection, bloodstream infections , wound infections and pneumonia[27,83]. Fifty percent of the 1 million cases of *A. baumannii* infections reported worldwide each year exhibit resistance to different antibiotics, including last-resort carbapenem β-lactams[83,84]. *A. baumannii* can evade carbapenem treatment through multiple mechanisms including reduced cell permeability, increased efflux and expression of various β-lactamase enzymes and is prone to rapid development of multidrug resistance[60,83,85]. Similar to Enterobacteriaceae, extensive drug resistant, and pan drug resistant isolates of *Acinetobacter baumannii* are now commonly reported[83,85].

β-lactam antibiotics

β-lactams are the most commonly prescribed antibiotics in the world due to their broad-spectrum activity against many important Gram-positive and Gram-negative

bacterial species[7,9,31,37,86]. These clinically significant antibiotics exert antimicrobial activity through perturbing cell wall biosynthesis[5,6]. β-lactam antibiotics target and inhibit penicillin-binding proteins (PBPs), which are essential for synthesis of the peptidoglycan layer of the Gram-negative bacterial cell envelope, resulting in lysis and ultimately death of the bacterial cell[7,87]. PBPs encode an active site serine residue which catalyzes the transpeptidation reaction in a two-step process. First, the active site serine residue reacts with the D-Ala-D-Ala terminus of a pentapeptide attached to the *N*-acetylmuramic acid of the peptidoglycan polymer resulting in the formation of an acyl-enzyme intermediate[88]. Next, the carbonyl carbon of the acyl-enzyme intermediate is attacked by the *m*-diaminopimelic acid (*m*DAP) residue of another pentapeptide to create a covalent bond between the peptides which serves to crosslink the peptidoglycan[7]. Crosslinking between adjacent strands creates a cage-like layer that encloses the inner (cytoplasmic) membrane by forming the peptidoglycan lattice, a load-bearing structural support that protects the cell from the internal turgor.

The β-lactam class of antibiotics are defined by a four-membered amide-containing β-lactam ring, which resembles the D-Ala-D-Ala region of pentapeptides attached to *N*-acetylmuramic acid. This D-Ala-D-Ala region is essential for peptidoglycan biosynthesis and therefore, serves as a substrate for PBP transpeptidase domain. The amide β-lactam ring covalently binds the active site serine residue of PBPs to form an acyl-enzyme intermediate that is sterically blocked from attack by the *m*DAP residue of another pentapeptide, as required for normal peptidoglycan biosynthesis[7,89,90]. This blocks peptidoglycan crosslinking by inhibiting PBP transpeptidase activity resulting in cell death[7,89,90]. Based on structure, β-lactam antibiotics have been divided into four clinically

relevant groups which include penams, cephams, monobactams and carbapenems[43]. Carbapenem β-lactams show broad-spectrum activity in their class which makes them important clinical therapeutics, especially against difficult to treat multidrug-resistant (MDR) Gram-negative bacterial infections[31,91]. Structurally similar to penicillin, carbapenems are bicyclic, consisting of the characteristic four-member β-lactam ring fused to a five-membered pyrroline ring containing a carbon instead of the sulfur at the C1 position and a double bond between C2 and C3 positions[8,31,92]. Modification of the groups around the β-lactam ring allow carbapenems to possess potent broad-spectrum activity and effectively resist many common resistance mechanisms[8,31,93]. In fact imipenem and meropenem are two carbapenems prescribed as last-line antibiotics in hospitals to treat MDR Gram-negative pathogens[94–98]. While both carbapenems are active against a broad scope of Gram-positive and Gram-negative bacteria, meropenem is reported to be slightly more effective against Gram-negative organisms[93,99]. However, despite restricting carbapenem use to treat only multidrug resistant bacterial infections, resistance mechanisms have inevitably emerged.

Gram-negative bacterial resistance to β-lactam antibiotics (β-lactamases)

There are several mechanisms by which bacteria can acquire resistance to antibiotics, including production of β-lactamase enzymes, increased efflux pump activity, reduced permeability and alterations in expression and/or function of porins and PBP/transpeptidase proteins[7,8]. However, acquisition of β-lactamase-encoding genes and subsequent production of these enzymes is the most common mechanism of resistance in Gram-negative bacteria[7,100]. Located in the periplasm, β-lactamases irreversibly open the β-lactam ring by hydrolyzing the amide bond, thereby inactivating

the drug and preventing it from reaching the PBP/transpeptidase targets[7,8]. These clinically significant enzymes have been classified into four classes (A, B, C, D) based on structural and sequence similarities, which can be separated into two biochemically distinct groups based on hydrolytic activity[8,101–103]. Class A, C, and D enzymes require an active-site serine residue to catalyze β-lactam hydrolysis; accordingly; they are labeled serine-β-lactamases (SβLs)[8,101,104]. In contrast, class B β-lactamases rely on one or two active site Zn^{2+} ions to inactivate β-lactam antibiotics and are therefore referred to as the metallo-β-lactamases (MβLs)[101,105–107]. MβLs have recently emerged in numerous clinically significant Gram-negative pathogens, including members of the Enterobacteriaceae family and *Acinetobacter baumannii,* causing a serious threat to our antibiotic repertoire[100,108–113]. The class B MβLs are further divided into 3 subclasses (B1, B2, B3) based on primary sequence homology and distinctive structural characteristics within the active site of these enzymes[105,114,115]. Mainly, B1 and B3 subclasses require two zinc ions in the active site to catalyze hydrolysis, while the B2 subclass enzymes are active with just a single zinc ion[7,8]. B1 subclass contains the largest number of known and clinically important MβLs including the imipenemase (IMP), verona integron-encoded metallo-β-lactamase (VIM)-type enzymes, and the New Delhi metallo-β-lactamase (NDM-1)[7,8,116].

New Delhi metallo-β-lactamase (NDM-1)

NDM-1 was first reported in 2008 in a *Klebsiella pneumoniae* isolate in a urine culture from a patient who had been hospitalized in India[110]. NDM-1 is unusually problematic in hospitals and healthcare settings due to its uncharacteristically broad substrate specificity which allows inactivation of all bicyclic β-lactam antibiotics, including

last-line carbapenem β-lactams. Moreover, organisms that produce NDM-1 are often reported to be resistant to other antimicrobial agents, which further limits therapeutic options[101]. The gene encoding NDM-1, *bla*$_{NDM-1}$, has been found on multiple plasmids and is efficiently transferred horizontally among Gram-negative bacterial populations along with other resistant genes the donor organism might be carrying[7,117]. Specifically, the rapid distribution and expansion of NDM-1 within clinically important Gram-negative pathogens is attributed to conserved association with the promiscuous class 1 integron ISCR1, which encodes additional MDR mechanisms[118,119]. Gram-negative pathogens carrying MβLs NDM, IMP, VIM are now considered to be among the most urgent antibiotic resistance problems worldwide[120,121].

β-lactamase inhibitors

β-lactam antibiotics susceptible to hydrolysis by serine-dependent β-lactamases are often co-administered with a β-lactamase inhibitor. For example, augmentin is a formulation of amoxicillin and clavulanic acid, which prevents β-lactam hydrolysis in the host[122,123]. These inhibitors tightly bind the serine-dependent β-lactamases active site to covalently modify the resistance enzyme with a stable intermediate. By deactivating hydrolysis, clavulanic acid essentially protects the β-lactam antibiotic, enabling it to exert its antimicrobial mechanism of action. While such inhibitors potentiate β-lactam treatments against some clinically relevant bacteria, the effective scope of these β-lactamase inhibitors is quite limited because inhibition is dependent on a catalytic serine[105,124]. Despite the prevalence and the clinical impact of these enzymes on the β-lactam repertoire, there are no MβL inhibitors approved for clinical use. However, some candidate MβL inhibitors are currently in development with several containing similar

structural motifs including zinc-binding sulfur atoms, zinc-binding dicarboxylates and other zinc binding moieties[125]. While competitive inhibitors are being characterized, the current MβL inhibitor repertoire represents a limited region of chemical space[125–127]. Additionally, recent high-throughput screening of small molecule libraries revealed some MβL inhibitory chemistries but these screens are often limited in size and performed with purified β-lactamases *in vitro*, implying that inhibition may be ineffective in cell-based systems, particularly against Gram-negative bacterial species[113,128,129]. While MβL inhibitor chemistries have proven difficult to target with small molecules, largely due to the shallow and featureless Zn-dependent active site and lack of a defining scaffold, peptide chemistries have shown promise[130].

Over the past few decades, there has been increased interest in developing antimicrobial peptides to supplement our antibiotic arsenal either for administration as monotherapy or combined with other currently available drugs[131–133]. The broad-spectrum activity of antimicrobial peptides, together with the potential to enhance the effect of other antimicrobial (mainly antibiotics) makes peptides an attractive therapeutic alternative to combat multidrug resistant bacterial infections[132]. Furthermore, acquisition of resistance to antimicrobial peptides is rare, largely due to the high metabolic cost to the bacterial cell[134].

Techniques such as phage display[135,136], ribosome display[137,138], and mRNA display[139,140] have been used to selectively screen for peptides that bind a target molecule or inhibit an enzyme within a cell[141]. For example, Sanschagrin *et al*. used a phage display screen to find peptides that bind the L1 MβL and identified a nine amino acid long peptide (Cys-Val-His-Ser-Pro-Asn-Arg-Glu-Cys) as a promising inhibitor of the L1 enzyme

showing mixed inhibition[130]. Another group described several cysteinyl peptides as competitive inhibitors of *Bacillus cereus* zinc β-lactamase and identified *N*-carbobenzoxy-D-cysteinyl-D-phenylalanine as the most potent reversible competitive inhibitor against this enzyme[142]. Yet another study identified a peptide inhibitor of class A β-lactamase TEM-1 that also inhibits the class A1 Bla1 β-lactamase and the class Cp99 β-lactamase[143]. While these techniques promote screening for peptides with desired properties, they also highlight several drawbacks. First, these techniques fail to provide a means to directly assess the functionality and relevance of the peptides and their interactions[141]. Furthermore, MβL inhibitory peptides discovered through these approaches often fail to show activity in synthetic form because they cannot pass through the cell membrane to reach their target[141]. Therefore, innovative techniques are required to explore increased chemical spaces for discovery of effective MβL inhibitors.

Peptide surface display system

A recent report outlined the potential of an antimicrobial discovery platform using high-throughput sequencing to identify new lead antimicrobial peptides with activity against Gram-negative bacteria[141]. This platform, labeled ***S***urface ***L***ocalized ***A***ntimicrobial Displa***Y*** (SLAY), exploits the massive depth of information gathered from high-throughput sequencing and was originally intended to advance discovery of antimicrobial peptides. To engineer this system, a randomly generated peptide was anchored to an outer membrane complex within a single Gram-negative cell to create a microenvironment around the bacterial cell and within the cell envelope. SLAY consists of an Lpp signal sequence that localizes the construct to the outer membrane, an OmpA transmembrane domain that anchors the surface display system to the outer membrane of the Gram-

negative bacterial cell envelope and an unstructured, low sequence complexity protein that acts as a flexible tether connecting the membrane-anchoring complex to a randomly generated peptide. The protein tether extends up to 20nm, allowing the attached peptide to interact with bacterial cell surface structures, periplasmic components, including the peptidoglycan cell wall, and even the cytoplasmic membrane. This innovative surface display of peptides allows millions of randomly generated peptide sequences to be sampled within a single tube through interaction and disruption of essential cell structures to restrict growth and/or lyse the cell, eliminating the target peptide sequences from the population[141]. As previously shown, transport of the machinery utilized by this system ensures that the peptide construct does not interact with cellular components until it is surface localized, alleviating the burden of intracellular activity[144]. Furthermore, this approach is significant not only because it enables us to explore a diverse chemical space in a cell-based system, which is a bottleneck to discover therapeutics effective against Gram-negative bacteria with translational potential, but also because peptide synthesis with the bacterial cell eliminates the costly need for chemical synthesis while increasing the potential composition and complexity of peptides that can be screened.

Transposon insertion sequencing (Tn-seq)

Another high-throughput sequencing technique that we leveraged in studying mechanisms of antibiotic treatment failure in bacteria is transposon insertion sequencing (Tn-seq). Transposon sequencing has enabled us to study links between bacterial genetic factors and observed phenotypes to gain meaningful insights into bacterial fitness during stress, like antibiotic treatment. Tn-seq is a broadly applicable technique that combines traditional transposon mutagenesis with massive parallel sequencing to enable rapid

examination of genotype-phenotype relationships on a genome-wide scale[145–147]. The basic steps of a Tn-seq protocol include generation of a saturating gene disruption library through transposon mutagenesis, pooling of the individual insertion mutants, extraction of genomic DNA (gDNA) from the pooled mutants followed by amplification and high-throughput sequencing of the transposon insertion junctions[145–148]. The *mariner*-family transposons have been particularly useful for generating saturating mutant libraries in diverse bacterial backgrounds[149–152]. *Mariner*-based transposons are characterized by their preferential insertion into thymine-adenine ("TA") motifs which results in reduced insertional bias and more robust downstream statistical analysis[148,149,153,154]. *Mariner* transposons are also host-independent which allows for stable random insertions without the need for host specific factors[155,156]. The plasmid-encoded *Himar1 mariner* transposon system, designed specifically for efficient transposon mutagenesis, carries kanamycin resistance cassette, used for mutant selection in *Acinetobacter baumannii,* flanked by the mariner transposon and a transposase encoding gene that is controlled by an *A. baumannii* specific promoter[157]. Since the transposition machinery is generally plasmid encoded, it can be easily modified by replacing the transposase promoter and the antibiotic selection marker to be applicable in diverse bacterial backgrounds. Overall, Tn-seq simplifies studying essential genes and pathways contributing to bacterial fitness in a variety of environmental conditions and stresses, such as antibiotic treatment. In the present work, we optimized and leveraged Tn-seq for use in *A. baumannii* to identify genetic factors required for carbapenem tolerance.

Bacterial tolerance to β-lactam antibiotics

The canonical response of susceptible *E. coli* isolates to β-lactam antibiotics is defined by digestion of the peptidoglycan cell wall resulting in cell morphological changes that ultimately lead to bacterial cell lysis and death[19,158–161]. Interestingly, several clinically significant Gram-negative bacterial species, such as *Enterobacter cloacae, P. aeruginosa, V. cholerae*, and *Burkholderia pseudomallei,* have been reported to exhibit high levels of tolerance to call wall acting β-lactam antibiotics, including last-resort carbapenem β-lactams[15,19,20,69]. *B. pseudomallei* is Gram-negative aerobic pathogen that causes the tropical disease melioidosis in both humans and animals[69,162]. There is a high number of relapse infections associated with melioidosis and many *Burkholderia* isolates exhibit high levels of tolerance to carbapenem β-lactams, indicating that carbapenem tolerance may play a role in occurrence of relapse infections[69,163–165].

In susceptible *E. cloacae, P. aeruginosa,* and *V. cholerae* isolates tolerance to β-lactam antibiotics is mediated by the formation of non-dividing, viable, cell wall defective spheroplasts that are like L-form bacteria[21,166,167]. However, there is one significant difference between spheroplasts and L-form bacteria which is that unlike L-forms, carbapenem-induced spheroplasts do not undergo division when the drug is present[19–21,166,167]. Importantly, when the antibiotic is removed, spheroplasts reportedly resume characteristic cell morphology and growth, providing further evidence that tolerance may potentially contribute to relapse/recurrent infections[21]. Previous studies have implicated components involved in peptidoglycan biosynthesis and outer membrane stability/integrity to be important for β-lactam tolerance in *V. cholerae*, which overlap with factors contributing to meropenem tolerance in *B. pseudomallei* to some degree[15,69].

Additionally, several cell envelope stress sensing components, including the alternative sigma factor RpoE and the VxrAB (or WigKR) two-component system (TCS), along with lipopolysaccharide (LPS) and peptidoglycan metabolic factors were identified to be important for recovery of β-lactam-induced spheroplast in *V. cholerae*[15,21,168]. However, little is known regarding incidence and mechanisms of carbapenem tolerance in many clinically relevant Gram-negative pathogens, including *E. cloacae, K. pneumoniae* and *A. baumannii*, which cause some of the most problematic nosocomial infections.

The Gram-negative bacterial cell envelope

The Gram-negative bacterial cell envelope is an important tripartite structure consisting of an outer membrane and an inner membrane separated by aqueous periplasmic space[22,23]. The inner membrane of Gram-negative bacteria is a symmetric bilayer composed of glycerol-based phospholipids that participates in nutrient transport, lipid biosynthesis and protein translocation[22,23]. The periplasmic space houses the essential peptidoglycan cell wall, which is a rigid, mesh-like polymer that maintains cell shape and bears the stress of cytoplasmic turgor pressure[22,23,169,170]. The outer membrane of Gram-negative bacteria is asymmetric, with an inner leaflet of glycerophospholipids and lipopolysaccharide (LPS) or lipooligosaccharide (LOS) (**Figure 2**) in the outer leaflet[22,23,171]. The LPS/LOS molecules in the outer leaflet of the OM function as a selective permeability barrier that protects the cell from environmental toxins and antibiotics[22,23,171].

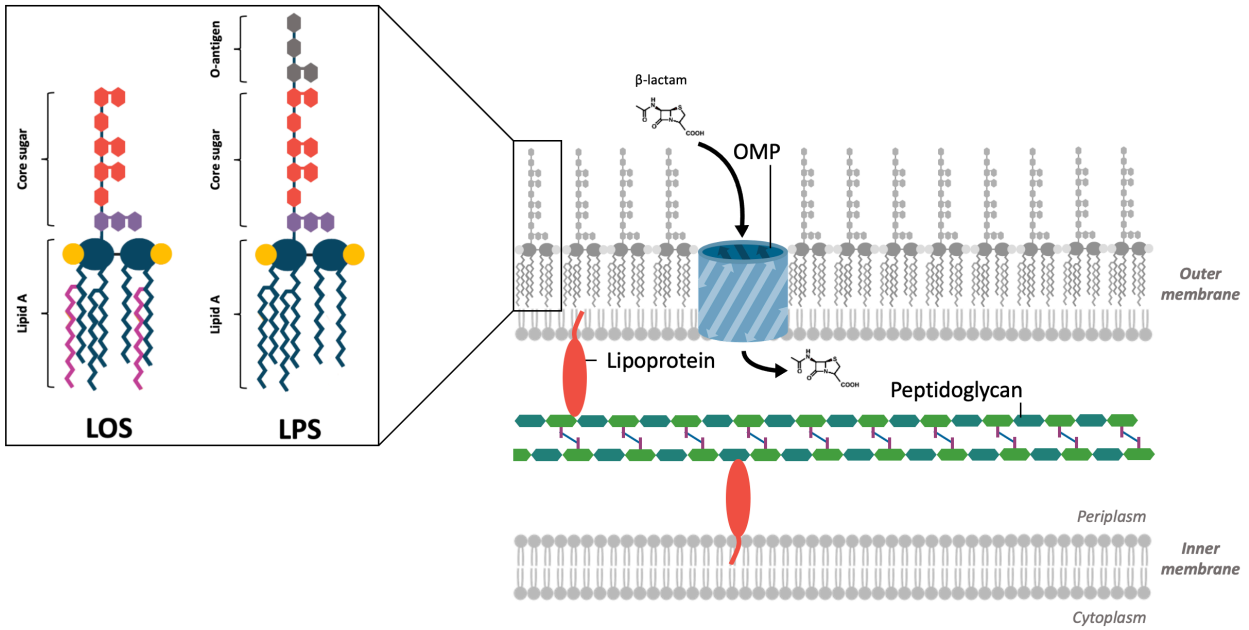

Figure 2: The Gram-negative bacterial cell envelope. Gram-negative bacteria are enclosed by a tripartite outer barrier consisting of an outer membrane, a periplasmic space containing peptidoglycan and an inner membrane.

Cell surface modifications

Several Gram-negative bacterial species have previously been shown to modify cell surface structures as a mechanism to evade antimicrobial threats[172]. For example, *E. cloacae* was found to increase the net negative charge of the outer membrane through PhoPQ-mediated incorporation of additional moieties to the lipid A molecule in order to prevent colistin binding and thereby escaping killing by colistin[172]. The PhoPQ two-component system (TCS) is a highly conserved cell envelope stress signaling system that regulates various lipid A modification enzymes in pathogenic Enterobacteriaceae[172–174]. The PhoPQ TCS is activated in conditions where divalent cations (Mg^{2+} and Ca^{2+}) are limited or cationic antimicrobial peptides are present[172,175] and directly regulates expression of an outer membrane acyltransferase, PagP, that adds acyl chains to the

lipid A moiety[176] and the *arn* operon which is involved in the synthesis and addition of the positively charged 4-amino-4-deoxy-L-arabinose (L-Ara4N) modification[172]. Addition of the L-Ara4N modification to lipid A increases the net negative charge on the surface of the cell preventing colistin from exerting its antimicrobial activity through displacement of divalent cations that form electrostatic interactions between adjacent LPS molecule. Most Gram-negative bacterial species canonically produce a hexa-acylated lipid A molecule and incorporate additional acyl chains through outer membrane PagP activity to form hepta-acylated lipid A molecules under certain stress conditions, like in the presence of antimicrobial peptides[23,177]. PagP-mediated hepta-acylation of lipid A in turn fortifies the outer membrane by reducing outer membrane fluidity through tighter packing of surface exposed LPS molecules[23].

Interestingly, unlike Enterobacteriaceae, *A. baumannii* does not encode many of the canonical cell envelope homeostasis components like PhoPQ and PagP. Instead, *A. baumannii* encodes an unique LpxM enzyme that acts as a dual-acyltransferase[177]. In Gram-negative bacteria, LpxM usually encodes the acyltransferase involved in attachment of the 6th acyl chain during the final step in lipid A biosynthesis[177]. However, due to the dual-acyltransferase function of LpxM, *A. baumannii* constitutively produces a hepta-acylated lipid A molecule and thereby a more rigid outer membrane barrier[23,177].

Outer membrane porins (OMPs)

In Gram-negative bacteria, the outer membrane is first line of defense against extracellular environments. For a long time, the outer membrane was only thought to be a protective barrier against harsh environments and toxic substances[23]. However, recently it was shown that the outer membrane also contributes to the mechanical

strength and stiffness of the Gram-negative bacterial cell envelope[178]. The outer membrane also provides Gram-negative bacteria intrinsic resistance to certain antimicrobial agents like daptomycin and vancomycin, which are unable to cross the outer membrane permeability barrier to reach their intracellular targets[179]. Along with LPS/LOS and phospholipids, the outer membrane also consists of lipoproteins that are embedded in the inner leaflet of the outer membrane and form covalent attachments with the periplasmic peptidoglycan layer[180]. In *E. coli* the most abundant lipoprotein is the Braun's lipoprotein, Lpp and it is thought to contribute to integrity and stability of the outer membrane by covalently linking it to the peptidoglycan cell wall (**Figure 2**)[23,180]. Outer membrane porins (OMPs) are another major group of outer membrane-associated proteins[23,181]. OMPs are generally transmembrane β-barrel proteins that form aqueous channels allowing the passage of small hydrophilic molecules across the outer membrane[23,182]. OMPs can be monomeric or trimeric and can allow non-specific or specific diffusion of small compounds into the periplasm[23,181,182]. β-lactam antibiotics, including carbapenems, have previously been reported to enter the periplasm through non-specific OMPs (**Figure 2**), which likely represent a major entryway for carbapenems to get into the cell to reach their PBP targets[180,182]. Outer membrane protein A (OmpA) is the most abundant non-specific OMP that is conserved across diverse Gram-negative bacterial species[23,182]. While localized in the outer membrane, OmpA is also known to non-covalently interact with the peptidoglycan cell wall via its periplasmic domain, thereby linking the outer membrane to the peptidoglycan and directly contributing to outer membrane stability[182,183]. Furthermore, OmpA was found to contribute to β-lactam resistance in *A. baumannii*, as deleting *ompA* resulted in increased susceptibility to these

antibiotics. This suggests that OmpA also contributes to outer membrane stability in the nosocomial pathogen *A. baumannii*.

Peptidoglycan maintenance and recycling

The peptidoglycan cell wall is an essential mesh-like structure that provides the cell shape and protects the bacteria from lysis due to internal turgor pressure[23,169,184]. Peptidoglycan synthesis begins in the cytoplasm with synthesis of the lipid II precursor which is flipped by MurJ across the inner (cytoplasmic) membrane into the periplasm, where it assembled into a continuous peptidoglycan sacculus by class A penicillin-binding proteins (aPBPs)[185–189]. More specifically, the aPBPs glycosyltransferase domain along with the Shape, Elongation, Division, and Sporulation (SEDS) proteins polymerize the *N*-acetylglucosamine (Glc*N*Ac)-*N*-acetylmuramic acid (Mur*N*Ac) backbone of the peptidoglycan polymer while aPBP/bPBP transpeptidase domains and, to a lesser extent, LD-transpeptidases (LDTs) form crosslinks between adjacent peptide stems to form the complete peptidoglycan mesh sacculus[185].

Expansion of the cell wall layer is an integral part of the bacterial growth cycle. During cellular growth, division and separation, the peptidoglycan sacculus is cleaved and remodeled to accommodate incorporation of newly synthesized peptidoglycan material[185,188]. In Gram-negative bacteria, many of the peptidoglycan fragments released from cell wall degradation during periplasmic remodeling are transported into the cytoplasm to be recycled into the *de novo* peptidoglycan synthesis pathway[190–193]. Therefore, the peptidoglycan synthesis, remodeling, and recycling machineries must be highly coordinated within the bacterial cell to maintain shape and integrity of the cell envelope and prevent lysis due to internal turgor pressure[193,194]. Periplasmic

peptidoglycan hydrolases, also called autolysins since unchecked activity of these enzymes often results in autolysis, play a critical role in peptidoglycan remodeling and recycling[185,188,195,196]. Autolysins include lytic transglycosylases and low molecular weight penicillin binding proteins (LMW-PBPs) that are specialized for cleaving specific bonds within the peptidoglycan sacculus[185,188,197].

Lytic transglucosylases facilitate peptidoglycan remodeling by cleaving glycosidic linkages between GlcNAc and MurNAc in the peptidoglycan backbone (**Figure 3**)[194,198]. LMW-PBPs are generally characterized to have either endopeptidase activity hydrolyzing the crosslink between *m*DAP of one peptide stem and D-Ala residue of another stem or DD-carboxypeptidase activity which leads to cleavage of the terminal D-Ala residue from penta-muropeptides[87,194,197,199,200]. PBP7, encoded by *pbpG,* has previously been identified as a LMW-PBP with endopeptidase activity in *E. coli* and *P. aeruginosa* [194,201,202]. Additionally, PBP7 has

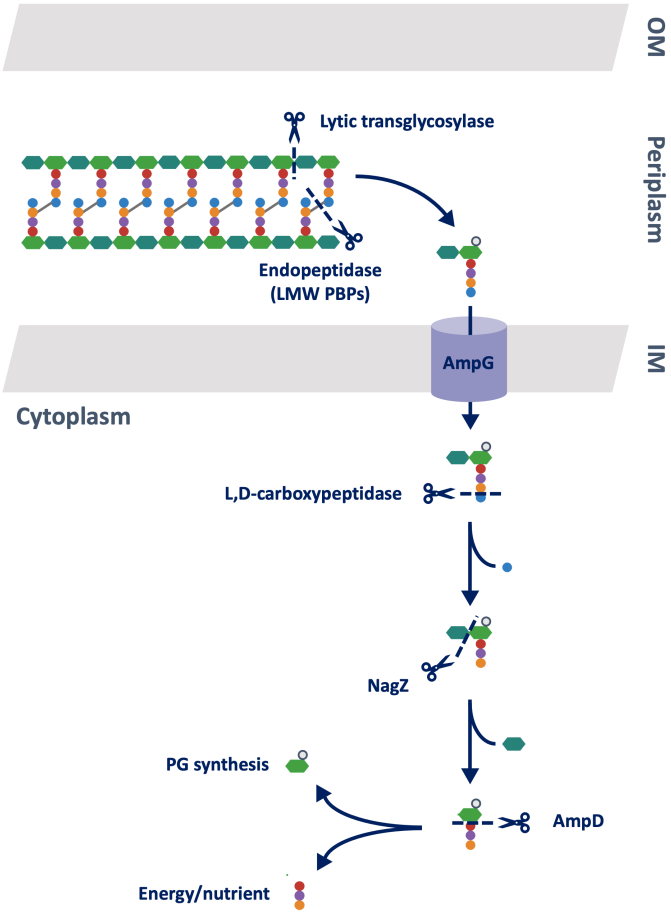

Figure 3: Peptidoglycan metabolism and recycling in Gram-negative bacteria. Schematic showing the cell wall remodeling and recycling pathway. Peptidoglycan turnover begins in the periplasm with lytic transglycosylases and endopeptidases releasing Glc*N*Ac 1,6-anhdro-Mur*N*Ac-peptides which are transported into the cytoplasm by the AmpG permease and further processed by LD-carboxypeptidases, NagZ and AmpD in the peptidoglycan recycling pathway.

been implicated *in vivo* survival of *A. baumannii* in ascites[203]. The endopeptidase activity of LMW-PBPs, like PBP7, cleaving crosslinks between adjacent peptidoglycan stem peptides aids in releasing the Glc*N*Ac 1,6-anhdro-Mur*N*Ac-tetrapeptide intermediates (**Figure 3**)[194,198].

These muropeptide intermediates generated by autolysins are next transported into the cytoplasm via the AmpG permease for further recycling (**Figure 3**)[194,204,205]. LD-carboxypeptidases play an important role in cytoplasmic peptidoglycan processing. After the Glc*N*Ac 1,6-anhdro-Mur*N*Ac-tetrapeptide intermediate is transported into the cytoplasm LD-carboxypeptidases are involved in cleaving the D-Ala residue in the fourth position of tetra-muropeptide stems to produce Glc*N*Ac 1,6-anhdro-Mur*N*Ac-tripeptides which are then be cleaved by the cytoplasmic β-*N*-acetylglucosaminidase NagZ which separates Glc*N*Ac from the 1,6-anhdro-MurNAc-tripeptide[194,206–208]. Following NagZ-mediated generation of 1,6-anhdro-Mur*N*Ac-tripeptides, the cytoplasmic amidase AmpD separates 1,6-anhdro-Mur*N*Ac from the tripeptide stem which can serve as a source of nutrients or energy and releases 1,6-anhdro-Mur*N*Ac to be further processed by the peptidoglycan recycling pathway (**Figure 3**)[194,206,208–212].

Additionally, Gram-negative bacteria detect disruptions in peptidoglycan biosynthesis, like those resulting from inhibition of PBP transpeptidase activity by β-lactam antibiotics and respond by activating various defense mechanism. Previous studies have reported that several Gram-negative pathogens induce expression of chromosomally encoded cryptic β-lactamases like AmpC in response to β-lactam antibiotics[209,213]. Inhibition of PBP transpeptidase activity by β-lactam antibiotics disrupts normal peptidoglycan biosynthesis causing increased peptidoglycan turnover by lytic

transglycosylases in the periplasm which results in increased levels of anhydromuropeptides being transported into the periplasm where they act as signal for AmpC β-lactamase induction[190,193,213].

The studies presented here investigate the importance of components associated with different subcellular compartments of the Gram-negative bacteria cell envelope in failure of antimicrobial therapy, starting with the contribution of periplasmic localized metallo-β-lactamases to carbapenem resistance in clinically significant Gram-negative bacterial species.

CHAPTER 3

DISCOVERY AND CHARACTERIZATION OF NEW DELHI METALLO-β-LACTAMASE-1 INHIBITOR PEPTIDES THAT POTENTIATE MEROPENEM-DEPENDENT KILLING OF CARBAPENEMASE-PRODUCING ENTEROBACTERIACEAE**

Misha I. Kazi[1], Blair W. Perry[1], Daren C. Card[1,2], Richard D. Schargel[1], Hana B. Ali[1], Victor C. Obuekwe[1,3], Madhab Sapkota[1], Katie N. Kang[1], Mark W. Pellegrino[1], David E. Greenberg[3,4], Todd A. Casatoe[1], Joseph M. Boll[#1]

[1]Department of Biology, University of Texas Arlington, Arlington, TX, USA; [2]Current Address: Department of Organismic & Evolutionary Biology and Museum of Comparative Zoology, Harvard University, Cambridge, Massachusetts, USA; [3]Department of Internal Medicine, University of Texas Southwestern Medical Center, Dallas, TX, USA; [4]Department of Microbiology, University of Texas Southwestern Medical Center, Dallas, TX, USA

[#]Correspondence: joseph.boll@uta.edu

** Published as: Kazi MI, Perry BW, Card DC, et al. Discovery and characterization of New Delhi metallo-β-lactamase-1 inhibitor peptides that potentiate meropenem-dependent killing of carbapenemase-producing Enterobacteriaceae. *J Antimicrob Chemother*. 2020;75(10):2843-2851. doi:10.1093/jac/dkaa242

Abstract

Metallo-β-lactamases (MBLs) are an emerging class of antimicrobial resistance enzymes that degrade β-lactam antibiotics, including last-resort carbapenems. Infections caused by carbapenemase-producing Enterobacteriaceae (CPE) are increasingly prevalent, but treatment options are limited. While several serine-dependent β-lactamase inhibitors are formulated with commonly prescribed β-lactams, no MBL inhibitors are currently approved for combinatorial therapies. New compounds that target MBLs to restore carbapenem activity against CPE are therefore urgently needed. Herein we identified and characterized novel synthetic peptide inhibitors that bound to and inhibited New Delhi MBL-1 (NDM-1), which is an emerging β-lactam resistance mechanism in CPE. We leveraged ***S***urface ***L***ocalized ***A***ntimicrobial displa***Y*** (SLAY) to identify and characterize peptides that inhibit NDM-1, which is a primary carbapenem resistance mechanism in CPE. Lead inhibitor sequences were chemically synthesized, and MBCs and MICs were calculated in the presence/absence of carbapenems. Kinetic analysis on recombinant NDM-1 and select peptides tested direct binding and supported NDM-1 inhibitor mechanisms of action. Inhibitors were also tested for cytotoxicity activity. We identified approximately 1700 sequences that potentiate carbapenem-dependent killing against NDM-1 *Escherichia coli*. Several also enhanced meropenem-dependent killing of other CPE. Biochemical characterization of a subset indicated the peptides penetrated the bacterial periplasm and directly bound NDM-1 to inhibit enzymatic activity. Additionally, each demonstrated minimal hemolysis and cytotoxicity against mammalian cell lines. Our approach advances a molecular platform for antimicrobial discovery, which complements the growing need for alternative antimicrobials. We also

discovered lead NDM-1 inhibitors, which serve as a starting point for further chemical optimization.

Introduction

β-lactams are an important class of antibiotics that not only possess activity toward Gram-positive bacteria, but also Gram-negatives, which include some of the most difficult-to-treat pathogens[9,86]. The defining β-lactam ring inhibits the transpeptidase activity of PBPs, which are essential bacterial enzymes that polymerize the peptidoglycan cell wall[7,87]. Disruption of peptidoglycan assembly leads to rapid cell lysis.

Carbapenems are important β-lactam therapeutics because they possess potent broad-spectrum activity and are not susceptible to common resistance mechanisms[8,93]. In fact, imipenem and meropenem are last-line carbapenem antibiotics used to treat multidrug resistant Gram-negative infections[94–98]. Despite restricting the use of carbapenems, resistance mechanisms have inevitably emerged.

The most common β-lactam resistance mechanism in Gram-negative organisms is production of β-lactamase enzymes[7,100]. β-lactamases hydrolyze the β-lactam ring, which prevents the antibiotic from binding its target PBP[7,8]. β-lactamases are divided into four classes (A, B, C, D) based on structural and sequence similarities, but comprise two distinct groups based on hydrolytic activity[8,101–103]. Serine-dependent β-lactamases (SBLs), including class A, C, and D, rely on an active-site serine for β-lactam degradation[8,101–104]. Class B β-lactamases rely on active-site Zn^{2+} ions to coordinate hydrolysis; hence, they are designated metallo-β-lactamases (MBLs)[101,105–107]. MBLs

recently emerged, but have rapidly spread among Gram-negative pathogens, which threatens our current antimicrobial treatment options[100,108–113].

New Delhi metallo-β-lactamase (NDM-1) was first reported in 2009 when *bla*$_{NDM-1}$ was found in a *Klebsiella pneumoniae* isolate from a patient in Sweden who had been hospitalized in India[110]. NDM-1 is particularly concerning because it quickly spread to all continents, is highly associated with other antibiotic resistance mechanisms, inactivates all bicyclic β-lactam antibiotics, including carbapenems, and is a primary resistance mechanism in many 'superbugs'[7,8,116,214]. Gram-negative pathogens carrying NDM and other MBL subclasses (i.e. IMP, VIM) are considered to be among the most urgent antibiotic resistance problems worldwide[120,121].

Class A, C, and D β-lactamase inhibitors were developed and include molecules that covalently modified the conserved serine residue (i.e. avibactam, tazobactam, sulbactam etc.) required for catalytic activity[215–218]. Administered in combination with prescription β-lactam antibiotics, inhibitors inactivate serine-dependent β-lactamases to restore antimicrobial activity. In contrast, we currently lack effective MBL inhibitors, including those that target the NDM subclass. ANT431 is a NDM-1 inhibitor in preclinical development, but does not possess broad-spectrum activity against MBLs and is not a candidate for further development[214,219]. Development of small molecule inhibitors has been challenging due to the flexibility of the MBL active site and challenges associated with metallo-enzymes. Alternatively, peptides with activity against MBLs have been reported[220–224].

Here, we used a cell-based high-throughput antimicrobial discovery system, termed ***S***urface ***L***ocalized ***A***ntimicrobial displa***Y*** (SLAY), to screen for synthetic

randomized peptides that potentiate carbapenem-dependent killing of NDM-1 *E. coli*.[225] We discovered thousands of peptides that restored NDM-1 *E. coli* susceptibility to carbapenems. A subset of leads were genetically validated and four were biochemically tested against recombinant NDM-1 for inhibitory activity. Kinetic analysis was performed to determine the inhibitory mechanism of each lead and cytotoxicity and hemolytic activity were assayed. Our results advanced our basic understanding of the chemical diversity of NDM-1 inhibition and further developed an innovative molecular platform for antimicrobial discovery.

Materials and Methods

Bacterial strains and antibiotics

Strains and plasmids used in this study are listed in Table S1. Primers are listed in Table S2. All strains were grown aerobically from freezer stocks on LB agar at 37°C. Antibiotics were used at the following concentrations: 75 mg/L carbenicillin (Fisher Scientific), 10 mg/L tetracycline (Sigma-Aldrich), 4 or 8 mg/L meropenem (TCI America), and 8 mg/L imipenem (Alfa Aesar).

Peptide library construction

SLAY for the NDM-1 screen was constructed on the broad host plasmid pMMB67EHTet, which was derived from pMMB67EH, where the *bla* gene was exchanged with a tetracycline resistance gene[225]. Peptide sequences were randomly generated using 30bp NNB codons to produce ten amino acid peptides. The sequences were cloned into the KpnI and SalI sites of pMMB67EHTet using primers homologous to the tether sequence on the reverse primer. Plasmid libraries were transformed into C2987

competent cells (NEB). Approximately 1.20 x 10^6 colonies were pooled. Plasmid DNA was isolated from the C2987 library and re-transformed into *E. coli* W3110/pNDM-1 to 3 times coverage.

Screening and sequencing the random peptide library

An aliquot of the frozen *E. coli* W3110/pNDM-1 peptide library was added to 5mL of LB supplemented with carbenicillin and tetracycline for growth, shaking at 37°C for 1 hour. Duplicate cultures were backdiluted into 5mL LB with carbenicillin and tetracycline to OD_{600} 0.01 supplemented with IPTG (MP Biomedicals). The remaining culture was used as the ‘‘input’’ sample for the peptide screen. Induced cultures were grown with shaking at 37°C. Cells were harvested at 4 hours, which was considered the “output” sample. Plasmids were isolated from “input” and “output” groups using the QIAprep Spin Miniprep kit. Primers with homologous regions to the plasmid were used to simultaneously amplify the peptide-encoding region of the plasmid and add sequencing adapters. Four reactions per sample were amplified for a total of 12 cycles. The reactions were pooled and cleaned using QIAquick PCR Purification kit. Libraries were gel purified using the QIAquick Gel Extraction kit. Amplicons were sequenced using 50bp single end reads on an Illumina HiSeq supplemented with Phi-X. DNA was sequenced at The University of Texas Genomic Sequencing and Analysis Facility.

Raw read processing

Raw Illumina reads each contained a 30bp sequence of interest (SOI) coding for the ten amino acid peptides, flanked on both sides by a library-specific amplicon pattern. For each library, we used custom scripts to identify the conserved flanking amplicon region sequences and raw reads without an exact match to expected flanking sequences

were excluded from subsequent analyses. Reads were also excluded if one or more nucleotides within the SOI had a Phred quality score less than 20 (i.e., 1% error rate) or if less than 90% of nucleotides within the SOI had a Phred score less than 30 (i.e., 0.1% error rate). The SOI for reads passing these filtering steps were translated into ten amino acid peptides.

Differential abundance analysis

Within each library, the number of sequences containing each unique peptide was tallied, and counts were normalized using trimmed mean of M-values normalization in edgeR to control for differences in sequencing depth between experiments[226]. Fisher's Exact Tests were performed in edgeR to identify significantly differentially abundant peptides between each "input" and "output" peptide population and the corresponding no-carbapenem control[226]. To control for type I errors resulting from thousands of statistical tests, we corrected p-values for each pairwise comparison using the independent hypothesis weighting (IHW) correction procedure with average normalized count per peptide as the covariate[227]. Peptides were considered NDM-1 inhibitors when the IHW p-value between comparisons was <0.05 and when there was a log2-fold average count depletion in the treatment group relative to the control. Because we were interested in peptides that potentiate carbapenem-dependent killing, peptides depleted only when carbapenems were added to the growth medium were reported. Physiochemical properties of NDM-1 inhibiting peptides were inferred using the Peptides package in R[228,229]. Peptide sequence logos and characterization of the physiochemical properties of NDM-1 inhibiting peptides were visualized using pheatmap (https://github.com/raivokolde/pheatmap) and ggseqlogo in R[230].

Bacterial growth curves using SLAY

Growth curves were performed as previously described with slight modifications[225]. Briefly, strains were grown on LB agar containing carbenicillin, tetracycline and 0.2% glucose overnight at 37°C. The next day, cultures were grown to mid-logarithmic phase (OD_{600} 0.4 – 0.6). Cultures were back diluted to OD_{600} 0.01 in 5 mL LB under three different conditions: (-) meropenem/ (-) IPTG, (+) meropenem/ (+) IPTG, and (+) meropenem/ (-) IPTG. Meropenem was used at 8 mg/L. Cultures were grown at 37°C with shaking and the OD_{600} was collected over a 4 h period using a Fisherbrand accuSkan GO UV/Vis Microplate Spectrophotometer with SkanIt Software 5.0. Each experiment was done twice in triplicate and a representative assay was reported. NDM-1 *E. coli* carrying the empty SLAY vector was used as a control.

Antimicrobial activity assays

MBC assays were adapted from previously described methods[225,231,232]. A small number of NDM-1 bacteria from an overnight plate were resuspended in 1 mL LB for OD_{600} measurement. Cultures were backdiluted to OD_{600} 0.05 in 5 mL LB containing carbenicillin and grown to logarithmic phase at 37°C with shaking. Cells were collected, washed twice with 5 mL 10 mM Tris (pH 7.4) + 25 mM NaCl + 0.1 % glucose and diluted to OD_{600} 0.001 in 5 mL 10mM Tris (pH 7.4) + 25 mM NaCl + 0.1% glucose either with or without a final concentration of 4 mg/L meropenem. 50 μL of bacteria were added to each well in a polypropylene 96-well plate (Greiner Bio-One). Chemically synthesized peptides (GenScript) were diluted to 512 μM in water and serial diluted to a volume of 75 μL. 50 μL of each peptide dilution was added to 50 μL of cells to result in final peptide concentration of 4, 8, 16, 32, 64, 128 and 256 μM. Plates were sealed and incubated at

37°C. At 24 h, each well was spotted on LB agar to assess killing (+) or (-) meropenem. MBCs were determined as the lowest concentration of peptide that results in at least 99.90 % of killing of the initial inoculums. Each experiment was performed twice in triplicate and the representative MBC was reported.

MIC assays were performed as previously described with slight modifications[233]. A small number of bacteria from an overnight plate were used to inoculate 5 mL LB at OD_{600} 0.05 and grown to logarithmic phase. Cells were washed twice with MOPS media + 0.1% glucose and diluted to OD_{600} 0.001. 50 μL of cells were added to each well of a polypropylene 96-well plate. Peptides were diluted in water to 256 μM and serial diluted. 50 μL of each peptide solution was added to 50 μL of cells at 0, 32, 64 and 128 μM. Increasing concentrations of meropenem (0.1 – 64 mg/L) were added to the appropriate well. Plates were sealed and incubated at 37°C overnight. MICs were determined by OD_{600} measurements where cell density was 0. Each experiment was performed twice in triplicate. A representative MIC was reported.

Permeability assays

Assays were performed as previously described[234]. A small number of bacteria was scraped from an overnight plate, resuspended in PBS and normalized to OD_{600} 0.2. CCCP (Acros Organics) was added at 200 μM to inhibit efflux pump activity. Ethidium bromide (EtBr) (MP Biomedicals) was added immediately prior to measurement to final concentration of 1.2 μM in 200 μL total volume. Readings were taken, using a BioTek Synergy Neo2 multi-mode reader, every 15 s for 30 min with samples assessed in triplicate in Greiner bio-one 96-well flat bottom black plates. Each experiment was performed twice in triplicate. One representative assay was reported.

Kinetic assays

NDM-1 was purified as previously described[235]. Kinetic assays were performed as previously reported with slight modifications[220]. NDM-1 inhibitory activity was calculated following hydrolysis of increasing concentrations of nitrocefin (BioVision, Inc.) (2-250 μM) in 10mM Tris, 50mM KCl, 5% glycerol; pH 8.0 (P6 and P9) or 10mM Tris, 50mM KCl, 5% glycerol 40% DMSO; pH 8.0 (P5 and P7) in the presence of (125 μM–3 mM) chemically synthesized peptides. Compound dilutions were performed in water (P6 and P9) or DMSO (P5 and P7). GraphPad Prism (8.4.1) was used to calculate the kinetic parameters for NDM-1 inhibition by each peptide using nonlinear regression and Michaelis-Menton enzyme kinetics, which determined the maximal velocity (V_{max}) and the Michaelis constant (K_m). Lineweaver-Burk plots were used to display the data where the slope = K_m/V_{max}, the y-intercept = $1/V_{max}$ and the x-intercept = $-1/K_m$. K_i values for NDM-1 inhibition were calculated using nonlinear regression with global curve fitting in Prism, where parameters were determined by finding the global best-fit value among all datasets for each inhibitor. The datasets were analyzed using the following models: Competitive inhibition model: $K_{mObserved} = K_m \times (1 + [I]/K_i)$, $Y = V_{max} \times X/K_{mObserved} + X)$; Noncompetitive inhibition model: $V_{max\ inh} = V_{max}/ (1 + I/K_i)$, $Y = V_{max\ inh} \times X/ (K_m + X)$, where I is the inhibitor concentration. The global fitting function was also used to support inhibitory mechanisms along with Michaelis-Menton kinetic analysis and Lineweaver-Burk plot values, which were reported.

MTT assays

MTT assays were performed as previously described[236]. Mode-K and HEK cell lines were used to assess peptide cytotoxicity. Initially, standard curves were calculated

to determine the linear range, which included a concentration of 75,000 cells for both cell lines. Cells were seeded in tissue culture-treated 96-well plates at a final volume of 100 μL and incubated for 24 hours to allow attachment. After 24 hours, media containing increasing concentrations of purified peptide inhibitors was added. Plates were incubated for 24 hours. Following incubation, 10 μL of 5 mg/L MTT (Sigma-Aldrich) solution in PBS was added to a final concentration of 0.45 mg/L and incubated at 37°C for 4 hours. Liquid was removed and 100 μL of 100% DMSO was added to each well to dissolve the formazan crystals. The plate was incubated in the dark at room temperature with shaking for 1 h and the absorbance was measured at 570 nm.

Hemolysis assays

Hemolysis assays were performed as described previously[225,237]. Briefly, human red blood cells (hRBC) were purchased (Rockland Immunochemicals, Inc.) and 50 μM solutions of chemically synthesized peptides were mixed in 10mM PBS at pH 7.4 for a total volume of 0.5 mL. The hRBC solution was made by washing 0.4 mL of the red blood cells twice with 7 mL of PBS. Precipitates were resuspended in 4 mL PBS. Hemolytic activity was measured by mixing the 0.5 mL peptide solutions with 0.4 mL hRBC solution at 37°C for 1 hour. The absorbance was measured at 540 nm. Percent hemolysis was calculated using the equation:

$$\% \text{ hemolysis} = \frac{\text{absorbance}_{\text{sample}} - \text{absorbance}_{\text{negative}} \times 100}{\text{absorbance}_{\text{positive}}}$$

Results

To screen for peptides that restore the antimicrobial activity of carbapenems against carbapenemase-producing Enterobacteriaceae (CPE), we generated a random synthetic library that encoded more than 1x 10^6 ten-amino acid peptides in the SLAY plasmid system (**Figure 4A**). Approximately 1700 unique sequences were identified that potentiate carbapenem-dependent killing of NDM-1 *E. coli* (**Figure 4B**), of which thirty-seven peptides were found to restrict growth in the presence of both imipenem and meropenem (**Figure 4B**, orange dots). We prioritized the thirty-seven peptides for analysis because increased susceptibility to multiple carbapenems suggested a conserved mechanism of action. Interestingly, the thirty-seven peptides only modestly increased CPE susceptibility to both meropenem and imipenem.

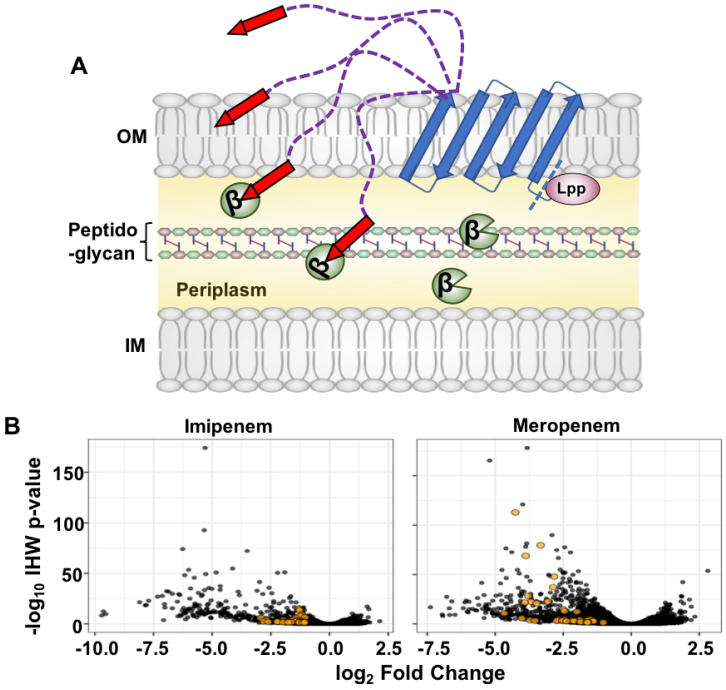

Figure 4: Self-screening of displayed peptides to discover NDM-1 inhibitors that potentiate killing of carbapenemase-producing *E. coli*. (A) Illustration of the surface localization display system (SLAY), including the OmpA (46–159) transmembrane protein (blue arrows), flexible tether (purple, dashed) and C-terminal peptide (red arrow). NDM-1 is localized to the periplasm (yellow). (B) Volcano plot of library sequences depleted in NDM-1 *E. coli* after 4 h of growth in imipenem (left) or meropenem (right). Sequences depleted in both conditions are labelled orange. This figure appears in color in the online version of *JAC* and in black and white in the printed version of *JAC*.

We computationally analyzed the amino acid composition of the thirty-seven peptides at each position to determine specific amino acids overrepresented within the pool (**Figure 5A**). Our analyses indicated enrichment of proline, arginine, leucine and isoleucine at site-specific positions. Furthermore, the physicochemical composition of the peptide pool highlighted a prevalence of basic, hydrophobic, and polar amino acids (**Figure 5B**). Twenty-six of the thirty-seven sequences were genetically validated using the SLAY system (**Figure 5C**).

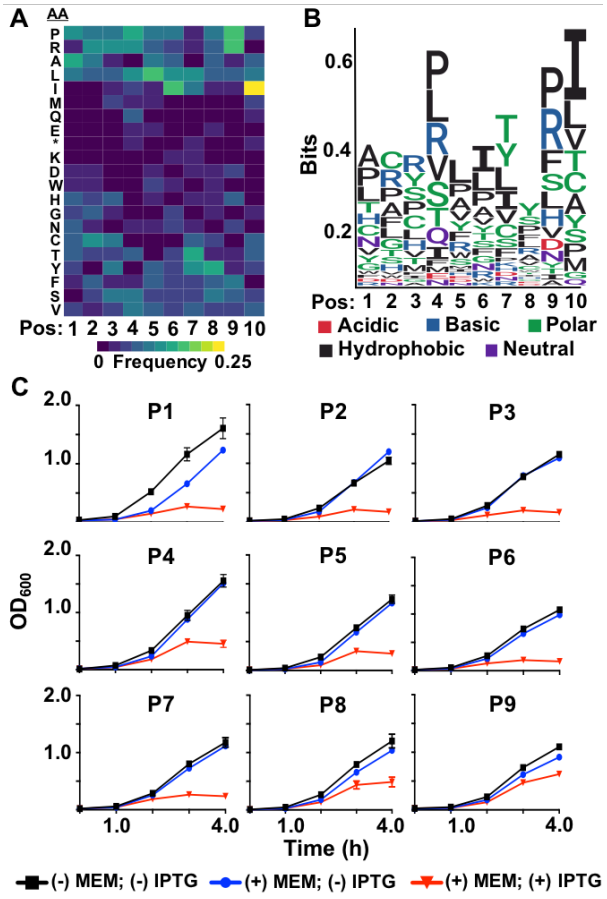

Figure 5: Physicochemical properties and genetic validation of inhibitor peptides that potentiate killing of NDM-1 *E. coli*. (A) Heat map of amino acids in each position of the depleted sequences in the screen. (B) Depleted sequences were used to build a consensus motif. Larger letters indicate stronger amino acid enrichment at each position. The chemical properties of each amino acid are color coded. (C) Growth curves of NDM-1 *E. coli* containing P1 - P9 cloned into the SLAY system. Cultures were grown in 8 mg/L meropenem (MEM) with or without 0.1 mM IPTG for 4 h. This figure appears in color in the online version of *JAC* and in black and white in the printed version of *JAC.*

The top nine validated peptides with the greatest inhibitory effect from the screen were chemically synthesized to measure meropenem activity against NDM-1 *E. coli* independent of SLAY localization. MBCs for each were determined when NDM-1 *E. coli* (*Ec*) was exposed to 4 mg/L of meropenem (**Table 1**), which is two-fold higher than the EUCAST breakpoint[238]. The reported MBCs represent the lowest concentration of peptide inhibitor that resulted in at least 99.90 % killing of the initial inoculum. MBC assays using increasing concentrations of synthesized peptides showed a correlative response with meropenem susceptibility, which indicated potentiation of meropenem-dependent killing independent of SLAY subcellular localization. Moreover, we tested peptide MBCs in two additional CPE, including NDM-1 *K. pneumoniae* (*Kp*) and *Enterobacter cloacae* (*Ecl*).

Table 1: Fold change (log_2) and NDM-1 inhibitor concentrations of peptides from SLAY

						MBC (μM)[a,b]		
Peptide	Sequence	Charge	Hydro-phobicity	log_2 Fold	p-value	*Ec* W3110 NDM-1	*Kp* NIH1 NDM-1	*Ecl* ATCC13047 NDM-1
P1	AFRPIPTHSC	1.026	-0.08	-4.26	<4.57e-118	8	32	32
P2	YNYSYIITRS	0.995	-0.52	-3.33	<1.50e-84	128	32	≥128
P3	PTTVHIIYRI	1.088	0.57	-3.88	<2.24e-73	16	16	64
P4	ASVTWLLYAM	-0.002	1.36	-2.83	<3.75e-52	128	128	≥128
P5	LRCLMLKFPI	1.935	1.31	-2.87	<3.62e-41	8	4	4
P6	CLRPSIISRA	1.936	0.49	-3.07	<2.24e-26	32	≥128	≥128
P7	WRYQWTILFI	0.997	0.38	-3.91	<1.81e-25	16	≥128	≥128
P8	FCIRLATYVI	0.935	1.76	-2.68	<2.02e-07	8	≤4	64
P9	PGHRVSCWLS	1.026	-0.17	-2.17	<5.36e-06	≤4	≤4	32

[a]MBCs were determined as the lowest concentration of peptide that results in at least 99.90% killing of the initial inoculums. Data are representative of three independent experiments.
[b]All MBCs were performed with 4 mg/L of meropenem.

Porins are the main entryways for carbapenems to penetrate the bacterial periplasm and are known to contribute to resistance[239]. Therefore, we first tested if membrane permeability increased when cells were treated with each peptide (**Figure 6**). 10 mg/L colistin, a cationic antimicrobial peptide (CAMP) known to perturb the outer membrane and lyse Gram-negative bacterial cells, was used as a positive control to indicate lysis[233,240,241]. Our data showed that high concentrations (256 μM) of select

peptides slightly increased cell permeability, whereas other peptides did not. Specifically, exposure to P5 and P9 marginally increased permeability. However, we reasoned the increased permeability was independent of meropenem-dependent killing (**Table 1**) because other peptides demonstrated a more robust increase in permeability, but the respective MBC values indicated less killing (i.e., P4 & P8). These data suggested an additional mechanism, independent of membrane permeability, to restore carbapenem susceptibility in NDM-1 *E. coli*. Therefore, we investigated how P5 and P9, which slightly increased permeability, and P6 and P7, which did not increase permeability, potentiate meropenem-dependent killing of NDM-1 *E. coli*.

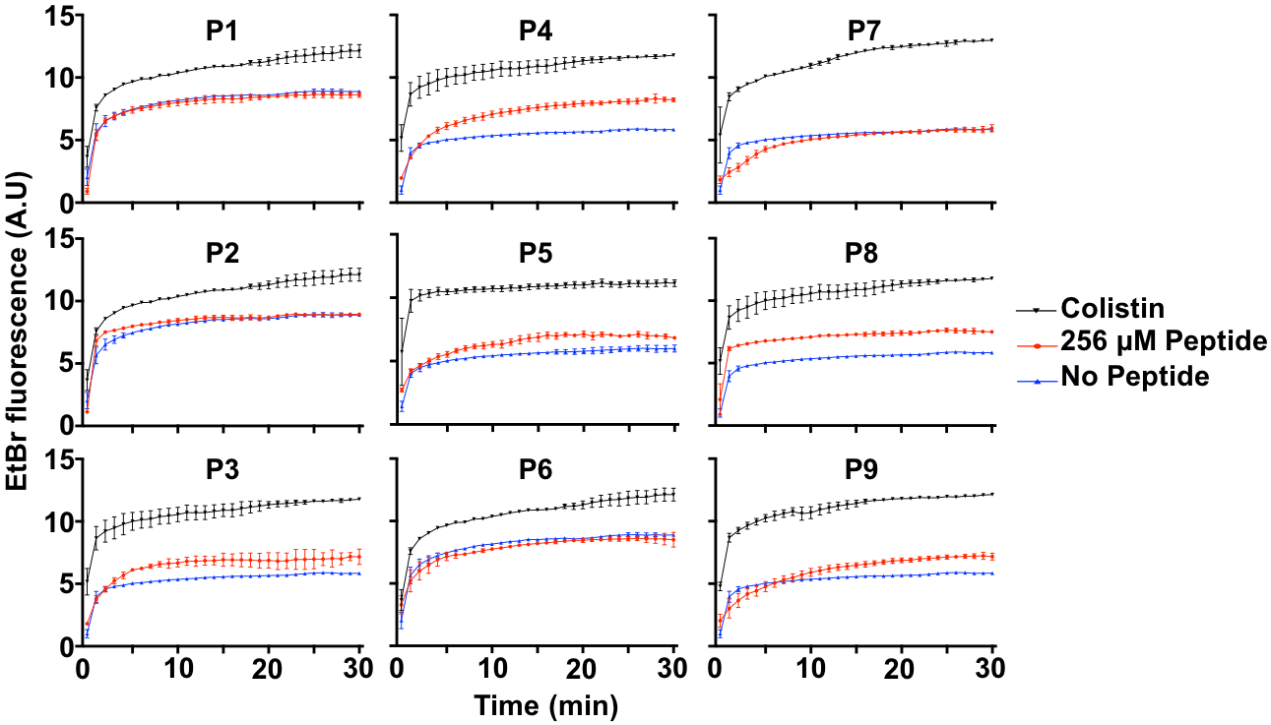

Figure 6: Permeability of NDM-1 *E. coli* when exposed to high concentrations of inhibitor peptides. Ethidium bromide uptake assay to measure outer membrane permeability of NDM-1 *E. coli* in the presence of 256 μM peptides. Colistin was used as a positive control at a concentration of 10 mg/L. A.U. is arbitrary units. This figure appears in color in the online version of *JAC* and in black and white in the printed version of *JAC*.

Next, we tested if peptides directly bound and inhibited NDM-1 activity using a biochemical assay to calculate NDM-1 hydrolysis of the β-lactam analog, nitrocefin. Hydrolysis of the amide bond in nitrocefin induces a measurable colorimetric shift (from 386 nm to 482 nm). Recombinant NDM-1, increasing inhibitor (P5, P6, P7 and P9) concentrations and nitrocefin were used to calculate the Michaelis-Menton kinetics of β-lactam hydrolysis[220,242,243]. NDM-1 was used at a concentration of 10 nM, nitrocefin concentrations were 0, 2, 10, 25, 50, 100, 200 and 250 μM, and peptide inhibitors were used at indicated concentrations (**Figure 7**). Importantly, Lineweaver-Burk plots of Michaelis-Menton kinetic analysis from three inhibitor peptides (P5, P6 and P9) suggested competitive inhibition of NDM-1, whereas P7 demonstrated non-competitive inhibition. We calculated the K_i of each kinetic reaction to determine inhibitor potency, where the lowest K_i observed was P6 (0.11 μM), followed by P9 (1.34 μM), P7 (158.60 μM) and P5 (176.50 μM).

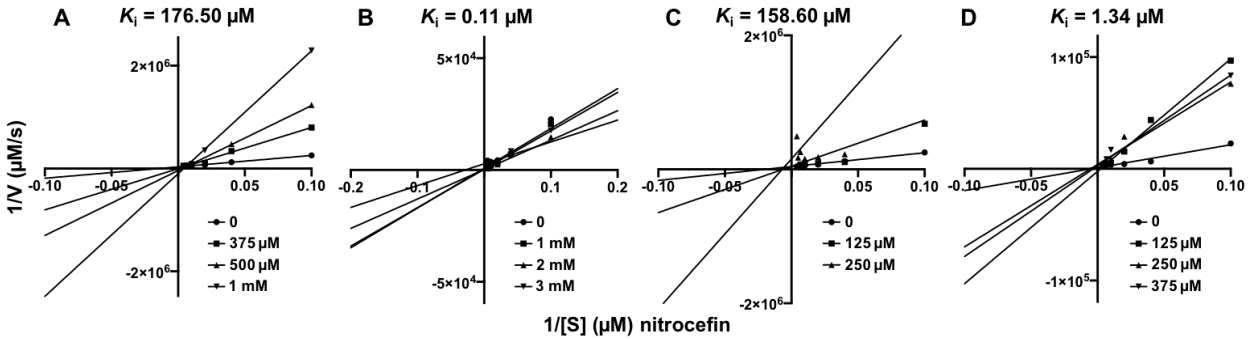

Figure 7: Lineweaver-Burk plots showing inhibition of NDM-1-dependent nitrocefin hydrolysis activity by inhibitor peptides. (A) P5, (B) P6, (C) P7 and (D) P9. Recombinant NDM-1 was used at 10 nM. Circles indicate hydrolysis without inhibitor. Squares, triangles and inverted triangles indicate increasing concentration of the respective inhibitor at the indicated concentrations. The position where the lines intersect indicates the type of inhibition, (P5, competitive; P6, competitive; P7, non-competitive; P9, competitive). The inhibitor constant (K_i) is indicated above each plot.

Meropenem MICs were calculated using increasing concentrations of the four NDM-1 inhibitors (**Table 2**). P5 and P9 strongly potentiated meropenem-dependent growth inhibition of NDM-1 *E. coli* at high and low peptide concentrations (32 μM), whereas P6 and P7 potentiated meropenem activity at higher concentrations (>64 μM). Meropenem MICs were also performed in NDM-1 *K. pneumoniae* and *E. cloacae* to determine if the NDM-1 inhibitors were broadly effective against CPE. While all peptides reduced the meropenem MIC in a concentration-dependent manner, P5 increased meropenem susceptibility to below the EUCAST breakpoint in all CPE tested, which indicated broad-spectrum activity.

Table 2: Meropenem MICs (mg/L) against NDM-1 Enterobacteriaceae

	E. coli W3110 NDM-1				*K. pneumoniae* NIH1 NDM-1				*E. cloacae* ATCC 13047 NDM-1			
	-	32uM	64uM	128 uM	-	32uM	64uM	128 uM	-	32uM	64uM	128 uM
P5	8	<0.5	<0.5	<0.5	32	8	<0.5	<0.5	16	8	2	<0.5
P6	8	8	4	4	32	16	16	8	16	8	4	4
P7	8	4	4	2	32	8	8	8	16	2	2	2
P9	8	2	<0.1	<0.1	32	16	16	16	16	8	8	8

As with any therapeutic compound, cytotoxicity is a concern to prioritize lead development. Cell viability in the presence of the NDM-1 inhibitor peptides was assessed by MTT assay in two cell lines, MODE-K and HEK293. None of the peptides exhibited notable cytotoxic activity when exposed to MODE-K cells, with each demonstrating well-below 20% lysis. The one exception was P7, when exposed at 256 μM, which was associated with the high concentration (9% of total concentration) of DMSO required to solubilize the peptide. While MODE-K cells showed minimal reduction of cell viability (**Figure 8A**), HEK293 cells showed a dose-dependent cytotoxic effect (**Figure 9**).

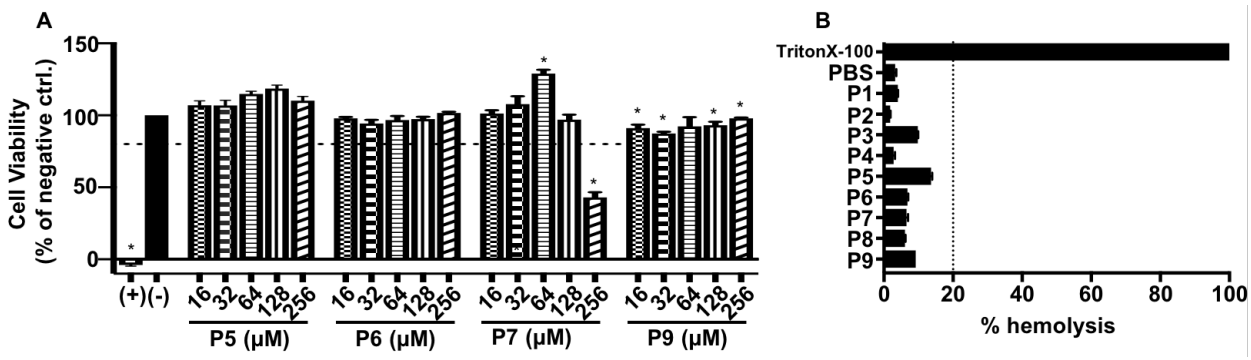

Figure 8: Cytotoxicity of NDM-1 inhibitor peptides against Mode-K cells. (A) MTT assays of Mode-K (intestinal epithelial) cells to measure viability after 24 h when exposed to increasing concentrations of NDM-1 inhibitor peptides. Cell viability is reported as the % of the no peptide control (-), which was normalized to 100. Triton X-100 was used as a positive control (+). Values with p-value > 0.05 are indicated by *. Dotted line indicates 80% cytotoxicity. (B) Hemolytic activity of selected peptides at 50 μM. Dotted line indicates 20% hemolysis.

Hemolysis is a known off-target effect of antimicrobial peptides, with several CAMPs showing marked hemolysis at therapeutically relevant concentrations[244]. We assayed the hemolytic activities of all synthesized peptides at 50 μM. The hemolytic activity of each is summarized in Figure 8B. None of the peptides tested exhibited notable hemolytic activity, with each demonstrating below 20% lysis.

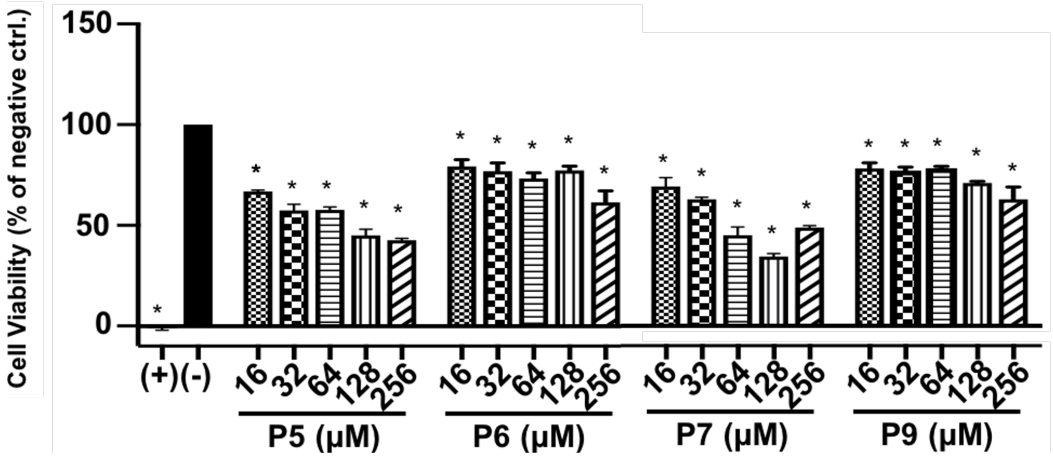

Figure 9: Cytotoxicity of NDM-1 inhibitor peptides against HEK 293 cells. MTT assays of HEK 293 cells to evaluate viability after 24 h when exposed to increasing concentration of NDM-1 inhibitor peptides. Cell viability is reported as the % of the no peptide control (-), which was normalized to 100. Triton X-100 was used as a positive control (+). Values with p-value > 0.05 are indicated by *.

Discussion

NDM-1 is a primary β-lactam resistance mechanism that has emerged in many Gram-negative 'superbugs', which threaten our antimicrobial repertoire. Here we used SLAY to identify and characterize peptides that restore the antimicrobial activity of carbapenems in NDM-1 Enterobacteriaceae. As anticipated, the vast majority of sequences in the random peptide screen did not restore carbapenem antimicrobial activity (99.99%). However, high-throughput sequencing identified approximately 1700 candidate inhibitors that potentiated NDM-1 *E. coli* killing via a carbapenem-dependent mechanism. Of these, only thirty-seven peptides increased susceptibility to both meropenem and imipenem based on our cutoffs, which suggested a conserved mechanism of action. Interestingly, these overlapped peptides only modestly increased carbapenem susceptibility (**Figure 4B**, orange dots), where the "best" peptides for one carbapenem did not function as well as the other in our screen.

Sequence analysis of the thirty-seven peptides suggested enrichment of specific amino acids, including enrichment of arginine, lysine and histidine residues, which contain positively charged side chains at pH 7.0, and proline residues. Interestingly, each sequence (with the exception of P6) encoded a positively charged residue at either the 2, 3 or 4 position (or reverse sequence). The conserved site-specific charge could contribute to NDM-1 inhibition or peptide penetration of the periplasm. Several lytic antimicrobial peptides require a cationic charge, which promotes electrostatic interactions with the negatively charged outer membrane to displace divalent ions to perturb the membrane[245–248]. In contrast, selected lead peptides in our study only slightly increased permeability, but strongly potentiated meropenem-dependent killing, which suggested an additional

membrane–independent mechanism of action. It is possible that the positive charge enriched NDM-1 inhibitor peptides at the negatively charged cell-surface, which distorted the membrane allowing periplasmic access, where the sequence bound and directly inhibited NDM-1. Consistent with this hypothesis, select peptides did not increase membrane permeability (i.e., P6 and P7) at a level we could detect (**Figure 6**), but nonetheless potentiated meropenem-dependent killing of CPE at higher concentrations (**Table 1**), likely through direct inhibition of NDM-1 (**Figure 7**).

Despite reports of several small molecule MBL inhibitors, none have been approved for therapeutic use for various reasons, including ineffectiveness across Enterobacteriaceae and poor pharmacokinetics/dynamics[214,249–254]. Several MBL peptide inhibitors have also been discovered with limited therapeutic efficacy[220,221,223,224,242]. Peptides offer diverse avenues to sample chemical space and SLAY provides a valuable platform to optimize and quickly test new sequence pools in a high-throughput manner to understand inhibitory motifs. Additionally, identified inhibitor motif combinations provide an opportunity to explore broad or narrow-spectrum inhibitors in a more directed fashion, which could be useful in future development of pathogen-specific therapeutics.

CHAPTER 4

HIGH-LEVEL CARBAPENEM TOLERANCE REQUIRES ANTIBIOTIC-INDUCED OUTER MEMBRANE MODIFICATIONS**

Andrew N. Murtha[*1,2], Misha I. Kazi[*3], Richard D. Schargel[3], Trevor Cross[1,2], Conrad Fihn[4], Vincent Cattoir[5,] Erin E. Carlson[4,6,7,8], Joseph M. Boll[#3], Tobias Dörr[#1,2,9]

[1]Weill Institute for Cell and Molecular Biology, Cornell University, Ithaca, NY, USA; [2]Department of Microbiology, Cornell University, Ithaca NY, USA; [3]Department of Biology, University of Texas Arlington, Arlington, TX, USA; [4]Department of Medicinal Chemistry, University of Minnesota, Minneapolis, MN, USA; [5]Department of Clinical Microbiology and National Reference Center for Antimicrobial Resistance (Lab Enterococci), Rennes University Hospital, Rennes, France; Inserm Unit U1230, University of Rennes 1, Rennes, France [6]Department of Chemistry, University of Minnesota, Minneapolis, MN, USA; [7]Department of Biochemistry, Molecular Biology, and Biophysics, University of Minnesota, Minneapolis, MN, USA; [8]Department of Molecular Pharmacology and Therapeutics, University of Minnesota, Minneapolis, MN, USA; [9]Cornell Institute of Host-Microbe Interactions and Disease, Cornell University, Ithaca, NY, USA

[#]Correspondence: tdoerr@cornell.edu, joseph.boll@uta.edu

*contributed equally

**_Accepted; In Press, PLoS Pathogens_

Abstract

Antibiotic tolerance is an understudied potential contributor to antibiotic treatment failure and the emergence of multidrug-resistant bacteria. The molecular mechanisms governing tolerance remain poorly understood. A prominent type of β-lactam tolerance relies on the formation of cell wall-deficient spheroplasts, which maintain structural integrity via their outer membrane (OM), an asymmetric lipid bilayer consisting of phospholipids on the inner leaflet and a lipid-linked polysaccharide (lipopolysaccharide, LPS) enriched in the outer monolayer on the cell surface. How a membrane structure like LPS, with its reliance on mere electrostatic interactions to maintain stability, is capable of countering internal turgor pressure is unknown. Here, we have uncovered a novel role for the PhoPQ two-component system in tolerance to the β-lactam antibiotic meropenem in Enterobacterales. We found that PhoPQ is induced by meropenem treatment and promotes an increase in 4-amino-4-deoxy-L-aminoarabinose [L-Ara4N] modification of lipid A, the membrane anchor of LPS. L-Ara4N modifications likely enhance structural integrity, and consequently tolerance to meropenem, in several Enterobacterales species. Importantly, mutational inactivation of the negative PhoPQ regulator *mgrB* (commonly selected for during clinical therapy with the last-resort antibiotic colistin, an antimicrobial peptide [AMP]) results in dramatically enhanced tolerance, suggesting that AMPs can collaterally select for meropenem tolerance via stable overactivation of PhoPQ. Lastly, we identify histidine kinase inhibitors (including an FDA-approved drug) that inhibit PhoPQ-dependent LPS modifications and consequently potentiate meropenem to enhance lysis of tolerant cells. In summary, our results suggest that PhoPQ-mediated LPS modifications play a significant role in stabilizing the OM, promoting survival when the primary integrity maintenance structure, the cell wall, is removed.

Introduction

The rapid rise of antibiotic treatment failure threatens our ability to prevent and control bacterial infections. Antibiotic resistance, the continued proliferation of bacteria in the presence of the antibiotic, can often explain failure of clinical therapy. However, the response to an antibiotic is oftentimes more nuanced than a simple dichotomy of resistance vs. susceptibility. Bacteria can survive treatment in a non- or slowly-proliferating state, readily reverting to healthy growth after removal of the antibiotic (such as the end of a treatment course), and this is typically referred to as "antibiotic tolerance"[12,65,255]. Importantly, tolerance to antibiotics has been shown to enhance the evolution of outright resistance mechanisms[63,75,256], and can thus serve as both a direct and indirect contributor to treatment failure.

β-lactams are the most widely prescribed antibiotic class used to treat bacterial infections. The β-lactam ring inhibits the activity of the penicillin-binding proteins (PBPs) through covalent modification of a catalytic residue. PBPs are enzymes that synthesize the cell wall, an essential structure composed mainly of the polysaccharide peptidoglycan (PG). In many well-studied model organisms, PBP inhibition induces cell wall degradation and often subsequent lysis through the action of cell wall degrading enzymes (collectively referred to as "autolysins") in a poorly-understood manner[65]. While lysis is the canonical response of model organisms like *Escherichia coli* K12, many formally β-lactam susceptible clinical isolates of Gram-negative pathogens (including prominent clinical isolates belonging to the Enterobacterales, like *Klebsiella spp.* and *Enterobacter spp.*) exhibit a unique type of β-lactam tolerance[19–21]. Like *E. coli*, these cells digest their PG upon exposure to β-lactams. However, instead of lysing, these pathogens survive

antibiotic-induced cell wall degradation by forming viable, non-dividing, cell wall-deficient spheroplasts, which presumably rely on the outer membrane to counter their internal turgor. Interestingly, spheroplasts do not absolutely require osmotic stabilization and form in diverse types of growth media, including human serum[21]. This cell wall-deficient phenotype is reminiscent of so-called L-forms[166,167,257], with the notable distinction that spheroplasts do not divide in the presence of the antibiotic.

Remarkably, spheroplasts formed in response to the carbapenem antibiotic meropenem readily resume growth and revert to wild type rod shape when the β-lactam is removed from the growth medium[20,21]. Little is known about the molecular mechanisms that facilitate spheroplast formation and survival. In *Vibrio cholerae*, the two-component system (TCS) VxrAB is essential for spheroplast recovery by upregulating cell wall synthesis and downregulating iron uptake into the cells, mitigating toxic free iron levels induced by β-lactam treatment and allowing the cell to avoid damage by oxidative stress[168,258]. Many questions remain, however, as to how the cell envelope maintains its integrity without a cell wall, the essential structure canonically thought to protect the cell against immense turgor pressure.

In this study, we used *Enterobacter cloacae* as a model Gram-negative pathogen to investigate genetic factors that contribute to bacterial tolerance to meropenem, which is used as a last-resort β-lactam to treat multidrug resistant bacterial infections[94,96,98]. We first show that tolerance is dependent on outer membrane modifications (specifically 4-amino-4-deoxy-L-aminoarabinose [L-Ara4N]) induced by the PhoPQ TCS, an important cell envelope stress sensor that has previously been shown to respond to magnesium limitation, cationic antimicrobial peptide exposure, osmotic challenge, and pH changes[175]. Both PhoPQ regulon transcription and modification of the lipopolysaccharide lipid A

domain are induced by meropenem treatment, suggesting a specific response to perturbations of PG synthesis in *E. cloacae*. These findings represent a novel mechanism of β-lactam tolerance in clinically relevant Enterobacterales, as well as an expanded role for the PhoPQ TCS.

Materials and Methods

Bacterial strains and growth

All strains were initially grown from freezer stocks on solid agar at 37°C. Isolated colonies were used to inoculate Luria-Bertani (LB), Brain heart infusion (BHI) or N-minimal medium (0.1M Bis-Tris, pH 7.5, 5 mM KCl, 7.5 mM $(NH_4)_2SO_4$, 0.5 M K_2SO_4, 1 mM KH_2PO_4, 0.10% casamino acids 0.2% glucose, 0.0002% thiamine, 15 μM $FeSO_4$, 10 mM $MgSO_4$) at 37°C. Where required, kanamycin was used at 50 μg/mL, meropenem was used at 10 μg/mL (300 x MIC; $MIC_{ATCC13047}$ = 0.03 μg/mL) and colistin was used at 20 μg/mL (1.25 x MIC; $MIC_{ATCC13047}$ = 16 μg/mL), unless noted otherwise. *K. pneumoniae* 1084 is an isolate AR0080 from the CDC AR isolate bank (https://wwwn.cdc.gov/arisolatebank/Search), cured of its imipenemase via spontaneous loss.

Meropenem killing experiments

Unless noted otherwise, killing experiments were conducted in 100-well honeycomb plates in a Bioscreen C growth curve analyzer (Growth Curves USA, Piscataway NJ). Overnight cultures were diluted 10-fold into fresh LB medium containing meropenem (10 μg/mL, 300x MIC) and transferred to honeycomb plates (200 μL volume/culture). OD_{600} was measured by plate reader; at indicated timepoints, the experiment was paused, and an aliquot was removed for CFU/mL determination or

microscopy. Rilu compounds were dissolved in DMSO as 50 mM (Rilu-2) or 500 mM (Riluzole) stocks and added directly to the LB medium containing meropenem at the indicated concentrations.

For *K. pneumoniae* killing experiments, we employed our standard tolerance assay as described previously[21], but with 0.2 % arabinose present for induction of plasmid-borne PhoP.

Colistin MIC experiment

Cultures were grown overnight at 37°C shaking, then diluted 1000-fold into fresh LB. Subcultures were grown for 1 hour at 37°C shaking before being diluted 1000-fold again into fresh LB to create a "seed culture". 100 μL of seed culture was subsequently diluted 2-fold into a 96-well plate containing colistin concentrations ranging 0.25 – 128 μg/mL. Reported values are medians of 4 technical replicates.

qRT-PCR

Strains were grown in 5 mL LB overnight at 37°C. 500 μL of overnight cultures was added to 4.5 mL pre-warmed BHI broth, either water or 10 μg/mL meropenem was added and cultures were incubated statically at 37°C for 0 and 30 mins. Following incubation, cells were harvested via centrifugation and resuspended in 500 μl RNA later and stored in -80°C prior to RNA extraction. Relative-abundance quantitative PCR (qPCR) was performed as previously described[259,260]. In brief, the Sybr Fast One-Step qRT-PCR kit (Kapa Biosystems) was used with 16S rDNA as the internal reference. The PCR was performed using the Bio-Rad CFX Connect Real-Time PCR System. Relative expression levels were calculated using the ΔΔCt method[261], with normalization of gene targets to 16S rDNA signals.

Flow cytometry GFP measurements

Cultures of strains harboring transcriptional P_{arnB}:msfGFP fusions were grown overnight in LB supplemented with 10 mM $MgSO_4$. Overnight cultures were then washed 2x in fresh LB before 10-fold dilution into fresh LB medium containing $MgSO_4$ (10 mM), Ethylenediaminetetraacetic acid (1 mM), or meropenem (10 μg/mL). Cultures were incubated statically for 3 hours at 37°C. Then, 500 μL of culture was harvested and run through a C6 Accuri flow cytometer (BD Biosciences) until 100,000 events (cells) had been analyzed. Mean green fluorescence as measured by the FL1-A channel was used as a readout for GFP.

Mutant construction

E. cloacae subsp. *cloacae* 13047 mutant strains (*phoPQ*, *arn* and *arnT*) were constructed as previously described using recombineering with the plasmid pKOBEG[172,262]. Briefly, linear PCR products were amplified from pKD3 and transformed into *E. cloacae* ATCC13047/pKOBEG strain by electroporation and plated on chloramphenicol selective media. Selected clones were transformed with pCP20 to cure the antibiotic resistance cassette. All mutants were verified by PCR.

pagP was deleted using the Wanner method as described previously[172]. Briefly, the chloramphenicol resistance cassette was amplified from pKD3 using primers TDP1532/TDP1533, which contain 75 bp flanking homology overhangs. The resulting PCR product was electroporated into *E. cloacae* ATCC13047 expressing lambda red recombinase from pACBSR-hyg[263] (a hygromycin-resistant derivative of pKD46[264]). Mutants were selected on chloramphenicol (100 μg/mL) and verified by PCR.

Other mutants were constructed using either lambda red recombinase[264] or the suicide vector pTox[265]. The *mgrB* gene was deleted using the suicide plasmid pTox5 as described in[265]. ~700 bp upstream and downstream flanking homology regions were amplified from ATCC13047 using primers TDP1767/68 and TDP1769/70, and cloned into pTox5 (digested with EcoRV) using isothermal assembly[266]. Successful pTox5Δ*mgrB* were conjugated into ATCC13047 using the *E. coli* donor strain MFD lambda *pir*; successful recombinants were selected on plates containing 100 μg/mL chloramphenicol. Upon single colony purification, colonies were directly streaked out on an M9 minimal medium plate containing 0.2 % casamino acids and 1 % rhamnose, followed by incubation at 30°C for 24 – 36 hours. Mutants were tested using primers TDP1771/72.

The *K. pneumoniae* Δ*phoPQ* mutant was constructed using pTox5. Upstream and downstream homology regions were amplified using primers TC120/TC344 and TC345/TC127. Allelic exchange was conducted as described above. Mutants were tested using flanking primers TC166/167. For the complementation construct, the PhoP open reading frame was synthesized as a gene block (gBlock TC391) with a 3x Flag tag (Twist Biosciences, South San Francisco, USA), and cloned into pBAD33 using isothermal assembly.

Lipid A isolation and mass spectrometry

Isolation of lipid A for analysis was performed as previously described[267] with slight modifications. To analyze lipid A after meropenem treatment, overnight cultures grown in BHI broth were diluted 1:10 in pre-warmed media with or without meropenem statically for 3 h. To assess Rilu-dependent modification of lipid A, 12.5 mL of *E. cloacae* was grown to OD_{600} 1.0. Rilu-2 was used at a final concentration of 200 μM. Bacteria were harvested

and lipid A extraction was carried out by mild-acid hydrolysis as previously described[268]. For mass spectrometry (MS), data were collected on a MALDITOF (Axima Confidence, Shimadzu) mass spectrometer in the negative mode, as previously done[172].

For quantification of lipid A, cultures were grown with 2.5 μCi/mL of ^{32}P ortho-phosphoric acid (^{32}P) (Perkin Elmer) and lipid A was extracted. Thin layer chromatography was done in a pyridine, chloroform, 88% formic acid, aqueous (50:50:16:5 v/v) tank for 3 hours. Plates were exposed to a phosphor screen, imaged, and densitometry was used to calculate the percentage of each lipid species. Reported densitometry was calculated using 2 replicates +/- standard deviation. For lipid A structural comparisons, purified ^{32}P-lipid A from *E. coli* W3110, WD101[174] were used in each experiment. These structures were comparable to previously published *E. cloacae* structures[269] and validated by mass spectrometry.

Results

The PhoPQ TCS system regulates carbapenem tolerance

We previously showed that many Gram-negative pathogens are highly tolerant to meropenem. Upon treatment, tolerant cells do not appreciably lyse. Instead, they form viable, enlarged, non-replicating spheroplasts that are devoid of detectable cell wall material[21]. Meropenem-induced spheroplast formation is quantifiable as an OD_{600} increase (**Figure 10A**) and concomitant with only a moderate decrease in survival, as measured by colony-forming units (CFU) (**Figure 10B**). In contrast, non-tolerant bacteria like many *E. coli* isolates rapidly lyse in the presence of meropenem, indicated by a decrease in both OD_{600} and survival (**Figure 10AB**). Since spheroplast integrity is

presumably maintained by the outer membrane, rather than the cell wall, we hypothesized that the strength of the outer membrane might correlate with tolerance. To test this, we repeated the killing experiments in the presence of the known outer membrane fortifying agents Mg^{2+} and Ca^{2+}, which link adjacent lipopolysaccharide molecules by forming ionic bridges between phosphate groups on the lipid A domain[270,271]. Addition of either divalent cation (Mg^{2+} or Ca^{2+}) supported spheroplast formation with a concomitant reduction in lysis during meropenem treatment in a concentration-dependent manner (**Figure 11AB**), particularly at very high concentrations. Furthermore, combinatorial addition of excess Ca^{2+} and Mg^{2+} completely prevented lysis (**Figure 11A**). Thus, divalent cations prevent lysis during meropenem treatment, potentially through increasing the mechanical load-bearing capacity of the outer membrane through lipopolysaccharide crosslinking to protect the spheroplast structure.

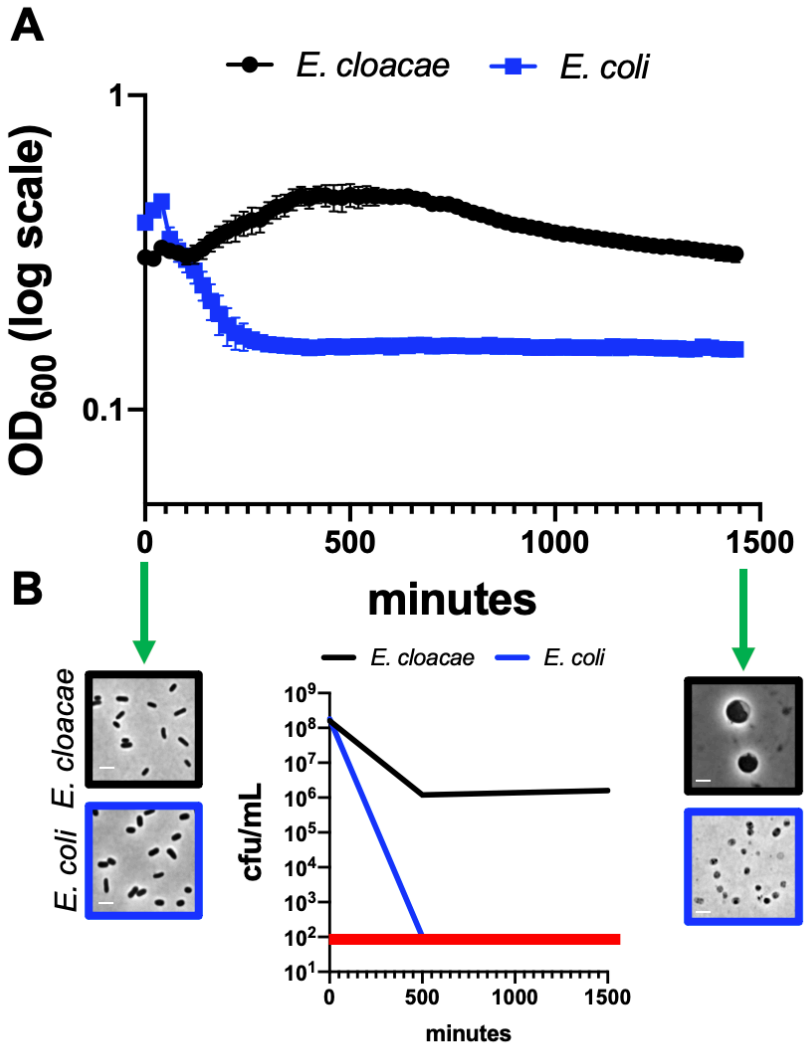

Figure 10: *Enterobacter cloacae* ATCC 13047 is highly meropenem tolerant. (A) Representative experiment demonstrating changes in OD_{600} measurements following meropenem treatment in *E. cloacae* relative to *E. coli.* Error bars represent the average of 3 technical replicates +/- standard deviation. (B) Survival was calculated as CFU/mL from the experiment depicted in (A). The red line denotes the limit of detection. Phase images from the same experiment show cells before and after meropenem exposure to illustrate spheroplast formation in *E. cloacae* and lysis in *E. coli* (only cell debris is visible in phase image). Scale bars, 2 μm.

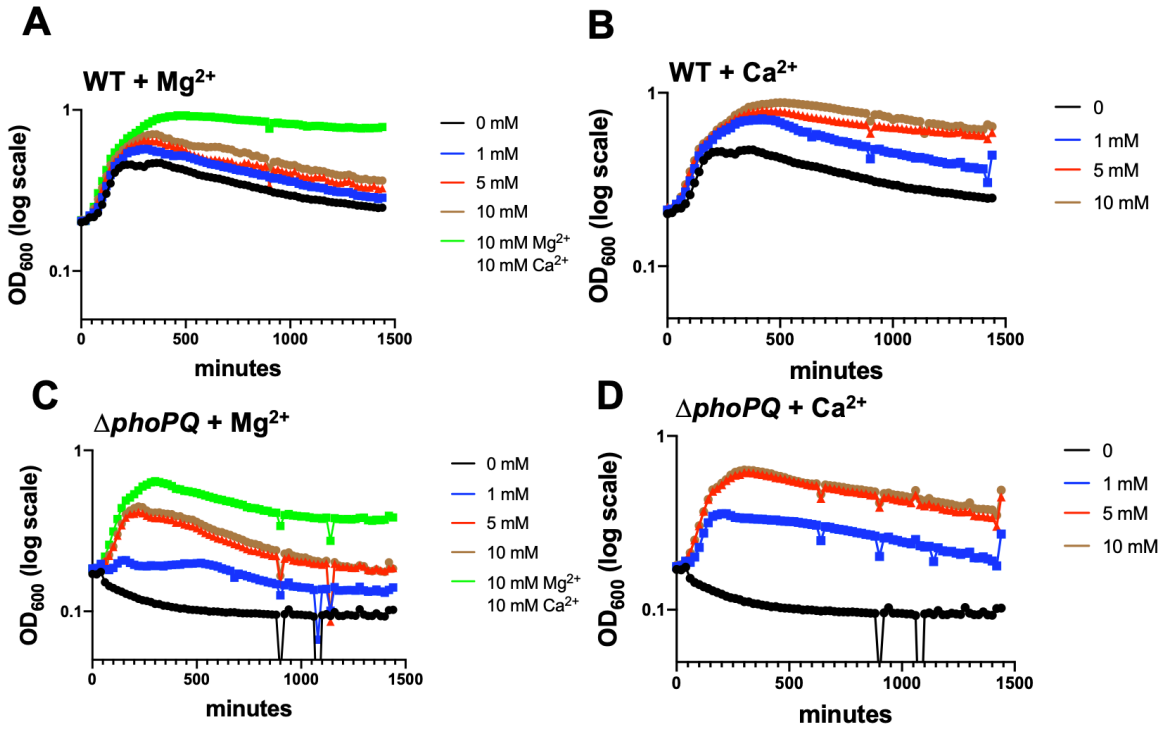

Figure 11: Addition of divalent cations prevents spheroplast lysis. Wild type (WT) (A-B) or its Δ*phoPQ* derivative (C-D) were treated as described in Figure 4.1A with addition of the indicated concentrations of (A,C) $MgSO_4$ (Mg^{2+}) or (B,D) $CaCl_2$ (Ca^{2+}). Data represent the average of 3 replicates +/- standard deviation.

When divalent cations are limiting, many Gram-negative pathogens induce outer membrane modifications (hyperacylation and/or increasing the positive charge of lipid A) to functionally substitute for divalent ionic bridges between lipopolysaccharide molecules[272]. In many Enterobacterales, these modifications are controlled by the well-studied PhoPQ two-component system (TCS)[175]. As shown in *E. cloacae*[172] and other Enterobacterales[173,273], the PhoPQ TCS directly regulates expression of the *arn* operon, which encodes enzymes that synthesize and transfer positively charged L-Ara4N moieties to lipid A, and partially regulates expression of *pagP* (coding for an outer membrane acyltransferase)[176]. In our strain of *E. cloacae*, the PhoPQ system is required to sustain “heteroresistance”, i.e. background resistance of a small subpopulation of cells

against therapeutic antimicrobial peptides like colistin[172,269,274]. To test whether the PhoPQ TCS contributes to meropenem tolerance, we measured spheroplast formation and stability over 24 hours in Δ*phoPQ.* Strikingly, OD_{600} declined sharply in Δ*phoPQ* relative to wild type, which could be fully complemented by ectopic expression of *phoPQ* (**Figure 12A**). The decline in spheroplast formation correlated with a robust 10-fold decrease in Δ*phoPQ* viability (measured by CFU/mL) relative to wild type (**Figure 12B**). Step-wise titration of Ca^{2+} and/or Mg^{2+} markedly enhanced Δ*phoPQ* tolerance (**Figure 11CD**), suggesting decreased tolerance (spheroplast formation) in Δ*phoPQ* is due to its inability to crosslink adjacent lipopolysaccharide molecules in the outer membrane[275]. To corroborate the involvement of PhoPQ, we sought to either enhance or reduce its activity and measured the effect of such perturbations on tolerance. PhoQ is antagonized by the small periplasmic MgrB protein; *mgrB* overexpression is thus expected to result in suppression of PhoPQ induction[276]. Indeed, *mgrB* overexpression from a plasmid reduced spheroplast formation (proxied by OD_{600} measurements) (**Figure 12C**) in the wild type, closely resembling the Δ*phoPQ* phenotype (**Figure 12A**). We next tested a strain deleted in *mgrB.* Modified lipid A structures in Δ*mgrB* were confirmed using matrix-assisted laser desorption ionization-time of flight mass spectrometry (MALDI-TOF MS) (**Figure 14AB**), and we also phenotypically validated this mutant. Since the PhoPQ system mediates colistin resistance and heteroresistance, the Δ*mgrB* mutant (where PhoPQ baseline levels are elevated) should be more resistant against colistin. As expected, colistin MIC was higher in the mutant (≥128 μg/mL) than in the wild type (16 μg/mL). Exposing Δ*mgrB* to meropenem resulted in an increase in OD_{600} (**Figure 13A**) that coincided with an approximately 1000-fold increased survival to meropenem relative

to wild type (**Figure 12B**). Lastly, two fully colistin-susceptible (non-heteroresistant) clinical isolates of *E. cloacae* from our collection exhibited a low-tolerance phenotype compared to ATCC 13047 (**Figure 13C**), consistent with the idea that the same OM modifications that cause colistin resistance also contribute to meropenem tolerance. Collectively, these data suggest that PhoPQ-dependent OM modifications contribute to meropenem tolerance.

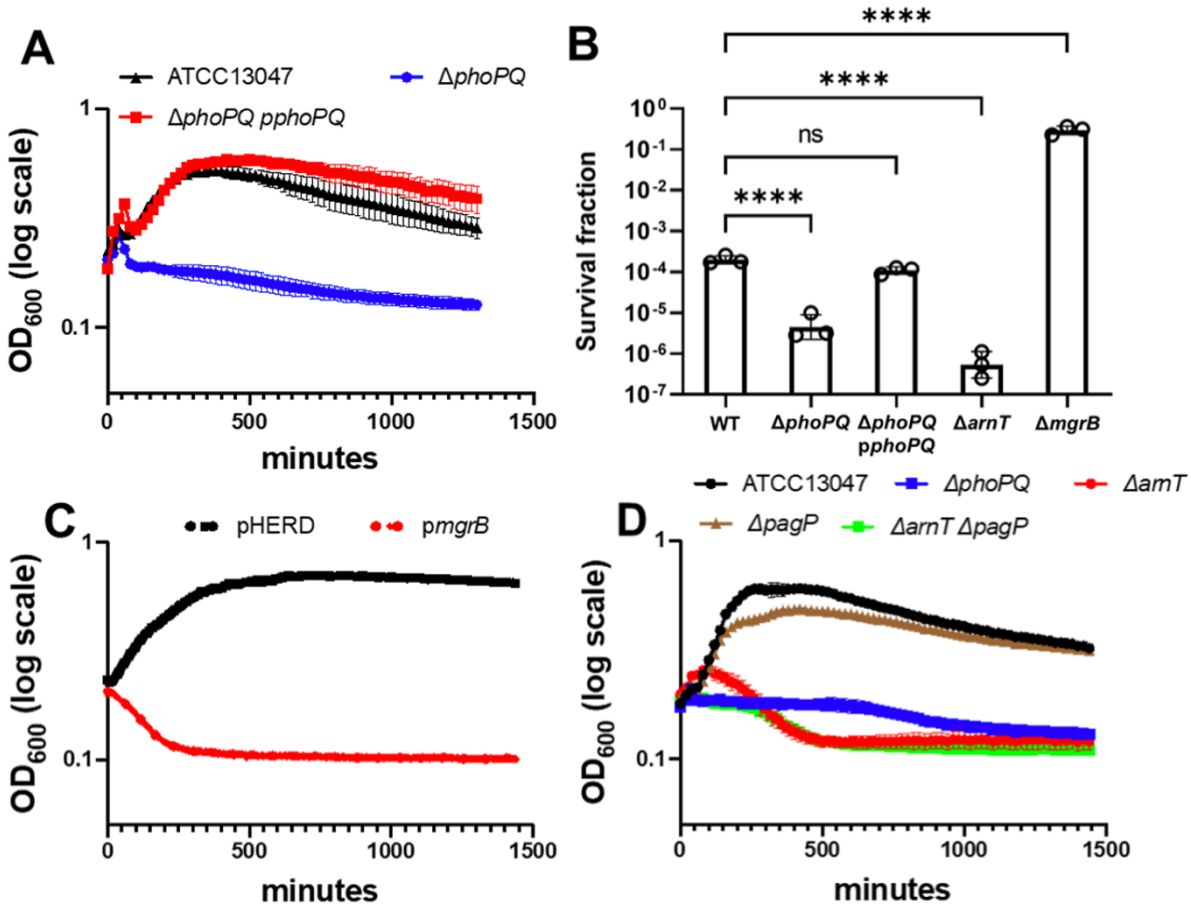

Figure 12: The PhoPQ system promotes meropenem tolerance in *E. cloacae*. (A) Spheroplast formation in response to meropenem treatment. Overnight cultures were diluted 10-fold into fresh LB medium containing 10 µg/mL meropenem and OD_{600} was measured. (B) Fraction of population surviving after 24 hours of meropenem exposure from experiments as described in (A). (C) MgrB overexpression reduces tolerance. Cells were treated as described in (A), but with the addition of 0.2 % arabinose (inducer). pHERD; empty vector. (D) The *arn* operon is required for meropenem tolerance. Experiments were conducted as described in (A). Data in each graph represent the average of 3 replicates +/- standard deviation; additional biological replicates are shown in Figure 4.4B. Statistical significance for survival fraction determined by one-way ANOVA of log transformed data, followed by Tukey's correction for multiple comparisons (ns, not significant; ****, $p \leq 0.0001$).

To dissect individual contributions of PhoPQ-regulated genes to tolerance, we created mutants in the *pagP* and *arn* loci. Specifically, we deleted *arnT*, which encodes the L-ara4N transferase which is necessary for aminoarabinose addition to lipid A[277]. While Δ*pagP* displayed spheroplast formation levels similar to wild type (**Figure 12D**), Δ*arnT* exhibited a drop in OD_{600} reminiscent of Δ*phoPQ* (**Figure 12D, Figure 13B**) and a concomitant 100-fold decrease in CFU/mL relative to wild type (**Figure 12B)**. Notably, the survival defect, as measured by CFU/mL, was consistently more pronounced in Δ*arnT* vs. Δ*phoPQ* (**Figure 12B**), suggesting either that residual L-Ara4N modification is retained in the absence of PhoPQ through basal expression of *arnT*, or that *phoPQ* induction in the absence of *arnT* is detrimental for an unknown reason.

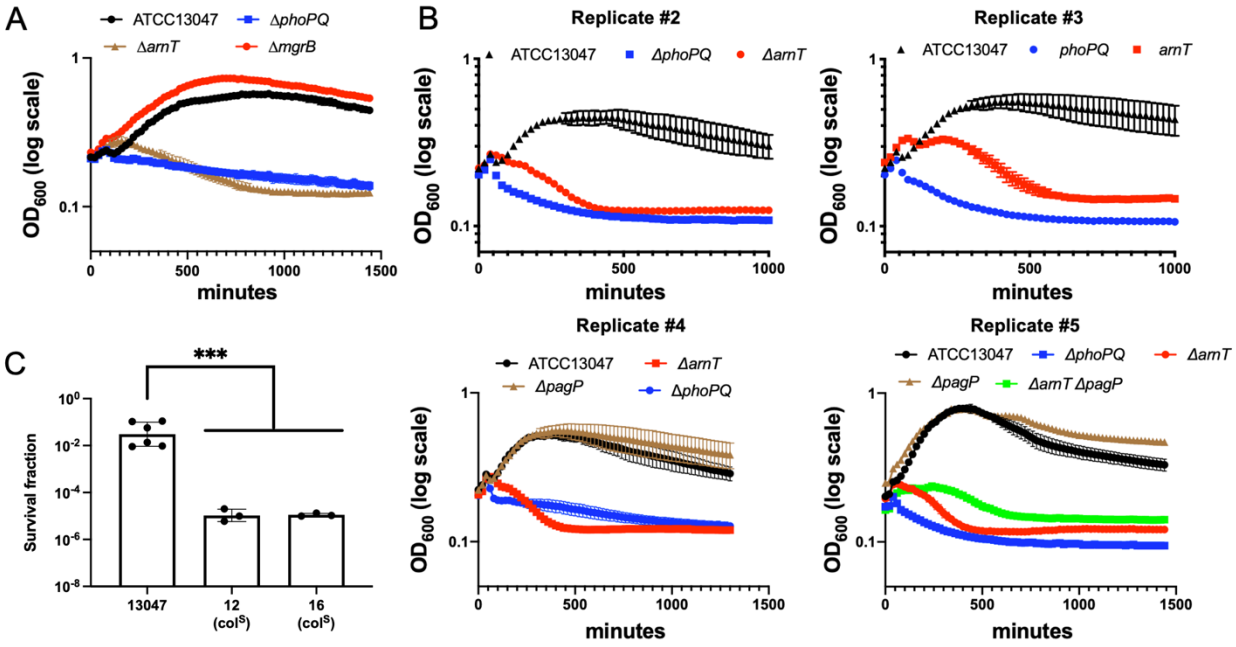

Figure 13: Independent biological replicates of experiments shown in Figure 4.1. (A) An *mgrB* mutation promotes a moderate increase in mass increase during meropenem exposure. (B) Experiments were conducted as described in Figure 4.1A legend; each graph represents experiments conducted on a different day. In addition, data in each graph represent the average of 3 biological replicates +/- standard deviation. (C) Fraction of surviving population from colistin-susceptible *E. cloacae* clinical isolates after 24 hours of meropenem exposure measured as described in Figure 4.3B.

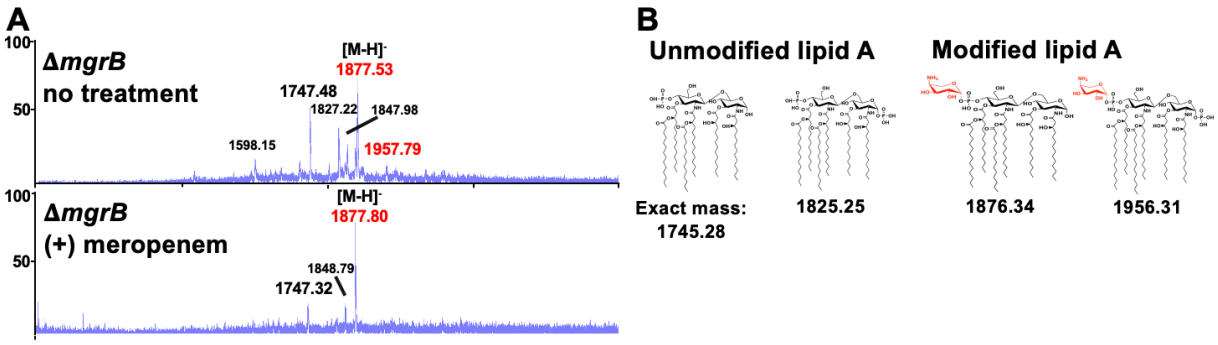

Figure 14: Analysis of lipid A from Δ*mgrB*. (A) MALDI-MS analysis of lipid A isolated from *E. cloacae* Δ*mgrB*. *m/z* corresponding with L-Ara4N modifications are illustrated in red. Each experiment was independently replicated three times, and one representative data set was reported. (B) Relevant lipid A chemical structures are shown.

Meropenem exposure induces the PhoPQ regulon

Expression of the *arn* operon in *E. cloacae* is directly regulated by phosphorylated PhoP [172]. Because we observed that PhoPQ was necessary for *arn*-mediated tolerance, we asked whether meropenem induced *arn* transcription in a PhoPQ-dependent manner. To test this, *E. cloacae* cells were exposed to meropenem for 30 minutes, after which *arnB* (the first gene in the *arn* operon and thus the most direct readout of promoter activity[172,278]), *pagP*, and *phoP* transcript levels were quantified (**Figure 15A**). Relative expression was calculated using 16s rRNA as an internal control. *phoP*, which is autoregulated[279], showed 2.5-fold higher expression in meropenem-treated cells relative to untreated. Additionally, *pagP* expression was 5-fold higher, and *arnB* expression was 6-fold higher after meropenem treatment. These results support a model where PhoPQ signaling, as well as transcription of its regulon, is induced in response to meropenem treatment.

To corroborate the qRT-PCR findings, we also constructed a fluorescent transcriptional reporter, fusing the *arnB* promoter with msfGFP, followed by fluorescence

measurements upon exposure to meropenem (**Figure 15B**). As a control, we first exposed cells to EDTA, which chelates divalent cations to destabilize the outer membrane and consequently activates PhoPQ[280]. As expected, P_{arnB}:msfGFP was induced by EDTA treatment in a *phoPQ*-dependent way (**Figure 15B**). Interestingly, meropenem treatment also robustly activated the P_{arnB}:msfGFP reporter, where a significant 3-fold fluorescence increase was measured, comparable to EDTA treatment. In contrast, meropenem only slightly (but reproducibly) increased *arnB* expression in the Δ*phoPQ* mutant under the same conditions. Thus, *arn* transcription is induced by meropenem in a primarily PhoPQ-dependent manner. conditions.

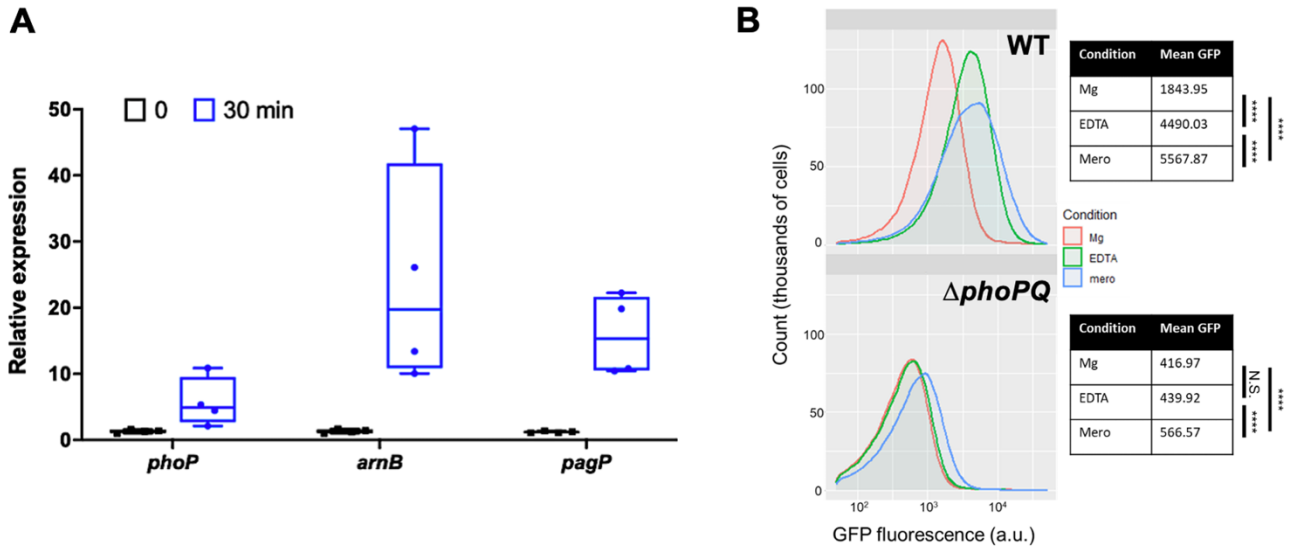

Figure 15: Expression of *arn*B in response to meropenem treatment is dependent on PhoPQ. (A) Relative expression reverse-transcription quantitative PCR (qRT-PCR) of PhoPQ regulon transcripts after meropenem exposure. Each experiment was independently replicated three times (individual data points of the three experiments are reported here). (B) Strains carrying transcriptional P_{arnB}:msGFP fusions were exposed to indicated conditions and analyzed on a C6 Accuri flow cytometer. Statistical difference between populations was determined with a one-way ANOVA followed by Tukey's correction for multiple comparisons (ns, not significant; ****, $p \leq 0.0001$).

Meropenem treatment promotes formation of L-Ara4N-*modified lipid A species in a PhoPQ-dependent manner*

The lipopolysaccharide lipid A domain is modified with L-Ara4N in a PhoPQ-dependent manner when Mg^{2+} is limiting[172]. To determine if the *E. cloacae* lipid A structure is modified with L-Ara4N in response to meropenem treatment, we isolated lipid A from treated and untreated cultures, which we then analyzed using MS and thin-layer chromatography (TLC). A distinct shift in lipid A structures was evident following 3 hours of meropenem treatment, where an increase in L-Ara4N modified vs. unmodified forms was observed (**Figure 16AB**). Notably, the lipid A species that dominated before treatment (hexa-acylated, bis-phosphorylated, *m/z* = 1825.25) decreased in abundance in favor of Arn- and PagP-modified lipid A. Doubly Arn/PagP-modified lipid A (*m/z* = 2114.14) was also produced following treatment. Notably, while L-Ara4N modification of lipid A was PhoPQ-dependent, PagP-dependent lipid A acylation was not (see below for discussion). Quantitative TLC supported the MS results and revealed a 12.21 (+/- 1.13)-fold increase in single-modified L-Ara4-N lipid A in a PhoPQ-dependent manner (**Figure 16C**).

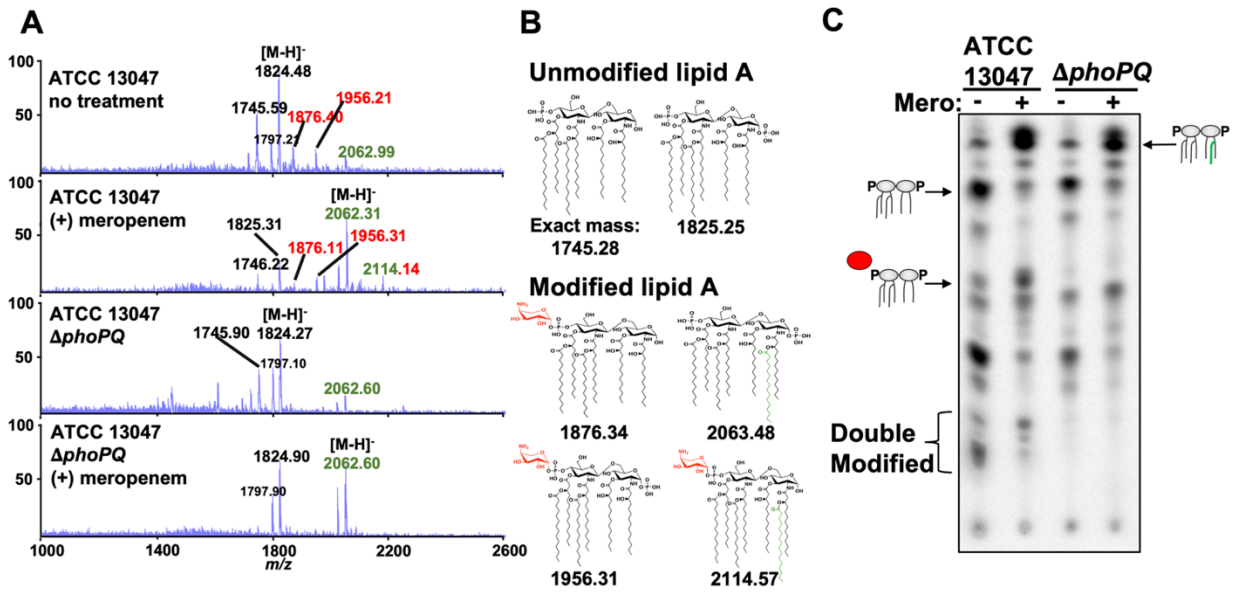

Figure 16: Analysis of *E. cloacae* lipid A after meropenem treatment. (A) MALDI-TOF MS analysis of lipid A extracted from wild-type or Δ*phoPQ E. cloacae* strains. L-Ara4N modifications are illustrated in red, while $C_{16:0}$ additions are green. Numbered labels that are both red and green contain both modifications. Each experiment was independently replicated three times, and one representative data set was reported. (B) Predicted lipid A chemical structures in wild type and Δ*phoPQ E. cloacae*. (C) ^{32}P-radiolabelled lipid A was extracted from treated or untreated wild-type or Δ*phoPQ E. cloacae.* Lipids were separated based on hydrophobicity using thin-layer chromatography. Red circle denotes L-Ara4N modification, while the green line indicates $C_{16:0}$ addition.

E. cloacae encodes a principal putative PagP acyltransferase that we denoted as PagP1 (Ecl_03072). Lipid A extracted from Δ*pagP* lacked the acyl chain induced upon meropenem treatment (**Figure 17A**), suggesting that PagP removes palmitate ($C_{16:0}$) from surface-exposed glycerophospholipids and transfers it to lipid A, as previously shown[281,282]. We also confirmed that meropenem-induced L-Ara4N modification was dependent on the *arn* operon (**Figure 17B**). Furthermore, MS analysis of Δ*phoPQ* Δ*pagP* (**Figure 17C**) and Δ*arnT* Δ*pagP* (**Figure 17D**) lipid A revealed that the mutants produced lipid A structures lacking all modifications following meropenem treatment, confirming that PagP and the *arn* operon products coordinate *E. cloacae* lipid A modifications in response to meropenem treatment. Interestingly, meropenem-induced hyperacylation was absent

in Δ*mgrB* cells (**Figure 14A**). One potential explanation is that meropenem-induced hyperacylation is a result of outer membrane glycerophospholipid accumulation in the outer leaflet of spheroplasts, a condition known to activate PagP enzymatic activity[280,283]. This model is also consistent with our observation that while PagP is partially under genetic control of PhoPQ[172], meropenem-induced hyperacylation is independent of PhoPQ (**Figure 16AC**). The absence of PagP-dependent modification in Δ*mgrB* might indicate increased outer membrane strength (and concomitant reduction in glycerophospholipid accumulation in the outer leaflet of the outer membrane) in this background. Further analysis of spheroplast membrane composition is necessary to support this model.

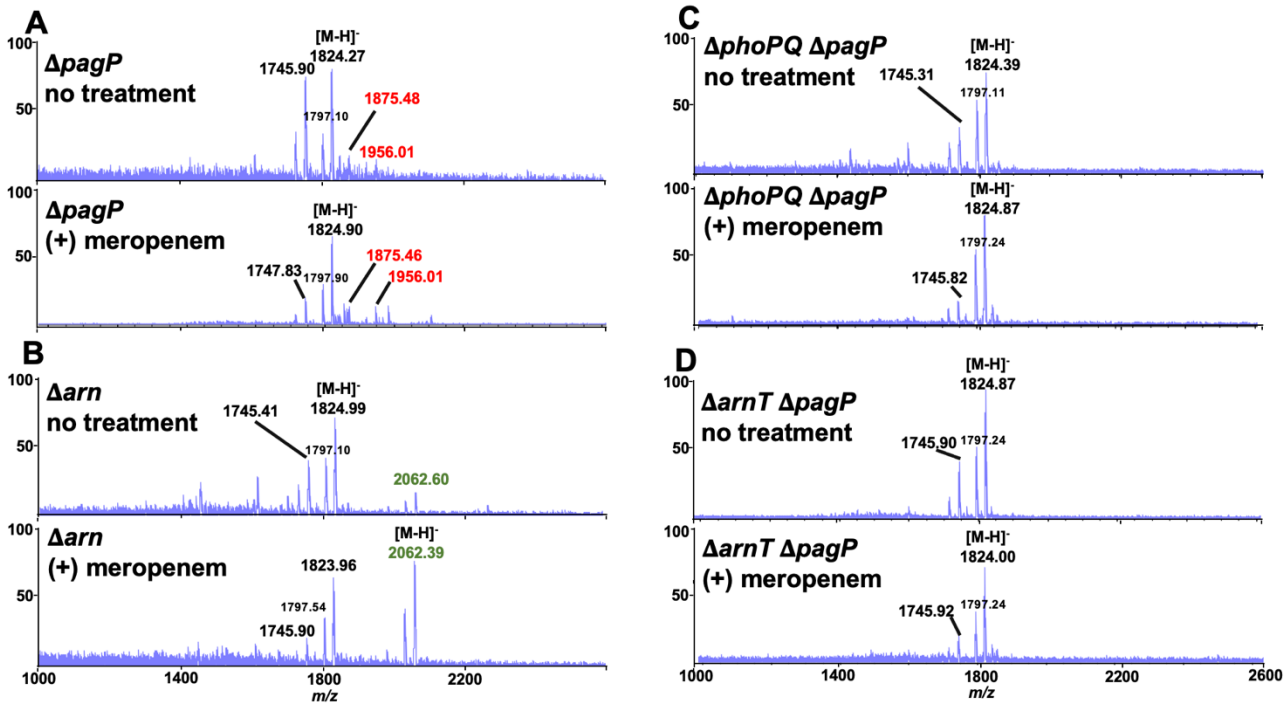

Figure 17: Analysis of lipid A from *E. cloacae* mutants. (A) MALDI-MS analysis of lipid A isolated from Δ*pagP,* (B) Δ*arn* (full operon deletion), (C) Δ*phoPQ* Δ*pagP and* (D) Δ*arnT* Δ*pagP*. *m/z* corresponding with L-Ara4N modifications are illustrated in red, while structures with altered acyl chain patterns are illustrated in green. Each experiment was independently replicated three times, and one representative data set was reported.

Based on the structural studies and our genetic evidence, we suggest PhoPQ-dependent tolerance is primarily mediated via L-Ara4N addition to lipid A. Presumably, L-Ara4N lipid A modification increases the structural integrity of the outer membrane through stabilization of lateral lipopolysaccharide interactions[275], which protects spheroplasts from high levels of internal turgor.

Colistin exposure primes* E. cloacae *for meropenem tolerance

Cationic antimicrobial peptides (CAMPs) are known inducers of the PhoPQ TCS[284]. Since our data above suggest that PhoPQ induction promotes tolerance, we hypothesized that pre-exposure to the CAMP colistin "primes" *E. cloacae* for tolerance to meropenem, potentially by inducing PhoPQ or more likely by selecting for cells that have a higher baseline level of PhoPQ induction. To test this, we measured the extent to which *E. cloacae* was killed by meropenem with and without prior growth in medium containing supra-MIC colistin; this is expected to enrich specifically for the heteroresistant (more heavily OM modified) subpopulation in *E. cloacae* ATCC 13047[172]. Interestingly, after pre-exposure to colistin, the fraction of cells surviving meropenem treatment was approximately 3.5-fold greater **(Figure 18)**. This suggests that CAMPs have the potential to induce tolerance to β-lactam antibiotics, but that the temporal conditions of treatment may determine the extent to which this effect is significant.

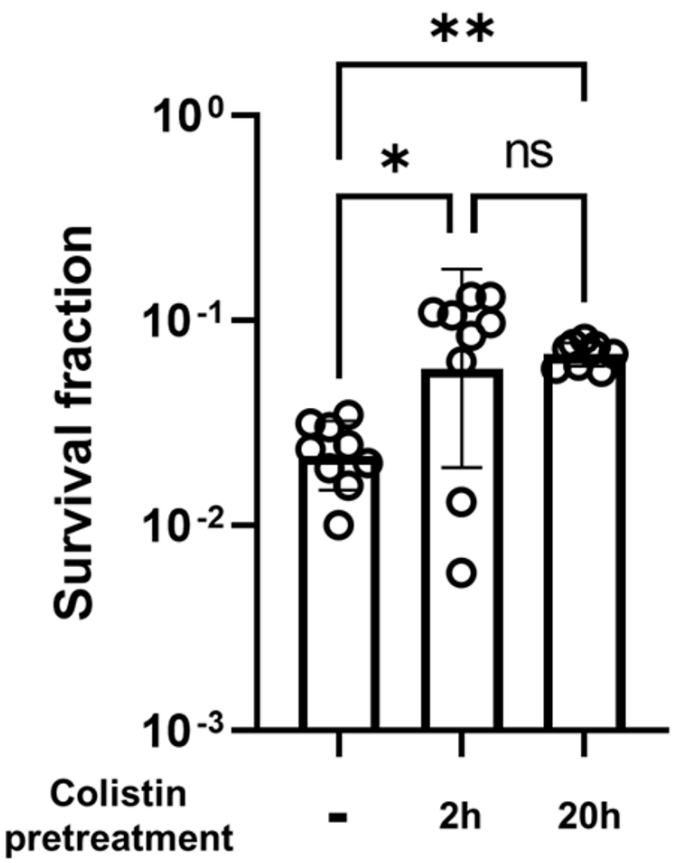

Figure 4.9: Colistin primes E. cloacae for meropenem tolerance. Overnight cultures were grown in LB +/- 20 µg/mL colistin, then diluted 10-fold into LB +/- 20 µg/mL colistin. Colistin pretreatment value represents total time exposed to colistin before exposure to 10 µg/mL meropenem. Cultures were then treated like other meropenem killing experiments (see methods). Survival fraction was calculated by dividing CFU/mL at 3h meropenem exposure by CFU/mL prior to meropenem exposure. Each bar represents the mean of 9 biological replicates, error bars represent standard deviation. Statistical significance determined by one-way ANOVA of log transformed data, followed by Tukey's correction for multiple comparisons (ns, not significant; *, $p \leq 0.05$; **, $p \leq 0.01$).

Outer membrane modifications are conserved β-lactam tolerance determinants in other Enterobacterales

We next sought to establish whether outer membrane modifications might promote tolerance in other Enterobacterales. We first turned to *Klebsiella pneumoniae* and used a hypertolerant clinical isolate (*Kp* 1084) and its Δ*phoPQ* derivative for killing experiments. We observed a striking, 10- (6 hours) to 10^5-fold (24 hours) decrease in viability in the

presence of meropenem, which could be fully complemented by expressing PhoP in trans (**Figure 19A**). We also analyzed a well-characterized *E. coli* K12 variant, WD101, engineered to constitutively upregulate the PmrAB two-component system[285] (which induces L-Ara4N modification of lipid A in *E. coli*) to test the hypothesis that outer membrane modifications increase tolerance in *E. coli* (**Figure 19B**). WD101 exhibited a dramatic, 10,000-fold increase in survival after 24 hours of meropenem exposure compared to the wild type parental strain, further supporting a role for outer membrane modifications in meropenem tolerance beyond *E. cloacae* ATCC13047.

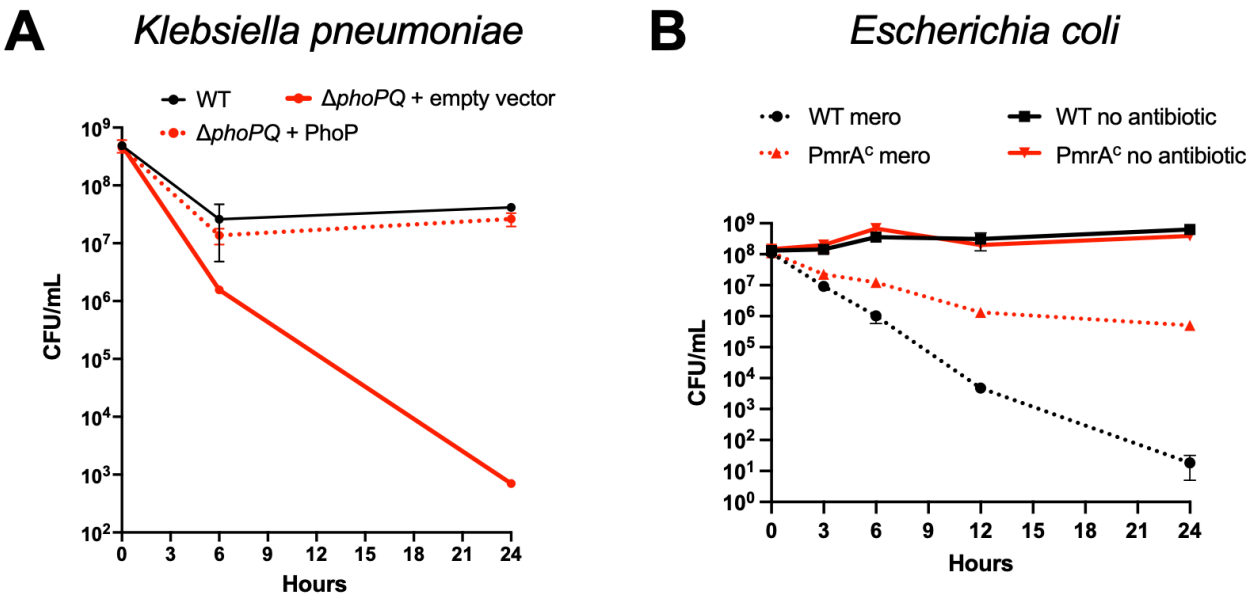

Figure 19: A conserved mechanism for meropenem tolerance in Enterobacterales. (A) *Klebsiella pneumoniae* 1084 carrying empty vector, and its Δ*phoPQ* derivative carrying either empty vector or pBAD33*phoP* ("Δ*phoPQ* + PhoP") was diluted 10-fold into BHI medium containing 10 µg/mL meropenem and 0.2 % arabinose for induction. Survival fraction is the CFU/mL after 6 hours of meropenem treatment divided by CFU/mL before treatment. Data represent averages of 3 replicates +/- standard deviation (B) *E. coli* strain W3110 (WT) or strain WD101, which has a constitutively active chromosomal copy of *pmrA* (*pmrA*^{C}), were cultured in N-minimal medium and treated with or without meropenem. Cultures were incubated statically at 37°C. CFU were enumerated at 0, 3, 6, 12 and 24 hours. Error bars indicate standard deviation. Each experiment was independently replicated three times in triplicate, and one representative data set was reported.

A small molecule inhibitor of PhoQ synergizes with meropenem and colistin in vitro

Tolerance is likely an under-appreciated contributor to antibiotic treatment failure. Antibiotic adjuvants that promote killing of tolerant cells thus have the potential to find a prominent place in our antibiotic armamentarium. Since histidine kinases like PhoQ are in principle targetable by small molecules, we tested whether his-kinase inhibitors synergized with meropenem. To this end, we turned to a previously developed suite of small molecules with potent histidine kinase inhibitory activity[286] and tested them in combination with meropenem. The anti-Amyotrophic Lateral Sclerosis (ALS) drug Riluzole, as well as its derivative Rilu-2, exhibited potent, concentration-dependent synergy in combination with meropenem to rapidly lyse tolerant *E. cloacae* cells *in vitro* (**Figure 20A, Figure 21A**). We also verified that Rilu-2 inhibited the formation of the L-ara4N lipid A structure using MALDI-TOF MS (**Figure 20B**). The peak corresponding to this modification (*m/z* 1876.29) is completely absent in Rilu-2-treated and Δ*phoPQ* cells. Since the PhoPQ system is primarily recognized for its contribution to CAMP resistance in many Enterobacterales, we next tested the Rilu compounds' ability to synergize with colistin. As expected, Rilu-2 and Riluzole indeed potentiated colistin-mediated killing (**Figure 21B**), lending additional support to a PhoQ-inhibitory role of these compounds and also confirming previous results in *Salmonella*[287]. Importantly, Riluzole is an FDA-approved treatment for ALS and could thus readily serve as an adjuvant against both meropenem-tolerant and colistin-resistant Enterobacterales.

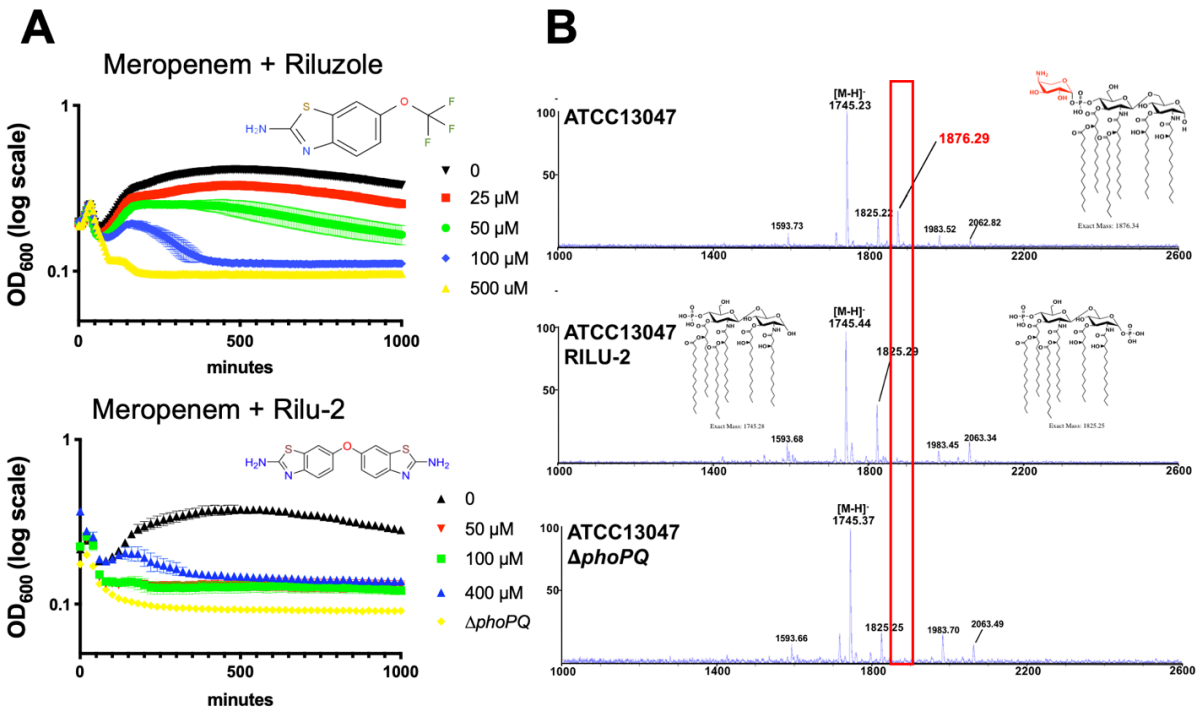

Figure 20: Rilu compounds synergize with meropenem to expedite *E. cloacae* killing. (A) Rilu compounds potentiate meropenem-induced lysis against *E. cloacae.* Overnight cultures were diluted 10-fold into fresh growth medium containing meropenem (10 µg/mL) and increasing concentrations of Riluzole or its derivative Rilu-2. Data represent the average of 3 technical replicates +/- standard deviation. (B) MALDI-MS analysis of lipid A isolated from untreated wild-type *E. cloacae*, cells treated with RILU-2 or Δ*phoPQ*. *m/z* corresponding with L-Ara4N modifications are illustrated in red. Relevant lipid A chemical structures are shown. Each experiment was independently replicated three times, and one representative data set is reported.

Discussion

While much work has been done in Enterobacterales to elucidate mechanisms of antibiotic resistance and persistence, the genetic and molecular determinants of tolerance, and especially spheroplast formation, have remained poorly understood. In contrast to resistance (continued growth) and persistence (dormancy), carbapenem-tolerant populations are initially susceptible to treatment (i.e., lose their cell wall). This phenotype is reminiscent of so-called "L-forms"[167], with the notable difference that spheroplasts do not replicate in this state, while L-forms do. This is likely a consequence

of L-forms being able to “escape” the outer membrane to then proliferate through stochastic membrane blebs[288,289].

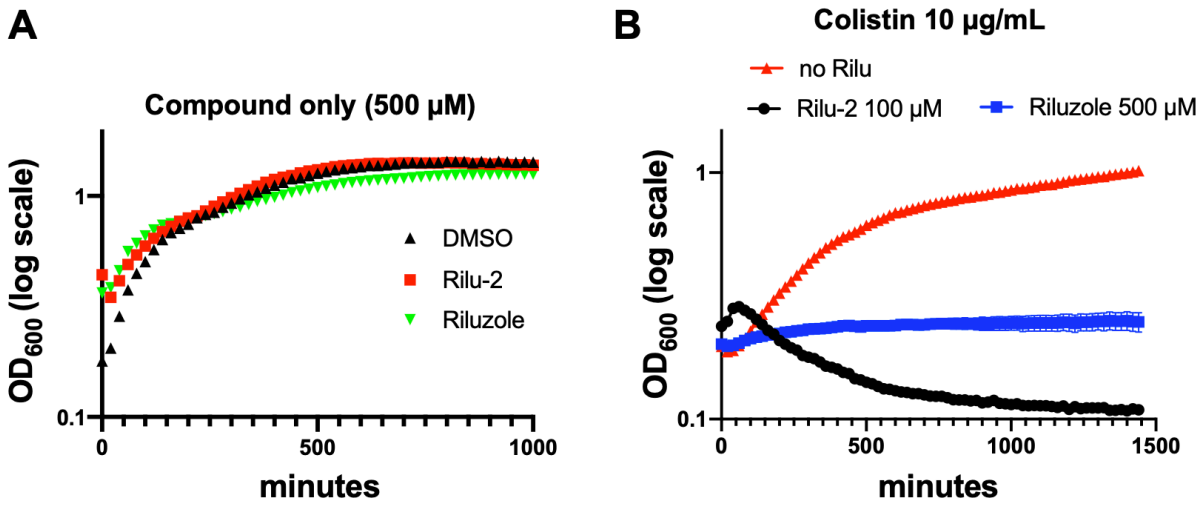

Figure 21: Rilu synergizes with colistin to enhance killing. (A) Rilu compounds do not cause lysis, but (B) potentiate colistin mediate killing. Experiments were conducted as described in Fig. 1A legend. Data represent the average of 3 replicates +/- standard deviation.

The remarkable ability of spheroplasts to survive without their PG layer lends support to the recent realization that the outer membrane has load-bearing capabilities[178] and prompted us to interrogate the molecular mechanism of outer membrane stabilization during antibiotic exposure. Our data suggest that L-Ara4N addition to lipid A is a key factor in spheroplast integrity. We propose that lipid A molecules with a positive charge increase outer membrane stability due to the enhancement of electrostatic interactions between adjacent lipopolysaccharide molecules on the surface-exposed face of the outer membrane[275]. Of note, the L-Ara4N modification has been previously implicated in resistance to CAMPs, such as colistin[172]. In this context, it is worrisome that colistin therapy can select for *mgrB* mutations[290–292], which we demonstrate here also confers high meropenem tolerance in addition to colistin resistance. Thus, treatment with antimicrobial peptide analogs (and we speculate that this may potentially apply to innate

AMPs as well) can select for bacteria that are stably tolerant to subsequent therapy with a β-lactam. Our data also suggest that colistin (and, by extension, potentially AMPs of the innate immune system) can induce transient β-lactam tolerance, likely through induction of the PhoPQ system and perhaps other protective stress responses.

However, the relationship between PhoPQ induction and tolerance is not absolute; a significant proportion of both colistin-pretreated and *mgrB*-deleted cells still lyse in the presence of meropenem. It is thus likely that colistin heteroresistant subsets are not the same as carbapenem tolerant cells. In our pre-treatment experiments with colistin, the PhoPQ system should be induced in all cells to similar degrees, yet only a fraction (0.1 %) of these cells was also meropenem tolerant. We speculate that β-lactam tolerance and colistin resistance, while relying on the same basic outer membrane modification, may each require a specific fraction of lipopolysaccharide molecules to be modified. Thus, within a sample, there may be a limited subset of cells exhibiting the correct amount of modification to enable both colistin resistance and meropenem tolerance (or even just optimal meropenem tolerance). This would explain why we observe only partial overlap between these two phenomena.

In summary, this work demonstrates a novel genetic determinant of carbapenem tolerance in clinically relevant Enterobacterales. Despite being a well-known regulator of polymyxin resistance, the PhoPQ two-component system was not previously known to respond or mediate tolerance to carbapenem treatment. As tolerance (and spheroplast formation in particular) is a possible culprit for antibiotic treatment failure[65,255,293], our results suggest a potential for combination therapies with histidine kinase inhibitors to increase the efficacy of carbapenems.

CHAPTER 5

PEPTIDOGLYCAN RECYCLING CONTRIBUTES TO OUTER MEMBRANE INTEGRITY AND CARBAPENEM TOLERANCE IN *ACINETOBACTER BAUMANNII***

Nowrosh Islam[*1], Misha I. Kazi[*1], Katie N. Kang[1], Jacob Biboy[2], Joe Gray[3], Feroz Ahmed[1], Richard D. Schargel[1], Cara C. Boutte[1], Tobias Dörr[4,5,6], Waldemar Vollmer[2], Joseph M. Boll[#1]

[1]Department of Biology, University of Texas Arlington, Arlington TX, USA; [2]Centre for Bacterial Cell Biology, Biosciences Institute, Newcastle University, Newcastle upon Tyne, United Kingdom; [3]Biosciences Institute, Newcastle University, Newcastle upon Tyne, United Kingdom; [4]Weill Institute for Cell and Molecular Biology, Cornell University, Ithaca NY, USA; [5]Department of Microbiology, Cornell University, Ithaca NY, USA; [6]Cornell Institute of Host-Microbe Interactions and Disease, Cornell University, Ithaca NY, USA

[#]Correspondence: joseph.boll@uta.edu

*Contributed equally

***In review, mBio*

Abstract

The Gram-negative cell envelope is an essential structure that not only protects the cell against lysis from the internal turgor, but also forms a barrier to limit entry of antibiotics. Some of our most potent bactericidal antibiotics, the β-lactams, exploit the essentiality of the cell envelope by inhibiting its biosynthesis, typically inducing lysis and rapid death. However, many Gram-negative bacteria exhibit “antibiotic tolerance”, the ability to sustain viability in the presence of β-lactams for extended time periods. Despite several studies showing that antibiotic tolerance contributes directly to treatment failure, and is a steppingstone in acquisition of true resistance, the molecular factors that promote intrinsic tolerance are not well-understood. *Acinetobacter baumannii* is a critical-threat nosocomial pathogen notorious for its ability to rapidly develop multidrug resistance. While typically reserved to combat multidrug resistant infections, carbapenem β-lactam antibiotics (i.e., meropenem) are first-line prescriptions to treat *A. baumannii* infections. Meropenem tolerance in Gram-negative pathogens is characterized by morphologically distinct populations of spheroplasts, but the impact of spheroplast formation is not fully understood. Here, we show that susceptible *A. baumannii* clinical isolates demonstrate high intrinsic tolerance to meropenem, form spheroplasts with the antibiotic and revert to normal growth after antibiotic removal. Using transcriptomics and genetics screens, we characterized novel tolerance factors and found that outer membrane integrity maintenance, drug efflux and peptidoglycan homeostasis collectively contribute to meropenem tolerance in *A. baumannii*. Furthermore, outer membrane integrity and peptidoglycan recycling are tightly linked in their contribution to meropenem tolerance in *A. baumannii*.

Introduction

The cell envelope is a dynamic barrier composed of an inner (cytoplasmic) membrane, a periplasm that includes a thin peptidoglycan (PG) layer and an outer membrane, which is a selective barrier that restricts entry of toxins and antibiotics. While the PG layer is known to protect against bursting due to the cell turgor, the outer membrane also protects against lysis when external osmotic conditions change[178]. Perturbation of the outer membrane or PG envelope layers induces lysis, but regulated responses that fortify the envelope can maintain envelope homeostasis to promote pathogen survival during stress exposure[294].

Antibiotic treatment failure is a growing threat to public health and has primarily been associated with antibiotic resistance (i.e., the ability to grow in the presence of antibiotics). However, antibiotic tolerance, a population's ability to survive otherwise toxic levels of transient antibiotic treatment for extended periods, likely acts as a stepping-stone to true resistance[63,75,256]. Antibiotic tolerance is characterized by survival of cell populations in a non-dividing state, where the minimal inhibitory concentration does not change and cells revert to normal growth when the antibiotic is removed, degraded or diluted[12,65,255]. Molecular factors that extend survival during treatment, increase the probability of resistance-conferring mutations or horizontal gene transfer to occur[75].

Carbapenems are important β-lactam therapeutics because they possess potent broad-spectrum activity and are not susceptible to common resistance mechanisms[8,93]. In fact, meropenem is a last-line carbapenem antibiotic used to treat multidrug resistant Gram-negative infections[94,98]. While meropenem treatment is typically reserved to fight multidrug resistant bacteria, it is a first-line prescription against the highly drug resistant

nosocomial pathogen, *Acinetobacter* baumannii[295,296]. Carbapenem-resistant *A. baumannii* has become commonplace among hospital acquired infections. In 2019 the Center for Disease Control listed carbapenem-resistant *A. baumannii* as one of the most urgent threats to public health[297], and a recent report by the World Health Organization prioritized the pathogen as critical for new antibiotic development[3], underscoring the severity.

We reasoned that since tolerance is a prerequisite for true resistance, factors that promote carbapenem tolerance may be widespread among susceptible *A. baumannii* strains. Defining intrinsic tolerance factors in *A. baumannii* may offer fundamental insight into how resistance mechanisms rapidly spread among populations and provide new targets to combat tolerant pathogens. While our understanding of resistance mechanisms that cause antibiotic treatment failure has been well-documented, tolerance factors that precede acquisition of true resistance are limited.

Here, we show that susceptible *A. baumannii* strains, including laboratory-adapted strains and recent clinical isolates, survive for extended periods (>24 h) in high levels of meropenem, demonstrating widespread tolerance. Meropenem induces cell wall-deficient spheroplast formation in *A. baumannii*, as shown in other Gram-negative pathogens[15,19,20]. After removal of the antibiotic, cells rapidly revert to the canonical *A. baumannii* coccobacilli morphology and resume growth. Transcriptome sequencing analysis at timepoints leading to spheroplast formation showed differential expression of genes that coordinate a regulatory response to reduce the intracellular meropenem concentration. During meropenem treatment, outer membrane integrity and permeability contribute to fitness, which we show are also impacted by defects in the PG recycling

pathway. PG recycling is also a major contributor to *A. baumannii* survival during meropenem treatment, where disruption of genes encoding periplasmic and cytoplasmic PG maintenance enzymes compromise outer membrane integrity. Lastly, we also define PBP7 (encoded by *pbpG*) and LdtK enzymatic activities, which are tolerance determinants in *A. baumannii.* Together, these studies show several pathways that coordinate in *A. baumannii* to limit meropenem-induced cell envelope damage. These findings provide new targets to direct antimicrobial therapies and prevent the spread of resistance.

Materials and Methods

Bacterial strains and growth

All *A. baumannii* strains were grown aerobically from freezer stocks on Luria-Bertani (LB) agar at 37°C. Antibiotics were used at the following concentrations unless noted otherwise: 25 mg/L kanamycin, 10 mg/L meropenem, 10 mg/L tetracycline.

Construction of genetic mutants

A. baumannii pbpG, ampD, ompA mutants were constructed as described previously[177,267], using the recombination-mediated genetic engineering (recombineering) method[177]. Briefly, a kanamycin resistance cassette flanked by FLP recombination target (FRT) sites was PCR amplified from the pKD4 plasmid using primers containing 125-bp flanking regions of homology to the gene of interest. The resulting linear PCR product was then transformed via electroporation into *A. baumannii* strains ATCC 17978 expressing pREC$_{Ab}$ (pAT03). Transformants were recovered in Luria broth and plated on

LB agar supplemented with 7.5 mg/L kanamycin. All genetic mutants were confirmed by PCR.

Following isolation of genetic mutants, the pMMB67EH::REC_{Ab} Tet^R plasmid was removed as described previously[177]. Isolated mutants were grown on LB agar supplemented with 2 mM nickel (II) chloride ($NiCl_2$) and replica plated on LB agar supplemented with kanamycin or tetracycline. Loss of pMMB67EH::REC_{Ab} Tet^R plasmid in mutants susceptible to tetracycline and resistant to kanamycin were confirmed using PCR. To excise chromosomal insertion of the kanamycin resistance cassette, cured mutants were transformed with pMMB67EH carrying the FLP recombinase (pAT08) and plated on LB agar supplemented with tetracycline and 2mM Isopropyl β-d-1thiogalactopyranoside (IPTG) to induce expression of FLP recombinase. Successful excision of the kanamycin resistance cassette was confirmed using PCR.

pPBP7 was constructed by amplifying the *pbpG* (A1S_0237) coding sequence (encoding PBP7) with 200-bp upstream and downstream flanking regions was amplified from *A. baumannii* ATCC 17978 chromosomal DNA (cDNA) and cloned into XhoI and KpnI restriction sites in the pABBRkn^R plasmid. The resulting pPBP7 plasmid was transformed into *A. baumannii* ATCC 17978 Δ*pbpG* background for complementation using the native promoter.

AmpD and OmpA complementation vectors were constructed similarly with slight alterations. The *ampD* (A1S_0045) and *ompA* (A1S_2840) coding sequences were amplified from *A. baumannii* ATCC 17978 cDNA and cloned into BamHI and SalI restriction sites in the pMMB67EHkn^R plasmid. The resulting pAmpD and pOmpA

plasmids were transformed into the respective mutant and induced with 2 mM IPTG for complementation.

Fluorescent NADA staining

Overnight cultures were grown with shaking at 37°C in 5 mL of BHI (BD Difco Bacto Brain Heart Infusion) broth. The following day, cultures were back diluted at 1:10 in fresh BHI media (total volume 5 mL) containing without or with meropenem. 2 μL of 10 mM NBD (linezolid-7-nitrobenz-2-oxa-1,3-diazol-4-yl)-amino-D-alanine (NADA) (Thermo Fisher) was added to each tube and incubated at 37°C. At noted time points 6, 12, and 24 h, cultures (5 mL) were washed twice in BHI broth and fixed with phosphate-buffered saline containing a (1:10) solution of 16% paraformaldehyde. For spheroplast recovery, 12 h treated cultures were washed 3 times in BHI to remove the excess meropenem and resuspended in fresh BHI. 10 mM NADA was added and incubated for 12 h at 37°C before fixing the cells for microscopy.

Microscopy

Paraformaldehyde-fixed cells were immobilized on 1.5% agarose pads and imaged using an inverted Nikon Eclipse Ti-2 widefield epifluorescence microscope equipped with a Photometrics Prime 95B camera and a Plan Apo 100x 1.45-numerical-aperture lens objective. Phase-contrast and fluorescence images were collected with NIS Elements software. Green fluorescence images were taken using a Sola LED light engine and filter cube with 632/60 or 535/50 emission filters.

Image analysis

Microscopy images were processed and pseudo colored with ImageJ Fiji[298]. A cyan lookup table was applied to NADA images. Cells shape (length, area, width and

fluorescence intensities) were quantified in MicrobeJ[299] and data were plotted in Prism 9 (GraphPad 9.2.0). Each experiment and independently replicated three times, one representative data was reported in the quantification and one representative image was included in the figure.

RNA-sequencing

Transcriptome sequencing analysis was performed as described previously with modification[260]. Briefly, the Direct-Zol RNA MiniPrep kit (Zymo Research) was used to extract total RNA from *A. baumannii* ATCC 17978 cultures either treated with meropenem or an equivalent volume of water as blank at 0.5, 3, and 9 h at 37°C in triplicate. Turbo DNA-free DNA removal kit (Invitrogen) was used to remove genomic DNA contamination. DNase-depleted RNA was sent to the Microbial Genome Sequencing Center (MiGS) for Illumina NextSeq 550 sequencing. CLC genomic workbench software (Qiagen) was used to align the resulting sequencing data to the *A. baumannii* ATCC 17978 genome annotations and determine the RPKM expression values and the weighted proportions fold change of expression values between meropenem treated and treated samples. Baggerley's test on proportions was used to generate a false discovery rate adjusted *P*-value. The weighted proportions fold change of expression values between samples was used to generate pathway-specific heatmaps in Prism 9. The sequencing data has been deposited in the National Center for biotechnology's Gene Expression Omnibus.

Transposon insertion sequencing

Transposon sequencing was performed as described previously[157,260,267,300]. Briefly, pJNW684 was conjugated into wild-type *A. baumannii* strain ATCC 17978 to generate a library of ~400,000 mutants. The transposon mutant library was pooled and

screened for survival with and without meropenem treatment at 6 h at 37°C. Genomic DNA (gDNA) from meropenem treated and untreated cultures was isolated, sheared and transposon junctions were amplified and sequenced. Frequency of transposon insertions was compared between meropenem treated and untreated conditions to determine fitness determinants that contribute to carbapenem tolerance in *A. baumannii.*

Time-dependent killing assays

Meropenem killing experiments were performed as previously described with slight alteration[21]. Wild type, mutant and complementation strains were grown overnight in Luria broth at 37°C. The following day, overnight cultures were back diluted 1:10 in fresh, prewarmed BHI broth containing meropenem or an equivalent volume of water. Diluted BHI cultures were then incubated at 37°C. At 0, 3, 6, 12, and 24 h, each sample was diluted 4-fold in blank BHI, and the optical density (OD_{600}) was measured. At each time point, cells were serially diluted 10-fold in fresh BHI broth and either 5 μL of each serial dilution was spot-plated, or 100 μL of each dilution was plated on LB agar. Spot-plates were imaged and CFUs were calculated after 24 h at 37°C. Each experiment was independently replicated three times, and one representative dataset was reported.

Construction of PBP7 and LdtK active-site mutants

Site-directed mutagenesis was performed, as previously described with *ldtK (*A1S_2806)[267]. Briefly, the *pbpG* coding sequence was amplified from *A. baumannii* ATCC 17978 cDNA, cloned into the BamHI restriction site in pUC19 and transformed into *E. coli* C2987 chemically competent cells (New England Biolabs, Inc). pUC19::PBP7 was used as a template for Pfu-mediated deletion mutagenesis. DpnI-digested PCR reactions were transformed into *E. coli* C2987 chemically competent cells and plated on LB agar

supplemented with 75 mg/L carbenicillin. All mutants were confirmed by PCR and Sanger sequencing.

Construction of PBP7 and LdtK overexpression strains

pbpG and *ldtK* coding sequences were amplified from *A. baumannii* ATCC 17978 cDNA and *pbpG*$_{S131A}$ and *ldtK*$_{C138S}$ were amplified from pUC19::*pbpG*$_{S131A}$ and pUC19::*ldtK*$_{C138S}$ plasmid DNA using primers containing his$_{8X}$-tag sequence. Amplicons were cloned into NdeI and BamHI restriction sites in pT7-7Kn and transformed into *E. coli* C2987 chemically competent cells, resulting pT7-7Kn::*pbpG,* pT7-7Kn::*pbpG*$_{S131A}$, pT7-7Kn::*ldtK* and pT7-7Kn::*ldtK*$_{C138S}$. Constructs were confirmed using Sanger sequencing and transformed into chemically competent *E. coli* C2527 (BL-21) (New England Biolabs, Inc) for purification, expression and western blotting.

Purification of recombinant PBP7 and LdtK

BL21 cells containing carrying pT7-7Kn::*pbpG,* pT7-7Kn::*pbpG*$_{S131A}$, pT7-7Kn::*ldtK* and pT7-7Kn::*ldtK*$_{C138S}$ were grown in 500 mL Luria broth and 1 mM IPTG at 37°C for 7 h. Cells were collected and washed in cold 1x Phosphate-buffered saline (PBS), pelleted and the supernatant was removed. The dry pellet was frozen at -80°C overnight. The pellet was thawed on ice and resuspended in 20 mL lysis buffer (20 mM Tris, 300 mM NaCl, 10 mM imidazole; pH 8). Samples were sonicated for 20 s on and off for 10 min at 60% amplitude (Qsonica Q125 Sonicator). Cells were centrifuged at 20,000 x g for 0.5 h at 4°C. Supernatant was incubated with lysis buffer washed HisPur Ni-NTA Resin (Thermo Scientific) on a rotator for 2 h at 4°C. Sample was added to a 10 mL protein purification column containing a porous polyethylene disk (Thermo Scientific) and allowed to gravity drip. The column was washed 3x with 20 mL lysis buffer and increasing concentrations of additional imidazole at each wash (0 mM, 15 mM, and 30 mM). 500 μl

of elution buffer (20 mM Tris, 300 mM NaCl, 250 mM imidazole; pH 8) was incubated with the column for 5 min then gravity eluted 9 times. The elution fractions containing protein, as determined by a protein gel, were injected into a 10 mW dialysis cassette (Thermo Scientific) and dialyzed over-night in dialysis buffer (10 mM Tris, 50 mM KCl, 0.1 mM EDTA, 5% glycerol; pH 8) at 4°C. Purified protein was collected and verified using western blot with an anti-his antibody.

Isolation of outer membrane vesicles

Outer membrane vesicles were isolated as described previously[267]. Briefly, overnight cultures were back-diluted to OD_{600} 0.01 in 100 mL Luria broth and grown to stationary phase at 37°C. Cultures were then pelleted at 5000 x g for 15 min at room temperature and the supernatant was filtered through a 0.45 mm bottle-top filter. Filtered supernatant was ultracentrifuged (Sorvall WX 80+ ultracentrifuge with AH-629 swinging bucket rotor) at 151,243 x g for 1h at 4°C. Following final ultracentrifugation, outer membrane vesicle pellet was resuspended in 500 mL cold membrane vesicle buffer (50 mM Tris, 5 mM NaCl, 1 mM $MgSO_4$; pH 7.5). Outer membrane vesicles were repeated three times in duplicate, one representative data set was reported.

Quantification of total outer membrane vesicle proteins

Bradford assay was used to determine outer membrane vesicle protein concentration, as previously described[267]. To generate a standard curve, bovine serum albumin (BSA) was diluted 0 to 20 mg/mL in Pierce Coomassie Plus assay reagent (ThermoFisher) to a final volume of 1 mL. Outer membrane vesicles were diluted 2, 5, 10, 15, 20 μL in reagent to a final volume of 1 mL. A microplate spectrophotometer (Fisherbrand AccuSkan) was used to measure the absorbance (OD_{595}) of standard and samples in a 96-well plate (BrandTech). Protein concentrations were determined by

comparing the optical densities of samples to the standard curve plotted in Microsoft Excel and final quantifications were graphed in GraphPad Prism 9. Experiments were reproduced three times from each outer membrane vesicle isolation, and one representative data set was reported.

Quantification of outer membrane vesicle 3-deoxy-D-manno-oct-2-ulosonic acid (Kdo) concentrations

Kdo assays were carried out as described previously[267,301]. For the standard curve, Kdo standard (Sigma) was diluted 0 to 128 μg/mL in 50 μL of DI water. 50 μL of 0.5 M sulphuric acid (H_2SO_4) was added to 50 μL of isolated outer membrane vesicles and freshly prepared 50 μL dilutions of the Kdo standard. Outer membrane versicles in 0.5 M H_2SO_4 were boiled for 8 min to release the Kdo sugars. Samples were allowed to cool for 10 min at room temperature. 50 μL of 0.1 M periodic acid was added to outer membrane vesicles and Kdo standards and incubated at room temperature for 10 min. Following incubation, 200 μL of 0.2 M sodium arsenite in 0.5 M hydrochloric acid (HCl) was added to outer membrane vesicles and Kdo standards followed by 800 μL of 0.6% freshly prepared thiobarbituric acid (TBA). All samples were boiled for 10 min and allowed to cool at room temperate for 30-40 min. Prior to optical density measurements, purified Kdo was extracted using *n*-butanol equilibrated with 0.5 M HCl. Optical density was measured at OD_{552} and OD_{509} (Fisherbrand AccuSkan microplate spectrophotometer) in disposable polystyrene cuvettes (Fisherbrand). A linear Kdo standard curve was generated by subtracting OD_{552} measurements from OD_{509} measurements in Microsoft Excel and final quantifications were graphed in GraphPad Prism 9. Experiments were reproduced three times from each outer membrane vesicle isolation, and one representative data set was reported.

Ethidium bromide permeability assay

Permeability assays were done as previously described[302], with slight modifications. Briefly, overnight cultures were grown in 5 mL BHI medium, normalized and back diluted (1:10) in BHI with and without meropenem. Cultures were withdrawn at 0, 6 and 12 h and washed 3 times with PBS and normalized based on OD_{600}. 180 μL of the cultures was added to 96 well black plate and 6 μM EtBr was added immediately before fluorescence measurements. The relative fluorescence unit was analyzed using synergy multi-mode plate reader (530 nm excitation filter, 590 nm emission filter and 570 nm dichroic mirror). The temperature was adjusted to 25°C and read at 15 s intervals for 0.5 h. Assays were repeated three times in triplicate, one representative data set was reported. The mean RFU for each sample was calculated and plotted by Prism 9. Experiments were reproduced three times, and one representative data set was reported.

PG isolation

Biological replicates were grown to mid-logarithmic or stationary phase in 400 mL of Luria broth. Cells were centrifuged (Avanti JXN-26 Beckman Coulter Centrifuge, Beckman Coulter JA-10 rotor) at 7,000 x g for 0.5 h at 4°C, resuspended in chilled 6 mL PBS and lysed via drop-wise addition to boiling 8% sodium dodecyl sulfate (SDS). PG was further purified as previously described[303]. Briefly, muropeptides were cleaved from PG by Cellosyl muramidase (Hoechst, Frankfurt am Main, Germany), reduced with sodium borohydride and separated on a 250 x 4.6 mm 3 μm Prontosil 120-3-C_{18} AQ reversed phase column (Bischoff, Leonberg, Germany). The eluted muropeptides were detected by absorbance at 205 nm. Eluted peaks were designated based on known

published chromatograms[260,267,304]; new peaks analyzed by MS/MS, as previously done[267].

Activity Assays

PBP7 activity assays were carried out in a final volume of 50 μl containing 20 mM Hepes pH 5.0, 6.0 or 7.5, 50 mM NaCl and 2 μM PBP7 or $PBP7_{S131A}$. PG from *E. coli* D456 was added, and the reaction mixture was incubated at 37°C for 16 h. The reaction was stopped by boiling the samples for 10 min. The reaction was reduced with sodium borohydride and acidified to pH 4.0-4.5. *E. coli* D456 PG at pH 5.0 buffer conditions served as control. Muropeptides were analyses as previously described[303].

LdtK activity assays were carried out in a final volume of 50 μl containing 20 mM NaP pH 5.0 and 10 μM LdtK or $LdtK_{C138S}$. PG from *E. coli* BW25113 (WT, tetra-muropeptide-rich) or CS703-1 (multiple mutations in penicillin-binding proteins, penta-muropeptide-rich) was added, and the reaction mixture was incubated at 37°C for 4 h. The reaction was stopped by boiling the samples for 10 min. Muropeptides were reduced with sodium borohydride. Muropeptides were analyses as previously described[303].

Protein Localization

Cells were grown to mid-logarithmic or stationary phase and normalized to a density of OD_{600} 0.75 in 20 mL. Cultures were washed twice with chilled 1x PBS + 0.1% gelatin (PBSG) and resuspended in chilled 2 mL PBSG containing 2 mg/mL Polymyxin B sulfate (MilliporeSigma) then agitated for 0.5 h at 4°C. Spheroplasts pelleted at 20,000 x g for 0.5 h at 4°C. The remaining supernatant was centrifuged at 20,000 x g for 0.5 h at 4°C. Supernatant was collected and saved as the periplasmic fraction. Previously pelleted spheroplasts were resuspended in 1 mL 10mM 4-(2-hydroxyethyl)-1-

piperazineethanesulfonic acid (HEPES) buffer solution (Gibco) and 100 μl was collected as whole spheroplasts. Remaining spheroplasts were sonicated 15 seconds on and 15 seconds off 10 times at 60% amplitude (Qsonica Q125 sonicator). Lysed spheroplasts were pelleted at 16,000 x g for 0.5 h at 4°C. Supernatant was centrifuged another 0.5 h for 16,000 x g at 4°C. Insoluble pellet was saved as total membrane fraction. Soluble supernatant was saved as the cytoplasmic fraction. Experiments were reproduced three times, and one representative data set was reported.

Immunoblots

All western blot analysis was performed using 4-12% Bis-Tris 10-well protein gels (Invitrogen) and NuPage MES SDS running buffer (Novex). Gels were transferred with NuPage transfer buffer (Novex) to 0.45 μm polyvinylidene difluoride (PVDF) (Amersham Hybond) membranes. All blots were blocked in 5% milk and 1x tris-buffered saline (TBS) for 2 h. Primary rabbit antisera, anti-LdtK and anti-RpoA were used at 1:750 dilution. Antirabbit horseradish peroxidase (HRP) secondary antibody was used at 1:10,000 (Thermo Fisher Scientific). Primary mouse antisera, 5x-His mouse anti-tag was used at 1:500 (Invitrogen). Anti-mouse HRP secondary antibody was used at 1:10,000 (Invitrogen). SuperSignal West Pico Plus (Thermo Fisher Scientific) was applied to detect relative protein concentrations.

For localization assays: whole cell lysate, whole spheroplasts and membrane fractions were mixed with 1x loading dye containing 4% 2-Mercaptoethanol (Fisher Chemical) and boiled for 10 min. 10 μl of each sample was used. 132 μl of the periplasmic or cytoplasmic fractions were added to 66 μl of 3x loading buffer containing 4% 2-Mercaptoethanol (Fisher Chemical) and boiled for 10 min. 60 μl of each sample was used.

Each sample was loaded into 4-12% Bis-Tris 10-well protein gels (Invitrogen) for immunoblotting.

For protein purification: 1 μg of purified protein was combined with 3x loading buffer containing 4% 2-Mercaptoethanol and boiled for 10 min. The sample was loaded into 412% Bis-Tris 10-well protein gel (Invitrogen) for immunoblotting.

Polyclonal antibody generation

Peptide fragments of LdtK and RpoA was used to generate two rabbit polyclonal antibodies against by Life Technologies Corporation (Grand Island, NY). Collected serum was tested for LdtK and RpoA reactivity in an enzyme-linked immunosorbent assay (ELISA) with peptide fragments and via western blot against whole-cell lysates.

Minimal inhibitory concentrations (MICs)

MICs were determined using the Broth Microdilution (BMD) method, as previously outlined[172]. Overnight cultures were back diluted to OD_{600} 0.01 and 100 μL of cells was added to each well of a 96-well round-bottom polypropylene plate (Grenier Bio-One). Meropenem diluted in water was serially diluted and 150 μL of each meropenem serial dilution was also added to each well. Plates were incubated overnight at 37° C and growth was measured by reading OD_{600} after 24 h of incubation. The lowest concentration of meropenem at which no bacterial growth was observed was determined to be the MIC. Assays were repeated three times in triplicate, one representative data set was reported.

Statistical Analysis

Tests for significance in cell morphology, fluorescence intensity, outer membrane vesicle production were conducted using the Student *t*-test (two-tailed distribution with

two-sample, equal variance calculations). Statistically significant differences between relevant strains possessed $P < 0.05$.

Results

Meropenem susceptible A. baumannii strains are tolerant, form spheroplasts and resume normal morphology and growth upon removal of the bactericidal antibiotic

It was previously shown that *Vibrio* cholerae[15,20], *Pseudomonas* aeruginosa[19] and pathogens in the Enterobacterales order[21,305] form viable, non-dividing spheroplasts when exposed to lethal concentration of β-lactam antibiotics over several hours. Importantly, spheroplasts revert to normal rod-shaped growth when the antibiotic concentration is sufficiently reduced[21], demonstrating a short-term survival mechanism that directly contributes to antibiotic treatment failure.

To determine if populations of *A. baumannii* strains can tolerate meropenem treatment over time, stationary phase cultures from susceptible *A. baumannii* isolates, including recent clinical isolates, were treated with high levels (10 μg/mL; 62.5-fold MIC in ATCC 17978) of the antibiotic. Treated cultures demonstrated only slight depletion after 24 h, relative to untreated (**Figure 22A; Figure 23A**). In contrast, meropenem treatment of cells in logarithmic growth phase showed rapid lysis (**Figure 23B**). Therefore, *A. baumannii* strains in stasis, a relevant physiological state during infection when the cell is known to fortify the cell envelope and slow growth/division[306], are highly tolerant to lethal meropenem concentrations. While these data agree with current dogma that β-lactam-dependent killing is strictly proportional with growth rate[65,307,308], subsequent analysis revealed that stationary phase *A. baumannii* cells experience significant cell envelope

damage upon meropenem treatment. After 12 h, stationary phase cells treated with meropenem demonstrated notable morphological changes typical of spheroplast formation relative to untreated cells (**Figure 22B; Figure 24**). All strains showed a measurable increase in surface area and width of treated cells relative to untreated (**Figure 22C; Figure 24**). A significant decrease in uptake of the fluorescent D-amino acid, NADA, was also evident (**Figure 22D; Figure 24**), suggesting degradation of the cell wall, as previously shown in other β-lactam tolerant Gram-negative bacteria[20,21]. Thus, tolerance under stationary phase conditions is not just a simple function of lack of growth, but rather an active response to significant cell envelope damage.

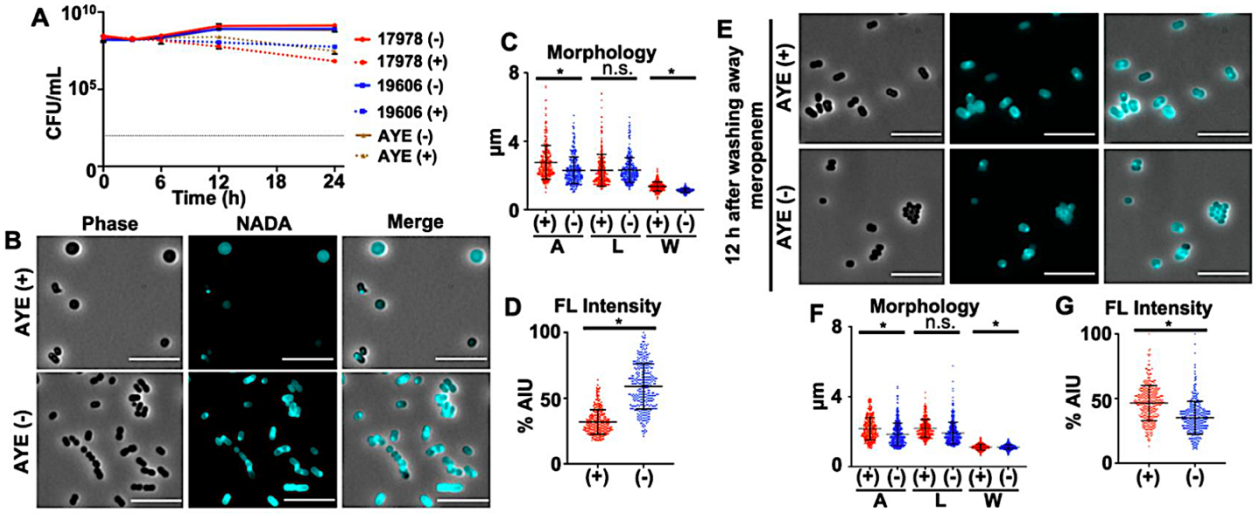

Figure 22: *Acinetobacter baumannii* strains are tolerant to meropenem. (A) Colony forming units (CFUs) of *A. baumannii* strains ATCC 17978, 19606 and AYE untreated (-) or treated (+) with meropenem over 24 h. Each killing assay was independently replicated three times, and one representative dataset was reported. Dotted black line indicates level of detection. (B) Phase and fluorescence microscopy of + or - *A. baumannii* strain AYE after 12 h. Scale bar is 10 µm. (C) Area (A), length (L) and width (W) quantitation of cells in panel B (n= 300). (D) Fluorescent (FL) signal intensity quantitation in percent arbitrary intensity units (AIU) of treated vs. untreated cells in panel B (n= 300). (E) Same as panel B, but 12 hours after meropenem removal showing the characteristic *A. baumannii* coccobacilli morphology is restored. (F) Area (A), length (L) and width (W) of cells in panel E (n= 300). (G) FL signal intensity in percent AIU treated vs. untreated in panel E (n= 300). Significance was determined using an unpaired t-test (P <0.05) in treated vs. untreated. An asterisk indicates significant differences between treated and untreated; n.s., not significant. Error bars indicate standard deviation from the mean.

Since we showed that *A. baumannii* spheroplasts were viable after plating (**Figure 22A**), we also wanted to determine if the characteristic *A. baumannii* coccobacilli morphology was restored after antibiotic removal. Cells were incubated statically in fresh media without antibiotic. At 12 h post-treatment, no spheroplast were found (**Figure 22E**), wild type morphology was restored (**Figure 22F**) and the cells showed incorporation of NADA (**Figure 22G**). Fluorescence intensity measurements were equivalent in treated and untreated cells. Furthermore, fluorescence intensity was higher at the midcell, where the divisome regulates daughter cell formation, suggesting the recovered population had resumed division (**Figure 22E**). Together, these data indicate that *A. baumannii* resumes wild type morphology and growth when meropenem treatment is stopped.

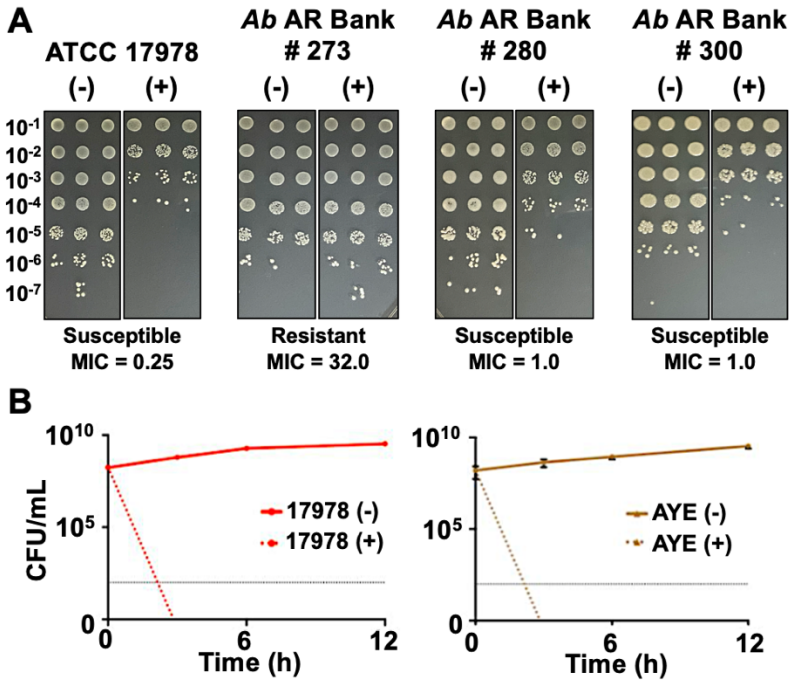

Figure 23: Tolerance in clinical *A. baumannii* isolates. (A) Dilution spot assays of *A. baumannii* strain ATCC 17978 and three recent clinical isolates, including a resistant (*A. baumannii* AR Bank #273) and two meropenem susceptible (*A. baumannii* AR Bank # 280 and # 300) strains for comparison. The calculated meropenem minimal inhibitory concentration (MIC) is indicated below each image. (B) Survival (CFU/mL) of *A. baumannii* strains ATCC 17978 and AYE in logarithmic phase cultures was calculated over 12 h during meropenem treatment. Each experiment was independently replicated two time, and one representative data set was reported. Dotted black line indicates level of detection. Error bars represent the average of 3 technical replicates +/- standard deviation.

Transcriptome analysis highlights differentially regulated pathways important for A. baumannii tolerance

Many Gram-negative pathogens form spheroplasts within 6 h to develop meropenem tolerance[20,21]; however, *A. baumannii* spheroplast formation is delayed. We first observe spheroplast formation only after 8 h, with large numbers within the population accumulating by 12 h (**Figure 22BCD; Figure 24**). To define transcriptional alterations associated with spheroplast-associated tolerance, we isolated RNA from treated and untreated cells at 0.5, 3 and 9 h. While subtle changes in gene expression were evident at 0.5 and 3 h, differential expression patterns were more obvious at 9 h in treated cultures relative to untreated (**Figure 25**). Genes associated with efflux were increasingly upregulated with each timepoint (**Figure 25A**), suggesting the cell quickly and continually responds to meropenem treatment by actively expelling the toxic compound. Upregulated efflux genes included *adeB*, *adeIJK* and *macABtolC*, which have all been implicated in antibiotic efflux[309–311]; specifically, β-lactam efflux has been reported associated with the AdeIJK RND-type pump[312,313].

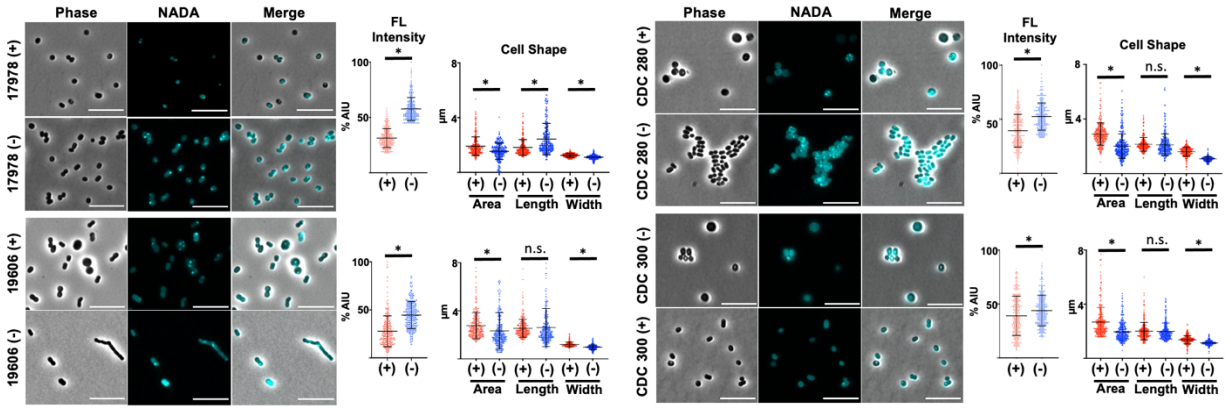

Figure 24: Spheroplast formation in *A. baumannii* isolates after 12 h of meropenem treatment. Phase and fluorescence microscopy of treated (+) or untreated (-) *A. baumannii* strains after 12 h. Scale bar is 10 μm. To the right of each image are fluorescence (FL) intensity quantifications reported in percent arbitrary intensity units (AIU) in treated (red, +) vs. untreated (blue, -) and cell shape quantifications including, area (A), length (L) and width (W) (n = 300). Significance was determined using an unpaired t-test ($P < 0.05$) in treated vs. untreated. Error bars indicate standard deviation relative to the mean. An asterisk indicates significant differences ($P < 0.05$); n.s., not significant.

Porins represent the major entryway for carbapenems such as meropenem to enter the periplasm[314], where they inhibit transpeptidation to cross-link the stem peptides of adjacent PG strands. Decreased expression of many porin-associated genes was found in treated cultures relative to untreated (**Figure 25B**), suggesting the cell also limits meropenem entry by reducing porin gene expression in response to treatment. However, temporal expression of porin-associated genes was delayed relative to efflux, in general. Deletion of *carO* is associated with carbapenem resistance in *A. baumannii*[315] and was found to be an influx channel for carbapenems[316], while OprD has also been associated with clinical carbapenem resistance in *A. baumannii*[317], suggesting reduced expression may strategically limit meropenem entry. Interestingly, the largest reduction in gene expression was associated with *ompW*, which encodes a predicted β-barrel protein (OmpW) that supports iron uptake[318], but our understanding of its biological function or how it contributes to carbapenem resistance or tolerance is limited. Notably, in *Vibrio*

cholerae, decreased iron uptake regulated by the VxrAB two-component system, promotes spheroplast recovery by reducing oxidative stress during β-lactam treatment[168,258].

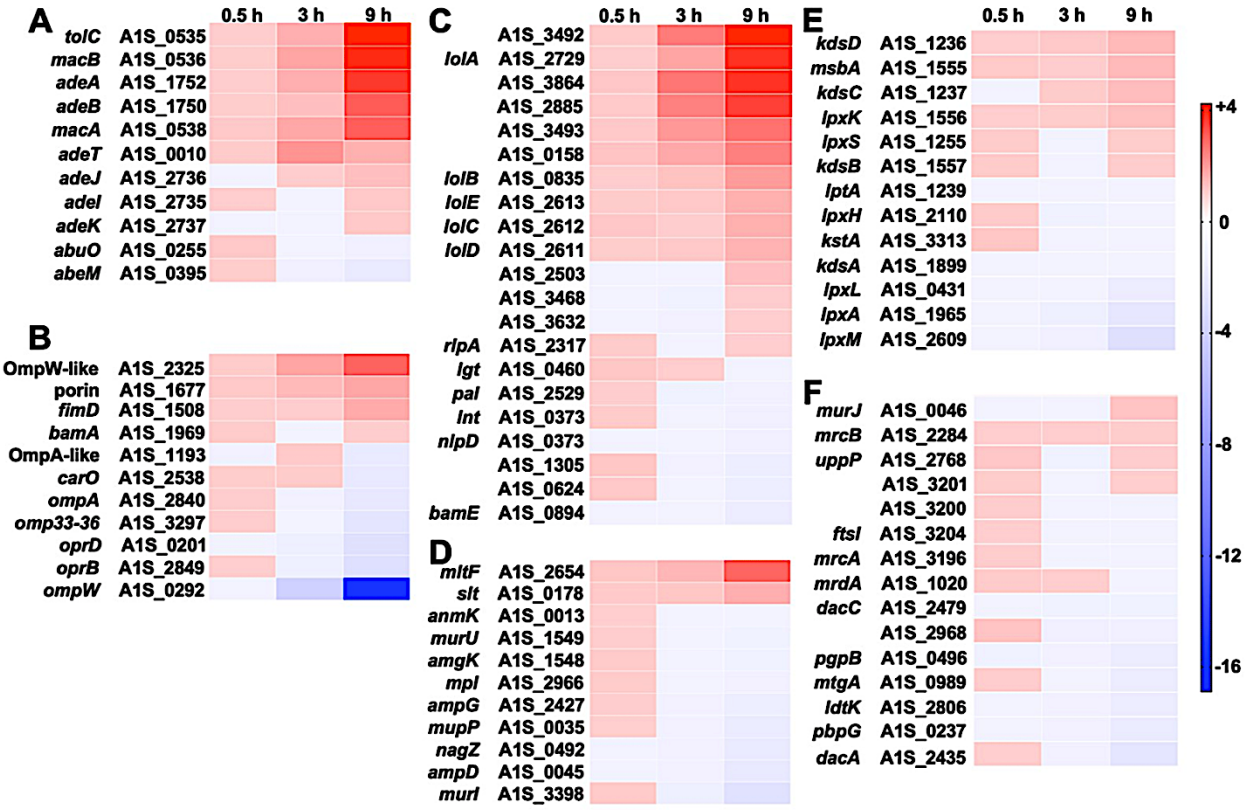

Figure 25: Differentially regulated genes in response to meropenem treatment in *A. baumannii*. Heat map showing the fold-change in genes expressed at 0.5, 3 and 9 h meropenem treatment relative to wild type ATCC 17978 (P <0.05). Pathways represented include genes associated with (A) efflux, (B) outer membrane porins, (C) outer membrane lipoproteins and their transporters, (D) peptidoglycan recycling, (E) LPS biosynthesis and (F) peptidoglycan biosynthesis.

As shown in separate *A. baumannii* transcriptional datasets in stress[260,319,320], meropenem treatment also induces expression of genes encoding putative outer membrane lipoproteins and their transporters (LolA-D) (**Figure 25C**). Remodeling the outer membrane with lipoproteins presumably fortifies the envelope by providing structural rigidity, where inner leaflet outer membrane lipoproteins are covalently attached to the underlying PG network[178,321]. Transcription of genes associated with PG remodeling

were only slightly altered with the notable exception of two genes encoding putative lytic transglycosylases, including membrane bound, MltF, and a soluble protein, Slt, which were both highly upregulated (**Figure 25D**). Lytic transglycosylases cleave *N*-acetylmuramic acid (Mur*N*Ac)-*N*-acetylglucosamine (Glc*N*Ac) bonds in PG to release soluble 1,6anhydroMur*N*Ac-containing muropeptides. Muropeptides excised by lytic transglycosylases can be secreted into the environment or imported into the cytoplasm and catabolized via the PG recycling pathway[322]. 1,6-AnhydroMur*N*Ac-containing muropeptides that feed into PG recycling can act as a source of nutrients, but also can be re-incorporated into the PG network through *de novo* biosynthesis or in some bacteria can also act as signals to induce β-lactamase expression[209,323]. Lastly, genes involved in lipooligosaccharide (LOS), and PG biosynthesis were slightly altered (**Figure 25EF**).

Genes and pathways that contribute to A. baumannii fitness during meropenem treatment

While transcriptome sequencing analyses offer insight into the stress response, one limitation of RNA-sequencing is that differentially regulated genes oftentimes do not impact fitness due to redundancy or pleiotropic effects. Therefore, we also performed transposon-sequencing on *A. baumannii* strain ATCC 17978, as previously done[267,300], and compared recovered insertional mutants from meropenem treated and untreated cultures. The screen was answered by several novel factors, some of which are the subject of a separate study, but also revealed the importance for outer membrane integrity and PG maintenance. To validate our screen, we calculated survival in several mutants, including Δ*ompA*, Δ*lpxM*, Δ*pbpG* and Δ*ldtK (also known as elsL*[324]*)*, in the presence and

absence of meropenem (**Figure 26A**). All mutants showed a 2-to-3-fold log depletion in the mutants relative to wild type at 12 h and >5-fold log depletion at 24 h. These studies suggest that *A. baumannii* fitness during meropenem treatment is dependent on outer membrane and PG maintenance factors.

OmpA is a highly conserved monomeric β-barrel protein with a periplasmic domain that noncovalently attaches the outer membrane to the PG network[325]. It is a highly abundant protein in *A. baumannii*[326] that couples with efflux pumps and can aid in export of antibacterial compounds from the periplasm[327,328]. OmpA is known to stabilize the outer membrane; *ompA* deletion/disruption increases formation of outer membrane vesicles and permeability[329]. To test the hypothesis that *ompA* deletion perturbs the outer membrane to promote carbapenem entry in *A. baumannii*, we performed two assays, including permeability measurements (**Figure 26B**) and outer membrane vesicle quantification (**Figure 26C**). Consistent with other reports[329], Δ*ompA* showed increased outer membrane vesicle formation and permeability to ethidium bromide, which is similar in size to meropenem. We also measured ethidium bromide influx in Δ*lpxM*, Δ*pbpG and* Δ*ldtK* (**Figure 26B**). Like Δ*ompA,* all isogenic mutations increased permeability relative to wild type and the respective complementation strain, which restored the permeability defect. Notably, meropenem treatment did not exacerbate permeability in wild type or any of the mutants (**Figure 26B**), suggesting it does not directly destabilize the outer membrane barrier function. Since we previously reported that Δ*ldtK* produces excess outer membrane vesicles[267] and all of the mutants showed increased permeability, we also tested vesicle formation in Δ*lpxM* and Δ*pbpG* (**Figure 26C**). Unexpectedly, Δ*pbpG*

produced excess outer membrane vesicles relative to wild type and all other mutants. In contrast, Δ*lpxM* did not.

Interestingly, Δ*lpxM* was the only strain that showed increased permeability but not hypervesiculation. LpxM catalyzes transfer of two lauroyl ($C_{12:0}$) groups from an acyl carrier protein to the *R*-3*'*- and *R*-2-hydroxymyristate positions of lipid A during LOS biosynthesis[177]. Mutations that reduce LOS acylation are known to increase fluidity of the lipid bilayer and could also impact folding/function of outer membrane porins[330,331]. Either/both mechanisms could increase entry of meropenem into the periplasmic space or disrupt efflux mechanisms that actively pump the compound out of the cell.

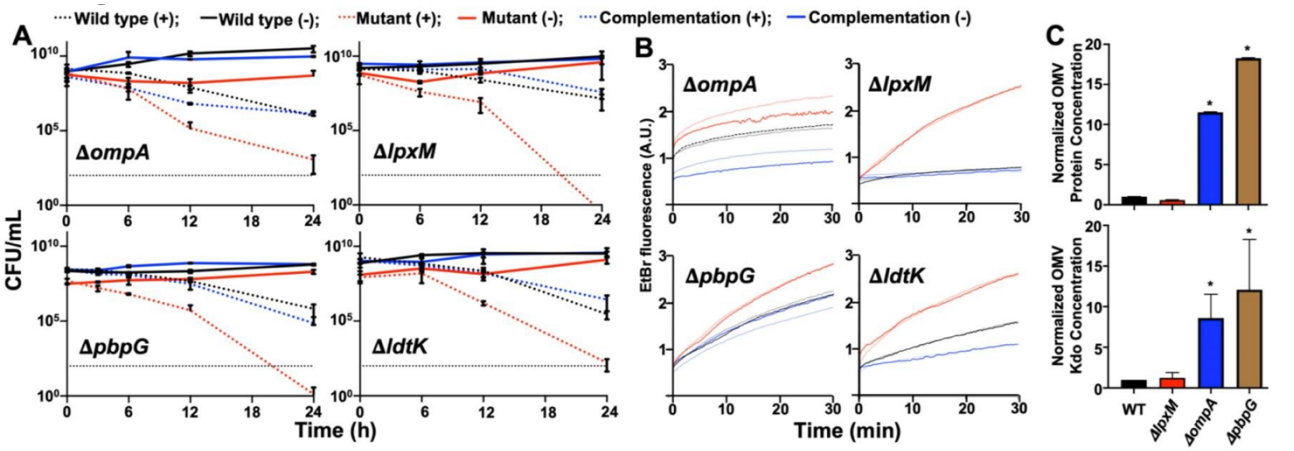

Figure 26: Genes encoding outer membrane integrity and peptidoglycan maintenance contribute to meropenem tolerance in *A. baumannii*. (A) Survival was calculated as CFU/mL over 24 h during meropenem treatment. Data were collected from two experiments in triplicate. Error bars represent the average of 3 technical replicates +/- standard deviation. (B) Permeability assays using ethidium bromide (EtBr) over 0.5 h. A.U.; arbitrary units. Lines shown depict the mean of three technical replicates. (C) Relative quantification of protein (top) and Kdo (bottom) concentrations of outer membrane vesicles (OMVs) in wild type (WT) and mutants. Each experiment was independently replicated three times, and one representative dataset was reported. Error bars indicate standard deviation. An asterisk indicates significant differences relative to the WT strain (P <0.05).

We also characterized the morphology of each mutant in growth (**Figure 27**). We found that relative to wild type, Δ*ompA* cells were chained and NADA incorporation was reduced (**Figure 27A**), suggesting that OmpA is required for proper function of PG

enzymes (division proteins and LD-/DD-transpeptidases that incorporate NADA and/or increased carboxypeptidase activity). Δ*lpxM* and Δ*pbpG* showed increased NADA incorporation (**Figure 27BC**), which is consistent with increased outer membrane permeability. Δ*pbpG* cells were also clumped (**Figure 27C**), suggesting the cells could not properly separate during division. As previously reported[267], Δ*ldtK* showed rounded cells (**Figure 5.6D**). We also calculated the meropenem minimal inhibitory concentrations in each mutant, which did not significantly deviate from the parent strain (**Figure 27E**).

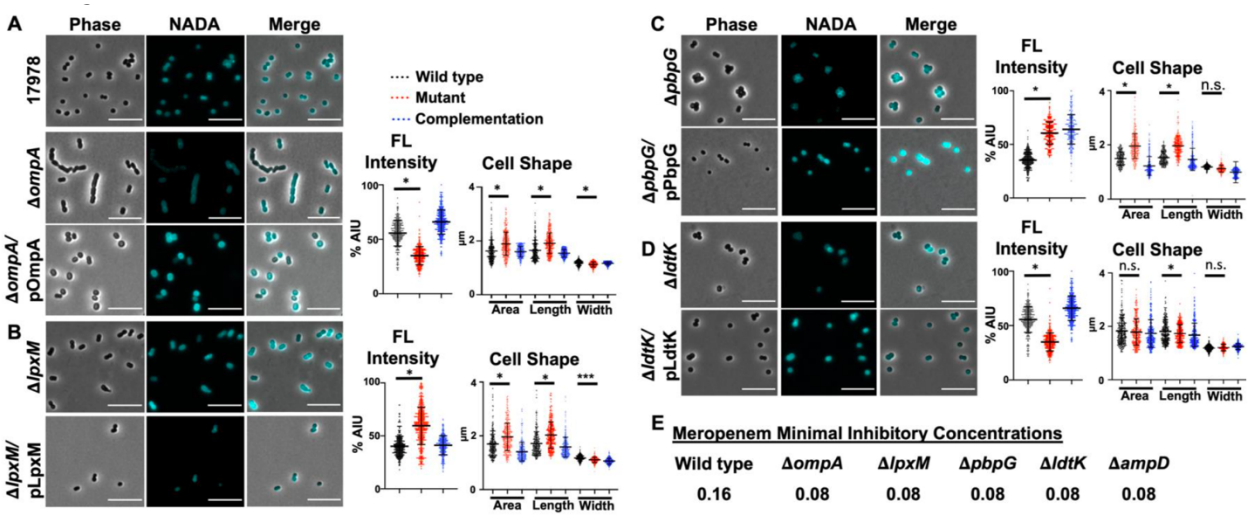

Figure 27: Morphology of wild type and mutant *A. baumannii* strains. (A) Phase and fluorescence microscopy of NADA-treated wild type and Δ*ompA,* (B) Δ*lpxM,* (C) Δ*pbpG* and (D) Δ*ldtK* with each respective complementation strain. Scale bar is 10 μm. Fluorescent (FL) signal intensity quantification in percent arbitrary intensity units (AIU) in wild type, mutant and complementation strains are to the right of mutant images. Cell shape quantifications including area (A), length (L) and width (W) (n = 300) are also included. Significance was determined using an unpaired t-test ($P < 0.05$). An asterisk indicates significant differences between wild type and mutant ($P < 0.05$); n.s., not significant. Error bars indicate standard deviation. (E) Minimal inhibitory concentrations of wild type and mutant strains.

While the contribution of the *A. baumannii* outer membrane proteins OmpA and LpxM to gate carbapenem entry to promote antibiotic tolerance is straightforward, we were intrigued by genetic links to PG maintenance (i.e., *pbpG* and *ldtK*). While mutation of *pbpG* and *ldtK* impact outer membrane integrity (**Figure 26**), we also wanted to define

their physiological role to determine specific pathways that contribute to meropenem tolerance.

PBP7 is a DD-carboxypeptidase and endopeptidase that catalyzes formation of tetrapeptides

To define the activity of *A. baumannii* PBP7 (encoded by *pbpG*), we isolated PG from wild type and Δ*pbpG* in growth (**Figure 28A; Table 3**) and stasis (**Figure 28B; Table 3**). Muropeptides were generated by treatment with muramidase, separated by high-performance liquid chromatography and uncharacterized peaks were analyzed by tandem mass spectrometry, as done previously[260,267,304]. PG composition from Δ*pbpG* in growth showed accumulation of two muropeptide peaks that were not present in wild type (**Figure 28A; Table 3**). MS analysis showed these peaks were enriched with pentapeptides and were identified as disaccharide pentapeptide (Penta, neutral mass: 1012.19 amu; theoretical: 1012.45 amu) and bis-disaccharide tetrapentapeptide (TetraPenta, neutral mass: 1935.60 amu; theoretical: 1935.84 amu) (**Figure 28C; Figure 29**), suggesting the enriched muropeptide pools represent PBP7 substrates in growth. Δ*pbpG* PG in stasis had depleted D-amino acid-modified muropeptide pools, including TetraTri-D-Lys- and TetraTri-D-Arg-peptides, and reduced 3-3 crosslink formation (**Figure 28BC; Table 3**), consistent with PBP7 DD-carboxypeptidase and endopeptidase activity to form tetrapeptides, which are the most abundant peptides in the PG in *A. baumannii*[260,267,304] and substrates of LD-transpeptidases. The periplasmic LD-transpeptidase, LdtJ, transfers D-amino acid to tetrapeptides and forms 3-3 crosslinks[267]. Therefore, it is likely that PBP7 provides at least some of the periplasmic substrates for LdtJ-dependent transpeptidase activity in stasis.

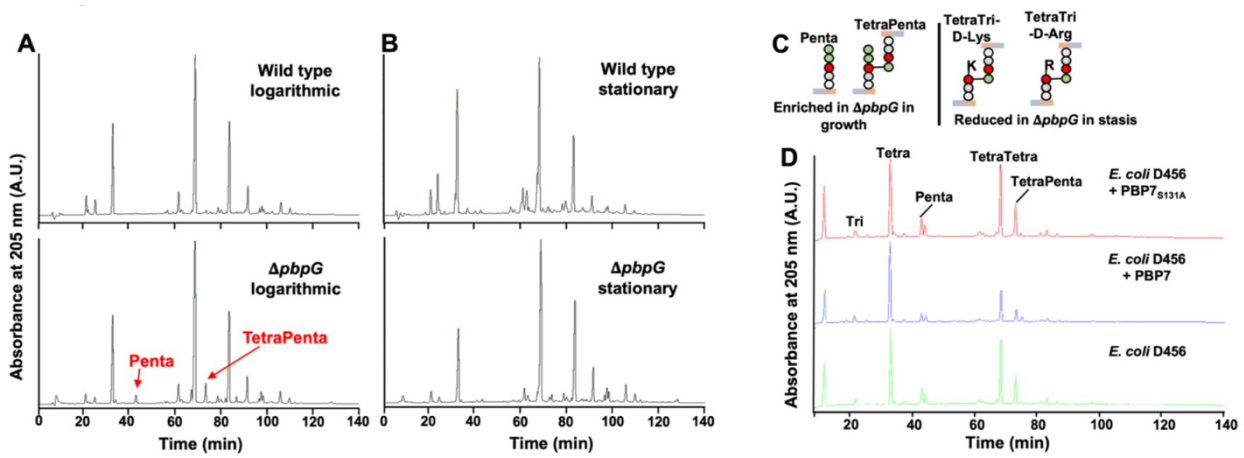

Figure 28: PBP7 is active against pentapeptides and DD-crosslinks. (A) PG isolated from wild type and Δ*pbpG* in growth phase was analyzed by HPLC. The muropeptides Penta and TetraPenta were enriched in Δ*pbpG.* (B) PG isolated from wild type and Δ*pbpG* in stationary phase was analyzed by HPLC. TetraTri-D-Lys and TetraTri-D-Arg were depleted in Δ*pbpG* relative to wild type. (C) Muropeptide structures are illustrated and were confirmed using MS/MS. (D) Recombinant PBP7 or the active-site mutant PBP7$_{S131A}$ was incubated with PG isolated from *E. coli* D456 which contains Tetra, Penta, TetraTetra and TetraPenta as the main muropeptides. PBP7 was active against pentapeptides (DD-CPase) and cross-linked muropeptides (DD-EPase).

To test the enzymatic activity, we purified recombinant PBP7 and a predicted catalytically inactive version in which alanine replaces the active site serine (PBP7$_{S131A}$). Purified proteins were incubated with PG from *E. coli* D456 (**Figure 28D**), a strain enriched with pentapeptides[332] and analyzed as previously done[333]. PBP7 was active against penta-, tetratetra- and tetrapentapeptides, where each muropeptide was trimmed to the tetrapeptide-form relative to the no-enzyme control. As expected, PBP7$_{S131A}$ did not show activity against any muropeptides. Together, these studies suggest that PBP7 not only hydrolyzes the bond between the terminal D-Ala residues, but also showed DD-endopeptidase activity and both activities enrich the periplasmic pool of monomeric tetrapeptides.

Table 3: Muropeptide composition of wild type and Δ*pbpG A. baumannii* strain ATCC 17978.

Peak No.	Muropeptide	Relative % of each muropeptide[a]			
		WT Logarithmic	WT Stationary	Δ*pbpG* Logarithmic	Δ*pbpG* Stationary
1	Tri	3.0 ± 0.4	3.2 ± 0.0	1.5 ± 0.2	2.0 ± 0.1
2	Tri-D-Asn	0.9 ± 0.1	0.1 ± 0.2	0.1 ± 0.3	0.1 ± 0.2
3	Tri-D-Lys	2.2 ± 0.7	4.8 ± 0.0	1.0 ± 0.0	1.1 ± 0.2
4	TetraGly4	0.0 ± 0.0	0.7 ± 0.1	0.0 ± 0.0	0.0 ± 0.0
5	Tetra-D-Lys	0.0 ± 0.0	2.6 ± 0.0	0.0 ± 0.0	0.0 ± 0.0
6	Tetra	17.6 ± 0.5	17.5 ± 0.4	16.1 ± 0.2	14.6 ± 0.3
7	Tetra-D-Arg	0.0 ± 0.0	0.4 ± 0.0	0.0 ± 0.0	0.1 ± 0.2
7B	Penta	0.0 ± 0.0	0.5 ± 0.0	1.3 ± 0.0	0.4 ± 0.0
8	TetraTriDapGly4	0.3 ± 0.0	0.8 ± 0.0	0.0 ± 0.0	0.2 ± 0.0
9	TriTri(Dap)/TriTriDap-D-Lys	0.5 ± 0.1	0.5 ± 0.0	0.1 ± 0.2	0.0 ± 0.0
10	TetraTri(Dap)	0.0 ± 0.0	1.8 ± 0.1	0.0 ± 0.0	0.4 ± 0.0
11	TetraTri	4.3 ± 0.2	3.4 ± 0.1	3.1 ± 0.0	1.9 ± 0.0
12	TetraTri-D-lys	0.6 ± 0.0	3.7 ± 0.0	0.5 ± 0.0	1.0 ± 0.0
13	TetraTri-D-lys	0.4 ± 0.0	0.7 ± 0.0	0.4 ± 0.0	0.0 ± 0.0
14	TetraTri-D-Arg	0.5 ± 0.1	6.0 ± 0.0	2.0 ± 0.0	1.7 ± 0.0
15	TetraTetra	36.2 ± 0.9	22.9 ± 0.4	39.6 ± 0.6	35.7 ± 0.2
15B	TetraPenta	0.5 ± 0.1	1.0 ± 0.1	2.9 ± 0.0	1.0 ± 0.1
16	TetraTetraTri or TetraTetraTriDap	0.1 ± 0.0	0.9 ± 0.0	0.9 ± 0.0	1.2 ± 0.1
17	TetraTetraTri or TetraTetraTriDap	0.3 ± 0.0	1.6 ± 0.0	0.3 ± 0.2	0.4 ± 0.0
18	TriTriDap-D-Met	0.6 ± 0.0	0.5 ± 0.0	0.2 ± 0.4	0.6 ± 0.0
19	TetraTetraTetra	17.9 ± 0.0	11.8 ± 0.3	16.9 ± 0.2	18.6 ± 0.1
20	TetraTri-D-Met	0.1 ± 0.2	0.7 ± 0.0	0.7 ± 0.0	0.2 ± 0.0
21	TetraTri Anh / TetraTetraTetraTri	4.4 ± 0.1	2.4 ± 0.2	3.9 ± 0.0	4.7 ± 0.0
22	TetraTetra Anh I	1.4 ± 0.0	0.8 ± 0.0	2.0 ± 0.0	2.2 ± 0.1
23	TetraTetra Anh II	0.7 ± 0.1	0.9 ± 0.0	1.0 ± 0.0	1.4 ± 0.1
24	TetraTetraTetra Anh	2.5 ± 0.1	1.6 ± 0.0	2.2 ± 0.0	3.2 ± 0.0
Sum of known peaks		95.8 ± 0.2	91.7 ±0.1	95.8 ± 0.2	92.8 ± 0.4
Monomers (Total)		24.8 ± 0.6	32.3 ±0.3	20.9 ± 0.0	19.7 ± 0.0
Monomers with modification		3.2 ± 0.6	9.3 ±0.2	1.1 ± 0.3	1.4 ± 0.3
Monomer tri		3.2 ± 0.5	3.5 ±0.0	1.6 ± 0.2	2.2 ± 0.1
Monomer tri-D-Asn		0.9 ± 0.1	0.1 ±0.3	0.1 ± 0.3	0.1 ± 0.2
Monomer tri-D-Lys		2.3 ± 0.7	5.2 ±0.0	1.0 ± 0.0	1.1 ± 0.2
Monomer tetraGly4		0.0 ± 0.0	0.8 ±0.1	0.0 ± 0.0	0.0 ± 0.0
Monomer tetra-D-Lys		0.0 ± 0.5	2.8 ±0.0	0.0 ± 0.0	0.0 ± 0.0
Monomer tetra		18.4 ± 0.5	19.0 ±0.4	16.8 ± 0.2	15.7 ± 0.4
Monomer tetra-D-Arg		0.0 ± 0.0	0.4 ±0.0	0.0 ± 0.0	0.1 ± 0.2
Monomer penta		0.0 ± 0.0	0.5 ±0.0	1.4 ± 0.0	0.4 ± 0.0
Dimers (Total)		52.5 ± 0.4	50.3 ±0.2	58.8 ± 0.2	55.1 ± 0.2
Dimers with modification		2.9 ± 0.5	14.1 ±0.1	4.1 ± 0.7	4.0 ± 0.1
Dimer chain ends (anhydroMur*N*Ac)		6.8 ± 0.0	4.4 ±0.2	7.2 ± 0.0	9.0 ± 0.1
Trimers (Total)		22.6 ± 0.2	17.4 ±0.5	21.2 ± 0.2	25.2 ± 0.1
Trimer chain ends (anhydroMur*N*Ac)		2.6 ± 0.1	1.7 ±0.0	2.3 ± 0.1	3.5 ± 0.0
Tripeptides (Total)		13.0 ± 1.2	20.8 ±0.4	9.0 ± 0.7	10.1 ± 0.2
Tripeptides with modifications		5.2 ± 0.9	13.0 ±0.3	3.4 ± 1.0	3.6 ± 0.1
Tetrapeptides (Total)		86.3 ± 1.3	77.5 ±0.4	89.0 ± 0.9	88.9 ± 0.1
Tetrapeptides with modifications		0.9 ± 0.2	10.5 ±0.1	1.9 ± 0.0	1.8 ± 0.3
Pentapeptides		0.2 ± 0.1	1.0 ±0.0	2.9 ± 0.0	1.0 ± 0.1
3-3 Crosslinks		1.1 ± 0.1	2.9 ±0.1	0.6 ± 0.3	1.2 ± 0.1
Chain ends (anhydroMur*N*Ac)		4.3 ± 0.0	2.8 ±0.1	4.3 ± 0.0	5.7 ± 0.1
Degree of crosslinkage		41.4 ± 0.3	36.7 ±0.2	43.6 ± 0.0	44.3 ± 0.0
% peptides in cross-links		75.2 ± 0.6	67.7 ±0.3	79.1 ± 0.0	80.3 ± 0.1

[a]Values are mean ± variation of two biological repeats.

LdtK is a cytoplasmic LD-carboxypeptidase active against tetrapeptides for PG recycling

During β-lactam treatment, autolysins (i.e., lytic transglycosylases) are activated[65,334], which increases the amount of PG turnover products with 1,6-anhydro-Mur*N*Ac residues. In *A. baumannii*, genes encoding the autolysins, MltF and Slt, were upregulated during meropenem treatment (**Figure 25D**), which likely increases periplasmic concentrations of TetraAnh, for cytoplasmic import. In *E. coli*, TetraAnh are substrates for the LD-carboxypeptidase LdcA, which trims tetrapeptides to tripeptides[206] that are catabolized by the conserved enzymes NagZ[335,336] to generate 1,6-anhMur*N*Ac-tripeptide and the amidase AmpD[337,338] to form free tripeptides, which can be further broken down into individual amino acids and used as energy. Furthermore, Mpl[339] can attach tripeptides to uridine diphosphate (UDP)-Mur*N*Ac to form UDP-Mur*N*Ac-tripeptide, an intermediate in the *de novo* PG biosynthesis pathway. However, no apparent LD-carboxypeptidase, orthologue to LdcA is encoded by *A. baumannii*.

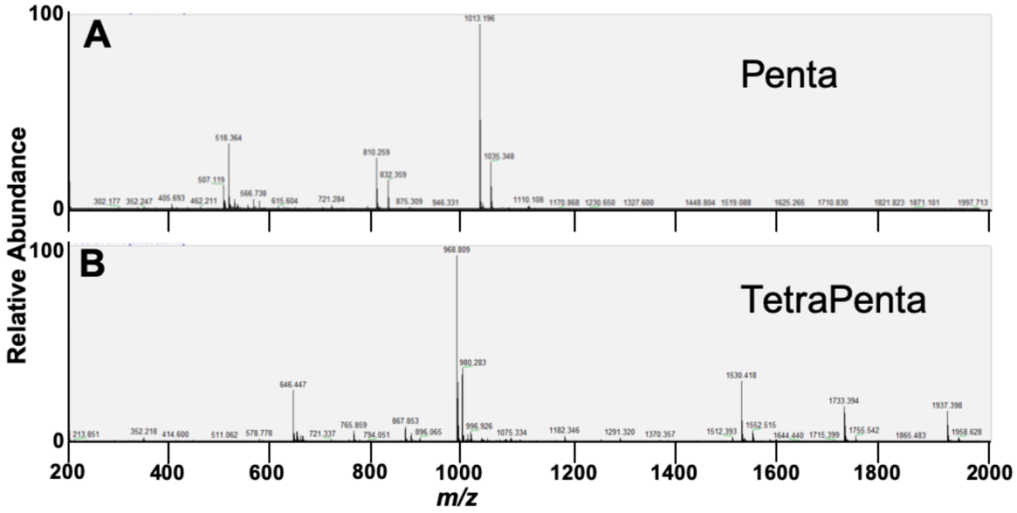

Figure 29: Unidentified peaks in logarithmic growth phase of Δ*pbpG*. Peaks at (A) 42 min and (B) 72 min were analyzed by mass spectrometry (MS). The peak in A was consistent with disaccharide pentapeptide (Penta, neutral mass: 1012.19 amu; theoretical: 1012.45 amu) and the peak in B was consistent with bis-disaccharide tetrapentapeptide (TetraPenta, neutral mass: 1935.60 amu; theoretical: 1935.84 amu).

LdtK was one potential LD-carboxypeptidase candidate for PG recycling because it encodes a putative LD-transpeptidase (YkuD) domain but does not encode a canonical secretion signal needed for export, suggesting it may be active in the cytoplasm. This observation coupled with a recent study showing that the *E. coli* YkuD homologue DpaA (also known as LdtF) is an amidase that hydrolyzes bonds formed by LD-transpeptidases[294,340], suggested that LdtK may indeed have LD-carboxypeptidase activity, which is essential for tripeptide formation in the recycling pathway.

First, we determined the subcellular localization of LdtK with a specific antibody that detects the native protein (**Figure 30A**). After fractionation of the subcellular compartments, we were only able to detect LdtK in the cytoplasmic fraction in growth and stasis, showing it is not exported to the periplasm.

Since LdtK is cytoplasmic, we sought to determine if it was active on tetra- and/or pentapeptide substrates. We purified recombinant LdtK and the active-site mutant, $LdtK_{C138S}$ and incubated both enzymes with muropeptides obtained from tetrapeptide-rich PG from *E. coli* BW25113 or pentapeptide-rich PG from *E. coli* CS7031[333] (**Figure 30B**). LdtK showed activity against tetrapeptides but not pentapeptides. The muropeptide profile showed the formation of disaccharide tripeptide and bis-disaccharide tetratripeptide, showing that LdtK cleaves the bond between the L-centre of *m*DAP and the terminal D-Ala in tetrapeptides, characteristic of LD-carboxypeptidase activity. Our data indicate that PBP7 trims pentapeptides and cleaves crosslinked peptides into tetrapeptides in the periplasmic PG network. Once 1,6-anhydro-Mur*N*Ac-containing muropeptides are released from the PG network by MltF, Slt or other lytic transglycosylases, they are transported into the cytoplasm and into tripeptides by LdtK in the PG recycling pathway.

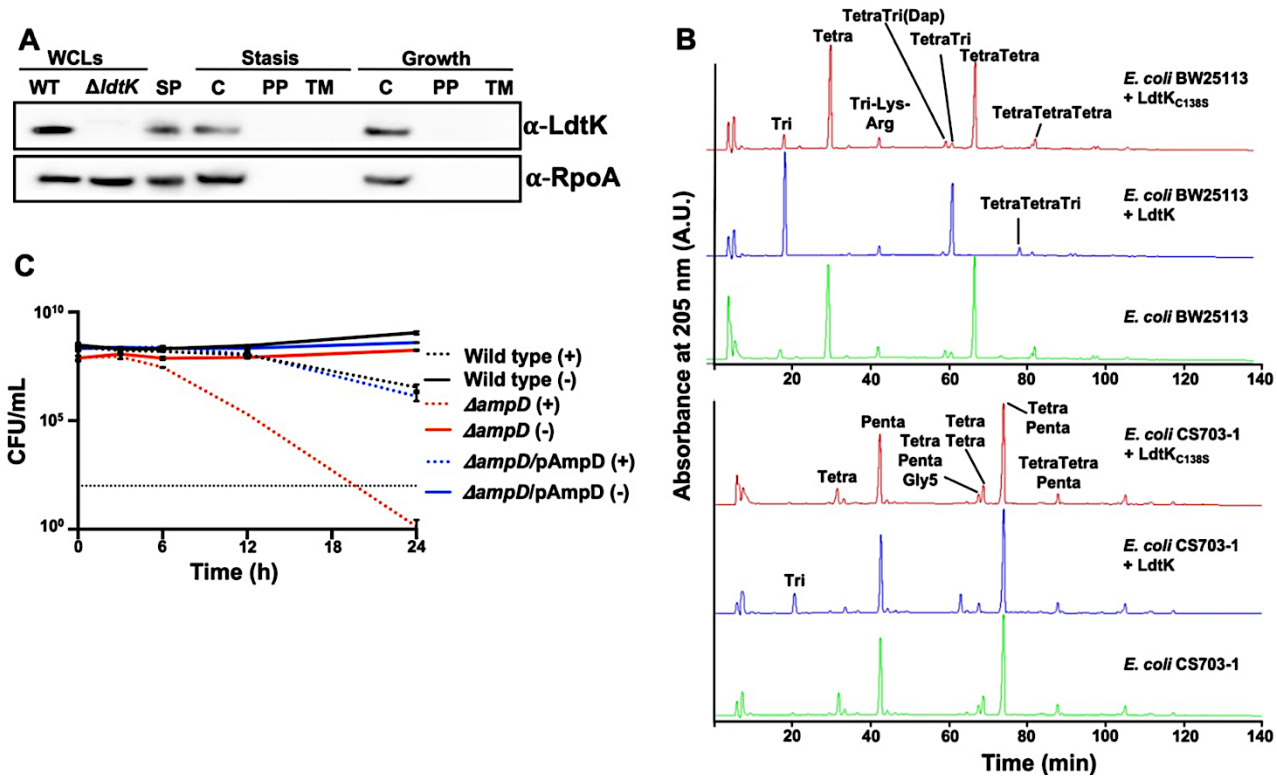

Figure 30: LdtK is active against Tetra and TetraTetra. (A) Western blot with α-LdtK and α-RpoA antisera. LdtK is 18.97 kDa, while RpoA is 37.27 kDa. WCL; whole-cell lysate, SP; spheroplast, C; cytoplasm, PP; periplasm, and TM; total membrane fractions. (B) Recombinant LdtK or the active-site mutant $LdtK_{C13S}$ was incubated with PG isolated from *E. coli strain* BW25113 (top, tetrapeptide-rich) or strain CS703-1 (bottom, pentapeptide-rich). LdtK was active against tetrapeptides but not pentapeptides. (C) Meropenem tolerance assay in Δ*ampD,* which encodes a well-conserved cytoplasmic enzyme required for PG recycling. Error bars represent the average of 3 technical replicates +/- standard deviation.

To further confirm if the cytoplasmic PG pathway contributes to meropenem tolerance in *A. baumannii*, we made an isogenic *ampD* mutant, which encodes *N*-acetylmuramyl-L-alanine amidase that releases the tripeptide from anhMur*N*Ac[338]. Like Δ*pbpG* and Δ*ldtK*, Δ*ampD* was also rapidly killed when treated with meropenem relative to wild type and the respective complementation strain (**Figure 30C**). Together, these studies strongly suggest that the PG recycling pathway contributes to meropenem tolerance in *A. baumannii*. Furthermore, the formation of cytoplasmic tripeptides or tetrapeptides appears to contribute to meropenem tolerance. Combinatorial therapies that

inhibit enzymes in both PG biosynthesis and recycling could provide an alternative treatment strategy.

Discussion

Many susceptible Gram-negative pathogens tolerate treatment with bactericidal antibiotics such as carbapenem β-lactams, but the molecular factors that underlie cell survival are not understood. Significant cell envelope damage is observed during treatment, characterized morphologically by cell wall-depleted spheroplasts[15,19–21,305]. Here, we show meropenem treatment induces spheroplast formation in *A. baumannii*, and that cell growth resumes upon removal of the antibiotic. Transcriptome sequencing analysis suggests *A. baumannii* responds to treatment by fortifying the structural integrity of the cell envelope through increased outer membrane lipoprotein and transporter gene expression and by inducing autolysins, which likely physically reinforce the envelope by providing stiffness and remodel the PG network, respectively. Treated cells also appear to limit intracellular meropenem concentrations through induced expression of efflux-associated genes and downregulation of porin genes, which both reduce periplasmic concentrations by actively pumping the antibiotic out of the cell and by limiting entry, respectively. A separate genetic (transposon) screen to identify fitness determinants, showed factors required for high level meropenem tolerance include genes that contribute to outer membrane permeability (*lpxM*, *ompA*, *pbpG* and *ldtK*) and cell envelope stability (*ompA*, *pbpG* and *ldtK*). Furthermore, genes in the cytoplasmic PG recycling pathway, *ldtK* and *ampD,* also answered the screen. Together the transcriptomics and genetic screen suggested factors that maintain cell envelope homeostasis through integrity

maintenance of the outer membrane and PG network contribute to meropenem tolerance in *A. baumannii*.

While we showed several tolerance factors are transcriptionally regulated, we do not know what transcription factors are involved. A previous study found that PhoPQ-dependent outer membrane modifications promoted survival in cell wall-deficient spheroplasts[305], presumably by fortifying the outer membrane to counter large loads of turgor pressure typically absorbed by the cell wall. Specifically, PhoPQ was activated in response to meropenem treatment. *A. baumannii* does not encode PhoPQ, but analogous mechanisms likely to contribute to cell envelope homeostasis to counter the turgor when the cell wall is compromised. One mechanism might include fortification of the cell envelope with lipoproteins, which occurs in stress in *A. baumannii*[260,319,320,341]; however, the underlying protective mechanism is not understood. Landmark studies in cell envelope mechanics have shown that outer membrane lipoprotein attachment to the PG impact cell envelope mechanics by increasing the load-bearing capacity of the cell envelope[178,321]. Outer membrane lipoproteins, specifically those that interact with the underlying PG network, increase outer membrane stiffness, which likely counterbalances the internal turgor. When the cell wall is perturbed during meropenem treatment, small fluctuations in turgor may be sufficient to induce lysis when lipoprotein-mediated attachment is absent. More studies are needed to tease apart the contribution of specific lipoproteins and how they contribute to cell envelope mechanics in stress. Furthermore, noncovalent attachments between the outer membrane and PG network via OmpA and hyperacylation of lipid A via LpxM may also increase the mechanical load-bearing capacity of the outer membrane to maintain envelope homeostasis when the cell wall is

defective. It is also possible that disruption of OmpA or LpxM has pleiotropic effects that reduce the barrier function to gate meropenem entry.

Unexpectedly, our data suggest that PG maintenance enzymes contribute to *A. baumannii* survival during meropenem treatment. Tetrapeptides represent the most abundant PG stem peptides in *A. baumannii*. They are formed, in part, by the DD-carboxypeptidase and endopeptidase activity of PBP7 from pentapeptides and DD-crosslinked muropeptides, respectively (**Figure 28A**). Tetrapeptides are substrates for LD-transpeptidase that form a small amount of 3-3 crosslinks in *A. baumannii*, but are needed to effectively repair PG defects in stressed *E. coli* cells[294]. Furthermore, tetrapeptides are also necessary for LD-transpeptidase-dependent covalent attachment of Braun's lipoprotein (Lpp) to *meso*-DAP residues in PG[342], which also fortifies the envelope[178]. Our data indicate that without PBP7, LdtJ-dependent 3-3 crosslink formation is reduced (**Figure** 28**A**), however less than 3% of all muropeptides contain 3-3 crosslinks and their contribution to PG integrity maintenance remain unclear.

The lytic transglycosylases MltF and Slt were induced in meropenem treatment (**Figure 25**), consistent with activation of autolysins in response to penicillin-binding protein inhibition during β-lactam treatment[20,65]. Lytic transglycosylase proteins cleave the glycosidic linkage between disaccharide subunits within the PG strands and perform an intramolecular transglycosylation in Mur*N*Ac to release soluble 1,6-anhydroMur*N*Ac containing muropeptides, which can be imported into the cytoplasm. The main turnover product, TetraAnh is transported into the cytoplasm by AmpG where they provide substrates for LdtK-dependent LD-carboxypeptidase activity to form TriAnh. Like other members of the YkuD family, LdtK retains preference for tetrapeptide substrates (**Figure**

30B) but represents the first known YkuD-containing enzyme that lacks a signal sequence and is active in the cytoplasm. LdtK is the second member of the YkuD family, after DpaA/LdtF that has a major role in cleaving amide bonds rather than generating them. Notably, the requirement for LdtK in meropenem tolerance is like how cells depend on outer membrane integrity maintenance (OmpA, LpxM, PBP7) during spheroplast formation. Lastly, LdtK (and LdtJ) were shown to be essential for *A. baumannii* survival without LOS[267], suggesting that PG recycling and modification of tetrapeptides are a general response to counter cell envelope stress in *A. baumannii*. It is also possible that cytosolic accumulation of tetrapeptides creates another problem in cells that are already sick and cannot be tolerated.

Hydrolysis of TriAnh by the dedicated enzymes NagZ and AmpD, which lead to the formation of anhMur*N*Ac-tripeptide, 1,6-anhMur*N*Ac and tripeptides, respectively, could be degraded into individual amino acids for utilization as nutrient or energy sources[210,212,323] to promote survival during tolerance. It is reasonable to expect the cell requires some nutrients during tolerance, and this pathway could provide energy to support basal metabolic processes. Alternatively, Mpl could ligate tripeptides to UDP-Mur*N*Ac in the recycling pathway[339,343]. UPD-Mur*N*Ac-tripeptide is an intermediate in the *de novo* PG synthesis pathway[344–346]; however, it is not obvious how *de novo* PG synthesis via recycling would benefit the bacterium during treatment because periplasmic PBPs and LD-transpeptidases, which are required for crosslinking, are inhibited by meropenem. Another possibility is that accumulation of cytoplasmic 1,6-anhydroMur*N*Ac-containing muropeptides provide signals to induce β-lactamase expression, which could localize in the periplasm to reduce meropenem concentrations to survivable levels. Two

mechanisms have been characterized in Gram-negative bacteria, including the AmpG-AmpR pathway and the BlrAB two-component system, which both induce β-lactamase expression in response to muropeptide concentrations[209]. Many genes in *A. baumannii* have not yet been characterized. Signaling pathways and potentially carbapenemases could be induced in response to 1,6-anhydroMur*N*Ac-containing muropeptide accumulation to promote meropenem degradation. A more detailed analysis is needed to characterize the PG recycling tolerance mechanism, which will inform more effective treatment strategies to combat *A. baumannii* infections. Furthermore, our studies also show that disruption of PG maintenance enzymes (i.e., PBP7, LdtK) compromised outer membrane integrity. It is also possible that outer membrane perturbations in these mutants induce unchecked antibiotic entry to impact fitness during meropenem treatment. Notably, regulatory links between the outer membrane and PG maintenance are not well-understood in *A. baumannii.*

CHAPTER 6

GENERATING TRANSPOSON INSERTION LIBRARIES IN GRAM-NEGATIVE BACTERIA FOR HIGH-THROUGHPUT SEQUENCING**

Misha I. Kazi[1], Richard D. Schargel[1], Joseph M. Boll[#1]

[1]Department of Biology, University of Texas Arlington, Arlington TX, USA

[#]Correspondence: joseph.boll@uta.edu

** Published as: Kazi MI, Schargel RD, Boll JM. Generating Transposon Insertion Libraries in Gram-Negative Bacteria for High-Throughput Sequencing. *J Vis Exp*. 2020;(161):10.3791/61612. Published 2020 Jul 7. Doi:10.3791/61612

Abstract

Transposon sequencing (Tn-seq) is a powerful method that combines transposon mutagenesis and massive parallel sequencing to identify genes and pathways that contribute to bacterial fitness under a wide range of environmental conditions. Tn-seq applications are extensive and have not only enabled examination of genotype-phenotype relationships at an organism level but also at the population, community and systems levels. Gram-negative bacteria are highly associated with antimicrobial resistance phenotypes, which has increased incidents of antibiotic treatment failure. Antimicrobial resistance is defined as bacterial growth in the presence of otherwise lethal antibiotics. The “last-line” antimicrobial colistin is used to treat Gram-negative bacterial infections. However, several Gram-negative pathogens, including Acinetobacter baumannii can develop colistin resistance through a range of molecular mechanisms, some of which were characterized using Tn-seq. Furthermore, signal transduction pathways that regulate colistin resistance vary within Gram-negative bacteria. Here we propose an efficient method of transposon mutagenesis in A. baumannii that streamlines generation of a saturating transposon insertion library and amplicon library construction by eliminating the need for restriction enzymes, adapter ligation, and gel purification. The methods described herein will enable in-depth analysis of molecular determinants that contribute to A. baumannii fitness when challenged with colistin. The protocol is also applicable to other Gram-negative ESKAPE pathogens, which are primarily associated with drug resistant hospital-acquired infections.

Introduction

The discovery of antibiotics is undoubtedly one of the most impactful health-related events of the 20th century. Not only do antibiotics quickly resolve serious bacterial infections, they also play a pivotal role in modern medicine. Major surgeries, transplants and advances in neonatal medicine and chemotherapy leave patients susceptible to life threatening infections and these therapies would not be possible without antibiotics[1,347]. However, rapid development and spread of antibiotic resistance among human pathogens has significantly decreased the efficacy of all clinically important classes of antibiotics[2]. Many bacterial infections that were once easily cleared with antibiotics treatment, no longer respond to classic treatment protocols, causing a serious threat to global public health[1]. Antimicrobial resistance (AMR) is where bacterial cells grow in otherwise lethal concentrations of antibiotics, regardless of the treatment duration[12,348]. There is an urgent need to understand molecular and biochemical factors that regulate AMR, which will help guide alternative antimicrobial development. Specifically, ESKAPE pathogens are problematic in clinical settings and associated with extensive AMR. These include *Enterococcus faecium*, *Staphylococcus aureus*, *Klebsiella pneumoniae*, *Acinetobacter baumannii*, *Pseudomonas aeruginosa* and *Enterobacter* spp. While several mechanisms contribute to AMR in ESKAPE pathogens, the latter four organisms are Gram-negative.

Gram-negative bacteria assemble a defining outer membrane that protects them from adverse environmental conditions. The outer membrane serves as a permeability barrier to restrict entry of toxic molecules, such as antibiotics, into the cell. Unlike other biological membranes, the outer membrane is asymmetrical. The outer leaflet is enriched

with surface-exposed lipopolysaccharide, while the inner leaflet is a mixture of phospholipids[272]. Lipopolysaccharide molecules are anchored to the outer membrane by a conserved lipid A moiety embedded within the lipid bilayer[349]. The canonical lipid A domain of Escherichia coli lipopolysaccharide is required for the growth of most Gram-negative bacteria and is synthesized by a nine-step enzymatic pathway that is one of the most fundamental and conserved pathways in Gram-negative organisms[272,349,350].

Polymyxins are cationic antimicrobial peptides that target the lipid A domain of lipopolysaccharide to perturb the outer membrane and lyse the cell. The electrostatic interaction between positively charged residues of polymyxins and the negatively charged lipid A phosphate groups disrupt the bacterial cell membrane ultimately leading to cell death[172,177,260,351,352]. Colistin (polymyxin E) is a last-resort antimicrobial used to treat infections caused by multidrug resistant Gram-negative nosocomial pathogens, such as *Acinetobacter baumannii*[353–355]. First discovered in 1947, polymyxins are produced by the soil bacteria, *Paenibacillus polymyxa*[356–358]. Polymyxins were prescribed to treat Gram-negative infections for years before their clinical use was limited due to reports of significant nephro- and neurotoxicity[359,360].

A. baumannii is a nosocomial Gram-negative pathogen that has dramatically increased the morbidity and mortality of patient outcomes over recent decades[361]. What was once regarded as a low-threat pathogen, now poses a significant risk for hospital-acquired infection throughout the world due to its incredible ability to acquire AMR and high risk of epidemic[27,362]. *A. baumannii* accounts for more than 10% of nosocomial infections in the United States. Disease manifests as pneumonia, bacteremia, urinary tract infections, skin and soft tissue infections, meningitis, and endocarditis[363]. Treatment

options for *A. baumannii* infections have dwindled due to resistance against almost all antibiotic classes, including β-lactams, fluoroquinolones, tetracycline, and aminoglycosides[27,362]. The prevalence of multidrug resistant, extensively drug-resistant and pan-drug resistant *A. baumannii* isolates has led to a resurgence in colistin treatment, which was thought to be one of the few remaining therapeutic options still effective against multidrug resistant *A. baumannii.* However, increased colistin resistance among *A. baumannii* isolates has further amplified its threat to the global public health[177,260,351,352,364–366].

Recent advances in high-throughput sequencing technologies, such as transposon sequencing (Tn-seq), have provided important tools to advance our understanding of bacterial fitness *in vitro* and *in vivo*. Tn-seq is a powerful tool that can be leveraged to study genotype-phenotype interactions in bacteria. Tn-seq is broadly applicable across bacterial pathogens, where it combines traditional transposon mutagenesis with massive parallel sequencing to rapidly map insertion sites, which can be used to link DNA mutations to phenotypic variants on a genome-wide scale[146,147,367,368]. While transposon mutagenesis methods have been previously described, the general steps are similar[146]. First, an insertion library is generated using transposon mutagenesis, where each bacterial cell within a population is restricted to a single transposon insertion within the genomic DNA (gDNA). Following mutagenesis, individual mutants are pooled. gDNA is extracted from the insertion mutant pool and the transposon junctions are amplified and subjected to high-throughput sequencing. The reads represent insertion sites, which can be mapped to the genome. Transposon insertions that reduce fitness quickly fall out of the population, while beneficial insertions

are enriched. Tn-seq has been instrumental to advance our understanding of how genes impact bacterial fitness in stress[146].

The *Himar1 mariner* transposon system encoded in pJNW684 was specifically constructed and optimized for the purpose of transposon mutagenesis. It includes a *mariner*-family transposon flanking the kanamycin resistance gene, which is used for the selection of transposon insertion mutants in *A. baumannii*. It also encodes an *A. baumannii* specific promoter that drives expression of the transposase encoding gene[157]. The *mariner*-based transposon also contains two translational terminators downstream of the kanamycin resistance gene, which prevents read-through downstream of the insertion[149]. pJNW684 also carries a RP4/oriT/oriR6K- conditional origin of replication which requires the *λpir* gene contributed by the donor strain to replicate[369]. In absence of the *λpir* gene, the pJNW684 vector carrying the transposition machinery will not be able to replicate in the *A. baumannii* recipient strain[157,260,369]. Therefore, during bacterial conjugation, only the transposon is inserted into the recipient genome without background insertion of the plasmid, which carries the transposase gene. This is significant because the loss of transposase activity along with the plasmid results in single, stable transposition event that prevents the transposon from moving to different locations once it inserts into the recipient genome.

pJNW648 has also been tested for activity in another Gram-negative organism, *E. coli*. Successful assembly of a saturating Tn-seq library in *E. coli* strain W3110 indicated the system is amenable to perform mutagenesis in a wide range of pathogens, including Enterobacteriaceae. Furthermore, the *A. baumannii* specific promoter that drives transposase expression can quickly be exchanged with a species-specific promoter.

Lastly, the kanamycin resistance gene can be exchanged for other resistance cassettes, depending on the AMR phenotype of the organism being studied.

One factor that contributes to colistin resistance in *A. baumannii* is administration of insufficient doses, where bacteria are exposed to selective pressure at non-lethal levels[370]. Several reports showed that subinhibitory antimicrobial concentrations can induce regulated responses that alter cell physiology to reduce susceptibility of the entire bacterial population[177,351,365,366]. Using Tn-seq, we discovered factors that regulate colistin resistance in *A. baumannii* strain ATCC 17978 after exposure to inhibitory[260] and subinhibitory concentrations of colistin. This example details a Tn-seq method that streamlines the construction and enrichment of a saturated transposon mutant library using the *mariner*-based family of transposons[155,156]. While several Tn-seq protocols generate 20,000 – 100,000 mutants[368,371–374], the protocol described herein can rapidly generate a transposon library of 400,000 + mutants, which roughly equates to a transposon insertion every 10-base pairs in *A. baumannii*[260]. Furthermore, the library size can be scaled up without significant additional effort. This method also eliminates the requirement for restriction endonucleases, adapter ligation and gel purification, which can reduce final library diversity.

Protocol

1. Bacterial strain preparation

1. Streak the "donor" strain (E. coli MFD DAP$^-$/pJNW684) for isolated colonies on Luria-Bertani agar supplemented with 600 μM diaminopimelic acid (DAP), 100 mg/L of ampicillin and 25 mg/L of kanamycin. Incubate overnight at 37°C. Using a single isolated colony, inoculate 50 mL of Luria broth (LB)

supplemented with 600 μM DAP, 100 mg/L of ampicillin and 25 mg/L of kanamycin in a 250 mL Erlenmeyer flask and label it as “donor”.

2. Streak the “recipient” strain (*A. baumannii* strain ATCC 17978) for isolated colonies on Luria-Bertani agar. Incubate overnight at 37°C. Using a single isolated colony, inoculate 50 mL of LB in a 250 mL Erlenmeyer flask and label it as “recipient”.
3. Incubate both cultures (“donor” and “recipient”) overnight at 37°C with shaking.

2. Bacterial mating

1. Transfer overnight cultures to 50 mL conical tubes.
2. Pellet both recipient and donor cultures using centrifugation at 5,000 × g for 7 min.
3. Discard the supernatant and resuspend the “donor” strain pellet in 35 mL of LB supplemented with DAP to wash away residual antibiotics.
4. Pellet the “donor” strain cells using centrifugation at 5,000 × g for 7 min.
5. Discard the supernatant and resuspend the “donor” strain pellet in 4.5 mL of LB supplemented with DAP. Use a 10 mL serological pipette.
6. Transfer the resuspended “donor” strain into “recipient” strain tube, which contains the pelleted “recipient” cells. Use the same 10 mL serological pipette from step 2.5 to mix the cultures. Immediately move to the next step.

   NOTE: The total volume of the final suspension should be 5 mL.
7. Distribute the mating suspension as individual 100 μL droplets on LB agar plates supplemented with DAP (5–7 droplets per plate) (**Figure 31A**).
8. Incubate plates at room temperature for 30 min.

9. Without disturbing the droplets, carefully transfer plates to a 37°C incubator and allow cultures to mate for 1 h.

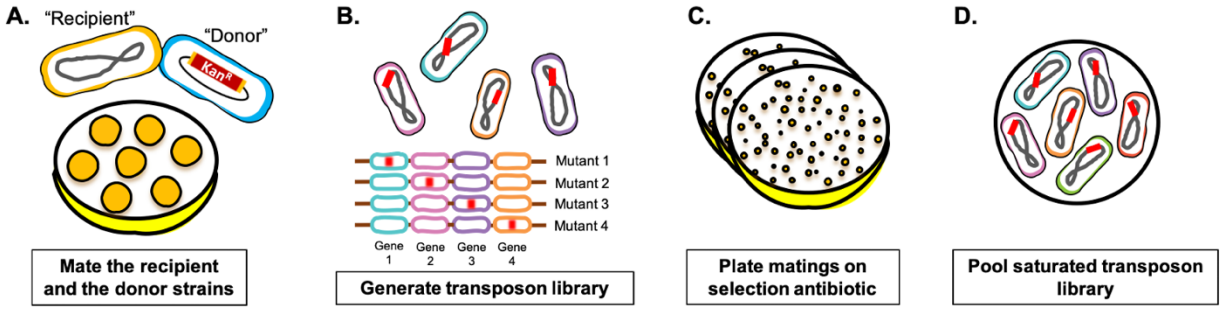

Figure 31: Schematic of transposon mutant library construction. (A) Bacterial conjugation. The "donor" strain, which encodes the transposition machinery, was mixed with the "recipient" strain. The mixture was spotted on LB agar plates and allowed to mate for 1 h. (B) Generation of transposon library. The plasmid carrying the transposition machinery was transferred from the "donor" strain to the "recipient" strain and the transposon was randomly inserted throughout the genome of the "recipient" strain. (C) Selection. Resulting cells were plated on agar plates supplemented with kanamycin to select for transposon insertion mutants. (D) Pooled library. Colonies were scraped from plates, resuspended in LB and pooled. Please click here to view a larger version of this figure.

NOTE: Incubation periods exceeding 1 h risks generation of sister mutants.

10. Following incubation, add 1.5 mL of LB onto each plate and harvest by resuspending bacteria from the plates. Use a 1 mL micropipette for resuspension. Final volume should be approximately 12–15 mL.
11. Combine harvested cells in a 50 mL conical tube.
12. Pellet the mated cells using centrifugation at 5,000 × g for 7 min.
13. Discard the supernatant and resuspend cells in 50 mL of LB to remove residual DAP.
14. Pellet the mating using centrifugation at 5,000 × g for 7 min.
15. Repeat the wash step (steps 2.13 and 2.14).

16. Using a 10 mL serological pipette, resuspend the pellet in 10 mL of LB supplemented with 25% glycerol.
17. Using washed cells, make five serial dilutions in LB broth (1:10, 1:100, 1:1000, 1:10,000, 1:100,000).
18. Spread 100 μL of each dilution on 4 different plates using sterile glass beads: Luria-Bertani agar supplemented with kanamycin, agar supplemented with ampicillin, agar supplemented with DAP and agar only.
19. Incubate plates at 37°C overnight.
20. Aliquot the remaining mating in 1 mL aliquots and store at-80°C.

3. **Determine the appropriate dilution of transposon library**

1. Record colony-forming units (CFU) from overnight plates.
2. Image a plate with countable colonies for each different plate condition (**Figure 32A**).

   NOTE: Both “donor” and “recipient” strains should grow on agar plates supplemented with DAP, so most plated dilutions will yield a lawn. Only the “recipient” strain can grow on agar plates. Neither the “donor” nor the “recipient” strain can grow on agar plates supplemented with ampicillin, so there should be none/minimal growth. Only target strain cells encoding the transposon insertion can grow on agar plates supplemented with kanamycin. Colonies should vary in size, indicating transposon insertions in genes that contribute to fitness on agar supplemented with kanamycin.
3. Calculate the number of transposon mutants in the frozen mating by counting the number of colonies on LB agar plates supplemented with kanamycin.

NOTE: For the A. baumannii genome (approximately 4 Mbps), the goal was to obtain about 400,000 colonies in order to generate a high-resolution mutant library (approximately one transposon insertion/10 base pairs). However, this number should be optimized based on genome size of the target species).

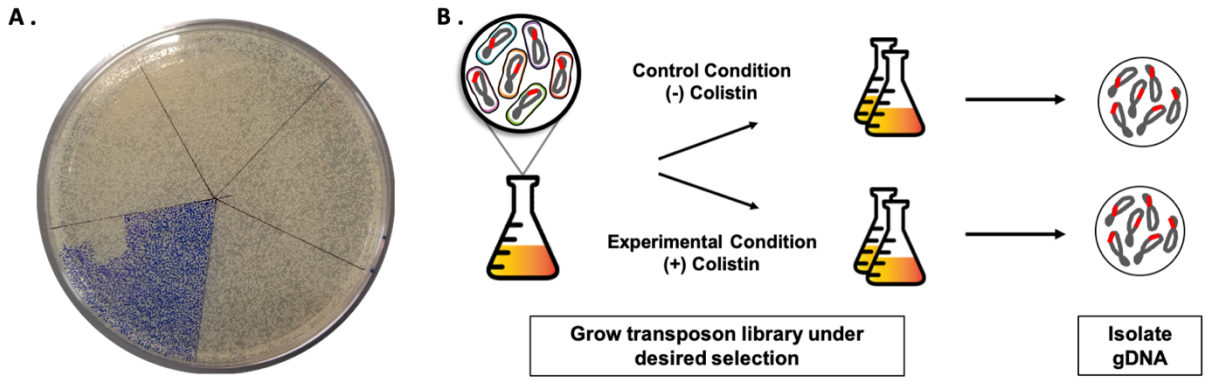

Figure 32: Representative bacterial conjugation results and a schematic of the colistin Tn-seq experiment. (A) Representative kanamycin selection plate. The plate is divided into five equal sections. Blue dots represent colony counting for estimation of A. baumannii transposon insertion mutants. At least three separate plates were counted to calculate the final estimation. (B) Identification of fitness factors at subinhibitory colistin concentrations. The pooled transposon library was grown to logarithmic growth phase either in the absence (control) or in the presence (experimental) of colistin. Once the cultures reached appropriate optical density, the cells were pelleted and gDNA was extracted from each sample. Each condition was tested in duplicate for a total of four samples. Please click here to view a larger version of this figure.

4. Generation of final bacterial mutant library

1. Thaw an aliquot of the frozen mating on ice.
2. Plate mating on 150 mm Luria-Bertani agar plates supplemented with kanamycin based on CFUs calculated in step 3.1. Adjust the volume with LB to yield 13,333 colonies per 150 μL before plating.

   NOTE: The CFU count here was determined to be about 10^5 CFU/mL, so the mating volume was adjusted to obtain 13,333 colonies per plate as this would

provide an optimal number of colonies on 30 plates for a high-resolution mutant library without overcrowding the plates.

3. Use sterile glass beads to spread 150 μL of the dilution per plate on 30 × 150 mm Luria-Bertani agar plates supplemented with kanamycin to obtain 400,000 colonies (**Figure 31C**).

   NOTE: Sterile rods or any kind of sterile spreader tool (*i.e.*, glass beads) may be used to spread the bacteria on plates.

4. Dispose of the used tube containing excess mating.

   NOTE: Freeze/thaw cycles adds selective pressures on the bacterial culture, which can skew the Tn-seq experiment results. Use a fresh aliquot each time.

5. Incubate plates at 37°C for 14 h.

   NOTE: The incubation time is optimized to prevent overgrowth (colonies touching). Minimizing growth by reducing the incubation time is suggested.

5. Estimating library density and pooling for storage

1. Count CFUs on each plate to estimate the total mutants in the transposon library. Count 20% of at least 3 plates to determine the colony count estimate for the entire group of plates (**Figure 32A**). Ensure that the colonies are not touching another colony.

2. After calculating the estimated colony yield, add 3–5 mL of LB (or more if needed) to each plate and scrape off the bacteria using a sterile scraping tool.

   NOTE: Sterile inoculating loops were used to efficiently scrape plates.

3. Pool bacterial suspensions from all plates into 50 mL conical tubes (**Figure 31D**). This will require multiple 50 mL conical tubes, at least 3.

4. Pellet pooled bacterial suspension using centrifugation at 5,000 × g for 7 min.
5. Discard the supernatant and resuspend pellet in 5 mL of LB supplemented with 30% glycerol.
6. Aliquot 1 mL of the transposon library into cryovials and store at −80°C.

6. Identification of factors that regulate colistin resistance in *A. baumannii*

1. Prepare 4 × 250 mL Erlenmeyer flasks with each containing 50 mL LB broth and label as (**Figure 32B**)
    1. *A. baumannii* strain ATCC 17978 Tn-seq library; (−) colistin_1
    2. *A. baumannii* strain ATCC 17978 Tn-seq library; (−) colistin_2
    3. *A. baumannii* strain ATCC 17978 Tn-seq library; (+) colistin_1
    4. *A. baumannii* strain ATCC 17978 Tn-seq library; (+) colistin_2

    NOTE: In the challenge growth described here, each condition, (−) colistin control and (+) colistin challenge, is being tested in duplicate. Therefore, the setup requires 4 × 250 mL Erlenmeyer flasks, two per condition.
2. Add 50 μL of 0.5 mg/L colistin to (+) colistin flasks (6.1.3 and 6.1.4) and 50 μL water to (−) colistin flasks (6.1.1 and 6.1.2).
3. Thaw a frozen Tn-seq library aliquot from step 5 on ice.
4. Pipette 1 μL of the thawed library into 1 mL of PBS.
5. Measure the optical density at 600 nm (OD_{600}) and multiply by 1,000.

    NOTE: This determines OD_{6OO} of 1 μL of the Tn-library.
6. Based on the calculation in step 6.5, inoculate each flask containing 50 mL LB to a final OD_{600} 0.001.

7. Grow cultures in a shaking incubator at 37°C to OD_{600} 0.5.

   NOTE: It is important that cultures remain in logarithmic growth phase, so if your strain is at a different OD_{600} during exponential growth, the OD_{600} needs to be adjusted to ensure the culture replicates as many times as possible within logarithmic growth phase. If the culture only replicates 3 times, the power to detect fitness defects in mutants is capped at 3-fold differences, in theory. Since different bacteria have different doubling times, it is important to seed the cultures at a fixed OD_{600} to normalize the starting inoculum. This ensures consistent representation of the entire library in all cultures.

8. Harvest cultures using centrifugation at 5,000 × g at 4°C for 7 min.
9. Remove the supernatant and wash with 50 mL of PBS.
10. Pellet using centrifugation at 5,000 × g at 4°C for 7 min.
11. Remove the supernatant and resuspend the pellet in 1 mL of PBS. Aliquot ~ 200 μL into 5 microcentrifuge tubes.
12. Pellet using centrifugation at 5,000 × g at 4°C for 5 min. Remove all of the supernatant using a pipette tip.
13. Store pellets at −20°C or proceed with gDNA extraction.

7. gDNA extraction

1. Thaw one cell pellet on ice.
2. Add 0.6 mL lysis buffer (9.34 mL TE buffer; 0.6 mL 10% SDS; 0.06 mL proteinase K [20 mg/L]) and vortex to completely resuspend the pellet.
3. Incubate at 37°C for 1 h.

4. Add 0.6 mL of phenol/chloroform/isoamyl alcohol to the sample and vortex vigorously.
5. Separate phases using centrifugation in a microcentrifuge at max speed at room temp for 5 min.
6. Transfer the upper aqueous phase to a new tube. Avoid disturbing the phase interface during transfer.
7. Add an equal volume of chloroform to the aqueous phase obtained above and vortex vigorously.
8. Separate phases using centrifugation in microcentrifuge at max speed at room temp for 5 min.
9. Transfer upper aqueous phase to a new tube.

   NOTE: Be sure to avoid disturbing the interface during transfer.
10. Add 2.5x aqueous phase volume of cold 100% ethanol and mix gently. Precipitated DNA will be visible.
11. Place tube at −80°C for at least 1 h.
12. Pellet DNA using centrifugation at max speed at 4°C for 30 min.
13. Carefully remove supernatant without disturbing the DNA pellet and wash with 150 μL of 70% ethanol by pipetting.
14. Pellet DNA using centrifugation at max speed at 4°C for 2 min.
15. Carefully remove the supernatant.
16. Repeat step 7.14 once. Carefully remove all remaining ethanol.
17. Dry DNA by incubating at room temp for 5–10 min.
18. Resuspend DNA pellet in 100 μL TE buffer by pipetting.

8. DNA shearing (Figure 33A)

1. Dilute gDNA with TE buffer to a concentration of 250 ηg/ mL in a total volume of 200 μL.
2. Place tubes in a water bath sonicator.
3. Sonicate DNA to yield fragments of approximately 300 nucleotides. Power: 60%, Total Time: 20 min, Cycles: 10 s ON and 10 s OFF at 4°C (**Figure 33A**).
4. Confirm DNA is sheared appropriately by separating 10 μL of unsheared DNA and 10 μL of sheared DNA on a 1% agarose gel. Repeat sonication or optimize as needed (**Figure 33B**).

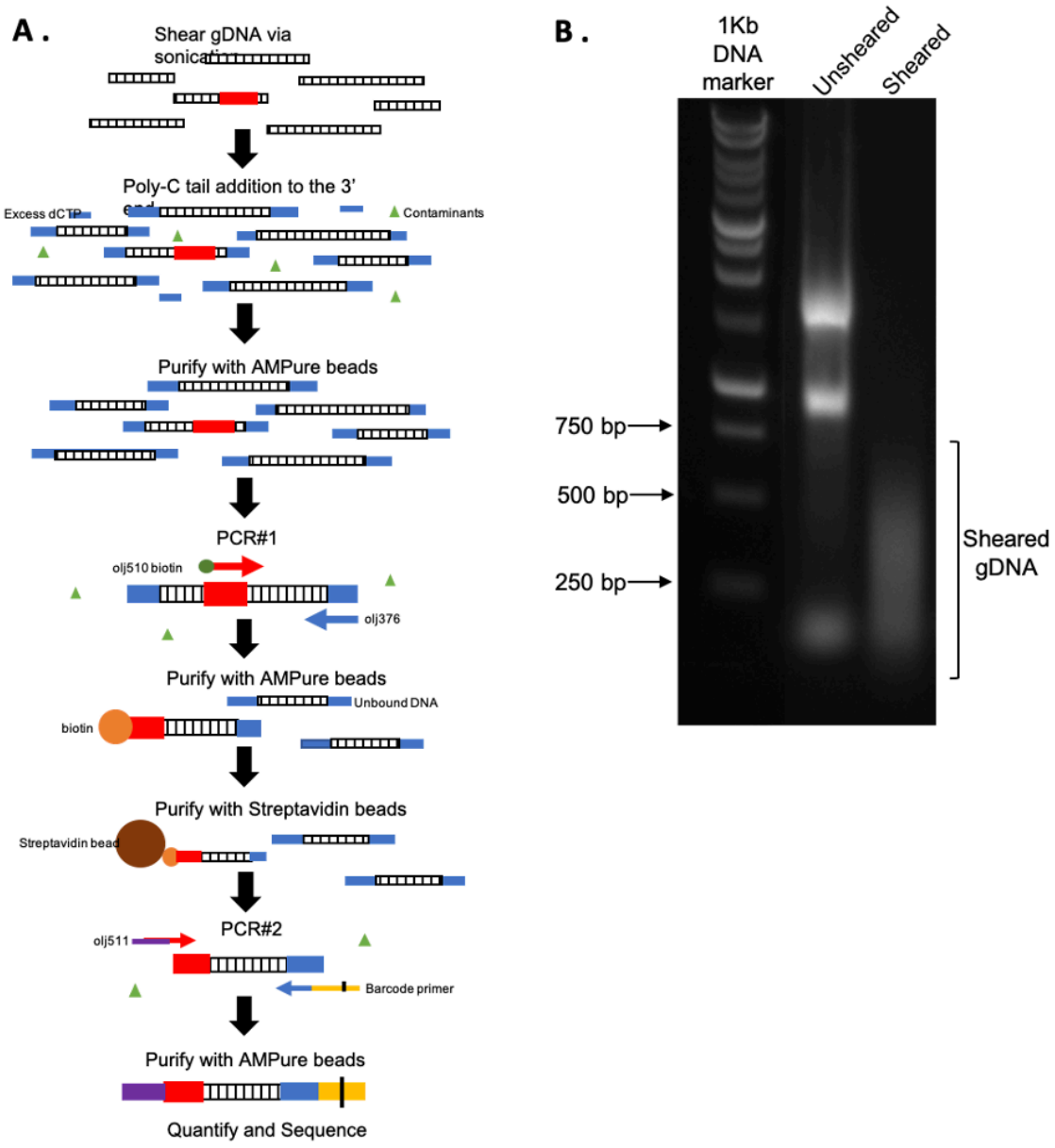

Figure 33: Flowchart of the DNA amplicon library build for massive parallel sequencing and representative sheared gDNA. (A) Tn-seq DNA library build schematic. Following extraction, gDNA was fragmented via mechanical shearing. Terminal deoxynucleotidyl transferase was used to add a poly-C tail to the 3' end of fragmented DNA before PCR amplification of the transposon-genome junctions and barcode addition. (B) 1% agarose gel of unsheared and sheared A. baumannii mutant libraries following gDNA shearing step. 1 Kb ladder was used as a DNA marker. Sheared gDNA smear primarily ranges between ~ 100 and 500 base pairs. Please click here to view a larger version of this figure.

9. **Poly-C tail addition to the 3' end (Figure 33A)**

1. Setup poly-C reaction according to the **Table 4**.
2. Incubate reaction at 37°C for 1 h.
3. Purify poly-C reaction with 40 μL of size-selection paramagnetic beads (**Figure 3**3**A**) by following the steps below.
    1. Add 40 μL of size-selection paramagnetic beads to each sample. Vortex ~ 5 s or pipette up and down.
    2. Incubate samples at room temperature for 5 min.
    3. Briefly, centrifuge tubes to collect liquid in the bottom of the tube (~ 2 s).
    4. Transfer tubes to a magnetic rack and incubate at room temperature for ~ 2 min until the solution is clear.
    5. With tubes on magnetic rack, carefully remove the supernatant.
    6. With tubes on magnetic rack, add 200 μL of freshly prepared 80% ethanol (do not disturb beads).
    7. Incubate samples for at least 30 s until solution is clear.
    8. With tubes on magnetic rack, carefully remove the supernatant.
    9. Repeat the wash step (steps 9.3.6 – 9.3.8).
    10. Collect liquid in the bottom of the tube using a brief centrifugation step (~ 2 s).
    11. Transfer tubes to the magnetic rack and remove any remaining liquid.
    12. Incubate at room temperature for 2–5 min to dry samples. Do not over dry.

13. Remove tubes from magnetic rack and add 25 μL of water to each. Vortex for ~ 5 s or pipette up and down.
14. Briefly, centrifuge tubes to collect liquid in the bottom of the tube (~ 2 s).
15. Transfer tubes to the magnetic rack and allow to sit for ~ 2 min until the solution is clear.
16. With tubes on the magnetic rack, remove liquid without disturbing the beads and transfer to a new tube (~23 μL of DNA).

Table 4: Reaction setup. Setup and conditions for poly-C, PCR 1 and PCR 2 reactions.

Reaction	Setup	Conditions
Poly-C reaction	30 μL of sheared gDNA 2.5 μL of 9.5 mM dCTP/0.5 mM ddCTP 10 μL of 5X Terminal deoxynucleotidyl transferase (Tdt) reaction buffer 1.25 μL of rTdt 6.25 μL of water to 50 μL	Incubate at 37°C for 1 hour
PCR 1	23 μL 3'-poly-C purified DNA (entire sample from previous step) 10 μL 10x high-fidelity DNA polymerase reaction mix 2 μL 10mM dNTPs 2 μL 50 mM MgS04 1 μL 30 μL 510 biotin 3 μL 30 μL olj 376 0.5 μL high-fidelity DNA polymerase 8.5 μL pure water to 50 μL total	1 cycle: 2 min 94 °C 15 cycles: 15 s 94 °C 30 s 60 °C 2 min 68 °C 1 cycle: 4 min 68 °C Hold: ∞ 4 °C
PCR 2	DNA bound beads from previous step 10 μL 10x high-fidelity DNA polymerase reaction mix 2 μL 10mM dNTP 2 μL 50 mM MgSO4 1 μL 30 μM olj 511 1 μL 30 μM barcode primer (Table 2) 0.5 μL high-fidelity DNA polymerase 33.5 μL pure water to 50 μL	1 cycle: 2 min 94 °C 15 cycles: 15 s 94 °C 30 s 60 °C 2 min 68 °C 1 cycle: 4 min 68 °C Hold: ∞ 4 °C

10. **Transposon junction amplification (Figure 33A)**

1. Setup PCR 1 as described in **Table 6.1** for the first nested PCR (**Table 5**).
2. Perform PCR 1 using conditions described in **Table 4**.
3. Purify PCR products with 40 μL of size-selection paramagnetic beads (steps 9.3.1 – 9.3–12). Elute in 50 μL of water (steps 9.3.13 – 9.3.16). At this point the samples can be stored at −20°C.
4. Prepare Streptavidin-coupled paramagnetic beads:
    1. Resuspend Streptavidin beads by shaking vigorously.
    2. Add 32 μL of beads per sample to a fresh microcentrifuge tube.

       NOTE: Beads for 6 + samples can be prepared in a single tube.
    3. Transfer the tube to a magnetic rack. Incubate for~ 2 min until solution is clear.
    4. With tube on magnetic rack, remove supernatant.
    5. Remove the tube from magnetic rack. Wash beads by resuspending in 1 mL 1x B&W buffer by pipetting up and down.
    6. Transfer the tube to magnetic rack. Incubate for ~ 2 min until solution is clear.
    7. With the tube on magnetic rack, remove the supernatant.
    8. Repeat wash step with 1 mL 1x B&W buffer (steps 10.4.5 – 10.4.7) twice more for a total of 3 washes.
    9. Remove tube from magnetic rack and resuspend beads in 52 μL of 2x B&W buffer per sample.

5. Combine 50 μL of the prepared beads with 50 μL of purified PCR1 (from step 10.3). Pipette to mix.
6. Rotate at room temperature for 30 min.
7. Wash away unbound DNA:
    1. Briefly, centrifuge to collect liquid at the bottom of the tube (~ 2 s).
    2. Transfer the tube to magnetic rack. Incubate for ~ 2 min until the solution is clear.
    3. With the tube on magnetic rack, remove the supernatant.
    4. Remove the tube from magnetic rack, wash beads by resuspending in 100 μL 1x B&W buffer and pipetting up and down.
    5. Transfer tube to magnetic rack. Incubate for ~ 2 min until the solution is clear.
    6. With tube on magnetic rack, remove supernatant.
    7. Repeat wash steps with 100 μL LoTE (steps 10.7.4 – 10.7.6) twice more for a total of 3 washes.
    8. Setup PCR 2 as described in **Table 4** to amplify transposon junctions and add a single barcode to each sample (**Table 5 and Table 6**).
    9. Perform PCR 2 using conditions described in **Table 4**.
    10. Purify with 40 μL of size-selection paramagnetic beads (steps 9.3.1 – 9.3.12). Elute in 17 μL of water (steps 9.3.13 – 9.3.16), collect ~ 15 μL.
    11. Quantify DNA concentration using a fluorometer. The final concentrations should be ~ 50 to 250 ηg/μL.

12. Assess DNA quality using chip-based capillary electrophoresis (**Figure 34A**).

Table 5: PCR amplification primers. PCR amplification primers used in the protocol to amplify the transposon junctions. The purpose of each is listed in the first column.

Purpose	Name	Sequence
Anneals to transposon	olj510-Biotin	Biotin-GATGGCCTTTTTGCGTTTCTACCTGCAGGGCGCG
Anneals to poly-C tail	olj376	GTGACTGGAGTTCAGACGTGTGCTCTTCCGATCTGG GGGGGGGGGGGGGG
Nested to transposon + P5 adapter:	olj511	AATGATACGGCGACCACCGAGATCTACACTCTTT
P5 capture site – P5 sequencing site–N5–Tn		CCCTACACGACGCTCTTCCGATCTNNNNNGGGGACTTA TCATCCAACCTGTTAG
Nested to olj376: P7 sequencing site – barcode xref- P7 capture site	BC##	CAAGCAGAAGACGGCATACGAGATxxxxxxGTGA CTGGAGTTCAGACGTGTG
see Table 3 for specific barcodes		

Representative Results

The outlined methods describe the generation of a high- density transposon library in *A. baumannii strain* ATCC 17978 through bacterial conjugation using *E. coli* MFD DAP$^-$, which replicates the plasmid pJNW684 (**Figure 34B**). The detailed protocol uses bi-parental bacterial conjugation for transfer of pJNW684 from the E. coli *λpir*+ donor strain to the *A. baumannii* recipient strain. This is an efficient and inexpensive method for generating dense transposon mutant libraries. Bacteria were mixed at optimized ratios and matings were spotted on Luria-Bertani agar plates for 1 h (**Figure 31A**). During mating, the transposon was transferred from the donor to recipient strain, where it inserted into the gDNA (**Figure 31B**). Matings were collected, approximately 10^5 CFU/mL were calculated and plated on 150 mm × 15 mm agar plates supplemented with kanamycin. After 14 h of growth at 37°C, plates contained thousands of colonies of varying size (**Figure 31C**) indicating successful generation of a transposon mutant library.

The transposon insertion mutants were pooled (**Figure 31D**) and frozen in aliquots to prevent repeated freeze-thaw cycles, which could add selective pressure on the insertion library.

Table 6: Barcode primers. Barcode primers are used in the second PCR step to amplify the transposon junctions while adding a P7 sequencing site and barcodes to the amplicon. Not all barcode primers are needed to generate a library. Only barcode primers for the number of samples are required.

Primer	Read	Barcode	Sequence
BC1	ATCACG	CGTGAT	CAAGCAGAAGACGGCATACGAGATCGTGATGTGACTGGAGTTCAGACGTGTG
BC2	CGATGT	ACATCG	CAAGCAGAAGACGGCATACGAGATACATCGGTGACTGGAGTTCAGACGTGTG
BC3	TTAGGC	GCCTAA	CAAGCAGAAGACGGCATACGAGATGCCTAAGTGACTGGAGTTCAGACGTGTG
BC4	TGACCA	TGGTCA	CAAGCAGAAGACGGCATACGAGATTGGTCAGTGACTGGAGTTCAGACGTGTG
BC5	ACAGTG	CACTGT	CAAGCAGAAGACGGCATACGAGATCACTGTGTGACTGGAGTTCAGACGTGTG
BC6	GCCAAT	ATTGGC	CAAGCAGAAGACGGCATACGAGATATTGGCGTGACTGGAGTTCAGACGTGTG
BC7	CAGATC	GATCTG	CAAGCAGAAGACGGCATACGAGATGATCTGGTGACTGGAGTTCAGACGTGTG
BC8	ACTTGA	TCAAGT	CAAGCAGAAGACGGCATACGAGATTCAAGTGTGACTGGAGTTCAGACGTGTG
BC9	GATCAG	CTGATC	CAAGCAGAAGACGGCATACGAGATCTGATCGTGACTGGAGTTCAGACGTGTG
BC10	TAGCTT	AAGCTA	CAAGCAGAAGACGGCATACGAGATAAGCTAGTGACTGGAGTTCAGACGTGTG
BC11	GGCTAC	GTAGCC	CAAGCAGAAGACGGCATACGAGATGTAGCCGTGACTGGAGTTCAGACGTGTG
BC12	CTTGTA	TACAAG	CAAGCAGAAGACGGCATACGAGATTACAAGGTGACTGGAGTTCAGACGTGTG
BC13	AGTCAA	TTGACT	CAAGCAGAAGACGGCATACGAGATTTGACTGTGACTGGAGTTCAGACGTGTG
BC14	AGTTCC	GGAACT	CAAGCAGAAGACGGCATACGAGATGGAACTGTGACTGGAGTTCAGACGTGTG
BC15	ATGTCA	TGACAT	CAAGCAGAAGACGGCATACGAGATTGACATGTGACTGGAGTTCAGACGTGTG
BC16	CCGTCC	GGACGG	CAAGCAGAAGACGGCATACGAGATGGACGGGTGACTGGAGTTCAGACGTGTG
BC17	GTAGAG	CTCTAC	CAAGCAGAAGACGGCATACGAGATCTCTACGTGACTGGAGTTCAGACGTGTG
BC18	GTCCGC	GCGGAC	CAAGCAGAAGACGGCATACGAGATGCGGACGTGACTGGAGTTCAGACGTGTG
BC19	GTGAAA	TTTCAC	CAAGCAGAAGACGGCATACGAGATTTTCACGTGACTGGAGTTCAGACGTGTG
BC20	GTGGCC	GGCCAC	CAAGCAGAAGACGGCATACGAGATGGCCACGTGACTGGAGTTCAGACGTGTG
BC21	GTTTCG	CGAAAC	CAAGCAGAAGACGGCATACGAGATCGAAACGTGACTGGAGTTCAGACGTGTG
BC22	CGTACG	CGTACG	CAAGCAGAAGACGGCATACGAGATCGTACGGTGACTGGAGTTCAGACGTGTG
BC23	GAGTGG	CCACTC	CAAGCAGAAGACGGCATACGAGATCCACTCGTGACTGGAGTTCAGACGTGTG
BC24	GGTAGC	GCTACC	CAAGCAGAAGACGGCATACGAGATGCTACCGTGACTGGAGTTCAGACGTGTG
BC25	ACTGAT	ATCAGT	CAAGCAGAAGACGGCATACGAGATATCAGTGTGACTGGAGTTCAGACGTGTG
BC26	ATGAGC	GCTCAT	CAAGCAGAAGACGGCATACGAGATGCTCATGTGACTGGAGTTCAGACGTGTG
BC27	ATTCCT	AGGAAT	CAAGCAGAAGACGGCATACGAGATAGGAATGTGACTGGAGTTCAGACGTGTG
BC28	CAAAAG	CTTTTG	CAAGCAGAAGACGGCATACGAGATCTTTTGGTGACTGGAGTTCAGACGTGTG
BC29	CAACTA	TAGTTG	CAAGCAGAAGACGGCATACGAGATTAGTTGGTGACTGGAGTTCAGACGTGTG
BC30	CACCGG	CCGGTG	CAAGCAGAAGACGGCATACGAGATCCGGTGGTGACTGGAGTTCAGACGTGTG
BC39	CTATAC	GTATAG	CAAGCAGAAGACGGCATACGAGATGTATAGGTGACTGGAGTTCAGACGTGTG
BC40	CTCAGA	TCTGAG	CAAGCAGAAGACGGCATACGAGATTCTGAGGTGACTGGAGTTCAGACGTGTG
BC42	TAATCG	CGATTA	CAAGCAGAAGACGGCATACGAGATCGATTAGTGACTGGAGTTCAGACGTGTG
BC43	TACAGC	GCTGTA	CAAGCAGAAGACGGCATACGAGATGCTGTAGTGACTGGAGTTCAGACGTGTG
BC44	TATAAT	ATTATA	CAAGCAGAAGACGGCATACGAGATATTATAGTGACTGGAGTTCAGACGTGTG
BC45	TCATTC	GAATGA	CAAGCAGAAGACGGCATACGAGATGAATGAGTGACTGGAGTTCAGACGTGTG
BC46	TCCCGA	TCGGGA	CAAGCAGAAGACGGCATACGAGATTCGGGAGTGACTGGAGTTCAGACGTGTG
BC47	TCGAAG	CTTCGA	CAAGCAGAAGACGGCATACGAGATCTTCGAGTGACTGGAGTTCAGACGTGTG
BC48	TCGGCA	TGCCGA	CAAGCAGAAGACGGCATACGAGATTGCCGAGTGACTGGAGTTCAGACGTGTG

The pooled *A. baumannii* transposon mutant library was used to identify fitness factors important for colistin resistance under subinhibitory concentrations of the antimicrobial (**Figure 32B**). The mutant library was grown to logarithmic phase in the absence/presence of 0.5 mg/L colistin in duplicate to deplete mutant cells encoding insertions in genes that contribute to colistin resistance. The total gDNA of the remaining library pool was isolated from control and experimental cultures and processed to prepare DNA for sequencing (**Figure 33A**).

Isolated gDNA was fragmented using mechanical shearing and a poly-C tail was added on the DNA fragments (**Figure 33A**). Following the addition of poly-C tail, DNA was purified and the transposon-genome junctions were enriched using the poly-C specific primer followed by a second round of PCR using another poly-C specific primer that introduced the P7 sequencing site which is required for binding the Illumina flow cell and cluster generation, and a six-base barcode that is used to demultiplex libraries post sequencing[149,375]. DNA concentrations were calculated, and the samples were analyzed using chip-based capillary electrophoresis to confirm successful library builds (**Figure 34A**), which are ready for high-throughput sequencing.

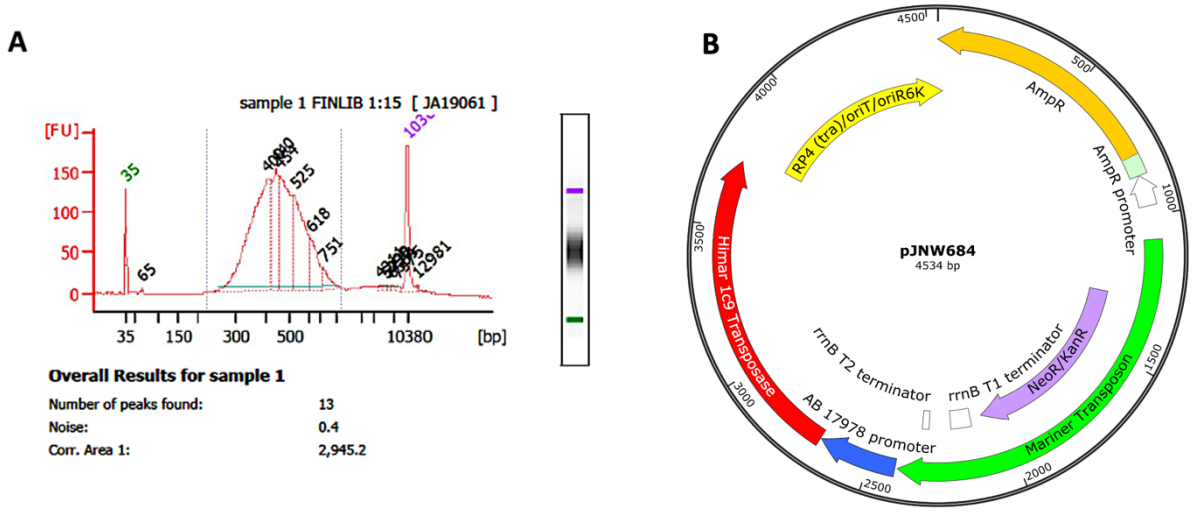

Figure 34: Representative quality control (QC) results and map of the plasmid carrying the transposition genes. (A) QC trace for a DNA library build. There is a peak at ~ **350** base pairs, indicating successful library build. If some larger DNA was detected in the QC results, the samples can be cleaned up further to remove large DNA fragments. (B) Plasmid pJNW684 consists of a Himar1 mariner transposon (green) with a kanamycin resistance cassette (purple) for mutant selection, a gene encoding the hyperactive mariner Himar1 C9 transposase (red) under control of an A. baumannii 17978 specific promoter (blue), an ampicillin resistance gene (bla, orange) and a RP4/oriT/oriR6K-conditional origin of replication (yellow). Please click here to view a larger version of this figure.

DNA libraries were sequenced by next generation sequencing. A single-end, 50 cycle run was performed, which yielded 30 million high-quality reads/sample providing 62.5-fold coverage of the transposon library. Transposon junctions (reads) were mapped to the reference genome[376], using commercially available bioinformatics analysis software. The number of reads at each insertion site in the input samples, (−) colistin control condition, were compared to the number of reads in the output samples, (+) colistin experimental condition, and fitness scores for each insertion site were calculated. The fitness scores were then grouped by gene. Genes demonstrating reduced scores when the library was grown in the presence of colistin relative to the input samples were considered fitness determinants for *A. baumannii* survival at subinhibitory concentrations of colistin. For example, transposon insertions within the PmrAB two-component system

were present in the input sample but were not found in the output sample. PmrAB directly regulates expression of *pmrC*, which transfers phosphoethanolamine onto lipid A to neutralize the charge on the cell surface[351,366]. Neutralization of bacterial surface charge is thought to reduce the electrostatic potential required for colistin-mediated killing. Identification of depleted genes known to contribute to the resistance phenotype validated the method.

Discussion

A. baumannii is an emerging threat to global public health due to the rapid acquisition of AMR against "last- line" therapeutics, such as colistin[27,177,260,351,362,365,366]. In recent decades, Tn-seq has played a critical role in elucidating genotype-phenotype interactions across numerous bacterial species and expanding our understanding of bacterial genetics[147,368,371,372]. Tn-seq protocols have been instrumental in identifying essential genes in diverse bacterial species such as *Campylobacter jejuni, Staphylococcus aureus*, the periodontal pathogen *Porphyromonas gingivalis*, and even *Mycobacterium tuberculosis*[149–152]. Beyond identification of essential genes, Tn-seq has been used to

identify antibiotic resistance genes in *Pseudomonas aeruginosa*, several conditionally essential genes in *Salmonella typhimurium*, and numerous genotype-phenotype relationships in *Streptococcus pneumoniae*[377–379]. More recently, transposon sequencing of *Vibrio cholerae* was employed in the infant rabbit model of Cholera to identify genes that are important for *in vivo* fitness during infection[375]. These studies demonstrate the versatility of Tn-seq as it can be utilized for both *in vitro* and *in vivo* studies.

The main advantage of Tn-seq over other methods, such as microarray technologies, 2D gel electrophoresis, and qPCR, is that it does not require prior knowledge of the genome or genomic information[380]. Therefore, transposon mutagenesis coupled with massive-parallel sequencing enables the study of known genes and genomes as well as discovery of novel genetic interactions. Here we have presented a comprehensive method for generating a highly dense transposon mutant library *in A. baumannii* to identify factors that are essential for bacterial fitness when exposed to subinhibitory concentrations of colistin. The described method has also been successfully used in *E. coli* (unpublished data), demonstrating the system is amenable to perform Tn-seq analysis in other Gram-negative pathogens, including Enterobacteriaceae.

Using *mariner* transposons for insertional mutagenesis has several advantages. The transposon family originated from eukaryotic hosts and have been widely used to generate saturating mutant libraries in diverse bacterial populations. *Mariner* transposons are host-independent, which means that stable random insertions can be achieved in the absence of specific host factors[155,156]. Additionally, *mariner* transposons have a defined number of insertion events because they preferentially insert into thymine-adenine ("TA") motifs, which reduces insertional bias and leads to more robust statistical analysis[148,149,153,154].

Several *mariner*-based Tn-seq methods use *MmeI* restriction digestion for gDNA fragmentation[367,371,372]. While enzymatic DNA fragmentation is a popular and successful method, it adds unnecessary steps to the procedure and increases potential bias[149]. Not only do these techniques require large quantities of starting materials, they can also potentially lead to unequal representation of insertion sequences in downstream

analyses[149,381]. Like some other methods that do not rely on *MmeI* nuclease activity[377,382,383] the method outlined herein relies on mechanical shearing to fragment gDNA, and TdT to add a poly-C tail to the 3' end of the DNA fragments. Compared to enzymatic DNA fragmentation and adapter ligation methods, this approach requires significantly smaller amounts of starting DNA while providing more consistent results, it also lowers the risk of DNA cross-contamination and reduces sample loss due to confinement in a sealed tube[149,381,384]. Furthermore, this method yields longer, high quality sequencing reads of 50 nucleotides which aid in more effective and precise mapping of sequences and a more robust downstream analysis[149,381]. The addition of a synthetic poly-C tail disregards potential overhangs that may result from fragmentation as this method relies on the exogenously added poly-C tail as a recognition site for the reverse primer, which contains 16 dG nucleotides at its 3' end and a sequence specific to next generation sequencing (*e.g.*, Illumina sequencing) at the 5' end, to prime synthesis[375,381]. The use of a synthetic nucleotide tail expands the application of this method to many distinct genomes independent of their native content[381]. Subsequently, transposon-genome junctions are amplified using the poly-C specific primer[149]. This alternative simplifies the procedure by eliminating the need for expensive restriction enzymes, adapter ligation, formation of adapter dimers and gel purification steps. We have further optimized the protocol to efficiently generate highly saturated transposon insertion libraries in several Gram-negative ESKAPE pathogens, including *Acinetobacter baumannii* and can be used to study genetic interactions under diverse *in vitro* and *in vivo* conditions[260].

One limitation of Tn mutagenesis is it relies on the antibiotic resistance markers for selection. However, many Gram-negative ESKAPE pathogens are multidrug or extensively drug resistant, meaning the user may need to exchange the resistance cassette according to the specific pathogen of interest. Furthermore, some clinical isolates are not amenable to transposon mutagenesis using the *mariner*-based transposon.

A critical step of the protocol is calculating the number of Tn mutants to plate. Plating too many colonies will result in a lawn that can complicate downstream analysis. If the colonies are too close or touching, they can add unwanted selective pressure on the library that can result in artifacts. Ideally, colonies would be not be touching and spaced evenly across the plate, as demonstrated (**Figure 6.2A**). Conversely, if too few colonies are plated, it will be difficult to isolate multiple Tn insertions in each gene.

It is also important to perform the controls listed in step 2.18. As stated in the Note of section of 3. 2, neither “donor” or “recipient” strain should grow on plates supplemented with Ampicillin. Since exogenous DAP is required for growth of the “donor” strain, any growth would indicate the “recipient” strain replicates pJNW684. This is a significant problem because if the transposon does not integrate into the gDNA, sequencing reads will only map to the plasmid, not an integration site. In this case the experiment will likely not yield useable data.

CHAPTER 7

CONCLUSIONS AND RECOMMENDATIONS

The studies herein are focused on elucidating and targeting mechanisms leading to antimicrobial treatment failure in clinically significant Gram-negative bacterial species to address the antibiotic resistance crisis. These data outline the discovery and characterization of synthetic peptide sequences that inhibit the NDM-1 resistance enzyme to prevent hydrolysis of carbapenem β-lactams. We also describe identification and characterization of genetic determinants important for carbapenem tolerance in two clinically important Gram-negative bacterial species including members of the Enterobacterales family and *Acinetobacter baumannii.* Lastly, we present a streamlined method for transposon insertion mutagenesis and sequencing that can be used to identify fitness factors in diverse Gram-negative bacteria.

Carbapenems are an important group of β-lactam antibiotics due to their broad-spectrum activity and use as last-resort treatment options against multidrug resistant Gram-negative bacterial infections[385]. Additionally, carbapenems are not susceptible to many common β-lactam resistance mechanisms[6,7]. However, the emergence and rapid spread of MβLs, like NDM-1, throughout significant nosocomial Gram-negative pathogens seriously threatens the efficacy of these important clinical therapeutics. There is an urgent need for development of novel β-lactamase inhibitors to restore the therapeutic utility of these last-line antibiotics and prolong their clinical use. While several inhibitors against serine-dependent β-lactamases have been approved for clinical use by the Food and Drug Administration (FDA), none of these are active against MβLs due to dramatic differences in the active site structure and catalytic mechanisms between these two types

of β-lactamases[385]. As such, there are currently no MβL inhibitors approved for clinical use.

A recent report outlined the innovative antimicrobial discovery platform SLAY that is designed to screen for peptide sequences with activity against Gram-negative bacteria[141]. The studies in chapter 3 outline current work to build on this platform by adapting SLAY to search for peptide sequences that target and inhibit the NDM-1 resistance enzyme. More than one million random ten amino acid peptide sequences were screened using the high-throughput cell-based SLAY system to discover thousands of peptide chemistries that increased susceptibility of NDM-1 encoded *E. coli* to the widely used carbapenems imipenem and meropenem. Thirty-seven of these peptides were found to be conserved between the imipenem and meropenem treatment conditions which could suggest broad-spectrum activity. Since meropenem demonstrates more potent activity against Gram-negative bacteria out of these two commonly used carbapenems, we focused primarily on characterizing peptide sequences that increased susceptibility of various carbapenemase-producing Enterobacterales (CPE) to meropenem. Molecular and biochemical validation was used to identify several peptides that enhanced meropenem activity against NDM-1 encoded *E. coli*, *Klebsiella pneumoniae*, and *Enterobacter cloacae,* directly bound and inhibited NDM-1 hydrolytic activity and demonstrated minimal cytotoxicity.

Antimicrobial peptides have recently gained attention as appealing alternative therapeutic options because they are fast acting and can be used as monotherapy or in combinatorial therapy[131–133]. Peptides demonstrate activity against resistant bacteria as well as dormant cells which makes them valuable candidates for development of

antimicrobial therapeutics[386,387]. Importantly, due to high metabolic expenditure, bacteria have a low propensity for developing resistance to antimicrobial peptides[134,386,387]. Previous work investigating peptide chemical diversity has been constrained due to limitation in screening and discovery of peptides such that the true therapeutic potential of chemistries within amino acid sequences has not been fully recognized. While high-throughput small molecule library screening has identified competitive and non-competitive MβL inhibitors, these screens highlight several shortcomings associated with previous methods[113,128,129]. First is that these screens were limited in size and secondly, they were carried out *in vitro* using purified β-lactamase enzymes, which fails to assess inhibitor efficacy in cell-based systems. The SLAY platform overcomes these limitations by allowing exploration of a diverse chemical space within a cell-based system, which has proven to be particularly challenging in discovery of effective therapeutics against Gram-negative bacteria.

The work outlined in chapter 3 further advances the SLAY drug discovery method to identify unique peptide sequences that specifically inhibit NDM-1-mediated hydrolysis of β-lactam antibiotics in carbapenemase-producing Enterobacterales (CPE). This demonstrates the versatility of the SLAY technology for discovering antimicrobial peptides with broad-spectrum activity against Gram-negative bacteria as well as sequences that target specific bacterial factors/resistance mechanisms. Additionally, lead NDM-1 inhibitors identified in this work serve as a starting point for continuous optimization and characterization of high-potency NDM-1 inhibitor peptides. Mutational analysis of the NDM-1 amino acid sequence and original parent sequences of lead inhibitors presented

in chapter 3 can provide valuable insights into NDM-1 inhibition and aid in characterizing high-potency inhibitor sequences that enhance carbapenem susceptibility in CPE.

Three out of the four peptide sequences identified through studies in chapter 3 demonstrated competitive inhibition of the NDM-1 enzyme. One important goal in combating carbapenem resistant bacteria and prolonging clinical efficacy of carbapenems is development of broad-spectrum inhibitors that are effective against all MβLs[105,119]. In the short-term, there is an urgent need to develop inhibitors that specifically inactivate the B1 subclass, since it consists of the largest number of clinically relevant and most worrisome MβLs[105,119]. Despite the low overall amino acid identities (~ 30%) between the three B1 subclass MβLs, all three enzymes share highly conserved features within their active sites, including substrate binding and catalytic mechanisms[119]. In fact, the three B1 subclass enzymes rely on H116, H118, and H196 residues to coordinate Zn1, while D120, C221, and H263 are used to coordinate Zn2. Based on this, it is likely that competitive inhibitors discovered herein will bind to the conserved zinc active site to inhibit MβL hydrolytic activity and therefore, serve as broad-spectrum inhibitors of the clinically relevant B1 subclass enzymes including New Delhi-type (NDMs), Imipenemase-type (IMPs) and Verona integron-encoded-type (VIMs) MβLs.

Overall, this work addresses the increasing need for development of alternative antimicrobial therapeutic strategies by advancing the innovative SLAY technology to discover unique MβL inhibitor peptides that can serve as candidates for further development to restore efficacy of last-resort carbapenem β-lactams. Additionally, the studies outlined in chapter 3 enhance our understanding of MβL inhibition and provide a starting point for development and optimization of high-potency inhibitors with

translational potential. As with most therapeutics, evaluating the therapeutic potential of lead compounds will be an important step for further development. Future studies measuring pharmacokinetic properties of inhibitors in physiologically relevant solutions, such as human serum, will be necessary to quantify peptide stability in physiological conditions that inhibitors might encounter upon administration and will provide valuable information about improving inhibitor potency. Additionally, further studies using a murine wound infection model to test carbapenem efficacy in combination with topical application of inhibitor peptides directly at the site of infection would serve as a useful tool for quickly analyzing therapeutic value of inhibitors *in vivo* and would lay a foundation for improving peptide delivery mechanisms and tissue penetration.

Chapter 4 and 5 of the present work investigate bacterial tolerance as another major factor contributing to the failure of carbapenem therapeutics against clinically significant Gram-negative pathogens. Antibiotic tolerance is the ability of a susceptible bacterial population to transiently survive exposure to otherwise lethal concentrations of bactericidal antibiotics (i.e., carbapenem β-lactams)[12,14,255]. Unlike resistance, tolerant populations do not grow in the presence of antibiotics therefore no change in antibiotic MIC is associated with tolerance[12,255]. This allows tolerant bacteria to evade detection with commonly used clinical testing methods, presenting a serious concern in effectively treating these infections[388]. Since tolerant populations are able to withstand antibiotic exposure for longer periods of time, high levels of antibiotic tolerance increase the probability to acquire resistance-conferring mutations as well as acquisition of resistance-conferring genes by providing a reservoir of adaptable cells for an extended period during the course of antimicrobial therapy[14]. Therefore, tolerance plays a direct and indirect role

in antibiotic treatment failure by contributing to high rates of recurrent/relapse infections and by serving as a steppingstone for evolution of true resistance[12,14,69,388,389]. *In vivo* studies using animal models have further supported the role of tolerance as an important determinant of clinical treatment outcomes[14,255,389–393]. Antibiotic tolerance is, therefore, now widely recognized as a significant factor contributing to the failure of antimicrobial therapeutics.

Interestingly, several clinically significant Gram-negative bacteria, including *E. cloacae*, *K. pneumoniae*, *P. aeruginosa,* and *V. cholerae*, demonstrate a unique type of tolerance to cell wall acting antibiotics, like carbapenem β-lactams, that is mediated by spheroplast formation[19,21]. As suggested by their name, spheroplasts have an uncharacteristically rounded cell morphology and are often observed to be cell wall deficient which is indicative of significant cell envelope damage[21]. While β-lactam induced spheroplasts do not replicate in the presence of these cell wall acting antibiotics, they are able to recover to characteristic cell morphology and normal growth once the antibiotic threat is removed[12,65,255]. These observations suggest that spheroplasts are able to "wait out" treatment with cell wall targeting agents until the antibiotic concentration is sufficiently decreased to resume default bacterial growth and structure[12,65,255]. It is likely that the stress-bearing outer membrane of Gram-negative bacteria significantly contributes to the ability of spheroplasts to survive and remain intact without or with a severely damaged peptidoglycan cell wall layer[178,394,395].

The studies performed in chapter 4 of the present work aim to elucidate genetic and molecular factors important for spheroplast-mediated carbapenem tolerance in important Enterobacterales, including *Enterobacter cloacae* and *Klebsiella pneumoniae*.

Members of the Enterobacterales have emerged as a serious nosocomial threat that often exhibit multidrug resistance to common therapeutics[172]. The PhoPQ TCS is a highly conserved and well-documented stress response in pathogenic Enterobacterales[172,174]. PhoPQ is generally activated under conditions where divalent cations, Mg^{2+} and Ca^{2+}, are limited and is known to transcriptionally regulate various lipid A modification determinants[396–399]. Gram-negative bacterial species are often reported to alter their outer membrane composition by addition of positively charged 4-amino-4-deoxy-L-arabinose (L-Ara4N)[201,400–402]. In Enterobacterales, expression of the *arn* operon, which is responsible for the L-Ara4N modification, is regulated by the PhoPQ TCS[172,173,176]. While the PhoPQ TCS has previously been described as a regulator of polymyxin resistance[402] and heteroresistance[172] in Enterobacterales, the present work uncovers a novel role for PhoPQ in Enterobacterales tolerance to carbapenem treatment. More specifically, it reveals that the PhoPQ TCS and its regulon are induced by meropenem treatment and pinpoints PhoPQ-dependent L-Ara4N lipid A modification as a key factor for carbapenem tolerance in Enterobacterales. Furthermore, suppression of PhoPQ induction by overexpression of MgrB, a small periplasmic protein, or through inhibition of the PhoQ histidine kinase by small molecule inhibitors Riluzole and its derivative Rilu-2 resulted in severe defects in spheroplast formation[276,286]. These observations support the hypothesis that meropenem treatment induces PhoPQ-mediated addition of positively charged lipid A modifications that increase outer membrane stability by strengthening electrostatic interactions between the negatively charged LPS molecules on the surface of the cell. This, in turn, fortifies and enhances load-bearing capabilities of the outer membrane promoting spheroplast survival when the peptidoglycan cell wall is weakened.

Importantly, this work demonstrates the value of small molecule histidine kinase inhibitors that synergize with meropenem to decrease spheroplast-mediated carbapenem tolerance in Enterobacterales. This can potentially be used for further development of novel therapeutic strategies where histidine kinase inhibitors are co-administered with carbapenem β-lactams to deter emergence of tolerant populations. Moreover, libraries of potent small molecule histidine kinase inhibitors already available provide a starting point for quick and easy testing of their synergistic activity with carbapenems against Enterobacterales tolerance[286]. Future studies using murine wound infection models will be useful for evaluating efficacy of meropenem in combination with Rilu and its derivative to counter carbapenem tolerance *in vivo.* Future studies should also focus on testing additional small molecule inhibitors for synergistic activity with meropenem and measuring pharmacokinetic properties of lead compounds in physiologically relevant solutions to determine therapeutic potential. Additionally, the SLAY platform may also serve as a powerful tool for discovering novel synthetic peptide sequences that inhibit carbapenem tolerance in Enterobacterales.

While the studies outlined in chapter 4 support the hypothesis that PhoPQ-dependent outer membrane alterations are a conserved mechanism for carbapenem tolerance among different Enterobacterales, *Acinetobacter baumannii* does not encode many of the canonical outer membrane modification components (i.e., PhoPQ) found in Enterobacterales and carbapenem tolerance in *A. baumannii* has not been extensively investigated. While, generally carbapenem use is limited to only treating serious multidrug resistant bacterial infection, meropenem serves as a first-line therapeutic against infections caused by *A. baumannii*, which has emerged as one of the most difficult to

combat nosocomial Gram-negative pathogens[295,296]. However, isolation of carbapenem-resistant *A. baumannii* (CRAB) has become increasingly prevalent, causing a serious global health concern. With the scarcity of new antimicrobial development in the pipeline and the rapid rise of bacterial antibiotic resistance, there is an urgent requirement for alternative therapeutic strategies to prolong the clinical efficacy of currently available antibiotics, like meropenem, against *A. baumannii* infections.

Since antibiotic tolerance has been reported to serve as a precursor for the development of true resistance, it is likely that susceptible *A. baumannii* isolates exhibit some level of tolerance to carbapenem β-lactams[73,75,255,256,393,403]. The work in chapter 5 first demonstrates that common carbapenem susceptible lab strains as well as recently isolated clinical *A. baumannii* strains are highly tolerant to meropenem. This indicates that carbapenem tolerance is a clinically prevalent adaptation among susceptible *A. baumannii* isolates that is not just limited to lab-adapted strains and it likely contributes to the failure of meropenem treatment against *A. baumannii* infections and promotes evolution of true resistance. Furthermore, *A. baumannii* carbapenem tolerance was found to be mediated by spheroplast formation and meropenem induced *A. baumannii* spheroplasts were able recover characteristic coccobacilli cell morphology and canonical growth upon removal of the antibiotic.

Upon observing high propensity of susceptible *A. baumannii* isolates for spheroplast-mediated tolerance to meropenem, we reasoned that elucidating genetic and molecular factors underlying carbapenem tolerance in *A. baumannii* may provide novel insight into the incredible ability of this pathogen to develop multidrug resistance and help uncover targets for combating carbapenem tolerance in *A. baumannii* to slow the

evolution of resistance. RNA-seq analyses revealed upregulation of genes involved in efflux of β-lactam antibiotics and decreased expression of genes encoding outer membrane porins (OMPs) in meropenem-induced spheroplasts compared to untreated *A. baumannii* cells. OMPs have been described previously as the major points of carbapenem entry into the cell[314], therefore these findings indicate that *A. baumannii* cells respond to meropenem treatment through increased efflux of the antibiotic out of the cell while simultaneously limiting influx of meropenem into the cell by downregulating OMPs to promote survival. Additionally, β-lactam antibiotics disrupt default peptidoglycan biosynthesis by inhibiting penicillin-binding protein (PBP) transpeptidase activity which indirectly induces lytic transglycosylases to increase periplasmic peptidoglycan turnover[190]. Most of these peptidoglycan turnover products released by lytic transglycosylases are transported back into the cytoplasm for peptidoglycan recycling where they can enter the *de novo* peptidoglycan biosynthesis pathway, serve as nutrient sources, or be used for induction of chromosomally encoded cryptic β-lactamase genes[209,323]. The transcriptomics data presented here also revealed increased expression of two genes encoding a putative membrane-associated lytic transglycosylase, MltF, as well as a putative soluble lytic transglycosylase, Slt, in meropenem treated versus untreated *A. baumannii.* This indicates that peptidoglycan remodeling is important for meropenem-induced spheroplast formation in *A. baumannii* as observed previously for spheroplast-mediated β-lactam tolerance in other Gram-negative pathogens[20,21], and suggests a potential role for peptidoglycan recycling in *A. baumannii* carbapenem tolerance. The RNA-seq analyses outlined in chapter 5 provide novel insights into the global transcriptional response associated with meropenem treatment and the formation

of meropenem-induced spheroplast formation that can be applied broadly to make predictions regarding carbapenem tolerance and failure of carbapenem therapy in numerous Gram-negative bacterial species.

Subsequently, Tn-seq was performed to pinpoint key fitness factors involved in *A. baumannii* carbapenem tolerance by comparing insertional mutants recovered from cultures treated with lethal meropenem concentrations and untreated *A. baumannii* cultures. This screen identified genes contributing to outer membrane stability, *ompA* and *lpxM*, as well as genes involved in peptidoglycan maintenance/recycling, *pbpG, ldtK* and *ampD*, as key fitness factors required for meropenem tolerance in *A. baumannii.* OmpA is an abundant monomeric β-barrel protein that is highly conserved among Gram-negative bacterial species[325]. OmpA is an outer membrane localized protein, but it also contains a periplasmic domain that non-covalently interacts with peptidoglycan, directly attaching the outer membrane to the cell wall and it has been shown to contribute to the outer membrane stability[325,329]. *Acinetobacter baumannii* encodes a unique LpxM enzyme that functions as a dual acyltransferase enabling *A. baumannii* to constitutively produce hepta-acylated lipid A[177]. Increased number of saturated acyl chains attached to the lipid A moiety results in tight assembly of LPS/LOS molecules exposed on the cell surface which contributes to outer membrane rigidity[23]. Based on this, the Tn-seq analysis supports the hypothesis that factors contributing to the structural integrity of the outer membrane are important for meropenem tolerance in *A. baumannii* like the findings with Enterobacterales in chapter 4. Increased outer membrane rigidity due to lipid A hepta-acylation by LpxM and stability provided by OmpA-mediated attachments between the outer membrane and the peptidoglycan cell wall likely contribute to the overall structural

and load-bearing capability of the outer membrane and this is important for maintaining cell envelope homeostasis in *A. baumannii* to promote survival when the cell wall is damaged.

Interestingly this screen also identified factors involved in peptidoglycan maintenance and recycling as key genetic determinants for meropenem tolerance in *A. baumannii.* Penicillin binding protein 7 (PBP7) is a low molecular weight (LMW) PBP encoded by *pbpG*[201]*.* PBP7 is grouped with the autolysins due to its endopeptidase activity hydrolyzing the D-Ala-*m*Dap bridge between adjacent peptidoglycan stem peptides in *E. coli* and other Gram-negative bacteria[200,202]. Data presented in chapter 5 indicate that in *A. baumannii* PBP7 functions not only as an endopeptidase, but also as a DD-carboxypeptidase. PBP7 is responsible for generating tetra-muropeptide substrates through both its endopeptidase activity cleaving TetraTetra and TetraPenta cross-linked muropeptides and its DD-carboxypeptidase activity removing the terminal D-Ala from monomeric penta-muropeptides. This is significant because tetra-muropeptides are used as substrates by LD-transpeptidases to catalyze formation of noncanonical 3-3 peptidoglycan crosslinks and D-amino acid addition[294]. In *E. coli* 3-3 crosslinks are mainly used to repair defects in peptidoglycan crosslinking during stationary phase but are also found to be important during cell envelope stress[294,342,404,405]. It might be that inhibiting PBP7 activity fails to provide adequate tetra-muropeptide substrates for LD-transpeptidases to form necessary 3-3 crosslinks which makes the peptidoglycan sacculus more vulnerable to further attack and disruption. Additionally, tetra-muropeptides are also required as substrates for LD-transpeptidases to covalently attach the major outer membrane lipoprotein Lpp, (or Braun's lipoprotein) to the peptidoglycan

cell wall in *E. coli*[342]. This is important for maintaining cell wall integrity and contributes to stabilizing the outer membrane to increase its load bearing capacity[178]. Additionally, deletion of *pbpG* in *A. baumannii* resulted in increased permeability and hyper-production of outer membrane vesicles suggesting a role for PBP7 in outer membrane stabilization. RNA-seq analysis also revealed upregulation of putative lipoproteins in meropenem treated cultures relative to untreated cultures. It is possible that PBP7 functions to provide tetrapeptide substrates for LD-transpeptidase-mediated attachment of outer membrane lipoproteins to peptidoglycan in *A. baumannii* to fortify the cell envelope under stress. Further characterization of outer membrane lipoproteins in *A. baumannii* will be important to inform the specific contribution of lipoproteins to *A. baumannii* cell envelope homeostasis.

PBP7 has also been reported to interact with the soluble lytic transglycosylase Slt70 in *E. coli* to stabilize the enzyme and stimulate its hydrolytic activity and complex with Slt70 and PBP3 *in vitro*[406]. Recently, PBP7 was reported to interact with the outer membrane localized lipoprotein NlpI to form multi-enzymatic complexes with other peptidoglycan hydrolases in *E. coli*[407]. Expression of genes encoding putative membrane-bound lytic transglycosylase (MltF) and soluble lytic transglycosylase (Slt) were highly upregulated in the RNA-seq analysis which could suggest that PBP7 might be performing similar functions in *A. baumannii* to promote survival. This work also suggests that PBP7 could be contributing to meropenem tolerance in *A. baumannii* by coordinating with MltF and Slt in the periplasm for the efficient release of muropeptide substrates that are transported into the cytoplasm for peptidoglycan recycling. Tn-seq analysis and subsequent validation indicate the importance of two cytoplasmic peptidoglycan recycling

enzymes, LdtK and AmpD, in *A. baumannii* tolerance to meropenem. LdtK represents the first known YkuD-domain containing protein that is localized in the cytoplasm rather than the periplasm. In the cytoplasm, LdtK uncharacteristically functions as a LD-carboxypeptidase cleaving the terminal D-Ala in the fourth position of imported 1,6-anhydroMurNAc tetra-muropeptides to generate 1,6-anhydroMurNAc tri-muropeptides. LdtK cytoplasmic LD-carboxypeptidase activity is significant because 1,6-anhydroMurNAc tri-muropeptides are used as substrates by AmpD for separating the tripeptide stem from 1,6-anhydroMurNAc. Cytoplasmic peptidoglycan muropeptide processing by LdtK and AmpD may be important for maintaining low-level metabolic activity required during *A. baumannii* meropenem tolerance since tripeptides generated from AmpD activity can be further broken down into individual amino acids for energy/nutrient use[210,212,323]. Tripeptide stems resulting from AmpD hydrolysis of 1,6-anhydroMurNAc tri-muropeptides can also be used as precursors in the downstream peptidoglycan recycling pathway, however the importance of *de novo* peptidoglycan biosynthesis in *A. baumannii* meropenem tolerance is less straightforward.

Overall, the studies outlined in chapter 5 of the present work first establish the prevalence of meropenem tolerance among susceptible *Acinetobacter baumannii* isolates and provides novel insights into the mechanisms underlying this process. It demonstrates a unique link between factors involved in peptidoglycan turnover/recycling and the maintenance of outer membrane integrity and stability that appears to be critical for meropenem tolerance in *A. baumannii.* Furthermore, this work identifies novel factors that can be therapeutically targeted to inhibit carbapenem tolerance and slow the spread of antibiotic resistance in *Acinetobacter baumannii.* We are currently performing Tn-seq

with meropenem treated and untreated *A. baumannii* at later timepoints which will further increase our understanding of the mechanisms regulating carbapenem tolerance in *A. baumannii* and allow us to more specifically identify factors that become essential for spheroplast integrity and survival. Future studies evaluating the contribution of peptidoglycan recycling in maintaining outer membrane stability and integrity as well as pinpointing the importance of specific autolysins will be important for further dissecting mechanisms underlying carbapenem tolerance in *A. baumannii.* Additionally, identifying specific PBP7 protein interactions will help expand its role in *A. baumannii* physiology and provide insights into how PBP7 contributes to outer membrane integrity maintenance and carbapenem tolerance. Future studies would also benefit from evaluating how cell envelope mechanics support spheroplast integrity and impact carbapenem tolerance.

The present work concludes in chapter 6 with a detailed outline of the transposon insertion sequencing (Tn-seq) method that we have optimized for building highly saturated transposon mutant libraries in *A. baumannii* and used widely in this work. Tn-seq has become a powerful tool for investigating essential bacteria fitness factors across diverse physiological conditions and innovations in high-throughput sequencing technologies have continued to make these techniques more accessible and more reliable. The Tn-seq method described in chapter 6 and used for identifying genetic determinants for *Acinetobacter baumannii* carbapenem tolerance in chapter 5 has also been used previously to determine genetic factors that are essential for fitness in Δ*mrcA* (encoding Pbp1A) background relative to wildtype *A. baumannii*[267]*.* This demonstrates the broad applicability of this technique for identifying essential fitness factors in a variety of stress conditions and genetic backgrounds. The method detailed in chapter 6 combines

standard transposon mutagenesis with massive parallel sequencing and follows the same basic steps as other protocols where a saturated transposon insertion library is generated and pooled followed by genomic DNA (gDNA) extraction and high throughput sequencing of transposon insertion junctions from control and experimental samples. Sequencing reads recovered from each condition can then be mapped to a reference genome and used to draw conclusions about genetic and phenotypic interactions.

One of the advantages of the Tn-seq method outline in the present work, aside from its versatile application, is that it uses a host-independent family of transposons and because these transposons have an insertional preference for thymine-adenine ("TA") motifs, they are limited to a defined number of insertions[148,149,153–156]. This eliminates the need for host-specific factors to achieve insertions that are both random and stable and results in reduced insertion bias leading to reproducible and robust downstream statical analyses[148,149,153–156]. While *MmeI* restriction digestion based enzymatic gDNA fragmentation is a commonly used method of building Tn-seq libraries for high-throughput sequencing, it does prove to be cumbersome with the addition of extra steps and has a potential to produce bias[149]. The present Tn-seq method eliminates the need for enzymatic DNA fragmentation by using a mechanical shearing method for fragmenting gDNA, and addition of a 3' poly-C tail for amplification of transposon-genome junctions using poly-C specific primers which contributes to the reproducibility of this method[149]. This streamlines the process by eliminating the need for tedious restriction digestion, adapter ligation and gel purification steps[149]. While Tn-seq protocols can generate libraries of 20,000 – 100,000 mutants, the protocol described here has been optimized to generate highly saturated libraries of + 400,000 mutants, which in *A. baumannii* is roughly

equal to an insertion every ten bases. Furthermore, the transposon mutagenesis system described in this work can be easily modified by replacing the antibiotic resistance gene cassette and the promoter regulating expression of the transposase gene for use in a variety of bacterial backgrounds to study genetic interactions both *in vivo* and *in vitro.*

Taken together, this work builds on innovative high-throughput technologies to search for novel strategies to combat clinical antimicrobial treatment failure. The studies described herein provide further evidence that there is an urgent need for development of novel therapeutic strategies with translational potential. Additionally, it warrants extensive investigation into “non-traditional” mechanisms of antibiotic treatment failure, such as tolerance, in difficult to treat nosocomial Gram-negative bacterial pathogens. It also emphasizes the need to address these noncanonical factors that contribute to failure of antimicrobial therapy in a clinical setting to identify potential methods to slow down the spread of antibiotic resistance and restore the efficacy of currently available antimicrobial therapeutics.

References:

1. Gould IM, Bal AM. New antibiotic agents in the pipeline and how they can help overcome microbial resistance. *Virulence*. 2013;4(2):185-191. doi:10.4161/viru.22507

2. Centers for Disease Control and Prevention (U.S.). *Antibiotic Resistance Threats in the United States, 2019*. Centers for Disease Control and Prevention (U.S.); 2019. doi:10.15620/cdc:82532

3. World Health Organization W. Global priority list of antibiotic-resistant bacteria to guide research, discovery, and development of new antibiotics. URL: http://www.who.int/medicines/publications/global-priority-list-antibiotic-resistant-bacteria/en/

4. Martens E, Demain AL. The antibiotic resistance crisis, with a focus on the United States. *The Journal of Antibiotics*. 2017;70(5):520-526. doi:10.1038/ja.2017.30

5. Waxman DJ, Strominger JL. Penicillin-binding proteins and the mechanism of action of beta-lactam antibiotics. *Annu Rev Biochem*. 1983;52:825-869. doi:10.1146/annurev.bi.52.070183.004141

6. Page MI. The mechanisms of reactions of .beta.-lactam antibiotics. *Accounts of Chemical Research*. 1984;17(4):144-151. doi:10.1021/ar00100a005

7. Palzkill T. Metallo-β-lactamase structure and function. *Ann N Y Acad Sci*. 2013;1277:91-104. doi:10.1111/j.1749-6632.2012.06796.x

8. Papp-Wallace KM, Endimiani A, Taracila MA, Bonomo RA. Carbapenems: past, present, and future. *Antimicrob Agents Chemother*. 2011;55(11):4943-4960. doi:10.1128/AAC.00296-11

9. Livermore DM. Fourteen years in resistance. *Int J Antimicrob Agents*. 2012;39(4):283-294. doi:10.1016/j.ijantimicag.2011.12.012

10. Moellering RC. NDM-1 — A Cause for Worldwide Concern. *N Engl J Med*. 2010;363(25):2377-2379. doi:10.1056/NEJMp1011715

11. Llarrull LI, Testero SA, Fisher JF, Mobashery S. The future of the β-lactams. *Current Opinion in Microbiology*. 2010;13(5):551-557. doi:10.1016/j.mib.2010.09.008

12. Brauner A, Fridman O, Gefen O, Balaban NQ. Distinguishing between resistance, tolerance and persistence to antibiotic treatment. *Nat Rev Microbiol*. 2016;14(5):320-330. doi:10.1038/nrmicro.2016.34

13. Trastoy R, Manso T, Fernández-García L, et al. Mechanisms of Bacterial Tolerance and Persistence in the Gastrointestinal and Respiratory Environments. *Clin Microbiol Rev*. 2018;31(4):e00023-18. doi:10.1128/CMR.00023-18

14. Windels EM, Michiels JE, Van den Bergh B, Fauvart M, Michiels J. Antibiotics: Combatting Tolerance To Stop Resistance. Epstein S, Rubin EJ, eds. *mBio*. 2019;10(5):e02095-19, /mbio/10/5/mBio.02095-19.atom. doi:10.1128/mBio.02095-19

15. Weaver AI, Murphy SG, Umans BD, et al. Genetic Determinants of Penicillin Tolerance in *Vibrio cholerae*. *Antimicrob Agents Chemother*. 2018;62(10):e01326-18, /aac/62/10/e01326-18.atom. doi:10.1128/AAC.01326-18

16. Meylan S, Andrews IW, Collins JJ. Targeting Antibiotic Tolerance, Pathogen by Pathogen. *Cell*. 2018;172(6):1228-1238. doi:10.1016/j.cell.2018.01.037

17. Martins D, McKay G, Sampathkumar G, Khakimova M, English AM, Nguyen D. Superoxide dismutase activity confers (p)ppGpp-mediated antibiotic tolerance to stationary-phase *Pseudomonas aeruginosa*. *Proc Natl Acad Sci USA*. 2018;115(39):9797-9802. doi:10.1073/pnas.1804525115

18. Bernabeu-Wittel M, García-Curiel A, Pichardo C, Pachón-Ibáñez ME, Jiménez-Mejías ME, Pachón J. Morphological changes induced by imipenem and meropenem at sub-inhibitory concentrations in Acinetobacter baumannii. *Clinical Microbiology and Infection*. 2004;10(10):931-934. doi:10.1111/j.1469-0691.2004.00944.x

19. Monahan LG, Turnbull L, Osvath SR, Birch D, Charles IG, Whitchurch CB. Rapid Conversion of Pseudomonas aeruginosa to a Spherical Cell Morphotype Facilitates Tolerance to Carbapenems and Penicillins but Increases Susceptibility to Antimicrobial Peptides. *Antimicrob Agents Chemother*. 2014;58(4):1956-1962. doi:10.1128/AAC.01901-13

20. Dörr T, Davis BM, Waldor MK. Endopeptidase-Mediated Beta Lactam Tolerance. Mougous JD, ed. *PLoS Pathog*. 2015;11(4):e1004850. doi:10.1371/journal.ppat.1004850

21. Cross T, Ransegnola B, Shin JH, et al. Spheroplast-Mediated Carbapenem Tolerance in Gram-Negative Pathogens. *Antimicrob Agents Chemother*. 2019;63(9):e00756-19, /aac/63/9/AAC.00756-19.atom. doi:10.1128/AAC.00756-19

22. Duong F, Eichler J, Price A, Rice Leonard M, Wickner W. Biogenesis of the Gram-Negative Bacterial Envelope. *Cell*. 1997;91(5):567-573. doi:10.1016/S0092-8674(00)80444-4

23. Silhavy TJ, Kahne D, Walker S. The Bacterial Cell Envelope. *Cold Spring Harbor Perspectives in Biology*. 2010;2(5):a000414-a000414. doi:10.1101/cshperspect.a000414

24. Hood MI, Jacobs AC, Sayood K, Dunman PM, Skaar EP. Acinetobacter baumannii Increases Tolerance to Antibiotics in Response to Monovalent Cations. *Antimicrobial Agents and Chemotherapy*. 2010;54(3):1029-1041. doi:10.1128/AAC.00963-09

25. Howard A, O'Donoghue M, Feeney A, Sleator RD. Acinetobacter baumannii: An emerging opportunistic pathogen. *Virulence*. 2012;3(3):243-250. doi:10.4161/viru.19700

26. Lin MF. Antimicrobial resistance in *Acinetobacter baumannii*: From bench to bedside. *WJCC*. 2014;2(12):787. doi:10.12998/wjcc.v2.i12.787

27. Peleg AY, Seifert H, Paterson DL. Acinetobacter baumannii: Emergence of a Successful Pathogen. *Clinical Microbiology Reviews*. 2008;21(3):538-582. doi:10.1128/CMR.00058-07

28. Lee A, Nolan A, Watson J, Tristem M. Identification of an ancient endogenous retrovirus, predating the divergence of the placental mammals. *Philosophical Transactions of the Royal Society B: Biological Sciences*. 2013;368(1626):20120503-20120503. doi:10.1098/rstb.2012.0503

29. D'Arezzo S, Capone A, Petrosillo N, Visca P. Epidemic multidrug-resistant Acinetobacter baumannii related to European clonal types I and II in Rome (Italy). *Clinical Microbiology and Infection*. 2009;15(4):347-357. doi:10.1111/j.1469-0691.2009.02668.x

30. Aminov RI. A Brief History of the Antibiotic Era: Lessons Learned and Challenges for the Future. *Front Microbio*. 2010;1. doi:10.3389/fmicb.2010.00134

31. Ribeiro da Cunha, Fonseca, Calado. Antibiotic Discovery: Where Have We Come from, Where Do We Go? *Antibiotics*. 2019;8(2):45. doi:10.3390/antibiotics8020045

32. Sneader W. *Drug Discovery: A History*. Repr. with corr. Wiley; 2006.

33. Hutchings MI, Truman AW, Wilkinson B. Antibiotics: past, present and future. *Current Opinion in Microbiology*. 2019;51:72-80. doi:10.1016/j.mib.2019.10.008

34. Zaffiri L, Gardner J, Toledo-Pereyra LH. History of Antibiotics. From Salvarsan to Cephalosporins. *Journal of Investigative Surgery*. 2012;25(2):67-77. doi:10.3109/08941939.2012.664099

35. Fleming A. On the antibacterial action of cultures of a penicillium, with special reference to their use in the isolation of B. influenzae. 1929. *Bull World Health Organ*. 2001;79(8):780-790.

36. Gaynes R. The Discovery of Penicillin—New Insights After More Than 75 Years of Clinical Use. *Emerg Infect Dis*. 2017;23(5):849-853. doi:10.3201/eid2305.161556

37. Aminov R. History of antimicrobial drug discovery: Major classes and health impact. *Biochemical Pharmacology*. 2017;133:4-19. doi:10.1016/j.bcp.2016.10.001

38. Chain E, Florey HW, Gardner AD, et al. PENICILLIN AS A CHEMOTHERAPEUTIC AGENT. *The Lancet*. 1940;236(6104):226-228. doi:10.1016/S0140-6736(01)08728-1

39. Hodgkin DC. The X-ray analysis of the structure of penicillin. *Adv Sci*. 1949;6(22):85-89.

40. Brunel J. Antibiosis from Pasteur to Fleming. *J Hist Med Allied Sci*. 1951;6(3):287-301. doi:10.1093/jhmas/vi.summer.287

41. Frost WD. The Antagonism Exhibited by Certain Saprophytic Bacteria against the Bacillus typhosus Gaffky. *The Journal of Infectious Diseases*. 1904;1(4):599-640.

42. Bo G. Giuseppe Brotzu and the discovery of cephalosporins. *Clin Microbiol Infect*. 2000;6 Suppl 3:6-9. doi:10.1111/j.1469-0691.2000.tb02032.x

43. Bush K. The coming of age of antibiotics: discovery and therapeutic value. *Ann N Y Acad Sci*. 2010;1213:1-4. doi:10.1111/j.1749-6632.2010.05872.x

44. Bush K, Bradford PA. β-Lactams and β-Lactamase Inhibitors: An Overview. *Cold Spring Harb Perspect Med*. 2016;6(8):a025247. doi:10.1101/cshperspect.a025247

45. Bush K. Proliferation and significance of clinically relevant β-lactamases. *Ann N Y Acad Sci*. 2013;1277:84-90. doi:10.1111/nyas.12023

46. Kahan JS, Kahan FM, Goegelman R, et al. Thienamycin, a new beta-lactam antibiotic. I. Discovery, taxonomy, isolation and physical properties. *J Antibiot (Tokyo)*. 1979;32(1):1-12. doi:10.7164/antibiotics.32.1

47. Bradley JS, Garau J, Lode H, Rolston KV, Wilson SE, Quinn JP. Carbapenems in clinical practice: a guide to their use in serious infection. *Int J Antimicrob Agents*. 1999;11(2):93-100. doi:10.1016/s0924-8579(98)00094-6

48. Kiratisin P, Chongthaleong A, Tan TY, et al. Comparative in vitro activity of carbapenems against major Gram-negative pathogens: results of Asia-Pacific surveillance from the COMPACT II study. *Int J Antimicrob Agents*. 2012;39(4):311-316. doi:10.1016/j.ijantimicag.2012.01.002

49. Baughman RP. The use of carbapenems in the treatment of serious infections. *J Intensive Care Med*. 2009;24(4):230-241. doi:10.1177/0885066609335660

50. Jorgensen JH, Maher LA, Howell AW. Activity of meropenem against antibiotic-resistant or infrequently encountered gram-negative bacilli. *Antimicrob Agents Chemother*. 1991;35(11):2410-2414. doi:10.1128/AAC.35.11.2410

51. Cielecka-Piontek J, Zajac M, Jelińska A. A comparison of the stability of ertapenem and meropenem in pharmaceutical preparations in solid state. *J Pharm Biomed Anal*. 2008;46(1):52-57. doi:10.1016/j.jpba.2007.08.024

52. Prescott WA, Gentile AE, Nagel JL, Pettit RS. Continuous-infusion antipseudomonal Beta-lactam therapy in patients with cystic fibrosis. *P T*. 2011;36(11):723-763.

53. Perry J, Waglechner N, Wright G. The Prehistory of Antibiotic Resistance. *Cold Spring Harb Perspect Med*. 2016;6(6):a025197. doi:10.1101/cshperspect.a025197

54. Uddin TM, Chakraborty AJ, Khusro A, et al. Antibiotic resistance in microbes: History, mechanisms, therapeutic strategies and future prospects. *J Infect Public Health*. Published online October 23, 2021:S1876-0341(21)00340-3. doi:10.1016/j.jiph.2021.10.020

55. Davies J, Davies D. Origins and evolution of antibiotic resistance. *Microbiol Mol Biol Rev*. 2010;74(3):417-433. doi:10.1128/MMBR.00016-10

56. Abraham EP, Chain E. An enzyme from bacteria able to destroy penicillin. 1940. *Rev Infect Dis*. 1988;10(4):677-678.

57. Dodds DR. Antibiotic resistance: A current epilogue. *Biochem Pharmacol*. 2017;134:139-146. doi:10.1016/j.bcp.2016.12.005

58. Durand GA, Raoult D, Dubourg G. Antibiotic discovery: history, methods and perspectives. *Int J Antimicrob Agents*. 2019;53(4):371-382. doi:10.1016/j.ijantimicag.2018.11.010

59. Fleming A. Penicillin. Published online December 11, 1945.

60. De Oliveira DMP, Forde BM, Kidd TJ, et al. Antimicrobial Resistance in ESKAPE Pathogens. *Clin Microbiol Rev*. 2020;33(3):e00181-19. doi:10.1128/CMR.00181-19

61. Magiorakos AP, Srinivasan A, Carey RB, et al. Multidrug-resistant, extensively drug-resistant and pandrug-resistant bacteria: an international expert proposal for interim standard definitions for acquired resistance. *Clinical Microbiology and Infection*. 2012;18(3):268-281. doi:10.1111/j.1469-0691.2011.03570.x

62. Sommer MOA, Munck C, Toft-Kehler RV, Andersson DI. Prediction of antibiotic resistance: time for a new preclinical paradigm? *Nat Rev Microbiol*. 2017;15(11):689-696. doi:10.1038/nrmicro.2017.75

63. Levin-Reisman I, Brauner A, Ronin I, Balaban NQ. Epistasis between antibiotic tolerance, persistence, and resistance mutations. *Proc Natl Acad Sci USA*. 2019;116(29):14734-14739. doi:10.1073/pnas.1906169116

64. Andrews JM. Determination of minimum inhibitory concentrations. *J Antimicrob Chemother*. 2001;48 Suppl 1:5-16. doi:10.1093/jac/48.suppl_1.5

65. Dörr T. Understanding tolerance to cell wall-active antibiotics. *Ann N Y Acad Sci*. 2021;1496(1):35-58. doi:10.1111/nyas.14541

66. Hobby GL, Meyer K, Chaffee E. Observations on the Mechanism of Action of Penicillin. *Experimental Biology and Medicine*. 1942;50(2):281-285. doi:10.3181/00379727-50-13773

67. Bigger JosephW. TREATMENT OF STAPHYLOCOCCAL INFECTIONS WITH PENICILLIN BY INTERMITTENT STERILISATION. *The Lancet*. 1944;244(6320):497-500. doi:10.1016/S0140-6736(00)74210-3

68. Sabath LD, Laverdiere M, Wheeler N, Blazevic D, Wilkinson BrianJ. A NEW TYPE OF PENICILLIN RESISTANCE OF STAPHYLOCOCCUS AUREUS. *The Lancet*. 1977;309(8009):443-447. doi:10.1016/S0140-6736(77)91941-9

69. Held K, Gasper J, Morgan S, Siehnel R, Singh P, Manoil C. Determinants of Extreme β-Lactam Tolerance in the Burkholderia pseudomallei Complex. *Antimicrob Agents Chemother*. 2018;62(4). doi:10.1128/AAC.00068-18

70. Kester JC, Fortune SM. Persisters and beyond: Mechanisms of phenotypic drug resistance and drug tolerance in bacteria. *Critical Reviews in Biochemistry and Molecular Biology*. 2014;49(2):91-101. doi:10.3109/10409238.2013.869543

71. Navarro Llorens JM, Tormo A, Martínez-García E. Stationary phase in gram-negative bacteria. *FEMS Microbiol Rev*. 2010;34(4):476-495. doi:10.1111/j.1574-6976.2010.00213.x

72. Moreillon P, Tomasz A. Penicillin Resistance and Defective Lysis in Clinical Isolates of Pneumococci: Evidence for Two Kinds of Antibiotic Pressure Operating in the Clinical Environment. *Journal of Infectious Diseases*. 1988;157(6):1150-1157. doi:10.1093/infdis/157.6.1150

73. Novak R, Henriques B, Charpentier E, Normark S, Tuomanen E. Emergence of vancomycin tolerance in Streptococcus pneumoniae. *Nature*. 1999;399(6736):590-593. doi:10.1038/21202

74. Nguyen D, Joshi-Datar A, Lepine F, et al. Active Starvation Responses Mediate Antibiotic Tolerance in Biofilms and Nutrient-Limited Bacteria. *Science*. 2011;334(6058):982-986. doi:10.1126/science.1211037

75. Levin-Reisman I, Ronin I, Gefen O, Braniss I, Shoresh N, Balaban NQ. Antibiotic tolerance facilitates the evolution of resistance. *Science*. 2017;355(6327):826-830. doi:10.1126/science.aaj2191

76. Schultz F, Anywar G, Tang H, et al. Targeting ESKAPE pathogens with anti-infective medicinal plants from the Greater Mpigi region in Uganda. *Sci Rep*. 2020;10(1):11935. doi:10.1038/s41598-020-67572-8

77. Rice LB. Federal Funding for the Study of Antimicrobial Resistance in Nosocomial Pathogens: No ESKAPE. *J INFECT DIS*. 2008;197(8):1079-1081. doi:10.1086/533452

78. Mulani MS, Kamble EE, Kumkar SN, Tawre MS, Pardesi KR. Emerging Strategies to Combat ESKAPE Pathogens in the Era of Antimicrobial Resistance: A Review. *Front Microbiol*. 2019;10:539. doi:10.3389/fmicb.2019.00539

79. Santajit S, Indrawattana N. Mechanisms of Antimicrobial Resistance in ESKAPE Pathogens. *BioMed Research International*. 2016;2016:1-8. doi:10.1155/2016/2475067

80. Ma Y, Wang C, Li Y, et al. Considerations and Caveats in Combating ESKAPE Pathogens against Nosocomial Infections. *Adv Sci*. 2020;7(1):1901872. doi:10.1002/advs.201901872

81. Sheu CC, Chang YT, Lin SY, Chen YH, Hsueh PR. Infections Caused by Carbapenem-Resistant Enterobacteriaceae: An Update on Therapeutic Options. *Front Microbiol*. 2019;10:80. doi:10.3389/fmicb.2019.00080

82. Thiolas A, Bollet C, La Scola B, Raoult D, Pagès JM. Successive Emergence of *Enterobacter aerogenes* Strains Resistant to Imipenem and Colistin in a Patient. *Antimicrob Agents Chemother*. 2005;49(4):1354-1358. doi:10.1128/AAC.49.4.1354-1358.2005

83. Piperaki ET, Tzouvelekis LS, Miriagou V, Daikos GL. Carbapenem-resistant Acinetobacter baumannii: in pursuit of an effective treatment. *Clinical Microbiology and Infection*. 2019;25(8):951-957. doi:10.1016/j.cmi.2019.03.014

84. Spellberg B, Rex JH. The value of single-pathogen antibacterial agents. *Nat Rev Drug Discov*. 2013;12(12):963. doi:10.1038/nrd3957-c1

85. Wong D, Nielsen TB, Bonomo RA, Pantapalangkoor P, Luna B, Spellberg B. Clinical and Pathophysiological Overview of Acinetobacter Infections: a Century of Challenges. *Clin Microbiol Rev*. 2017;30(1):409-447. doi:10.1128/CMR.00058-16

86. Livermore DM, Woodford N. The beta-lactamase threat in Enterobacteriaceae, Pseudomonas and Acinetobacter. *Trends Microbiol*. 2006;14(9):413-420. doi:10.1016/j.tim.2006.07.008

87. Sauvage E, Kerff F, Terrak M, Ayala JA, Charlier P. The penicillin-binding proteins: structure and role in peptidoglycan biosynthesis. *FEMS Microbiol Rev*. 2008;32(2):234-258. doi:10.1111/j.1574-6976.2008.00105.x

88. Lee W, McDonough MA, Kotra L, et al. A 1.2-A snapshot of the final step of bacterial cell wall biosynthesis. *Proc Natl Acad Sci USA*. 2001;98(4):1427-1431. doi:10.1073/pnas.98.4.1427

89. Buynak JD. Cutting and stitching: the cross-linking of peptidoglycan in the assembly of the bacterial cell wall. *ACS Chem Biol*. 2007;2(9):602-605. doi:10.1021/cb700182u

90. Shi Q, Meroueh SO, Fisher JF, Mobashery S. A computational evaluation of the mechanism of penicillin-binding protein-catalyzed cross-linking of the bacterial cell wall. *J Am Chem Soc*. 2011;133(14):5274-5283. doi:10.1021/ja1074739

91. El-Gamal MI, Brahim I, Hisham N, Aladdin R, Mohammed H, Bahaaeldin A. Recent updates of carbapenem antibiotics. *Eur J Med Chem*. 2017;131:185-195. doi:10.1016/j.ejmech.2017.03.022

92. Lohans CT, Freeman EI, Groesen E van, et al. Mechanistic Insights into β-Lactamase-Catalysed Carbapenem Degradation Through Product Characterisation. *Sci Rep*. 2019;9(1):13608. doi:10.1038/s41598-019-49264-0

93. Bassetti M, Nicolini L, Esposito S, Righi E, Viscoli C. Current status of newer carbapenems. *Curr Med Chem*. 2009;16(5):564-575.

94. Torres JA, Villegas MV, Quinn JP. Current concepts in antibiotic-resistant gram-negative bacteria. *Expert Rev Anti Infect Ther*. 2007;5(5):833-843. doi:10.1586/14787210.5.5.833

95. Boon JM, Smith BD. Chemical control of phospholipid distribution across bilayer membranes. *Med Res Rev*. 2002;22(3):251-281.

96. Paterson DL. Recommendation for treatment of severe infections caused by Enterobacteriaceae producing extended-spectrum beta-lactamases (ESBLs). *Clin Microbiol Infect*. 2000;6(9):460-463.

97. Paterson DL. Serious infections caused by enteric gram-negative bacilli--mechanisms of antibiotic resistance and implications for therapy of gram-negative sepsis in the transplanted patient. *Semin Respir Infect*. 2002;17(4):260-264. doi:10.1053/srin.2002.36446

98. Paterson DL, Bonomo RA. Extended-spectrum beta-lactamases: a clinical update. *Clin Microbiol Rev*. 2005;18(4):657-686. doi:10.1128/CMR.18.4.657-686.2005

99. Zhanel GG, Simor AE, Vercaigne L, Mandell L, Canadian Carbapenem Discussion Group. Imipenem and meropenem: Comparison of in vitro activity, pharmacokinetics, clinical trials and adverse effects. *Can J Infect Dis*. 1998;9(4):215-228.

100. Queenan AM, Bush K. Carbapenemases: the versatile beta-lactamases. *Clin Microbiol Rev*. 2007;20(3):440-458, table of contents. doi:10.1128/CMR.00001-07

101. Zmarlicka MT, Nailor MD, Nicolau DP. Impact of the New Delhi metallo-beta-lactamase on beta-lactam antibiotics. *Infect Drug Resist*. 2015;8:297-309. doi:10.2147/IDR.S39186

102. Ambler RP, Coulson AF, Frère JM, et al. A standard numbering scheme for the class A beta-lactamases. *Biochem J*. 1991;276 (Pt 1):269-270.

103. Bush K, Jacoby GA. Updated functional classification of beta-lactamases. *Antimicrob Agents Chemother*. 2010;54(3):969-976. doi:10.1128/AAC.01009-09

104. Ghuysen JM. Serine beta-lactamases and penicillin-binding proteins. *Annu Rev Microbiol*. 1991;45:37-67. doi:10.1146/annurev.mi.45.100191.000345

105. Bebrone C. Metallo-beta-lactamases (classification, activity, genetic organization, structure, zinc coordination) and their superfamily. *Biochem Pharmacol*. 2007;74(12):1686-1701. doi:10.1016/j.bcp.2007.05.021

106. Wang Z, Fast W, Valentine AM, Benkovic SJ. Metallo-beta-lactamase: structure and mechanism. *Curr Opin Chem Biol*. 1999;3(5):614-622.

107. Crowder MW, Spencer J, Vila AJ. Metallo-beta-lactamases: novel weaponry for antibiotic resistance in bacteria. *Acc Chem Res*. 2006;39(10):721-728. doi:10.1021/ar0400241

108. Laraki N, Galleni M, Thamm I, et al. Structure of In31, a blaIMP-containing Pseudomonas aeruginosa integron phyletically related to In5, which carries an unusual array of gene cassettes. *Antimicrob Agents Chemother*. 1999;43(4):890-901.

109. Lauretti L, Riccio ML, Mazzariol A, et al. Cloning and characterization of blaVIM, a new integron-borne metallo-beta-lactamase gene from a Pseudomonas aeruginosa clinical isolate. *Antimicrob Agents Chemother*. 1999;43(7):1584-1590.

110. Yong D, Toleman MA, Giske CG, et al. Characterization of a new metallo-beta-lactamase gene, bla(NDM-1), and a novel erythromycin esterase gene carried on a unique genetic structure in Klebsiella pneumoniae sequence type 14 from India. *Antimicrob Agents Chemother*. 2009;53(12):5046-5054. doi:10.1128/AAC.00774-09

111. Walsh TR. Clinically significant carbapenemases: an update. *Curr Opin Infect Dis*. 2008;21(4):367-371. doi:10.1097/QCO.0b013e328303670b

112. Walsh TR. Emerging carbapenemases: a global perspective. *Int J Antimicrob Agents*. 2010;36 Suppl 3:S8-14. doi:10.1016/S0924-8579(10)70004-2

113. Poirel L, Naas T, Nicolas D, et al. Characterization of VIM-2, a carbapenem-hydrolyzing metallo-beta-lactamase and its plasmid- and integron-borne gene from a Pseudomonas aeruginosa clinical isolate in France. *Antimicrob Agents Chemother*. 2000;44(4):891-897.

114. Galleni M, Lamotte-Brasseur J, Rossolini GM, et al. Standard numbering scheme for class B beta-lactamases. *Antimicrob Agents Chemother*. 2001;45(3):660-663. doi:10.1128/AAC.45.3.660-663.2001

115. Garau G, García-Sáez I, Bebrone C, et al. Update of the standard numbering scheme for class B beta-lactamases. *Antimicrob Agents Chemother*. 2004;48(7):2347-2349. doi:10.1128/AAC.48.7.2347-2349.2004

116. Cornaglia G, Giamarellou H, Rossolini GM. Metallo-β-lactamases: a last frontier for β-lactams? *Lancet Infect Dis*. 2011;11(5):381-393. doi:10.1016/S1473-3099(11)70056-1

117. Castanheira M, Deshpande LM, Farrell SE, Shetye S, Shah N, Jones RN. Update on the prevalence and genetic characterization of NDM-1-producing Enterobacteriaceae in Indian hospitals during 2010. *Diagn Microbiol Infect Dis*. 2013;75(2):210-213. doi:10.1016/j.diagmicrobio.2012.10.017

118. Chen YT, Liao TL, Liu YM, Lauderdale TL, Yan JJ, Tsai SF. Mobilization of qnrB2 and ISCR1 in plasmids. *Antimicrob Agents Chemother*. 2009;53(3):1235-1237. doi:10.1128/AAC.00970-08

119. Mojica MF, Bonomo RA, Fast W. B1-Metallo-β-Lactamases: Where Do We Stand? *Curr Drug Targets*. 2016;17(9):1029-1050.

120. Tacconelli E. GLOBAL PRIORITY LIST OF ANTIBIOTIC-RESISTANT BACTERIA TO GUIDE RESEARCH, DISCOVERY, AND DEVELOPMENT OF NEW ANTIBIOTICS. :7.

121. Tacconelli E, Carrara E, Savoldi A, et al. Discovery, research, and development of new antibiotics: the WHO priority list of antibiotic-resistant bacteria and tuberculosis. *Lancet Infect Dis*. 2018;18(3):318-327. doi:10.1016/S1473-3099(17)30753-3

122. Reading C, Cole M. Clavulanic acid: a beta-lactamase-inhiting beta-lactam from Streptomyces clavuligerus. *Antimicrob Agents Chemother*. 1977;11(5):852-857.

123. Fisher J, Belasco JG, Charnas RL, Khosla S, Knowles JR. Beta-lactamase inactivation by mechanism-based reagents. *Philos Trans R Soc Lond, B, Biol Sci*. 1980;289(1036):309-319. doi:10.1098/rstb.1980.0048

124. Rotondo CM, Wright GD. Inhibitors of metallo-β-lactamases. *Current Opinion in Microbiology*. 2017;39:96-105. doi:10.1016/j.mib.2017.10.026

125. Fast W, Sutton LD. Metallo-β-lactamase: Inhibitors and reporter substrates. *Biochimica et Biophysica Acta (BBA) - Proteins and Proteomics*. 2013;1834(8):1648-1659. doi:10.1016/j.bbapap.2013.04.024

126. King DT, Strynadka NCJ. Targeting metallo-β-lactamase enzymes in antibiotic resistance. *Future Med Chem*. 2013;5(11):1243-1263. doi:10.4155/fmc.13.55

127. Drawz SM, Papp-Wallace KM, Bonomo RA. New β-lactamase inhibitors: a therapeutic renaissance in an MDR world. *Antimicrob Agents Chemother*. 2014;58(4):1835-1846. doi:10.1128/AAC.00826-13

128. Ktari S, Arlet G, Mnif B, et al. Emergence of multidrug-resistant Klebsiella pneumoniae isolates producing VIM-4 metallo-beta-lactamase, CTX-M-15 extended-spectrum beta-lactamase, and CMY-4 AmpC beta-lactamase in a Tunisian university hospital. *Antimicrob Agents Chemother*. 2006;50(12):4198-4201. doi:10.1128/AAC.00663-06

129. Patel G, Bonomo RA. "Stormy waters ahead": global emergence of carbapenemases. *Front Microbiol*. 2013;4:48. doi:10.3389/fmicb.2013.00048

130. Sanschagrin F, Levesque RC. A specific peptide inhibitor of the class B metallo-beta-lactamase L-1 from Stenotrophomonas maltophilia identified using phage display. *J Antimicrob Chemother*. 2005;55(2):252-255. doi:10.1093/jac/dkh550

131. Hancock REW, Sahl HG. Antimicrobial and host-defense peptides as new anti-infective therapeutic strategies. *Nat Biotechnol*. 2006;24(12):1551-1557. doi:10.1038/nbt1267

132. Zasloff M. Antimicrobial peptides of multicellular organisms. *Nature*. 2002;415(6870):389-395. doi:10.1038/415389a

133. Padhi A, Sengupta M, Sengupta S, Roehm KH, Sonawane A. Antimicrobial peptides and proteins in mycobacterial therapy: current status and future prospects. *Tuberculosis (Edinb)*. 2014;94(4):363-373. doi:10.1016/j.tube.2014.03.011

134. Nizet V. Antimicrobial peptide resistance mechanisms of human bacterial pathogens. *Curr Issues Mol Biol*. 2006;8(1):11-26.

135. Zwick MB, Shen J, Scott JK. Phage-displayed peptide libraries. *Curr Opin Biotechnol*. 1998;9(4):427-436.

136. Smith GP, Petrenko VA. Phage Display. *Chem Rev*. 1997;97(2):391-410.

137. Hanes J, Plückthun A. In vitro selection and evolution of functional proteins by using ribosome display. *Proc Natl Acad Sci USA*. 1997;94(10):4937-4942.

138. Hanes J, Jermutus L, Weber-Bornhauser S, Bosshard HR, Plückthun A. Ribosome display efficiently selects and evolves high-affinity antibodies in vitro from immune libraries. *Proc Natl Acad Sci USA*. 1998;95(24):14130-14135.

139. Roberts RW, Szostak JW. RNA-peptide fusions for the in vitro selection of peptides and proteins. *Proc Natl Acad Sci USA*. 1997;94(23):12297-12302.

140. Nemoto N, Miyamoto-Sato E, Husimi Y, Yanagawa H. In vitro virus: bonding of mRNA bearing puromycin at the 3'-terminal end to the C-terminal end of its encoded protein on the ribosome in vitro. *FEBS Lett*. 1997;414(2):405-408.

141. Tucker AT, Leonard SP, DuBois CD, et al. Discovery of Next-Generation Antimicrobials through Bacterial Self-Screening of Surface-Displayed Peptide Libraries. *Cell*. 2018;172(3):618-628.e13. doi:10.1016/j.cell.2017.12.009

142. Bounaga S, Galleni M, Laws AP, Page MI. Cysteinyl peptide inhibitors of Bacillus cereus zinc beta-lactamase. *Bioorg Med Chem*. 2001;9(2):503-510.

143. Huang W, Beharry Z, Zhang Z, Palzkill T. A broad-spectrum peptide inhibitor of beta-lactamase identified using phage display and peptide arrays. *Protein Eng*. 2003;16(11):853-860.

144. Francisco JA, Earhart CF, Georgiou G. Transport and anchoring of beta-lactamase to the external surface of Escherichia coli. *Proc Natl Acad Sci USA*. 1992;89(7):2713-2717.

145. van Opijnen T, Lazinski DW, Camilli A. Genome-Wide Fitness and Genetic Interactions Determined by Tn-seq, a High-Throughput Massively Parallel Sequencing Method for Microorganisms: Tn-seq: High-Throughput Sequencing for Microorganisms. *Current Protocols in Microbiology*. 2017;36(1):1E.3.1-1E.3.24. doi:10.1002/9780471729259.mc01e03s36

146. Kwon YM, Ricke SC, Mandal RK. Transposon sequencing: methods and expanding applications. *Appl Microbiol Biotechnol*. 2016;100(1):31-43. doi:10.1007/s00253-015-7037-8

147. Yamaichi Y, Dörr T. Transposon Insertion Site Sequencing for Synthetic Lethal Screening. In: Espéli O, ed. *The Bacterial Nucleoid*. Vol 1624. Methods in Molecular Biology. Springer New York; 2017:39-49. doi:10.1007/978-1-4939-7098-8_4

148. Barquist L, Boinett CJ, Cain AK. Approaches to querying bacterial genomes with transposon-insertion sequencing. *RNA Biology*. 2013;10(7):1161-1169. doi:10.4161/rna.24765

149. Klein BA, Tenorio EL, Lazinski DW, Camilli A, Duncan MJ, Hu LT. Identification of essential genes of the periodontal pathogen Porphyromonas gingivalis. *BMC Genomics*. 2012;13(1):578. doi:10.1186/1471-2164-13-578

150. Stahl M, Stintzi A. Identification of essential genes in C. jejuni genome highlights hyper-variable plasticity regions. *Funct Integr Genomics*. 2011;11(2):241-257. doi:10.1007/s10142-011-0214-7

151. Chaudhuri RR, Allen AG, Owen PJ, et al. Comprehensive identification of essential Staphylococcus aureus genes using Transposon-Mediated Differential Hybridisation (TMDH). *BMC Genomics*. 2009;10(1):291. doi:10.1186/1471-2164-10-291

152. Griffin JE, Gawronski JD, Dejesus MA, Ioerger TR, Akerley BJ, Sassetti CM. High-resolution phenotypic profiling defines genes essential for mycobacterial growth and

cholesterol catabolism. *PLoS Pathog*. 2011;7(9):e1002251. doi:10.1371/journal.ppat.1002251

153. Perry BJ, Yost CK. Construction of a mariner-based transposon vector for use in insertion sequence mutagenesis in selected members of the Rhizobiaceae. *BMC Microbiol*. 2014;14(1):298. doi:10.1186/s12866-014-0298-z

154. Plasterk RHA, Izsvák Z, Ivics Z. Resident aliens: the Tc1/ mariner superfamily of transposable elements. *Trends in Genetics*. 1999;15(8):326-332. doi:10.1016/S0168-9525(99)01777-1

155. Lampe DJ, Churchill ME, Robertson HM. A purified mariner transposase is sufficient to mediate transposition in vitro. *EMBO J*. 1996;15(19):5470-5479.

156. Mazurkiewicz P, Tang CM, Boone C, Holden DW. Signature-tagged mutagenesis: barcoding mutants for genome-wide screens. *Nat Rev Genet*. 2006;7(12):929-939. doi:10.1038/nrg1984

157. Wang N, Ozer EA, Mandel MJ, Hauser AR. Genome-Wide Identification of Acinetobacter baumannii Genes Necessary for Persistence in the Lung. Sperandio V, ed. *mBio*. 2014;5(3):e01163-14. doi:10.1128/mBio.01163-14

158. Kong KF, Schneper L, Mathee K. Beta-lactam antibiotics: from antibiosis to resistance and bacteriology. *APMIS*. 2010;118(1):1-36. doi:10.1111/j.1600-0463.2009.02563.x

159. Spratt BG, Cromie KD. Penicillin-binding proteins of gram-negative bacteria. *Rev Infect Dis*. 1988;10(4):699-711. doi:10.1093/clinids/10.4.699

160. Tomasz A. Penicillin-binding proteins and the antibacterial effectiveness of beta-lactam antibiotics. *Rev Infect Dis*. 1986;8 Suppl 3:S260-278. doi:10.1093/clinids/8.supplement_3.s260

161. Trautmann M, Heinemann M, Zick R, Möricke A, Seidelmann M, Berger D. Antibacterial activity of meropenem against Pseudomonas aeruginosa, including antibiotic-induced morphological changes and endotoxin-liberating effects. *Eur J Clin Microbiol Infect Dis*. 1998;17(11):754-760. doi:10.1007/s100960050180

162. Wiersinga WJ, van der Poll T, White NJ, Day NP, Peacock SJ. Melioidosis: insights into the pathogenicity of Burkholderia pseudomallei. *Nat Rev Microbiol*. 2006;4(4):272-282. doi:10.1038/nrmicro1385

163. Hemsley CM, Luo JX, Andreae CA, Butler CS, Soyer OS, Titball RW. Bacterial Drug Tolerance under Clinical Conditions Is Governed by Anaerobic Adaptation but not Anaerobic Respiration. *Antimicrob Agents Chemother*. 2014;58(10):5775-5783. doi:10.1128/AAC.02793-14

164. Nierman WC, Yu Y, Losada L. The In vitro Antibiotic Tolerant Persister Population in Burkholderia pseudomallei is Altered by Environmental Factors. *Front Microbiol*. 2015;6. doi:10.3389/fmicb.2015.01338

165. Hamad MA, Austin CR, Stewart AL, Higgins M, Vázquez-Torres A, Voskuil MI. Adaptation and Antibiotic Tolerance of Anaerobic Burkholderia pseudomallei. *Antimicrob Agents Chemother*. 2011;55(7):3313-3323. doi:10.1128/AAC.00953-10

166. Errington J. Cell wall-deficient, L-form bacteria in the 21st century: a personal perspective. *Biochemical Society Transactions*. 2017;45(2):287-295. doi:10.1042/BST20160435

167. Errington J, Mickiewicz K, Kawai Y, Wu LJ. L-form bacteria, chronic diseases and the origins of life. *Phil Trans R Soc B*. 2016;371(1707):20150494. doi:10.1098/rstb.2015.0494

168. Dörr T, Alvarez L, Delgado F, Davis BM, Cava F, Waldor MK. A cell wall damage response mediated by a sensor kinase/response regulator pair enables beta-lactam tolerance. *Proc Natl Acad Sci U S A*. 2016;113(2):404-409. doi:10.1073/pnas.1520333113

169. Vollmer W, Blanot D, De Pedro MA. Peptidoglycan structure and architecture. *FEMS Microbiol Rev*. 2008;32(2):149-167. doi:10.1111/j.1574-6976.2007.00094.x

170. Huang KC, Mukhopadhyay R, Wen B, Gitai Z, Wingreen NS. Cell shape and cell-wall organization in Gram-negative bacteria. *Proceedings of the National Academy of Sciences*. 2008;105(49):19282-19287. doi:10.1073/pnas.0805309105

171. May KL, Grabowicz M. The bacterial outer membrane is an evolving antibiotic barrier. *Proc Natl Acad Sci USA*. 2018;115(36):8852-8854. doi:10.1073/pnas.1812779115

172. Kang KN, Klein DR, Kazi MI, et al. Colistin heteroresistance in *Enterobacter cloacae* is regulated by PhoPQ-dependent 4-amino-4-deoxy- L -arabinose addition to lipid A. *Mol Microbiol*. 2019;111(6):1604-1616. doi:10.1111/mmi.14240

173. Mitrophanov AY, Jewett MW, Hadley TJ, Groisman EA. Evolution and Dynamics of Regulatory Architectures Controlling Polymyxin B Resistance in Enteric Bacteria. Guttman DS, ed. *PLoS Genet*. 2008;4(10):e1000233. doi:10.1371/journal.pgen.1000233

174. Needham BD, Trent MS. Fortifying the barrier: the impact of lipid A remodelling on bacterial pathogenesis. *Nat Rev Microbiol*. 2013;11(7):467-481. doi:10.1038/nrmicro3047

175. Groisman EA, Duprey A, Choi J. How the PhoP/PhoQ System Controls Virulence and Mg^{2+} Homeostasis: Lessons in Signal Transduction, Pathogenesis, Physiology, and Evolution. *Microbiol Mol Biol Rev*. 2021;85(3). doi:10.1128/MMBR.00176-20

176. Bishop RE, Kim SH, El Zoeiby A. Role of lipid A palmitoylation in bacterial pathogenesis. *J Endotoxin Res*. 2005;11(3):174-180. doi:10.1179/096805105X35242

177. Boll JM, Tucker AT, Klein DR, et al. Reinforcing Lipid A Acylation on the Cell Surface of Acinetobacter baumannii Promotes Cationic Antimicrobial Peptide Resistance and Desiccation Survival. *mBio*. 2015;6(3):e00478-00415. doi:10.1128/mBio.00478-15

178. Rojas ER, Billings G, Odermatt PD, et al. The outer membrane is an essential load-bearing element in Gram-negative bacteria. *Nature*. 2018;559(7715):617-621. doi:10.1038/s41586-018-0344-3

179. Blair JMA, Webber MA, Baylay AJ, Ogbolu DO, Piddock LJV. Molecular mechanisms of antibiotic resistance. *Nat Rev Microbiol*. 2015;13(1):42-51. doi:10.1038/nrmicro3380

180. Delcour AH. Outer membrane permeability and antibiotic resistance. *Biochimica et Biophysica Acta (BBA) - Proteins and Proteomics*. 2009;1794(5):808-816. doi:10.1016/j.bbapap.2008.11.005

181. Uppalapati SR, Sett A, Pathania R. The Outer Membrane Proteins OmpA, CarO, and OprD of Acinetobacter baumannii Confer a Two-Pronged Defense in Facilitating Its Success as a Potent Human Pathogen. *Front Microbiol*. 2020;11:589234. doi:10.3389/fmicb.2020.589234

182. Choi U, Lee CR. Distinct Roles of Outer Membrane Porins in Antibiotic Resistance and Membrane Integrity in Escherichia coli. *Front Microbiol*. 2019;10:953. doi:10.3389/fmicb.2019.00953

183. Samsudin F, Ortiz-Suarez ML, Piggot TJ, Bond PJ, Khalid S. OmpA: A Flexible Clamp for Bacterial Cell Wall Attachment. *Structure*. 2016;24(12):2227-2235. doi:10.1016/j.str.2016.10.009

184. Aliashkevich A, Cava F. LD-transpeptidases: the great unknown among the peptidoglycan cross-linkers. *FEBS J*. Published online June 22, 2021:febs.16066. doi:10.1111/febs.16066

185. Dörr T, Moynihan PJ, Mayer C. Editorial: Bacterial Cell Wall Structure and Dynamics. *Front Microbiol*. 2019;10:2051. doi:10.3389/fmicb.2019.02051

186. Taguchi A, Welsh MA, Marmont LS, et al. FtsW is a peptidoglycan polymerase that is functional only in complex with its cognate penicillin-binding protein. *Nat Microbiol*. 2019;4(4):587-594. doi:10.1038/s41564-018-0345-x

187. Ruiz N. Bioinformatics identification of MurJ (MviN) as the peptidoglycan lipid II flippase in *Escherichia coli*. *PNAS*. 2008;105(40):15553-15557. doi:10.1073/pnas.0808352105

188. Typas A, Banzhaf M, Gross CA, Vollmer W. From the regulation of peptidoglycan synthesis to bacterial growth and morphology. *Nat Rev Microbiol*. 2012;10(2):123-136. doi:10.1038/nrmicro2677

189. Meeske AJ, Sham LT, Kimsey H, et al. MurJ and a novel lipid II flippase are required for cell wall biogenesis in *Bacillus subtilis*. *Proc Natl Acad Sci USA*. 2015;112(20):6437-6442. doi:10.1073/pnas.1504967112

190. Cho H, Uehara T, Bernhardt TG. Beta-Lactam Antibiotics Induce a Lethal Malfunctioning of the Bacterial Cell Wall Synthesis Machinery. *Cell*. 2014;159(6):1300-1311. doi:10.1016/j.cell.2014.11.017

191. Fisher JF, Mobashery S. The sentinel role of peptidoglycan recycling in the β-lactam resistance of the Gram-negative Enterobacteriaceae and Pseudomonas aeruginosa. *Bioorg Chem*. 2014;56:41-48. doi:10.1016/j.bioorg.2014.05.011

192. Goodell EW. Recycling of murein by Escherichia coli. *J Bacteriol*. 1985;163(1):305-310. doi:10.1128/jb.163.1.305-310.1985

193. Jacobs C, Frère JM, Normark S. Cytosolic intermediates for cell wall biosynthesis and degradation control inducible beta-lactam resistance in gram-negative bacteria. *Cell*. 1997;88(6):823-832. doi:10.1016/s0092-8674(00)81928-5

194. Dhar S, Kumari H, Balasubramanian D, Mathee K. Cell-wall recycling and synthesis in Escherichia coli and Pseudomonas aeruginosa – their role in the development of resistance. *Journal of Medical Microbiology*. 2018;67(1):1-21. doi:10.1099/jmm.0.000636

195. Johnson JW, Fisher JF, Mobashery S. Bacterial cell-wall recycling: Bacterial cell-wall recycling. *Annals of the New York Academy of Sciences*. 2013;1277(1):54-75. doi:10.1111/j.1749-6632.2012.06813.x

196. van Heijenoort J. Peptidoglycan hydrolases of Escherichia coli. *Microbiol Mol Biol Rev*. 2011;75(4):636-663. doi:10.1128/MMBR.00022-11

197. Goffin C, Ghuysen JM. Multimodular penicillin-binding proteins: an enigmatic family of orthologs and paralogs. *Microbiol Mol Biol Rev*. 1998;62(4):1079-1093. doi:10.1128/MMBR.62.4.1079-1093.1998

198. Höltje JV, Mirelman D, Sharon N, Schwarz U. Novel type of murein transglycosylase in Escherichia coli. *J Bacteriol*. 1975;124(3):1067-1076. doi:10.1128/jb.124.3.1067-1076.1975

199. Izaki K, Matsuhashi M, Strominger JL. Glycopeptide transpeptidase and D-alanine carboxypeptidase: penicillin-sensitive enzymatic reactions. *Proc Natl Acad Sci U S A*. 1966;55(3):656-663. doi:10.1073/pnas.55.3.656

200. Vollmer W, Joris B, Charlier P, Foster S. Bacterial peptidoglycan (murein) hydrolases. *FEMS Microbiol Rev*. 2008;32(2):259-286. doi:10.1111/j.1574-6976.2007.00099.x

201. Henderson TA, Templin M, Young KD. Identification and cloning of the gene encoding penicillin-binding protein 7 of Escherichia coli. *J Bacteriol*. 1995;177(8):2074-2079. doi:10.1128/jb.177.8.2074-2079.1995

202. Song J, Xie G, Elf PK, Young KD, Jensen RA. Comparative analysis of Pseudomonas aeruginosa penicillin-binding protein 7 in the context of its membership in the family of low-molecular-mass PBPs. *Microbiology (Reading)*. 1998;144 (Pt 4):975-983. doi:10.1099/00221287-144-4-975

203. Russo TA, MacDonald U, Beanan JM, et al. Penicillin-binding protein 7/8 contributes to the survival of Acinetobacter baumannii in vitro and in vivo. *J Infect Dis*. 2009;199(4):513-521. doi:10.1086/596317

204. Jacobs C, Huang LJ, Bartowsky E, Normark S, Park JT. Bacterial cell wall recycling provides cytosolic muropeptides as effectors for beta-lactamase induction. *EMBO J*. 1994;13(19):4684-4694.

205. Park JT. Turnover and recycling of the murein sacculus in oligopeptide permease-negative strains of Escherichia coli: indirect evidence for an alternative permease system and for a monolayered sacculus. *J Bacteriol*. 1993;175(1):7-11. doi:10.1128/jb.175.1.7-11.1993

206. Templin MF, Ursinus A, Höltje JV. A defect in cell wall recycling triggers autolysis during the stationary growth phase of Escherichia coli. *EMBO J*. 1999;18(15):4108-4117. doi:10.1093/emboj/18.15.4108

207. Yem DW, Wu HC. Purification and properties of beta-N-acetylglucosaminidase from Escherichia coli. *J Bacteriol*. 1976;125(1):324-331. doi:10.1128/jb.125.1.324-331.1976

208. Sonnabend MS, Klein K, Beier S, et al. Identification of Drug Resistance Determinants in a Clinical Isolate of Pseudomonas aeruginosa by High-Density Transposon Mutagenesis. *Antimicrob Agents Chemother*. 2020;64(3). doi:10.1128/AAC.01771-19

209. Irazoki O, Hernandez SB, Cava F. Peptidoglycan Muropeptides: Release, Perception, and Functions as Signaling Molecules. *Front Microbiol*. 2019;10:500. doi:10.3389/fmicb.2019.00500

210. Schroeder U, Henrich B, Fink J, Plapp R. Peptidase D of Escherichia coli K-12, a metallopeptidase of low substrate specificity. *FEMS Microbiol Lett*. 1994;123(1-2):153-159. doi:10.1111/j.1574-6968.1994.tb07215.x

211. Uehara T, Park JT. Identification of MpaA, an Amidase in *Escherichia coli* That Hydrolyzes the γ- D -Glutamyl- *meso*- Diaminopimelate Bond in Murein Peptides. *J Bacteriol*. 2003;185(2):679-682. doi:10.1128/JB.185.2.679-682.2003

212. Schmidt DMZ, Hubbard BK, Gerlt JA. Evolution of Enzymatic Activities in the Enolase Superfamily: Functional Assignment of Unknown Proteins in *Bacillus subtilis* and *Escherichia coli* as L -Ala- D / L -Glu Epimerases. *Biochemistry*. 2001;40(51):15707-15715. doi:10.1021/bi011640x

213. Zeng X, Lin J. Beta-lactamase induction and cell wall metabolism in Gram-negative bacteria. *Front Microbiol*. 2013;4. doi:10.3389/fmicb.2013.00128

214. Everett M, Sprynski N, Coelho A, et al. Discovery of a Novel Metallo-β-Lactamase Inhibitor That Potentiates Meropenem Activity against Carbapenem-Resistant Enterobacteriaceae. *Antimicrob Agents Chemother*. 2018;62(5). doi:10.1128/AAC.00074-18

215. Reading C, Cole M. Clavulanic acid: a beta-lactamase-inhiting beta-lactam from Streptomyces clavuligerus. *Antimicrob Agents Chemother*. 1977;11(5):852-857.

216. English AR, Retsema JA, Girard AE, Lynch JE, Barth WE. CP-45,899, a beta-lactamase inhibitor that extends the antibacterial spectrum of beta-lactams: initial bacteriological characterization. *Antimicrob Agents Chemother*. 1978;14(3):414-419.

217. Fisher J, Belasco JG, Charnas RL, Khosla S, Knowles JR. Beta-lactamase inactivation by mechanism-based reagents. *Philos Trans R Soc Lond, B, Biol Sci*. 1980;289(1036):309-319.

218. Ehmann DE, Jahić H, Ross PL, et al. Avibactam is a covalent, reversible, non–β-lactam β-lactamase inhibitor. *Proc Natl Acad Sci U S A*. 2012;109(29):11663-11668. doi:10.1073/pnas.1205073109

219. Bush K, Bradford PA. Interplay between β-lactamases and new β-lactamase inhibitors. *Nat Rev Microbiol*. 2019;17(5):295-306. doi:10.1038/s41579-019-0159-8

220. Sanschagrin F, Levesque RC. A specific peptide inhibitor of the class B metallo-beta-lactamase L-1 from Stenotrophomonas maltophilia identified using phage display. *J Antimicrob Chemother*. 2005;55(2):252-255. doi:10.1093/jac/dkh550

221. Sun Q, Law A, Crowder MW, Geysen HM. Homo-cysteinyl peptide inhibitors of the L1 metallo-beta-lactamase, and SAR as determined by combinatorial library synthesis. *Bioorg Med Chem Lett*. 2006;16(19):5169-5175. doi:10.1016/j.bmcl.2006.07.001

222. Walter MW, Felici A, Galleni M, et al. Trifluoromethyl alcohol and ketone inhibitors of metallo-β-lactamases. *Bioorganic & Medicinal Chemistry Letters*. 1996;6(20):2455-2458. doi:10.1016/0960-894X(96)00453-2

223. King AM, Reid-Yu SA, Wang W, et al. Aspergillomarasmine A overcomes metallo-β-lactamase antibiotic resistance. *Nature*. 2014;510(7506):503-506. doi:10.1038/nature13445

224. Liu XL, Yang KW, Zhang YJ, et al. Optimization of amino acid thioesters as inhibitors of metallo-β-lactamase L1. *Bioorg Med Chem Lett*. 2016;26(19):4698-4701. doi:10.1016/j.bmcl.2016.08.048

225. Tucker AT, Leonard SP, DuBois CD, et al. Discovery of Next-Generation Antimicrobials through Bacterial Self-Screening of Surface-Displayed Peptide Libraries. *Cell*. 2018;172:618-628. doi:10.1016/j.cell.2017.12.009

226. Robinson MD, McCarthy DJ, Smyth GK. edgeR: a Bioconductor package for differential expression analysis of digital gene expression data. *Bioinformatics*. 2010;26(1):139-140. doi:10.1093/bioinformatics/btp616

227. Ignatiadis N, Klaus B, Zaugg JB, Huber W. Data-driven hypothesis weighting increases detection power in genome-scale multiple testing. *Nat Methods*. 2016;13(7):577-580. doi:10.1038/nmeth.3885

228. Osorio D, Rondón-Villarreal P, Torres R. Peptides: A Package for Data Mining of Antimicrobial Peptides. *The R Journal*. 2015;7(1):4. doi:10.32614/RJ-2015-001

229. R Core Team. *R: A Language and Environment for Statistical Computing*. R Foundation for Statistical Computing; 2019. http://www.R-project.org/

230. Wagih O. ggseqlogo: a versatile R package for drawing sequence logos. *Bioinformatics*. 2017;33(22):3645-3647. doi:10.1093/bioinformatics/btx469

231. Mah TF. Establishing the minimal bactericidal concentration of an antimicrobial agent for planktonic cells (MBC-P) and biofilm cells (MBC-B). *J Vis Exp*. 2014;(83):e50854. doi:10.3791/50854

232. Qaiyumi, S. Macro- and Microdilution Methods of Antimicrobial Susceptibility Testing. In Antimicrobial susceptibility testing protocols, A.C. In: Goodwin, R. Schwalbe and L.Steele-Moore; :75-79.

233. Kang KN, Klein DR, Kazi MI, et al. Colistin heteroresistance in Enterobacter cloacae is regulated by PhoPQ-dependent 4-amino-4-deoxy-l-arabinose addition to lipid A. *Mol Microbiol*. 2019;111(6):1604-1616. doi:10.1111/mmi.14240

234. Kamischke C, Fan J, Bergeron J, et al. The Acinetobacter baumannii Mla system and glycerophospholipid transport to the outer membrane. *Elife*. 2019;8. doi:10.7554/eLife.40171

235. Docquier JD, Lamotte-Brasseur J, Galleni M, Amicosante G, Frère JM, Rossolini GM. On functional and structural heterogeneity of VIM-type metallo-beta-lactamases. *J Antimicrob Chemother*. 2003;51(2):257-266. doi:10.1093/jac/dkg067

236. Alatrash N, Narh ES, Yadav A, et al. Synthesis, DNA Cleavage Activity, Cytotoxicity, Acetylcholinesterase Inhibition, and Acute Murine Toxicity of Redox-Active Ruthenium(II) Polypyridyl Complexes. *ChemMedChem*. 2017;12(13):1055-1069. doi:10.1002/cmdc.201700240

237. Zhang SK, Song JW, Gong F, et al. Design of an α-helical antimicrobial peptide with improved cell-selective and potent anti-biofilm activity. *Sci Rep*. 2016;6:27394. doi:10.1038/srep27394

238. Rodloff AC, Goldstein EJC, Torres A. Two decades of imipenem therapy. *J Antimicrob Chemother*. 2006;58(5):916-929. doi:10.1093/jac/dkl354

239. Pagès JM, James CE, Winterhalter M. The porin and the permeating antibiotic: a selective diffusion barrier in Gram-negative bacteria. *Nat Rev Microbiol*. 2008;6(12):893-903. doi:10.1038/nrmicro1994

240. Boll JM, Crofts AA, Peters K, et al. A penicillin-binding protein inhibits selection of colistin-resistant, lipooligosaccharide-deficient Acinetobacter baumannii. *Proc Natl Acad Sci USA*. 2016;113(41):E6228-E6237. doi:10.1073/pnas.1611594113

241. Boll JM, Tucker AT, Klein DR, et al. Reinforcing Lipid A Acylation on the Cell Surface of Acinetobacter baumannii Promotes Cationic Antimicrobial Peptide Resistance and Desiccation Survival. *MBio*. 2015;6(3):e00478-00415. doi:10.1128/mBio.00478-15

242. Thomas PW, Spicer T, Cammarata M, Brodbelt JS, Hodder P, Fast W. An altered zinc-binding site confers resistance to a covalent inactivator of New Delhi metallo-beta-lactamase-1 (NDM-1) discovered by high-throughput screening. *Bioorg Med Chem*. 2013;21(11):3138-3146. doi:10.1016/j.bmc.2013.03.031

243. Makena A, Brem J, Pfeffer I, et al. Biochemical characterization of New Delhi metallo-β-lactamase variants reveals differences in protein stability. *J Antimicrob Chemother*. 2015;70(2):463-469. doi:10.1093/jac/dku403

244. Edwards IA, Elliott AG, Kavanagh AM, Zuegg J, Blaskovich MAT, Cooper MA. Contribution of Amphipathicity and Hydrophobicity to the Antimicrobial Activity and Cytotoxicity of β-Hairpin Peptides. *ACS Infect Dis*. 2016;2(6):442-450. doi:10.1021/acsinfecdis.6b00045

245. Trent MS, Ribeiro AA, Lin S, Cotter RJ, Raetz CR. An inner membrane enzyme in Salmonella and Escherichia coli that transfers 4-amino-4-deoxy-L-arabinose to lipid A: induction on polymyxin-resistant mutants and role of a novel lipid-linked donor. *J Biol Chem*. 2001;276(46):43122-43131. doi:10.1074/jbc.M106961200

246. Raetz CRH, Reynolds CM, Trent MS, Bishop RE. Lipid A modification systems in gram-negative bacteria. *Annu Rev Biochem*. 2007;76:295-329. doi:10.1146/annurev.biochem.76.010307.145803

247. Peterson AA, Fesik SW, McGroarty EJ. Decreased binding of antibiotics to lipopolysaccharides from polymyxin-resistant strains of Escherichia coli and Salmonella typhimurium. *Antimicrob Agents Chemother*. 1987;31(2):230-237.

248. Lehrer RI, Barton A, Daher KA, Harwig SS, Ganz T, Selsted ME. Interaction of human defensins with Escherichia coli. Mechanism of bactericidal activity. *J Clin Invest*. 1989;84(2):553-561. doi:10.1172/JCI114198

249. Klingler FM, Wichelhaus TA, Frank D, et al. Approved Drugs Containing Thiols as Inhibitors of Metallo-β-lactamases: Strategy To Combat Multidrug-Resistant Bacteria. *J Med Chem*. 2015;58(8):3626-3630. doi:10.1021/jm501844d

250. Yusof Y, Tan DTC, Arjomandi OK, Schenk G, McGeary RP. Captopril analogues as metallo-β-lactamase inhibitors. *Bioorg Med Chem Lett*. 2016;26(6):1589-1593. doi:10.1016/j.bmcl.2016.02.007

251. Arjomandi OK, Hussein WM, Vella P, et al. Design, synthesis, and in vitro and biological evaluation of potent amino acid-derived thiol inhibitors of the metallo-β-lactamase IMP-1. *Eur J Med Chem*. 2016;114:318-327. doi:10.1016/j.ejmech.2016.03.017

252. Brem J, van Berkel SS, Aik W, et al. Rhodanine hydrolysis leads to potent thioenolate mediated metallo-β-lactamase inhibition. *Nat Chem*. 2014;6(12):1084-1090. doi:10.1038/nchem.2110

253. Brem J, Cain R, Cahill S, et al. Structural basis of metallo-β-lactamase, serine-β-lactamase and penicillin-binding protein inhibition by cyclic boronates. *Nat Commun*. 2016;7:12406. doi:10.1038/ncomms12406

254. Yang SK, Kang JS, Oelschlaeger P, Yang KW. Azolylthioacetamide: A Highly Promising Scaffold for the Development of Metallo-β-lactamase Inhibitors. *ACS Med Chem Lett*. 2015;6(4):455-460. doi:10.1021/ml500534c

255. Westblade LF, Errington J, Dörr T. Antibiotic tolerance. Leong JM, ed. *PLoS Pathog*. 2020;16(10):e1008892. doi:10.1371/journal.ppat.1008892

256. Liu J, Gefen O, Ronin I, Bar-Meir M, Balaban NQ. Effect of tolerance on the evolution of antibiotic resistance under drug combinations. *Science*. 2020;367(6474):200-204. doi:10.1126/science.aay3041

257. Mercier R, Kawai Y, Errington J. General principles for the formation and proliferation of a wall-free (L-form) state in bacteria. *Elife*. 2014;3. doi:10.7554/eLife.04629

258. Shin JH, Choe D, Ransegnola B, et al. A multifaceted cellular damage repair and prevention pathway promotes high-level tolerance to β-lactam antibiotics. *EMBO Rep*. 2021;22(2):e51790. doi:10.15252/embr.202051790

259. Davies BW, Bogard RW, Mekalanos JJ. Mapping the regulon of Vibrio cholerae ferric uptake regulator expands its known network of gene regulation. *Proc Natl Acad Sci U S A*. 2011;108(30):12467-12472. doi:10.1073/pnas.1107894108

260. Boll JM, Crofts AA, Peters K, et al. A penicillin-binding protein inhibits selection of colistin-resistant, lipooligosaccharide-deficient *Acinetobacter baumannii*. *Proc Natl Acad Sci USA*. 2016;113(41):E6228-E6237. doi:10.1073/pnas.1611594113

261. Livak KJ, Schmittgen TD. Analysis of relative gene expression data using real-time quantitative PCR and the 2(-Delta Delta C(T)) Method. *Methods*. 2001;25(4):402-408. doi:10.1006/meth.2001.1262

262. Guérin F, Isnard C, Cattoir V, Giard JC. Complex Regulation Pathways of AmpC-Mediated β-Lactam Resistance in Enterobacter cloacae Complex. *Antimicrob Agents Chemother*. 2015;59(12):7753-7761. doi:10.1128/AAC.01729-15

263. Huang TW, Lam I, Chang HY, Tsai SF, Palsson BO, Charusanti P. Capsule deletion via a λ-Red knockout system perturbs biofilm formation and fimbriae expression in Klebsiella pneumoniae MGH 78578. *BMC Res Notes*. 2014;7:13. doi:10.1186/1756-0500-7-13

264. Datsenko KA, Wanner BL. One-step inactivation of chromosomal genes in Escherichia coli K-12 using PCR products. *Proceedings of the National Academy of Sciences*. 2000;97(12):6640-6645. doi:10.1073/pnas.120163297

265. Lazarus JE, Warr AR, Kuehl CJ, Giorgio RT, Davis BM, Waldor MK. A New Suite of Allelic-Exchange Vectors for the Scarless Modification of Proteobacterial Genomes. *Appl Environ Microbiol*. 2019;85(16):e00990-19. doi:10.1128/AEM.00990-19

266. Gibson DG, Young L, Chuang RY, Venter JC, Hutchison CA, Smith HO. Enzymatic assembly of DNA molecules up to several hundred kilobases. *Nat Methods*. 2009;6(5):343-345. doi:10.1038/nmeth.1318

267. Kang KN, Kazi MI, Biboy J, et al. Septal Class A Penicillin-Binding Protein Activity and LD -Transpeptidases Mediate Selection of Colistin-Resistant Lipooligosaccharide-Deficient Acinetobacter baumannii. Sperandio V, ed. *mBio*. 2021;12(1). doi:10.1128/mBio.02185-20

268. Zhou Z, Lin S, Cotter RJ, Raetz CR. Lipid A modifications characteristic of Salmonella typhimurium are induced by NH4VO3 in Escherichia coli K12. Detection of 4-amino-4-deoxy-L-arabinose, phosphoethanolamine and palmitate. *J Biol Chem*. 1999;274(26):18503-18514. doi:10.1074/jbc.274.26.18503

269. Band VI, Crispell EK, Napier BA, et al. Antibiotic failure mediated by a resistant subpopulation in Enterobacter cloacae. *Nat Microbiol*. 2016;1(6):16053. doi:10.1038/nmicrobiol.2016.53

270. Snyder S, Kim D, McIntosh TJ. Lipopolysaccharide bilayer structure: effect of chemotype, core mutations, divalent cations, and temperature. *Biochemistry*. 1999;38(33):10758-10767. doi:10.1021/bi990867d

271. Garidel P, Rappolt M, Schromm AB, et al. Divalent cations affect chain mobility and aggregate structure of lipopolysaccharide from Salmonella minnesota reflected in a decrease of its biological activity. *Biochim Biophys Acta*. 2005;1715(2):122-131. doi:10.1016/j.bbamem.2005.07.013

272. Henderson JC, Zimmerman SM, Crofts AA, et al. The Power of Asymmetry: Architecture and Assembly of the Gram-Negative Outer Membrane Lipid Bilayer. *Annu Rev Microbiol*. 2016;70(1):255-278. doi:10.1146/annurev-micro-102215-095308

273. Lin QY, Tsai YL, Liu MC, Lin WC, Hsueh PR, Liaw SJ. Serratia marcescens *arn* , a PhoP-Regulated Locus Necessary for Polymyxin B Resistance. *Antimicrob Agents Chemother*. 2014;58(9):5181-5190. doi:10.1128/AAC.00013-14

274. Band VI, Weiss DS. Heteroresistance: A cause of unexplained antibiotic treatment failure? *PLoS Pathog*. 2019;15(6):e1007726. doi:10.1371/journal.ppat.1007726

275. Rice A, Wereszczynski J. Atomistic Scale Effects of Lipopolysaccharide Modifications on Bacterial Outer Membrane Defenses. *Biophys J*. 2018;114(6):1389-1399. doi:10.1016/j.bpj.2018.02.006

276. Lippa AM, Goulian M. Feedback inhibition in the PhoQ/PhoP signaling system by a membrane peptide. *PLoS Genet*. 2009;5(12):e1000788. doi:10.1371/journal.pgen.1000788

277. Trent MS, Ribeiro AA, Lin S, Cotter RJ, Raetz CR. An inner membrane enzyme in Salmonella and Escherichia coli that transfers 4-amino-4-deoxy-L-arabinose to lipid A: induction on polymyxin-resistant mutants and role of a novel lipid-linked donor. *J Biol Chem*. 2001;276(46):43122-43131. doi:10.1074/jbc.M106961200

278. Gunn JS, Lim KB, Krueger J, et al. PmrA-PmrB-regulated genes necessary for 4-aminoarabinose lipid A modification and polymyxin resistance. *Molecular Microbiology*. 1998;27(6):1171-1182. doi:10.1046/j.1365-2958.1998.00757.x

279. Soncini FC, Véscovi EG, Groisman EA. Transcriptional autoregulation of the Salmonella typhimurium phoPQ operon. *J Bacteriol*. 1995;177(15):4364-4371. doi:10.1128/jb.177.15.4364-4371.1995

280. Jia W, El Zoeiby A, Petruzziello TN, Jayabalasingham B, Seyedirashti S, Bishop RE. Lipid trafficking controls endotoxin acylation in outer membranes of Escherichia coli. *J Biol Chem*. 2004;279(43):44966-44975. doi:10.1074/jbc.M404963200

281. Hwang PM, Choy WY, Lo EI, et al. Solution structure and dynamics of the outer membrane enzyme PagP by NMR. *Proceedings of the National Academy of Sciences*. 2002;99(21):13560-13565. doi:10.1073/pnas.212344499

282. Bishop RE, Gibbons HS, Guina T, Trent MS, Miller SI, Raetz CR. Transfer of palmitate from phospholipids to lipid A in outer membranes of gram-negative bacteria. *EMBO J*. 2000;19(19):5071-5080. doi:10.1093/emboj/19.19.5071

283. Malinverni JC, Silhavy TJ. An ABC transport system that maintains lipid asymmetry in the Gram-negative outer membrane. *Proceedings of the National Academy of Sciences*. 2009;106(19):8009-8014. doi:10.1073/pnas.0903229106

284. Bader MW, Sanowar S, Daley ME, et al. Recognition of Antimicrobial Peptides by a Bacterial Sensor Kinase. *Cell*. 2005;122(3):461-472. doi:10.1016/j.cell.2005.05.030

285. Trent MS, Ribeiro AA, Doerrler WT, Lin S, Cotter RJ, Raetz CRH. Accumulation of a Polyisoprene-linked Amino Sugar in Polymyxin-resistant Salmonella typhimurium andEscherichia coli. *Journal of Biological Chemistry*. 2001;276(46):43132-43144. doi:10.1074/jbc.M106962200

286. Wilke KE, Francis S, Carlson EE. Inactivation of multiple bacterial histidine kinases by targeting the ATP-binding domain. *ACS Chem Biol*. 2015;10(1):328-335. doi:10.1021/cb5008019

287. Thielen MK, Vaneerd CK, Goswami M, Carlson EE, May JF. 2-Aminobenzothiazoles Inhibit Virulence Gene Expression and Block Polymyxin Resistance in Salmonella enterica. *Chembiochem*. 2020;21(24):3500-3503. doi:10.1002/cbic.202000422

288. Mercier R, Kawai Y, Errington J. Excess membrane synthesis drives a primitive mode of cell proliferation. *Cell*. 2013;152(5):997-1007. doi:10.1016/j.cell.2013.01.043

289. Billings G, Ouzounov N, Ursell T, et al. De novo morphogenesis in L-forms via geometric control of cell growth. *Mol Microbiol*. 2014;93(5):883-896. doi:10.1111/mmi.12703

290. Poirel L, Jayol A, Bontron S, et al. The mgrB gene as a key target for acquired resistance to colistin in Klebsiella pneumoniae. *J Antimicrob Chemother*. 2015;70(1):75-80. doi:10.1093/jac/dku323

291. Cannatelli A, D'Andrea MM, Giani T, et al. In vivo emergence of colistin resistance in Klebsiella pneumoniae producing KPC-type carbapenemases mediated by insertional inactivation of the PhoQ/PhoP mgrB regulator. *Antimicrob Agents Chemother*. 2013;57(11):5521-5526. doi:10.1128/AAC.01480-13

292. López-Camacho E, Gómez-Gil R, Tobes R, et al. Genomic analysis of the emergence and evolution of multidrug resistance during a Klebsiella pneumoniae outbreak including carbapenem and colistin resistance. *J Antimicrob Chemother*. 2014;69(3):632-636. doi:10.1093/jac/dkt419

293. Roberts D, Higgs E, Rutman A, Cole P. Isolation of spheroplastic forms of Haemophilus influenzae from sputum in conventionally treated chronic bronchial sepsis using selective medium supplemented with N-acetyl-D-glucosamine: possible reservoir for re-emergence of infection. *Br Med J (Clin Res Ed)*. 1984;289(6456):1409-1412. doi:10.1136/bmj.289.6456.1409

294. Morè N, Martorana AM, Biboy J, et al. Peptidoglycan Remodeling Enables Escherichia coli To Survive Severe Outer Membrane Assembly Defect. Kline KA, ed. *mBio*. 2019;10(1). doi:10.1128/mBio.02729-18

295. Maragakis LL, Perl TM. Antimicrobial Resistance: *Acinetobacter baumannii:* Epidemiology, Antimicrobial Resistance, and Treatment Options. *CLIN INFECT DIS*. 2008;46(8):1254-1263. doi:10.1086/529198

296. Rahal JJ. Antimicrobial Resistance among and Therapeutic Options against Gram-Negative Pathogens. *CLIN INFECT DIS*. 2009;49(s1):S4-S10. doi:10.1086/599810

297. About Antimicrobial Resistance | Antibiotic/Antimicrobial Resistance | CDC. Accessed December 20, 2018. https://www.cdc.gov/drugresistance/about.html

298. Schindelin J, Arganda-Carreras I, Frise E, et al. Fiji: an open-source platform for biological-image analysis. *Nat Methods*. 2012;9(7):676-682. doi:10.1038/nmeth.2019

299. Ducret A, Quardokus EM, Brun YV. MicrobeJ, a tool for high throughput bacterial cell detection and quantitative analysis. *Nat Microbiol*. 2016;1(7):16077. doi:10.1038/nmicrobiol.2016.77

300. Kazi MI, Schargel RD, Boll JM. Generating Transposon Insertion Libraries in Gram-Negative Bacteria for High-Throughput Sequencing. *J Vis Exp*. 2020;(161). doi:10.3791/61612

301. Marolda CL, Lahiry P, Vinés E, Saldías S, Valvano MA. Micromethods for the Characterization of Lipid A-Core and O-Antigen Lipopolysaccharide. In: *Glycobiology Protocols*. Vol 347. Humana Press; 2006:237-252. doi:10.1385/1-59745-167-3:237

302. Kazi MI, Perry BW, Card DC, et al. Discovery and characterization of New Delhi metallo-β-lactamase-1 inhibitor peptides that potentiate meropenem-dependent killing of carbapenemase-producing Enterobacteriaceae. *J Antimicrob Chemother*. 2020;75(10):2843-2851. doi:10.1093/jac/dkaa242

303. Glauner B, Höltje JV, Schwarz U. The composition of the murein of Escherichia coli. *J Biol Chem*. 1988;263(21):10088-10095.

304. Le NH, Peters K, Espaillat A, et al. Peptidoglycan editing provides immunity to *Acinetobacter baumannii* during bacterial warfare. *Sci Adv*. 2020;6(30):eabb5614. doi:10.1126/sciadv.abb5614

305. Murtha AN, Kazi MI, Schargel RD, et al. *High-Level Carbapenem Tolerance Requires Antibiotic-Induced Outer Membrane Modifications*. Microbiology; 2021. doi:10.1101/2021.09.25.461800

306. McLeod GI, Spector MP. Starvation- and Stationary-phase-induced resistance to the antimicrobial peptide polymyxin B in Salmonella typhimurium is RpoS (sigma(S)) independent and occurs through both phoP-dependent and -independent pathways. *J Bacteriol*. 1996;178(13):3683-3688. doi:10.1128/jb.178.13.3683-3688.1996

307. Tuomanen E, Cozens R, Tosch W, Zak O, Tomasz A. The Rate of Killing of Escherichia coli by -Lactam Antibiotics Is Strictly Proportional to the Rate of Bacterial Growth. *Microbiology*. 1986;132(5):1297-1304. doi:10.1099/00221287-132-5-1297

308. Lee AJ, Wang S, Meredith HR, Zhuang B, Dai Z, You L. Robust, linear correlations between growth rates and β-lactam–mediated lysis rates. *Proc Natl Acad Sci USA*. 2018;115(16):4069-4074. doi:10.1073/pnas.1719504115

309. Lin MF, Lin YY, Tu CC, Lan CY. Distribution of different efflux pump genes in clinical isolates of multidrug-resistant Acinetobacter baumannii and their correlation with antimicrobial resistance. *Journal of Microbiology, Immunology and Infection*. 2017;50(2):224-231. doi:10.1016/j.jmii.2015.04.004

310. Yoon EJ, Courvalin P, Grillot-Courvalin C. RND-Type Efflux Pumps in Multidrug-Resistant Clinical Isolates of Acinetobacter baumannii: Major Role for AdeABC Overexpression and AdeRS Mutations. *Antimicrob Agents Chemother*. 2013;57(7):2989-2995. doi:10.1128/AAC.02556-12

311. Rajamohan G, Srinivasan VB, Gebreyes WA. Novel role of Acinetobacter baumannii RND efflux transporters in mediating decreased susceptibility to biocides. *Journal of Antimicrobial Chemotherapy*. 2010;65(2):228-232. doi:10.1093/jac/dkp427

312. Damier-Piolle L, Magnet S, Brémont S, Lambert T, Courvalin P. AdeIJK, a Resistance-Nodulation-Cell Division Pump Effluxing Multiple Antibiotics in *Acinetobacter baumannii*. *Antimicrob Agents Chemother*. 2008;52(2):557-562. doi:10.1128/AAC.00732-07

313. Kornelsen V, Kumar A. Update on Multidrug Resistance Efflux Pumps in Acinetobacter spp. *Antimicrob Agents Chemother*. 2021;65(7). doi:10.1128/AAC.00514-21

314. Pagès JM, James CE, Winterhalter M. The porin and the permeating antibiotic: a selective diffusion barrier in Gram-negative bacteria. *Nat Rev Microbiol*. 2008;6(12):893-903. doi:10.1038/nrmicro1994

315. Mussi MA, Relling VM, Limansky AS, Viale AM. CarO, an *Acinetobacter baumannii* outer membrane protein involved in carbapenem resistance, is essential for L -ornithine uptake. *FEBS Letters*. 2007;581(29):5573-5578. doi:10.1016/j.febslet.2007.10.063

316. Mussi MA, Limansky AS, Viale AM. Acquisition of Resistance to Carbapenems in Multidrug-Resistant Clinical Strains of *Acinetobacter baumannii* : Natural Insertional Inactivation of a Gene Encoding a Member of a Novel Family of β-Barrel Outer Membrane Proteins. *Antimicrob Agents Chemother*. 2005;49(4):1432-1440. doi:10.1128/AAC.49.4.1432-1440.2005

317. Dupont M, Pagès JM, Lafitte D, Siroy A, Bollet C. Identification of an OprD Homologue in *Acinetobacter b aumannii*. *J Proteome Res*. 2005;4(6):2386-2390. doi:10.1021/pr050143q

318. Catel-Ferreira M, Marti S, Guillon L, et al. The outer membrane porin OmpW of *Acinetobacter baumannii* is involved in iron uptake and colistin binding. De la Rosa M, ed. *FEBS Lett*. 2016;590(2):224-231. doi:10.1002/1873-3468.12050

319. Henry R, Vithanage N, Harrison P, et al. Colistin-Resistant, Lipopolysaccharide-Deficient Acinetobacter baumannii Responds to Lipopolysaccharide Loss through Increased Expression of Genes Involved in the Synthesis and Transport of Lipoproteins, Phospholipids, and Poly-β-1,6- *N* -Acetylglucosamine. *Antimicrob Agents Chemother*. 2012;56(1):59-69. doi:10.1128/AAC.05191-11

320. Henry R, Crane B, Powell D, et al. The transcriptomic response of *Acinetobacter baumannii* to colistin and doripenem alone and in combination in an *in vitro* pharmacokinetics/pharmacodynamics model. *J Antimicrob Chemother*. 2015;70(5):1303-1313. doi:10.1093/jac/dku536

321. Mathelié-Guinlet M, Asmar AT, Collet JF, Dufrêne YF. Lipoprotein Lpp regulates the mechanical properties of the E. coli cell envelope. *Nat Commun*. 2020;11(1):1789. doi:10.1038/s41467-020-15489-1

322. Scheurwater EM, Clarke AJ. The C-terminal Domain of Escherichia coli YfhD Functions as a Lytic Transglycosylase. *Journal of Biological Chemistry*. 2008;283(13):8363-8373. doi:10.1074/jbc.M710135200

323. Uehara T, Park JT. Peptidoglycan Recycling. Slauch JM, ed. *EcoSal Plus*. 2008;3(1):ecosalplus.4.7.1.5. doi:10.1128/ecosalplus.4.7.1.5

324. Geisinger E, Mortman NJ, Dai Y, et al. Antibiotic susceptibility signatures identify potential antimicrobial targets in the Acinetobacter baumannii cell envelope. *Nat Commun*. 2020;11(1):4522. doi:10.1038/s41467-020-18301-2

325. Park JS, Lee WC, Yeo KJ, et al. Mechanism of anchoring of OmpA protein to the cell wall peptidoglycan of the gram-negative bacterial outer membrane. *FASEB j*. 2012;26(1):219-228. doi:10.1096/fj.11-188425

326. Gribun A, Nitzan Y, Pechatnikov I, Hershkovits G, Katcoff DJ. Molecular and Structural Characterization of the HMP-AB Gene Encoding a Pore-Forming Protein from a Clinical Isolate of Acinetobacter baumannii. *Curr Microbiol*. 2003;47(5). doi:10.1007/s00284-003-4050-4

327. Smani Y, Fàbrega A, Roca I, Sánchez-Encinales V, Vila J, Pachón J. Role of OmpA in the Multidrug Resistance Phenotype of Acinetobacter baumannii. *Antimicrob Agents Chemother*. 2014;58(3):1806-1808. doi:10.1128/AAC.02101-13

328. Tsai YK, Liou CH, Lin JC, Fung CP, Chang FY, Siu LK. Effects of different resistance mechanisms on antimicrobial resistance in Acinetobacter baumannii: a strategic system for screening and activity testing of new antibiotics. *International Journal of Antimicrobial Agents*. 2020;55(4):105918. doi:10.1016/j.ijantimicag.2020.105918

329. Moon DC, Choi CH, Lee JH, et al. Acinetobacter baumannii outer membrane protein a modulates the biogenesis of outer membrane vesicles. *J Microbiol*. 2012;50(1):155-160. doi:10.1007/s12275-012-1589-4

330. Horne JE, Brockwell DJ, Radford SE. Role of the lipid bilayer in outer membrane protein folding in Gram-negative bacteria. *Journal of Biological Chemistry*. 2020;295(30):10340-10367. doi:10.1074/jbc.REV120.011473

331. Storek KM, Auerbach MR, Shi H, et al. Monoclonal antibody targeting the β-barrel assembly machine of *Escherichia coli* is bactericidal. *Proc Natl Acad Sci USA*. 2018;115(14):3692-3697. doi:10.1073/pnas.1800043115

332. Edwards D, Donachie W. Construction of a Triple Deletion of Penicillin-Binding Proteins 4, 5, and 6 in Escherichia coli. In: *Bacterial Growth and Lysis: Metabolism and Structure of the Bacterial Sacculus.* Springer US; 1993:369-374.

333. Potluri L, Karczmarek A, Verheul J, et al. Septal and lateral wall localization of PBP5, the major D,D-carboxypeptidase of Escherichia coli, requires substrate recognition and membrane attachment: PBP5 localizes at peptidoglycan synthesis sites. *Molecular Microbiology*. 2010;77(2):300-323. doi:10.1111/j.1365-2958.2010.07205.x

334. Kohlrausch U, Höltje JV. Analysis of murein and murein precursors during antibiotic-induced lysis of Escherichia coli. *J Bacteriol*. 1991;173(11):3425-3431. doi:10.1128/jb.173.11.3425-3431.1991

335. Cheng Q, Park JT. Substrate Specificity of the AmpG Permease Required for Recycling of Cell Wall Anhydro-Muropeptides. *J Bacteriol*. 2002;184(23):6434-6436. doi:10.1128/JB.184.23.6434-6436.2002

336. Vötsch W, Templin MF. Characterization of a β-N-acetylglucosaminidase ofEscherichia coli and Elucidation of Its Role in Muropeptide Recycling and β-Lactamase Induction. *Journal of Biological Chemistry*. 2000;275(50):39032-39038. doi:10.1074/jbc.M004797200

337. Höltje JV, Kopp U, Ursinus A, Wiedemann B. The negative regulator of beta-lactamase induction AmpD is a N-acetyl-anhydromuramyl-L-alanine amidase. *FEMS Microbiol Lett*. 1994;122(1-2):159-164. doi:10.1111/j.1574-6968.1994.tb07159.x

338. Jacobs C, Joris B, Jamin M, et al. AmpD, essential for both beta-lactamase regulation and cell wall recycling, is a novel cytosolic N-acetylmuramyl-L-alanine amidase. *Mol Microbiol*. 1995;15(3):553-559. doi:10.1111/j.1365-2958.1995.tb02268.x

339. Mengin-Lecreulx D, van Heijenoort J, Park JT. Identification of the mpl gene encoding UDP-N-acetylmuramate: L-alanyl-gamma-D-glutamyl-meso-diaminopimelate ligase in Escherichia coli and its role in recycling of cell wall peptidoglycan. *J Bacteriol*. 1996;178(18):5347-5352. doi:10.1128/jb.178.18.5347-5352.1996

340. Bahadur R, Chodisetti PK, Reddy M. Cleavage of Braun's lipoprotein Lpp from the bacterial peptidoglycan by a paralog of l,d-transpeptidases, LdtF. *Proc Natl Acad Sci USA*. 2021;118(19):e2101989118. doi:10.1073/pnas.2101989118

341. Powers MJ, Trent MS. Phospholipid retention in the absence of asymmetry strengthens the outer membrane permeability barrier to last-resort antibiotics. *Proc Natl Acad Sci USA*. 2018;115(36):E8518-E8527. doi:10.1073/pnas.1806714115

342. Magnet S, Bellais S, Dubost L, et al. Identification of the L,D-transpeptidases responsible for attachment of the Braun lipoprotein to Escherichia coli peptidoglycan. *J Bacteriol*. 2007;189(10):3927-3931. doi:10.1128/JB.00084-07

343. Das D, Hervé M, Feuerhelm J, et al. Structure and Function of the First Full-Length Murein Peptide Ligase (Mpl) Cell Wall Recycling Protein. Pastore A, ed. *PLoS ONE*. 2011;6(3):e17624. doi:10.1371/journal.pone.0017624

344. White RJ, Pasternak CA. The purification and properties of *N* -acetylglucosamine 6-phosphate deacetylase from *Escherichia coli*. *Biochemical Journal*. 1967;105(1):121-125. doi:10.1042/bj1050121

345. Uehara T, Suefuji K, Valbuena N, Meehan B, Donegan M, Park JT. Recycling of the Anhydro- *N* -Acetylmuramic Acid Derived from Cell Wall Murein Involves a Two-Step Conversion to *N* -Acetylglucosamine-Phosphate. *J Bacteriol*. 2005;187(11):3643-3649. doi:10.1128/JB.187.11.3643-3649.2005

346. Uehara T, Suefuji K, Jaeger T, Mayer C, Park JT. MurQ Etherase Is Required by *Escherichia coli* in Order To Metabolize Anhydro- *N* -Acetylmuramic Acid Obtained

either from the Environment or from Its Own Cell Wall. *J Bacteriol*. 2006;188(4):1660-1662. doi:10.1128/JB.188.4.1660-1662.2006

347. Holzheimer RG. Antibiotic induced endotoxin release and clinical sepsis: a review. *J Chemother*. 2001;13 Spec No 1(1):159-172. doi:10.1179/joc.2001.13.Supplement-2.159

348. Scholar EM, Pratt WB. *The Antimicrobial Drugs*. 2nd ed. Oxford University Press; 2000.

349. Whitfield C, Trent MS. Biosynthesis and export of bacterial lipopolysaccharides. *Annu Rev Biochem*. 2014;83:99-128. doi:10.1146/annurev-biochem-060713-035600

350. Raetz CRH, Whitfield C. Lipopolysaccharide endotoxins. *Annu Rev Biochem*. 2002;71:635-700. doi:10.1146/annurev.biochem.71.110601.135414

351. Arroyo LA, Herrera CM, Fernandez L, Hankins JV, Trent MS, Hancock REW. The pmrCAB operon mediates polymyxin resistance in Acinetobacter baumannii ATCC 17978 and clinical isolates through phosphoethanolamine modification of lipid A. *Antimicrob Agents Chemother*. 2011;55(8):3743-3751. doi:10.1128/AAC.00256-11

352. Harris TL, Worthington RJ, Hittle LE, Zurawski DV, Ernst RK, Melander C. Small molecule downregulation of PmrAB reverses lipid A modification and breaks colistin resistance. *ACS Chem Biol*. 2014;9(1):122-127. doi:10.1021/cb400490k

353. Vaara M. Agents that increase the permeability of the outer membrane. *Microbiol Rev*. 1992;56(3):395-411. doi:10.1128/mr.56.3.395-411.1992

354. Vaara M. Polymyxins and their novel derivatives. *Curr Opin Microbiol*. 2010;13(5):574-581. doi:10.1016/j.mib.2010.09.002

355. Kassamali Z, Rotschafer JC, Jones RN, Prince RA, Danziger LH. Polymyxins: wisdom does not always come with age. *Clin Infect Dis*. 2013;57(6):877-883. doi:10.1093/cid/cit367

356. Ainsworth GC, Brown AM, Brownlee G. Aerosporin, an antibiotic produced by Bacillus aerosporus Greer. *Nature*. 1947;159(4060):263. doi:10.1038/160263a0

357. Benedict RG, Langlykke AF. Antibiotic activity of Bacillus polymyxa. *J Bacteriol*. 1947;54(1):24.

358. Stansly PG, Shepherd RG, White HJ. Polymyxin: a new chemotherapeutic agent. *Bull Johns Hopkins Hosp*. 1947;81(1):43-54.

359. Hermsen ED, Sullivan CJ, Rotschafer JC. Polymyxins: pharmacology, pharmacokinetics, pharmacodynamics, and clinical applications. *Infect Dis Clin North Am*. 2003;17(3):545-562. doi:10.1016/s0891-5520(03)00058-8

360. Pedersen MF, Pedersen JF, Adsen PO. A clinical and experimental comparative study of sodium colistimethate and polymyxin B sulfate. *Invest Urol*. 1971;9(3):234-237.

361. Falagas ME, Bliziotis IA. Pandrug-resistant Gram-negative bacteria: the dawn of the post-antibiotic era? *Int J Antimicrob Agents*. 2007;29(6):630-636. doi:10.1016/j.ijantimicag.2006.12.012

362. Beceiro A, Tomás M, Bou G. Antimicrobial resistance and virulence: a successful or deleterious association in the bacterial world? *Clin Microbiol Rev*. 2013;26(2):185-230. doi:10.1128/CMR.00059-12

363. Maragakis LL, Perl TM. Acinetobacter baumannii: epidemiology, antimicrobial resistance, and treatment options. *Clin Infect Dis*. 2008;46(8):1254-1263. doi:10.1086/529198

364. Moffatt JH, Harper M, Harrison P, et al. Colistin Resistance in Acinetobacter baumannii Is Mediated by Complete Loss of Lipopolysaccharide Production. *AAC*. 2010;54(12):4971-4977. doi:10.1128/AAC.00834-10

365. Chin CY, Gregg KA, Napier BA, Ernst RK, Weiss DS. A PmrB-Regulated Deacetylase Required for Lipid A Modification and Polymyxin Resistance in Acinetobacter baumannii. *Antimicrob Agents Chemother*. 2015;59(12):7911-7914. doi:10.1128/AAC.00515-15

366. Beceiro A, Llobet E, Aranda J, et al. Phosphoethanolamine modification of lipid A in colistin-resistant variants of Acinetobacter baumannii mediated by the pmrAB two-component regulatory system. *Antimicrob Agents Chemother*. 2011;55(7):3370-3379. doi:10.1128/AAC.00079-11

367. van Opijnen T, Lazinski DW, Camilli A. Genome-Wide Fitness and Genetic Interactions Determined by Tn-seq, a High-Throughput Massively Parallel Sequencing Method for Microorganisms. *Curr Protoc Mol Biol*. 2014;106:7.16.1-24. doi:10.1002/0471142727.mb0716s106

368. Goodman AL, McNulty NP, Zhao Y, et al. Identifying Genetic Determinants Needed to Establish a Human Gut Symbiont in Its Habitat. *Cell Host & Microbe*. 2009;6(3):279-289. doi:10.1016/j.chom.2009.08.003

369. Ferrieres L, Hemery G, Nham T, et al. Silent Mischief: Bacteriophage Mu Insertions Contaminate Products of Escherichia coli Random Mutagenesis Performed Using Suicidal Transposon Delivery Plasmids Mobilized by Broad-Host-Range RP4 Conjugative Machinery. *Journal of Bacteriology*. 2010;192(24):6418-6427. doi:10.1128/JB.00621-10

370. Lim LM, Ly N, Anderson D, et al. Resurgence of Colistin: A Review of Resistance, Toxicity, Pharmacodynamics, and Dosing. *Pharmacotherapy*. 2010;30(12):1279-1291. doi:10.1592/phco.30.12.1279

371. Goodman AL, Wu M, Gordon JI. Identifying microbial fitness determinants by insertion sequencing using genome-wide transposon mutant libraries. *Nat Protoc*. 2011;6(12):1969-1980. doi:10.1038/nprot.2011.417

372. van Opijnen T, Camilli A. Transposon insertion sequencing: a new tool for systems-level analysis of microorganisms. *Nat Rev Microbiol*. 2013;11(7):435-442. doi:10.1038/nrmicro3033

373. Liu H, Bouillaut L, Sonenshein AL, Melville SB. Use of a mariner-based transposon mutagenesis system to isolate Clostridium perfringens mutants deficient in gliding motility. *J Bacteriol*. 2013;195(3):629-636. doi:10.1128/JB.01288-12

374. Singer JT, Finnerty WR. Insertional specificity of transposon Tn5 in Acinetobacter sp. *J Bacteriol*. 1984;157(2):607-611. doi:10.1128/jb.157.2.607-611.1984

375. Shull LM, Camilli A. Transposon Sequencing of Vibrio cholerae in the Infant Rabbit Model of Cholera. In: Sikora AE, ed. *Vibrio Cholerae*. Vol 1839. Methods in Molecular Biology. Springer New York; 2018:103-116. doi:10.1007/978-1-4939-8685-9_10

376. Smith MG, Gianoulis TA, Pukatzki S, et al. New insights into Acinetobacter baumannii pathogenesis revealed by high-density pyrosequencing and transposon mutagenesis. *Genes Dev*. 2007;21(5):601-614. doi:10.1101/gad.1510307

377. Gallagher LA, Shendure J, Manoil C. Genome-scale identification of resistance functions in Pseudomonas aeruginosa using Tn-seq. *mBio*. 2011;2(1):e00315-00310. doi:10.1128/mBio.00315-10

378. Khatiwara A, Jiang T, Sung SS, et al. Genome scanning for conditionally essential genes in Salmonella enterica Serotype Typhimurium. *Appl Environ Microbiol*. 2012;78(9):3098-3107. doi:10.1128/AEM.06865-11

379. van Opijnen T, Camilli A. A fine scale phenotype-genotype virulence map of a bacterial pathogen. *Genome Res*. 2012;22(12):2541-2551. doi:10.1101/gr.137430.112

380. Hurd PJ, Nelson CJ. Advantages of next-generation sequencing versus the microarray in epigenetic research. *Briefings in Functional Genomics and Proteomics*. 2009;8(3):174-183. doi:10.1093/bfgp/elp013

381. Lazinski DW, Camilli A. Homopolymer tail-mediated ligation PCR: a streamlined and highly efficient method for DNA cloning and library construction. *BioTechniques*. 2013;54(1). doi:10.2144/000113981

382. Gawronski JD, Wong SMS, Giannoukos G, Ward DV, Akerley BJ. Tracking insertion mutants within libraries by deep sequencing and a genome-wide screen for Haemophilus genes required in the lung. *Proc Natl Acad Sci U S A*. 2009;106(38):16422-16427. doi:10.1073/pnas.0906627106

383. Langridge GC, Phan MD, Turner DJ, et al. Simultaneous assay of every Salmonella Typhi gene using one million transposon mutants. *Genome Res*. 2009;19(12):2308-2316. doi:10.1101/gr.097097.109

384. Quail MA, Swerdlow H, Turner DJ. Improved Protocols for the Illumina Genome Analyzer Sequencing System. *Current Protocols in Human Genetics*. 2009;62(1). doi:10.1002/0471142905.hg1802s62

385. Mojica MF, Rossi MA, Vila AJ, Bonomo RA. The urgent need for metallo-β-lactamase inhibitors: an unattended global threat. *The Lancet Infectious Diseases*. Published online July 2021:S1473309920308689. doi:10.1016/S1473-3099(20)30868-9

386. Yeaman MR, Yount NY. Mechanisms of antimicrobial peptide action and resistance. *Pharmacol Rev*. 2003;55(1):27-55. doi:10.1124/pr.55.1.2

387. Brogden NK, Brogden KA. Will new generations of modified antimicrobial peptides improve their potential as pharmaceuticals? *Int J Antimicrob Agents*. 2011;38(3):217-225. doi:10.1016/j.ijantimicag.2011.05.004

388. Liu Y, Yang K, Zhang H, Jia Y, Wang Z. Combating Antibiotic Tolerance Through Activating Bacterial Metabolism. *Front Microbiol*. 2020;11:577564. doi:10.3389/fmicb.2020.577564

389. Santi I, Manfredi P, Maffei E, Egli A, Jenal U. Evolution of Antibiotic Tolerance Shapes Resistance Development in Chronic Pseudomonas aeruginosa Infections. Buchrieser C, ed. *mBio*. 2021;12(1):e03482-20. doi:10.1128/mBio.03482-20

390. Kaiser P, Regoes RR, Dolowschiak T, et al. Cecum Lymph Node Dendritic Cells Harbor Slow-Growing Bacteria Phenotypically Tolerant to Antibiotic Treatment. Schneider DS, ed. *PLoS Biol*. 2014;12(2):e1001793. doi:10.1371/journal.pbio.1001793

391. Adams RH, Schield DR, Card DC, Blackmon H, Castoe TA. GppFst: genomic posterior predictive simulations of FST and dXY for identifying outlier loci from population genomic data. *Bioinformatics*. 2017;33(9):1414-1415. doi:10.1093/bioinformatics/btw795

392. Brennan RO, Durack DT. Therapeutic significance of penicillin tolerance in experimental streptococcal endocarditis. *Antimicrob Agents Chemother*. 1983;23(2):273-277. doi:10.1128/AAC.23.2.273

393. Van den Bergh B, Michiels JE, Fauvart M, Michiels J. Should we develop screens for multi-drug antibiotic tolerance? *Expert Rev Anti Infect Ther*. 2016;14(7):613-616. doi:10.1080/14787210.2016.1194754

394. Claessen D, Errington J. Cell Wall Deficiency as a Coping Strategy for Stress. *Trends in Microbiology*. 2019;27(12):1025-1033. doi:10.1016/j.tim.2019.07.008

395. Osawa M, Erickson HP. L form bacteria growth in low-osmolality medium. *Microbiology (Reading)*. 2019;165(8):842-851. doi:10.1099/mic.0.000799

396. García Véscovi E, Soncini FC, Groisman EA. Mg2+ as an extracellular signal: environmental regulation of Salmonella virulence. *Cell*. 1996;84(1):165-174. doi:10.1016/s0092-8674(00)81003-x

397. Gunn JS, Richards SM. Recognition and integration of multiple environmental signals by the bacterial sensor kinase PhoQ. *Cell Host Microbe*. 2007;1(3):163-165. doi:10.1016/j.chom.2007.05.001

398. Prost LR, Miller SI. The Salmonellae PhoQ sensor: mechanisms of detection of phagosome signals. *Cell Microbiol*. 2008;10(3):576-582. doi:10.1111/j.1462-5822.2007.01111.x

399. Gunn JS. The Salmonella PmrAB regulon: lipopolysaccharide modifications, antimicrobial peptide resistance and more. *Trends Microbiol*. 2008;16(6):284-290. doi:10.1016/j.tim.2008.03.007

400. Ernst RK, Guina T, Miller SI. Salmonella typhimurium outer membrane remodeling: role in resistance to host innate immunity. *Microbes Infect*. 2001;3(14-15):1327-1334. doi:10.1016/s1286-4579(01)01494-0

401. Raetz CRH, Reynolds CM, Trent MS, Bishop RE. Lipid A Modification Systems in Gram-Negative Bacteria. *Annu Rev Biochem*. 2007;76(1):295-329. doi:10.1146/annurev.biochem.76.010307.145803

402. Olaitan AO, Morand S, Rolain JM. Mechanisms of polymyxin resistance: acquired and intrinsic resistance in bacteria. *Front Microbiol*. 2014;5. doi:10.3389/fmicb.2014.00643

403. Windels EM, Michiels JE, Fauvart M, Wenseleers T, Van den Bergh B, Michiels J. Bacterial persistence promotes the evolution of antibiotic resistance by increasing survival and mutation rates. *ISME J*. 2019;13(5):1239-1251. doi:10.1038/s41396-019-0344-9

404. Pisabarro AG, de Pedro MA, Vázquez D. Structural modifications in the peptidoglycan of Escherichia coli associated with changes in the state of growth of the culture. *J Bacteriol*. 1985;161(1):238-242. doi:10.1128/jb.161.1.238-242.1985

405. Mueller EA, Egan AJ, Breukink E, Vollmer W, Levin PA. Plasticity of Escherichia coli cell wall metabolism promotes fitness and antibiotic resistance across environmental conditions. *eLife*. 2019;8:e40754. doi:10.7554/eLife.40754

406. Romeis T, Höltje JV. Specific interaction of penicillin-binding proteins 3 and 7/8 with soluble lytic transglycosylase in Escherichia coli. *J Biol Chem*. 1994;269(34):21603-21607.

407. Banzhaf M, Yau HC, Verheul J, et al. Outer membrane lipoprotein NlpI scaffolds peptidoglycan hydrolases within multi-enzyme complexes in *Escherichia coli*. *EMBO J*. 2020;39(5). doi:10.15252/embj.2019102246